# CHARACTERISATION OF CMV CD8+T-CELL MEMORY-INFLATION TO IMMEDIATE EARLY HLA-C RESTRICTED TARGETS AND THE POTENTIAL OF CMV AS A VACCINE VECTOR FOR CANCER THERAPY

**Miss Louise Christine Hosie**

A thesis submitted to the University of Birmingham for the degree of DOCTOR OF PHILOSOPHY

**21st of October 2016**

**49 533 Words**

**282 pages**

**(excluding text in tables, figure legends and bibliography)**


UNIVERSITY OF BIRMINGHAM

**Institute of Immunology and Immunotherapy**

**University of Birmingham**

**October 2016**

# CONTENTS

.

# LIST OF FIGURES

**Chapter1;**



**Chapter 2;**



**Chapter 3;**

**Chapter 4;**

# LIST OF TABLES

# ABBREVIATIONS

aa – amino acid
APC – Antigen presenting cell
ARF(s) – Alternative reading frame/s
$\beta_2$M – Beta macroglobulin
BAC – Bacterial artificial chromosome
BFa - Brefeldin A
BSA – Bovine serum albumin
CCR7 – Chemokine receptor 7
CFC - carboxymethylcellulose
CFSE - Carboxyfluorescein succinimidyl ester
CMV – Cytomegalovirus
D – Diversity
DC – Dendritic cell
DMS0 – Dimethyl sulfoxide
DS – Double stranded
DTT - Dithiothreito
EBV – Epstein Barr virus
E – Early
E/L – Early/late
ER – Endoplasmic reticulum
FCS – Fetal calf serum
gCMV – Guinea pig CMV
gB – glycoprotein B
gH/gL – glycoprotein H/glycoprotein L
GMCSF - Granulocyte macrophage colony-stimulating factor'
IE – Immediate early
IE-1 – Immediate early 1 protein
IL-2 – Interleukin 2
IFN-γ – Interferon gamma
HCMV – Human Cytomegalovirus
HIV – Human Immunodeficieny virus
HFFF2 – Human fetal foreskin fibroblasts
HSV-1 – Herpes Simplex Virus 1
J - Joining
L - Late
LCLs -
PBMCs - Peripheral blood mononuclear cells
PBS – Phosphate buffered saline
PFA - Paraformaldehyde
PHA – Phytohaemagglutinin
PI – Propidium iodide
PRR – Pathogen recognition receptor
P/S – Penicillin/Stretpamicin

MCMV – Murine Cytomegalovirus
MHC I – MHC class I
MHC II – MHC class II
MHC I tetramer - MHC class I tetramer
MIEP – Major immediate early promoter
NK – Natural killer
NURD – Nucleosome remodeling deacetylase
ORFs – Open reading frames
O/N – Overnight
Q - Glutamine
RhCMV – Rhesus Macaque CMV
RT – Room temperature
SEREX - Serological analysis of cDNA expression libraries
SIV – Simian Immunodeficiency Virus
TA – Tumor antigen
TAP – Transporter associated with antigen
TCR – T cell receptor
TLR2 – Toll like receptor 2
$T_{CM}$ – T Central memory cell
$T_{EM}$ – T Effector memory cell
$T_{EMRA}$ – T Effector memory revertant cell
$T_N$ – T Naïve cell
TNF-α – Tumor necrosis factor alpha
TMB –
UL – Unique long
US – unique short
V – Variable
VSV – Vesicular Stomatitis virus

# ABSTRACT

CMV CD8+T-cell memory-inflation can occupy up to 50% of the total CD8+ T cell pool. Studies using an MHC class I immunevasion-deleted strain revealed novel peptide-epitopes across the virus genome both in-frame and translated in a non-canonical manner. This study functionally and phenotypically characterised CD8+T-cells responding to these CMV-derived epitopes with age. They were found to be frequent component of the *in vivo* repertoire dedicated towards HCMV during latency. A HLA-Cw*0702-restricted immunodominant CD8+T-cell response that accumulated within elderly donors was identified to reach 32% of the total CD8+T-cell pool producing IFN-γ/TNF-α. Subsequently, HLA-Cw*0702-restricted memory-inflation was observed to a further two peptides dominating the CD8+T-cell memory compartment. HLA-Cw*0702 CD8+T-cells demonstrated a $T_{EMRA}$ phenotype - $CD45RA^{+}/CD27^{-}/CD28^{-}/CCR7^{-/}perforin^{high}/granzymeB^{high}$ - and represented promising candidates for inclusion in HSCT adoptive immunotherapies. Consequently, the global HCMV-specific CD8+T-cell response is being vastly underestimated by restricting studies to; in-frame translation products, HLA-A/-B-restricted peptide-epitopes and utilising WT-strains to characterise novel CD8+T-cell targets. Lastly, understanding why particular HCMV antigens induce inflationary CD8+T-cells will facilitate harnessing HCMV as a cancer therapy. In an attempt to direct HCMV-mediated inflationary responses towards malignancies, a HCMV-based vaccine vector expressing the NYESO1 CTAg was generated. Preliminary results indicate the immunogenicity of such a vaccine *in vitro.*

# ACKNOWLEDGMENTS

Firstly, I wish to thank my supervisor Professor Paul Moss for the opportunity to undertake my PhD within his research group and for the encouragement and inspiration throughout.

Secondly, I wish to thank my supervisor Dr Annette Pachnio for the constant support and guidance, friendship all through my time at Birmingham and for being my Cytomegalovirus guru.

I am extremely grateful to my supervisor Dr Jianmin Zuo for providing his molecular biology expertise, help at a moment's notice and for never failing to make me laugh.

I wish to thank all the participants of the 1000 elder's cohort and all of the donors from the institute who participated in this research study whom without this research could not have been conducted.

A special thank you to my collaborators. Dr Stanley Riddell for generously providing the sequences of the HCMV peptide-epitopes. Dr Richard Stanton, for his expertise and guidance in generating the HCMV-NYESO1 recombinant vaccine.

A massive thanks to past and present members of the Paul moss research group for all of your support. In particular Dr Suzy Elderhsaw and Dr Hayden Pearce who provided invaluable help and friendship in the lab. To Luke Maggs and Amandeep Johl thank you for constantly making me smile on those long research days, nights and weekends! Also a thank you to Jusnara Begum for being an amazing source of experimental CMV knowledge and reagents.

Lastly, I wish to thank the Medical research Council for funding this investigative study.

# DEDICATION

**“It is impossible to live without failing at something,**

**unless you live so cautiously that you might as well not have lived at all**

**— in which case, you fail by default.”**

**J.K. Rowling**

This work is the culmination of years of never ending support and ceaseless love from the Hosie and Vint families.

Samantha Hosie - thank you for being my constant weird best friend

Sarah Vint - thank you for being the craziest and most supportive gran

Lorraine Hosie - never forgotten and I hope this makes you proud

But without a doubt I would not be here today without the selfless help and encouragement of Gordon Hosie. You are my hero.

**This work is dedicated to you Dad.**

# CHAPTER 1 – INTRODUCTION

## 1.1 - Human Cytomegalovirus (HCMV)

*Herpesviridae* are a family of large DNA viruses that establish lifelong persistence and consists of three major subfamilies - the α, β, and γ- *Herpesviridae*. Human Cytomegalovirus (HCMV) is a member of the β-Herpesvirus subfamily that infects up to 90% of the world's population depending upon socioeconomic status with seropositivity tending to increase with age [1]. HCMV is well controlled within healthy individuals typically causing an asymptomatic infection. However, HCMV disease represents one of the major causes of morbidity and mortality within immunocompromised patients e.g. new-borns and high risk groups such as AIDS or both solid organ transplant (SOT) and haematopoietic stem cell transplant (HSCT) patients. Despite an asymptomatic primary infection within healthy individuals, HCMV is now being linked to the development of several disease states. Within healthy individuals, the pro-inflammatory response to HCMV replication over the course of the host's lifetime is believed to contribute to the development of atherosclerosis [2, 3]. In chronic kidney disease patients, HCMV has been identified as a risk factor for arterial stiffening (arteriosclerosis) however the mechanisms behind this are unclear [4]. HCMV is also implicated in poor responses to vaccines such as Influenza and contributing to both aging and immune senescence within the elderly [5-7]. CMV is a highly species-specific virus i.e. HCMV will infect only humans and murine CMV (MCMV) infects only mice. Despite this species barrier, animal models of CMV have proven invaluable. For example, MCMV has provided insight into the virus life cycle, latency and pathogenesis of CMV and allowed for the investigation of potential immunotherapies for CMV-mediated disease [8, 9]. The guinea pig model of CMV disease has facilitated studies into congenital infection and immune protection as guinea CMV (gCMV) is readily able to cross the placental barrier [10]. Recently, the Rhesus macaque CMV (RhCMV) model has been successfully used to study the ability of CMV as a vaccine vector against SIV [11-13].

After an initial acute infection, HCMV establishes a life-long chronic infection whose major site of latency is postulated to be the $CD34^+$ myeloid progenitor lineage such as monocyte or dendritic cells [14]. In this lineage, the reactivation of HCMV is hypothesised to be closely linked to the differentiation status of the $CD34^+$ myeloid cells [15]. HCMV has an extensive cell tropism including, but most likely not restricted to; endothelial, epithelial, dendritic cells and fibroblasts [14]. During acute infection, HCMV is able to disseminate throughout the host and infect almost all organs within the human body [16] including the liver, lungs and kidneys. In addition, viral antigens have been detected in several different cell types within these organs, such as hepatocytes, monocytes, endothelial, epithelial and smooth muscle cells [16].

HCMV has a genome of ~235Kb separated into unique long (UL) and unique short (US) gene regions encoding for approximately 192 open reading frames (ORFs). The virion of HCMV consists of a double stranded (DS) DNA genome enclosed by the icosahedral nucleocapsid (Fig-1). The nucleocapsid is surrounded by the proteinaceous tegument layer formed of phosphoproteins (Fig-1). This layer contains over half of the HCMV-encoded virion proteins [17]. Lastly, the tegument is enveloped by a lipid bilayer that contains the glycoprotein complexes.

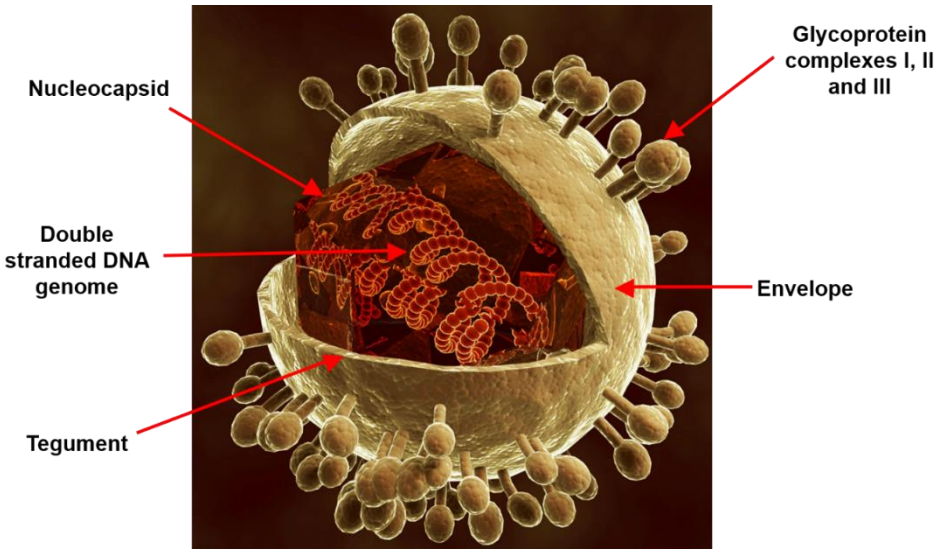


***Fig 1 – Schematic of a HCMV infectious virion***. Adapted from Rogers et al. [18] Rights and permission obtained from Nature Immunology licence number 3946961120363.

The infectious life cycle begins when the glycoprotein envelope protein gB attaches to viral cellular receptors e.g. heparin sulphate proteoglycans, followed by fusion of the virus envelope to the cellular membrane mediated by the gH/gL complex (Fig-2) (For a review of the lifecycle [19]). The uncoating of the virus and exposure of the nucleocapsid triggers its transport to the host cell nucleus, thought to be mediated by the viral tegument proteins, utilising host microtubules. Within the nucleus viral proteins utilise the host-cell transcription machinery to replicate the genome. The transcription of the HCMV genome occurs in temporally controlled phases: immediate early (IE), early (E) and late (L). The transcripts from the IE genes are the first to be produced and represent the viral transactivators IE-1 and IE-2 which drive the transcription of the E transcripts of the genome. The proteins encoded by the E genes function to modulate the host environment and immune response so that replication of the viral genome may continue unimpeded. The last transcripts to be produced are from the L genes representing the structural proteins that will form the new

virions. Once the newly formed DNA genomes are exported out of the nucleus, tegument acquisition occurs within the ER-Golgi intermediate compartment. Final envelopment with the glycoprotein complexes occurs in the cytoplasm with mature and fully enveloped virions egressing from infected cells via a budding and exocytosis event. The entire infectious life cycle is approximately 72 hours from entry to infectious virion release

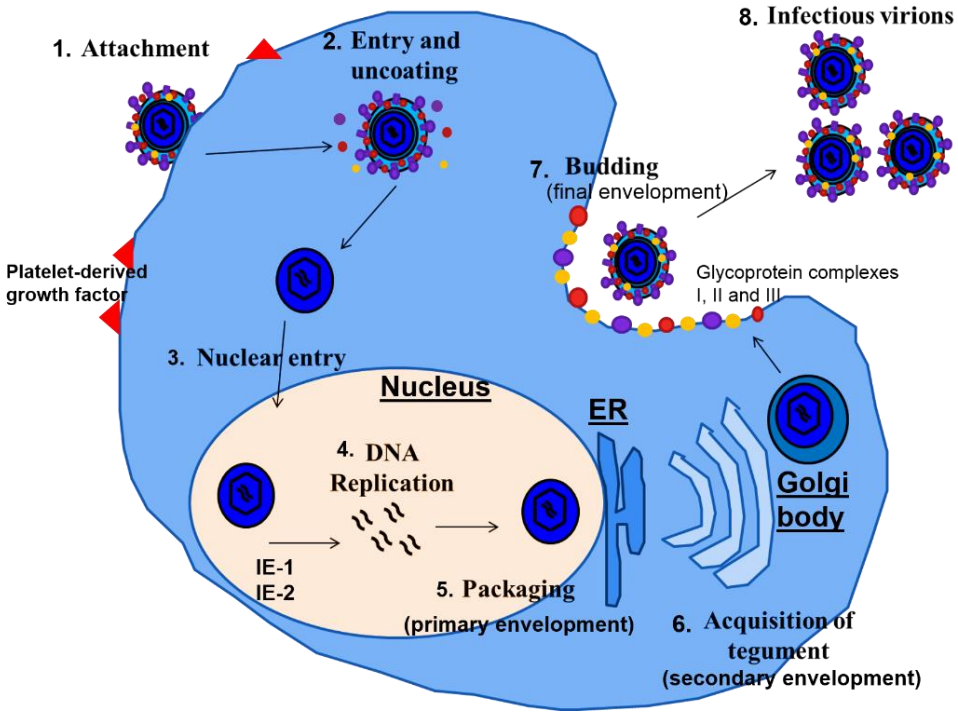


***Fig 2 – Schematic representation of the HCMV lifecycle.*** Adapted from Crough and Khanna et al [20]. The infectious life cycle of HCMV within a human cell. 1. HCMV attaches to a host cell via interaction of the viral glycoproteins (gB and gH) with specific surface cell receptors such as 'platelet-derived growth factor α'. 2. Entry of the virus is then facilitated via a fusion event of the viral glycoprotein envelope with the host cellular membrane. This leads to the uncoating of the virus and release of the viral nucleocapsid into the host cell cytoplasm. 3. Nucleocapsids are transported to and enter the host cell nucleus. 4. The expression of the viral IE-1/IE-2 transactivators leads to the initiation of viral DNA replication. 5. Newly replicated viral DNA is encapsulated within newly formed capsids, known as primary envelopment, and these then egress to the host cell cytoplasm. 6. At the ER-Golgi body interface, newly formed viral capsids acquire the proteinaceous tegument layer, known as secondary envelopment. 7. Mature infectious virions are produced after acquiring the viral glycoproteins, final envelopment, after a budding event. 8. Infectious virions are released by exocytosis. The entire life cycle is approximately 72 hours.

## 1.2 – CD8+T-cell immunology

T-cell mediated immunity consists of two main components -– one for extracellularly-derived pathogens (CD4+T-cells) and one for intracellularly-derived pathogens (CD8+T-cells). T-cells recognise peptides derived from pathogens that are presented on the cell surface within the complex of either an MHC class I (MHC-I) or class II (MHC-II) molecule via engagement of their ‘T cell receptor’ (TCR).

CD4+T-cells are a critical component in the fight against extracellular pathogens such as bacteria and eukaryotic pathogens and are pivotal in providing co-stimulation and cytokines to the CD8+T-cell response (review on CD4+T-cell function [21]). CD4+T-cells have recently been demonstrated to directly kill virally infected cells via their ‘T-cell receptor’ (TCR) recognising peptide:MHC-II complexes on ‘Antigen presenting cells’ (APCs). The focus of this study will however be upon the CD8+T-cell arm of the adaptive immune response.

CD8+T-cells are responsible for clearing intracellular viruses and aberrant host cells. Their TCR recognises peptides 8-10 amino acids (aa) long derived from intracellular pathogens that are presented on the cell surface within an MHC-I molecule. The peptides are generated via cytoplasmic proteolytic degradation of infected cells by the proteasome and their subsequent transport into the Endoplasmic Reticulum (ER) lumen via the membrane associated 'Transporter associated with Antigen Processing' (TAP). Within the ER lumen, the peptides are trimmed and loaded onto newly synthesised MHC-I molecules and the MHC:peptide complex is released to the cell surface [22].

The TCR is a complex of membrane bound proteins that facilitate the binding to foreign or self-derived peptides presented in the MHC molecules. Within humans around 95% of CD8+T-cells contain a TCR formed of a CD8 heterodimer of αβ chains bound in a non-covalent complex with the invariant chains of CD3 molecules. These are known as αβ

CD8+T-cells. The remaining 5% are formed of γδ chains [23]. This investigation will focus on the αβ CD8+T-cell population.

When the TCR complex engages a peptide:MHC-I complex an immunological synapse forms– defined as the contact point between the TCR, co-receptors on the APC (e.g. CD28 and CTLA-4), peptide:MHC complex and host signalling pathway molecules (LCK, ZAP70, ITK, PLC) (reviews [24, 25]). This results in signalling cascades terminating in the proliferation, antigen driven differentiation and cytokine/effector molecule production of the CD8+T-cell. This in turn leads to the activation-induced cell death and elimination of infected target cells via two major cytotoxic pathways: the perforin/granzyme or the Fas ligand/Fas receptor apoptosis pathway [26]. In the former pathway, TCR engagement causes secretory granules to translocate to the immunological synapse allowing perforin molecules to be released and form pores within the target cells [25]. This facilitates the entry of granzyme molecules which induce the apoptosis caspase pathways. In the FAS mediated pathway, FAS ligands present on the CD8+T-cell engage FAS molecules (a member of the TNF receptor superfamily) on the surface of the target cell to be killed. This then also activates the apoptosis caspase pathways within the target cell.

The CD8+T-cell repertoire within the human body has to be capable of responding to all potential pathogens encountered during a life time. The immune system must generate enough diversity of CD8+T-cell populations with distinct TCRs and therefore differing antigen specificity. To do this genetic recombination occurs within the thymus between the encoded segments – constant (C), variable (V), diversity (D) and joining (J) – of the α and β chains. This determines the structure of the antigen binding site of the TCR and the large overall diversity (Fig-3) [27]. The hypervariable sections of the TCR known as the ‘complementarity determining regions’ (CDRs) 1 and 2 regions are germline encoded within the V gene (Fig-3) and they play a role in binding to the MHC-I molecule. The third hypervariable region, CDR3, is situated between the V, D and J sections on both the α and β chains and is responsible for

recognising the peptide:MHC complex and therefore provides the antigenic specificity. Further diversity in the TCR chains is provided by the insertion of non-template encoded nucleotides within the CDR3 region (referred to as 'N', Fig-3). The CDR3 regions vary between different TCRs whilst the CDR1/2 sequences do not as they are germline encoded, however, the usage of common chains between TCRs varies. In total, within the human TCR loci, there are 43 V and 58 J α gene segments and 42 V, 2 D and 12 J β gene segments [28]. It has been postulated that the overall antigenic diversity of the human CD8+T-cell response exceeds 1 x $10^{15}$ distinct TCR receptors [27]**.**

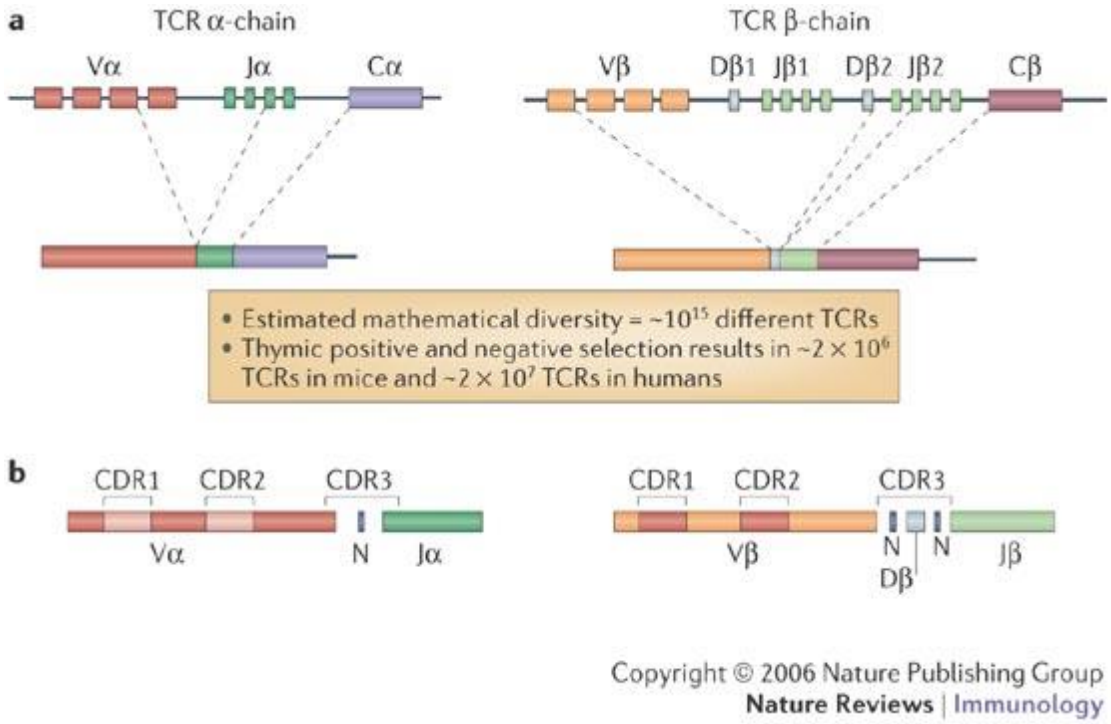


***Fig 3 – Somatic recombination of the TCR α and β chains.*** **[27]**. Permission to reuse content in this thesis obtained from Nature Reviews Immunology. Licence number 3885290794359. A) TCRs are formed of a heterodimer of an α and β chain generated by somatic gene recombination between the V-J (α chain) and V-D-J (β chain) segments. B) Hypervariable CDR regions. CDR1 and CDR2 are germline encoded within the V gene segment. CDR3 is situated between the V and J gene segments. N refers to the sites of additional non-template encoded nucleotides to increase antigenic diversity of the TCR repertoire.

## 1.3 – CD8+T-cell memory subsets

During an immune response to pathogens, CD8+T-cells transit through three distinct phases; antigen-stimulation and expansion, death of effector cells and the formation of a pathogen-specific memory CD8+T-cell pool (Reviewed [29]). Once the primary infection has been cleared and the pathogen eliminated, ~95% of effector T-cells (defined by high proliferative capacity and cytotoxicity) die via apoptosis [30]. This leaves a small pool of about 5-10% of long lived pathogen-specific memory CD8+T-cells. These reside in organs until antigenic rechallenge. This memory CD8+T-cell pool is maintained for life and can be broadly categorised into 4 memory subsets; 'Central memory T-cells' ($T_{CM}$), Effector memory T-cells ($T_{EM}$), 'T-cell Effector Memory Revertant' ($T_{EMRA}$) and the recently defined 'Tissue resident memory T-cells' ($T_{RM}$) (review [31]).

Naïve CD8+T-cells ($T_N$) that have not yet encountered cognate antigen, express selectins and chemokine receptors allowing migration to the secondary lymphoid organs e.g. lymph nodes. The cell surface expression of the CD45RA isoform and chemokine receptor 7 (CCR7) are used to differentiate naïve T-cells from antigen experienced T-cells. Within the secondary lymphoid organs they encounter their cognate antigen and mature into effector T-cells. Effector T-cells – activated T-cells – lack CCR7/CD62L expression so that they are able to migrate to non-lymphoid sites of inflammation, kill infected cells and resolve the infection. Once the acute infection has been resolved and antigen stimulation removed, ~90% of these effector cells die off and the remaining differentiate into resting memory CD8+T-cells subsets demonstrating differing surface phenotypes and effector functions.

$T_{CM}$ patrol are memory CD8+T-cells that patrol between the blood and secondary lymphoid organs e.g. lymph nodes and tonsils, produce IL-2 and are able to proliferate efficiently. Their surface phenotype is $CCR7^+$, $CD45RO^+$, $CD27^+/CD28^+$ (co-stimulatory markers) $CD127^+$ (IL-7 receptor) and $CD62L^+$ (lymph node homing ligand). These $T_{CM}$ cells provide long term protective responses from within secondary organs such as the lymph nodes

initiate secondary immune responses to generate a second wave of effector CD8+T-cells which are able to enter the periphery [31, 32]. However, as this subset does not have immediate effector function they cannot initially contain secondary viral infections [31, 33] .

$T_{EM}$ are memory CD8+T-cells that circulate the blood and peripheral tissues e.g. gut mucosa, have immediate effector function and secrete potent amounts of IFN-γ. Their surface phenotype is $CCR7^-$, $CD45RO^+$, $CD62L^-$, and $CD27^-/CD28^-$ (Reviewed [32, 34]). These $T_{EM}$ cells provide protection from secondary infections at peripheral sites where the primary infection occurred or subsequent infections are likely to occur [32]. Typically once the acute infection has been controlled, $T_{EM}$ in the periphery decline to low stable numbers until antigenic rechallenge.

In addition to the $T_{CM}$ and $T_{EM}$ memory subsets, a CD8+T-cell memory subset representing highly differentiated memory T-cells has been described that patrols the periphery. The subset is termed 'T-cell Effector Memory Revertant' ($T_{EMRA}$) based upon their re-acquisition of the CD45RA isoform. These are a subset of highly cytotoxic memory CD8+T-cells that lose CCR7 expression and are perforin and granzymeB positive (Reviewed [34]). The development of this subset has been linked to the chronic stimulation of the T-cells by viral antigen [29, 35]. The re-expression of the CD45RA isoform is thought either due to prolonged periods of antigen absence or is re-acquired to provide long term survival signals to the CD8+T-cell [36] [37].

Recently, a subset of memory CD8+T-cells termed ‘Tissue resident memory T-cells) ($T_{RM}$) have been described that are $CD69^+CD103^+$ (review [38, 39]). $T_{RM}$ maintain large peripheral tissue numbers after resolution of an acute infection but do not circulate throughout the periphery. $T_{RM}$ therefore represent an anatomically distinct population to the peripherally located $T_{EM}$ and $T_{EMRA}$. At this tissue location they provide a first line of immunosurveillance and defence against secondary infections due to their high proliferative capacity.

## 1.4 – Immune Response to CMV

HCMV is arguably one of the most immunogenic human pathogens studied to date. The virus induces both the innate and adaptive arms of the immune response including inflammatory cytokines, neutralising antibodies, Natural Killer (NK) cells and CD4+ and CD8+T-cells [40].

The first line of host defence upon HCMV entering cells is provided by the innate signalling pathway - initiated via the interaction of the glycoprotein B (gB) and glycoprotein H (gH) with Toll-like receptor 2 (TLR2) on target cells. This ultimately leads to the production of inflammatory cytokines such as 'Interferon gamma' (IFN-γ) and 'Tumour necrosis factor alpha' (TNF-α) via the NF-κB dependent signal transduction pathway [41]. This inflammatory environment recruits NK-cells to the point of viral replication. NK-cells are now well recognised as being an important primary defence against viral pathogens [42] as viral infection leads to the up-regulation of activating ligands for NK-cells such as MICA/B and ULBP6 [43]. Conversely, this cytokine induced pro-inflammatory environment may be beneficial to HCMV replication. IFN-γ and TNF-α recruit myeloid immune cells such as dendritic cells and macrophages to the site of viral infection which are permissible to HCMV infection [14]. This inflammatory environment therefore represents a potential method of HCMV dissemination to establish foci throughout the peripheral system [44, 45].

Little is still currently known on the role of NK-cells in controlling HCMV infection. The adoptive transfer of MCMV-specific NK-cells recognising the m157 protein from MCMV-infected mice to non-infected mice provided protection from CMV challenge [46]. This implicates NK-cells as important in the initial control of the virus. Foley et al. have recently associated a population of MCMV-specific NK-cells expanding over a period of time expressing the NKG2C activating receptor [47]. Recently, Redeker et al. demonstrated a positive correlation between NK-cells and a reduced MCMV viral load by day 4 after primary

MCMV infection of WT mice – thus further implicating the role of NK-cells in early MCMV control [3].

Antibodies also play a recognised role in control of CMV. The majority of antibodies directed towards HCMV are directed towards the pentameric envelope complex gH/gL(ul128-131) but have also been detected for pp65, pp150 (Reviewed [48]). Antibodies specific for the multimeric gH/gL (UL128-131) complex demonstrate viral neutralisation properties preventing dissemination [33]. However, a recent study indicated that these HCMV-specific antibodies are not sufficient to prevent the cell to cell spread of HCMV [49]. Importantly, HCMV-specific IgG titre has been demonstrated to increase with age. This correlated with an increased HCMV viral load within older donors and a decrease in the IE-1-specific cellular T-cell response. Indicating that the adaptive response is more critical than humoral for viral control in older age [50].

The CD4+ and CD8+T-cell responses represent the critical component of the immune response for HCMV control. Their development and maintenance is essential to maintaining the control of viral reactivation events and therefore preventing the production of new infectious virions. This is supported by the fact that immunosuppressed individuals develop uncontrolled viral replication in the absence of adaptive control [51]. The frequencies and magnitudes of peripheral T-cells specific for HCMV are the largest recorded for a viral pathogen to date, vary greatly between seropositive individuals, dominate the T-cell memory compartments and reduce the naïve T-cell compartment (discussed in section 1.5/1.7). Within young donors the HCMV-specific T-cells also represent a significant percentage of the memory T-cell population (discussed in section 1.5-7).

Evidence supporting the role of CD4+T-cells in controlling CMV infection is provided by studies in renal transplant patients who acquire primary HCMV infection. Within otherwise healthy asymptomatic patients the emergence of HCMV-specific CD4+T-cells was at an

earlier time-point than CD8+T-cells. However in renal transplant patients who presented with a delayed CD4+T-cell response, HCMV disease developed [52]. Furthermore, the maintenance of adoptively transferred HCMV-specific CD8+T-cells required CD4+T-cell help to control HCMV within bone marrow transplant patients [53-55]. Lastly, within HSCT patients an inverse correlation between CMV-specific CD4+T-cell levels and viral reactivation episodes was observed indicating their critical role in controlling CMV viral load [56].

The CD4+T-cell response to HCMV is broadly directed across the genome [57, 58] including towards but not limited to the gB, pp65, UL86, IE and gH proteins. HCMV-specific CD4+T-cell responses within young donors have been reported to reach 10% of the total peripheral CD4+T-cell pool. These CD4+T-cells display a phenotype of decreased CD27/CD28 expression, a concomitant decrease in IL-2 production and are $CD57^+$ with age [59]. They can have cytotoxic phenotypes expressing high levels of GranzymeB and Th1 cytokines [60, 61]. MCMV and HCMV-specific cytotoxic CD4+T-cells have been shown recently to directly kill peptide-loaded targets *in vitro* [61, 62] and express high levels of CX3CR1 postulated to direct them towards infected endothelium *in vivo* [61].

Evidence supporting the crucial role of CD8+T-cells in MCMV control includes the adoptive transfer of IE-1-specific CD8+T-cells into mice depleted for CD8+T-cells. These mice were protected from a lethal challenge with MCMV [63]. Within humans, the same principle has been applied by Riddell at al. where HCMV-specific CD8+T-cells that were expanded *ex vivo,* protected patients from primary and reoccurring HCMV manifestations [64].

## 1.5 – The CD8+T-cell response to CMV

The *ex vivo* CMV-specific CD8+T-cell response has been extensively investigated due to the use of validated methods such as; enzyme-linked immunosorbent spot (ELISpot) assays, *in vitro* peptide stimulation followed by intracellular cytokine staining (ICS) by flow cytometry

and the development of MHC-I tetramer technology. These methods have increased the knowledge of the breadth and magnitude of the HCMV-specific CD8+T-cell response and allowed comparison to other antiviral CD8+T-cell populations [65, 66].

HCMV primary infection is difficult to investigate due to its asymptomatic nature; therefore the natural progression of the HCMV-specific CD8+T-cell response with age is poorly understood. However, using HCMV seronegative renal transplant patients who acquire HCMV post-transplant, it has been shown that during primary infection HCMV-specific CD4+T-cells precede the emergence of CD8+T-cells. Additionally that most peripheral CMV-specific CD8+T-cells during primary infection are of an earlier differentiated phenotype - $CCR7^{-}CD27^{+}CD28^{+/-}CD45RA^{-}CD45R0^{+}$ [67, 68]. As these renal transplant patients enter latency, the peripheral CD8+T-cells progress to a later differentiated $T_{EMRA}$ phenotype - $CCR7^{-}CD27^{-}CD28^{-}CD45RA^{+}CD45R0^{-}$ [67, 68].

The main defining features of latent CMV-specific CD8+T-cells are; $CD45RA^{+}$ reexpression, high cytotoxic potential (defined by intracellular perforin and granyzmeB granules) [69] and loss of CD27/CD28 expression [70]. Altogether, CMV-specific CD8+T-cells display features that typically indicate a T-cell further down the maturation pathway yet are still functional [71]. A unique feature of the CMV-specific CD8+T-cell populations is the high expression of the fractalkine receptor CX3CR1. This has also been shown at the transcriptional level to be present on CMV-specific CD8+T-cells during acute infection and maintained through to latency [72]. CX3CR1 may be responsible for homing CMV-specific memory CD8+T-cells to the endothelium. This provides a plausible hypothesis for why these highly cytotoxic CMV-CD8+T-cells have been implicated in causing cardiovascular disease/damage [2, 4]

HCMV encodes for >160 antigenic proteins [73]. The first HCMV-specific CD8+T-cell responses detected were against the 72KDa IE-1 transactivator protein [74] followed by the pp65 phosphoprotein [75]. The IE-1 and pp65 proteins in particular were focused upon as

they are the first viral protein to be expressed and most abundant tegument protein respectively. This has led to the assumption that they are the immunodominant proteins of HCMV and facilitated numerous studies into pp65/IE-1-specific CD8+T-cell responses [76-79].

Recent focus has been on evaluating the global CD8+T-cell repertoire dedicated towards CMV. One study investigated synthetic peptides from 14 HCMV proteins: gH, gB, IE-1, US2, US3, US6, US11, UL16, UL18, pp28, pp50, pp65, pp71 and pp150 to analyse the HCMV-specific CD8+T-cell responses *ex vivo*. The results identified CD8+T-cell responses to all peptides, albeit at differing magnitudes, and new CD8+T-cell epitopes were subsequently characterised [58].

The most detailed study to date analysed the CD4+ and CD8+T-cell response to all 213 HCMV open reading frames (ORFs) [57]. Synthetic peptides were generated and T-cell responses against them investigated in 33 seropositive donors by detection of IFN-γ producing CD4+ and CD8+T-cells using flow cytometry [57]. A median of 8 and a total of 151 ORFs elicited HCMV-specific CD8+T-cell responses within these donors. This study provided the first global picture of the breadth of the T-cell response to HCMV. However, this study by Sylwester et al. did not identify specific CMV-derived T-cell epitopes.

However, HCMV encodes for several proteins that interfere with viral MHC-I presentation to the immune response [80, 81]. The above are two examples of studies that were carried out with donors infected with WT strains containing the MHC-I immunomodulatory proteins. Therefore there was the possibility that the magnitude or breadth of the HCMV-specific CD8+T-cell response detected was masked by the down-regulation of MHC-I within the seropositive donors. In order to characterise the HCMV-specific CD8+T-cell response in the absence of the US genes, Khan et al. utilised a US2-US11 immunevasin deleted strain of HCMV termed 'RV798' developed by Jones et al. [82, 83]. This was to allow all potential

HCMV antigenic epitopes to be displayed upon the surface of infected cells without the interference of MHC-I down-regulation [84]. Increased surface levels of MHC-I were observed on RV798 infected fibroblasts, compared to the WT- infected fibroblasts, which subsequently led to an increased CD8+T-cell recognition by both IE-1 and pp65-specific CD8+T-cell clones – up to 10-fold. After this finding, the authors then also defined novel target antigens of HCMV-specific CD8+T-cells and found them to be directed across the HCMV genome functioning in both the early and late phases of the viral life cycle. HCMV-specific CD8+T-cells were then screened for killing ability with 'Modified Vaccinia Ankara' (MVA) modified to express individual HCMV proteins. CD8+T-cells co-cultured with RV798 cells were efficiently able to target a broader range of HCMV targets including, pp150, pp50, IE-2 and gB.

Manley et al. also utilised the RV798 strain to analyse both the specificity and frequency of HCMV-specific CD8+T-cells [82]. Fibroblasts, derived from healthy seropositive donors, were infected with RV798 and the overall CD8+T-cell response analysed. The authors found the CD8+T-cell recognition of the RV798 infected fibroblasts to be increased 40-fold compared to those infected with the WT strain. The results observed that the majority of the CD8+T-cells were directed towards the pp65 and IE-1 proteins as previously published, but interestingly, CD8+T-cell responses were detected towards IE and E proteins not yet characterised. Utilising single knockout strains of CMV to identify which proteins the CD8+T-cell clones were specific for by observing the loss of killing, Riddell and colleagues then characterised the CD8+T-cell epitopes. The sequences of a selection of 16 epitopes were kindly provided to our research group (Table-7, [85]). The epitopes were found to be derived from HCMV antigens broadly spread across all phases of the viral life cycle including UL16, UL17, UL23, UL24, UL28, UL33, UL36, UL52, UL56, UL84, UL105, UL122 and US23. The same work by Riddell et al. identified novel peptides derived from the US22 and US34 proteins that are translated in a non-canonical method – via translation of an alternative ORF

that begins +2aa from the canonical methionine start codon. These were termed ‘cryptic’ CD8+T-cell epitopes (Riddell et al. unpublished data Table-10).

Clearly, the CD8+T-cell response to HCMV is one of the broadest and largest documented to a viral pathogen to date.

**1.6 - HCMV memory-inflation**

Memory-inflation defines the phenomenon whereby virus specific CD8+T-cells increase substantially within the periphery with age. The term ‘memory-inflation’ was first devised after investigating virus-specific T-cell responses in MCMV infected mice longitudinally using utilising MHC-I tetramer technology. Large peripheral increases in CMV-specific CD8+T-cells was observed with age [86]. Memory-inflation has since been observed during infection with other human viral pathogens [29, 87, 88]. For example, after systemic ‘Herpes Simplex Virus 1’ (HSV-1) infection, gB-specific CD8+T-cells accumulate in the periphery [89]. A third Herpesvirus ‘Epstein Barr Virus’ (EBV) induces CD8+T-cells specific for an immunodominant epitope that increase with age [90]. However, the total number of EBV-specific CD8+T-cells within the periphery did not alter with age. Memory-inflation is therefore most pronounced for HCMV [87, 91-93] and has also been demonstrated within several animal models of CMV infection e.g. mice and monkeys [76, 94, 95].

There is currently no model for EBV infection, therefore the availability of the MCMV and ‘Rhesus CMV’ (RhCMV) model provides a good platform to study the phenomenon of memory inflation. An advantage to using animal models, in particular MCMV, is the ability to longitudinally study the generation and maintenance of memory inflation during the animal’s lifetime. However there are some drawbacks to the use of such animal models and the translation of data obtained from these models to HCMV memory inflation. For example, the immunology of MCMV and RhCMV may lack important aspects of human immunology [96,

97]. Additionally, as CMV's are highly species specific, the replication and pathogenesis of MCMV and RhCMV may differ to HCMV *in vivo*. For example, unlike HCMV, MCMV genomes and reactivation can be observed within the lungs of infected mice [98]. Therefore it is also important to study the phenomenon of memory inflation within the context of HCMV, cross-sectionally, and where possible longitudinally, within seropositive individuals.

CMV specific CD4+T-cells have been documented to undergo memory-inflation however not to the extent of CD8+T-cells [59]. CD4+T-cell memory-inflation within the murine model has been documented against a single epitope $m09_{133-147}$ [99]. With regards to HCMV, the total CMV-specific CD4+T-cell population has recently been demonstrated to increase with age from 2.2% (donors <50 years) to 4.7% of the total CD4+T-cells (donors >65 years) [59] [60]. However unlike CD8+T-cell memory inflation, this does not lead to an imbalance of the ratio of the memory compartments and has been poorly investigated. The exaggerated CD8+T-cell memory-inflation will be the focus of this investigation.

To date, HCMV represents the largest immunodominant pathogen to the human immune response. Within elderly seropositive individuals, the HCMV-specific CD8+T-cell response is reported to be on average 10% of the total peripheral CD8+T-cell pool compared to 2% within the young [77]. Investigations by Moss et al. and Lang et al. demonstrated HCMV-specific CD8+T-cell responses could reach 21% and 50% of the total peripheral CD8+T-cell pool towards a single pp65 epitope respectively [87, 100]. CD8+T-cell responses to the pp65 and IE-1 proteins have additionally been documented to account for 50% of the total peripheral CD8+T-cell response within elderly individuals [77] and represent immunodominant antigens [71, 75, 101, 102]. The scale of HCMV epitopes that display memory-inflation or have the potential to inflate has not yet been identified or investigated. This is largely a result of the difficulty in distinguishing when individuals first become CMV-positive making it almost impossible to longitudinally follow specific CD8+T-cell populations and pin-point when they begin to inflate. It is for this reason that memory-inflation has been

best studied within the murine model where CMV primary infection can be followed to latency. These studies have led to the identification of two distinct types of MCMV CD8+T-cell epitopes– ‘stable’ vs ‘inflationary’ – whereby only ‘inflationary’ epitopes elicit CD8+T-cell populations that undergo memory-inflation [[103, 104].

Stable CD8+T-cell epitopes e.g. $M45_{985-993}$ MCMV epitope, elicit CD8+T-cell responses that follow the classical pattern of T-cell expansion, contraction and maintenance at low level after a typical pathogen infection. These CD8+T-cell populations demonstrate a $T_{CM}$ phenotype. The opposite is seen with inflationary CD8+T-cell epitopes e.g. $M38_{316-323}$ MCMV epitope. Here the specific CD8+T-cells accumulate over time and represent a $T_{EMRA}$ phenotype. It should be noted that these distinct CD8+T-cell responses are not restricted to the M45 and M38 proteins and both stable and inflationary CD8+T-cell populations have also been identified towards the $M57_{816-824}$ or $m139_{419-426}$ and $IE3_{416-423}$ peptides respectively [105].

Within humans, this distinction between CD8+T-cell populations has not yet been made. However, through cross-sectional studies of chronically infected donors, it has been identified that peripherally inflated HCMV-specific CD8+T-cell responses have a unique phenotype associated with ‘dysfunctional’ or ‘end stage’ CD8+T-cells during latency [70, 87, 106-108]. They have been identified as; $CCR7^-/CD27^-/CD28^-/CD45RA^+/CD57^+$ therefore representing a $T_{EMRA}$ phenotype [71, 106]. This is in comparison to earlier-differentiated HCMV-specific CD8+T-cells detected during primary infection being; $Ki67^+/CD45RO^+/CD45RA^-/CD27^+$ [109]. It has since been established that inflationary CMV CD8+T-cells are still functional and capable of exerting anti-viral effects [87, 91]. They are extremely Th1 cytokine producing, with the exception of IL-2, and high for perforin and granzymeB [70, 72, 87, 91]. Importantly, they show no signs of functional exhaustion with age [91, 110].

The mechanisms driving memory-inflation and its maintenance are at present undefined. However, the unique $T_{EMRA}$ phenotype of CMV CD8+T-cell accumulations likely point to low level antigen presentation to these peripheral CD8+T-cells throughout the lifetime of the infected host. The presence of CD45RA on HCMV-specific CD8+T-cell expansions may suggest that they have not encountered their cognate antigen for a period of time [111]. CD45RO is now known to require persistent antigen-stimulation to remain expressed on the surface of CD8+T-cells [37]. On the other hand, others state that CD45RA re-expression is a product of chronic antigen stimulation and is providing survival signals to the CD8+T-cell [36]**.**

It is clear that the CD8+T-cell response is effective at limiting the production of infectious virions by halting replication at the IE/E stage within the lungs of infected mice [112, 113]. These foci of viral IE/E gene expression may represent reservoirs of antigen source for the chronic stimulation of the IE/E-specific CD8+T-cell response. Infection of mice with a mutant strain of MCMV (termed ΔgL-MCMV) unable to replicate more than once due to a deletion in the glycoprotein L (gL), still allows for the development of memory-inflation but at a lower magnitude [114]. Interestingly indicating that the continuous production of infectious particles over time is not required for memory-inflation. However, our research group has utilised a highly replication attenuated strain of MCMV, termed tsm5, to infect mice and followed the resulting CD8+T-cell response. The study demonstrated that memory-inflation is abolished. The difference between the two mutant CMV strains is that ΔgL-MCMV can complete viral DNA synthesis during reactivation events within the cells infected during primary infection but newly infectious virions cannot enter new cells. Conversely the tsm5 strain cannot complete viral DNA synthesis.

Together this data therefore supports a hypothesis that sporadic viral reactivations resulting in CMV gene expression and MHC-I presentation of these proteins is required to re-stimulate the initial CD8+T-cell pools primed during primary HCMV infection. The production of fully

infectious progeny is not required. Over time this stimulation results in a CD8+T-cell population with an 'end-stage' $T_{EMRA}$ phenotype. This will be termed the 'antigen encounter theory' in this investigation.

Further studies supporting the antigen encounter theory were conducted in mice whereby the adoptive transfer of HCMV-specific CD8+T-cells with a $T_{CM}$ phenotype differentiated into a $T_{EMRA}$ phenotype that quickly migrated to the periphery - suggesting antigen stimulation is driving their differentiation [115]. The recruitment of new CD8+T-cells into the periphery from the thymus was found as a dispensable factor for memory-inflation maintenance within thymectomized mice - suggesting the inflated CD8+T-cell populations may be maintained by peripheral antigen encounter [116]**.**

A study by our research group implicates the replication of MCMV genomes as sufficient to maintain memory-inflation [117]. Moss et al. discovered that the treatment of MCMV-infected mice with valaciclovir over a period of 12 months, seemingly resolved memory-inflation and increased the total naïve CD8+T-cell pool. Furthermore, the degree of T-cell differentiation of inflated populations was decreased within the mice. This indicated that DNA synthesis during MCMV reactivation plays a role in both the maintenance and driving the differentiation of the inflated CD8+T-cell responses.

The last study supporting the antigen encounter theory to be discussed is one by Snyder and colleagues who demonstrated that the memory-inflation pool of MCMV-specific CD8+T-cells is maintained by the constant replenishing of MCMV-specific effector cells as they are short-lived [103, 118]. Adoptively transferred MCMV-specific CD8+T-cells into latently infected mice were described as infrequently dividing but instead replaced by new effector CD8+T-cells from lymphoid organs they hypothesise in response to antigen stimulation by reactivating virus.

## 1.7 – Stable vs. inflationary CMV CD8+T-cell populations and epitopes – what factors define whether a CD8+T-cell response will inflate?

Clearly, the antigen encounter theory does not explain why only certain CD8+T-cell population's specific for particular epitopes within individual CMV proteins inflate. Some explanations as to why some CMV-peptide-epitopes demonstrate inflationary capacities have been provided within the literature.

1. Gene expression context

One of the most obvious explanations as to why an epitope may have an inflationary advantage over others is the expression kinetics during the virus lifecycle. Those expressed earlier during the lifecycle will have an enhanced opportunity, over those expressed with L kinetics, for presentation to the CD8+T-cell response before elimination of the infected cell. Kurz et al. presented evidence of MCMV replication frequently within the lungs of infected mice that did not lead to the production of new infectious progeny i.e. L stages of reactivation [112, 113]. Reddehase and colleagues further demonstrated that MCMV RNA present within the lungs was transcribed from the IE genes with no E or L RNA present. This indicated the quick control or abortion of complete viral reactivation by IE/E-specific MCMV-specific CD8+T-cells before viral progeny production. In support of these findings, Simon et al. demonstrated the removal of MCMV-infected cells by IE-1-specific CD8+T-cells during stochastic reactivation events in the lung [119]. Proving that IE-derived antigens can reach the cell surface during a reactivation event leading to the CD8+T-cell removal of the cell before antigens derived from the E-L phases can also reach the cell surface. Thus preferentially expanding the IE-specific CD8+T-cell pool.

Dekhtiarenko et al. showed that the fusion of a Herpes Simplex Virus 1 (HSV-1) peptide-epitope to a MCMV promoter with IE kinetics, lead to the development of a specific CD8+T-cell population with inflationary kinetics. Conversely, the fusion of the same HSV-1 epitope to the M45 promoter expressed with E kinetics, led to the development of a stable CD8+T-cell population.

Overall these studies clearly implicate the expression kinetics of the CMV protein as important in whether an epitope derived from said protein will be inflationary. However, these studies do not explain why several CMV proteins such as M102 encode for CD8+T-cell epitopes displaying both stable and inflationary characteristics within the same open reading frame. Therefore, other factors must ultimately also contribute to the overall ability of an epitope to be inflationary.

2. Peptide-epitope processing and competition for peptide-epitope at the APC level

It would be reasonable to assume that memory-inflated CD8+T-cell pools may have arisen in part due to the availability of mature epitope:MHC complexes on APCs. An important factor that determines the surface concentration of a peptide-epitope in a stable complex with MHC-I is the efficient generation of the mature epitope [120].

The immunoproteasome is a derivative of the classical proteasome whose synthesis in non-haematopoietic cells requires stimulation by IFN-γ inflammatory environments but is expressed constitutively in haematopoietic cells [121]. It has been proposed that stable ($M45_{985-993}$) vs inflationary ($M38_{316-323}$) epitopes are generated by the immunoproteasome vs classical proteasome respectively [122]. The authors hypothesise that once latency has been established, and the inflammatory signals have been removed, only the non-haematopoietic cells expressing the classical proteasome can process epitopes during a viral reactivation event. These can then drive the accumulation of the resulting CD8+T-cell pool. This is important as non-haematopoietic cells are implicated as the cell type responsible for driving memory-inflation during latency [104, 123].

Studies in the murine model have led to the identification that competition between differing CD8+T-cell population's for peptide:MHC-I complexes on the same MCMV-infected cells, influences the overall immunodominance of the CD8+T-cell repertoire. Farrington et al. infected mice with a recombinant MCMV expressing the SIINFEKL peptide (MCMV-GFP-SL8) under the control of the IE2 promoter [124]. Within these mice SIINFEKL-CD8+T-cell responses inflated and WT MCMV-inflation was abolished. However, a co-infection of mice with both WT-MCMV and the MCMV-GFP-SL8 strain allowed the development of inflationary

CD8+T-cell responses specific for both MCMV epitopes and SIINFEKL [124]. The authors hypothesised that the higher avidity of the SIINFEKL peptide within MCMV-GFP-SL8 infected mice led to an increased surface concentration of SIINFEKL:H-2K$^{b}$ complexes over the MCMV:H-2K$^{b}$ complexes. However during co-infection, the WT MCMV vs MCMV-GFP-SL8 strains established distinct loci of infected cells allowing the presentation of MCMV peptides vs SIINFEKL on different APCs. This suggests that sufficient antigen:MHC complexes must be available on infected cells to be presented to the CD8+T-cell response for them to inflate.

3. CD8+T-cell avidity

It has also been proposed that MCMV-specific CD8+T-cell populations with a higher avidity for cognate peptide are preferentially maintained during latency by the host immune response to more effectively control viral reactivation events [125]. In support of this, are numerous studies that document the oligoclonality and increase in avidity of HCMV-specific CD8+T-cell populations with age [126] [87] [127]. Notably, that this high avidity TCR usage is also conserved between several different HCMV positive individuals [128]**.** Inflated HCMV-specific CD8+T-cell populations have been documented as derived from single CD8+T-cell clones undergoing stimulation and expansions within hosts *in vivo* [76] [129]. Importantly, conflicting evidence has been provided where an accumulation of a low affinity CD45RA+ pp65-specific CD8+T-cell population was observed within older adults [130]. Therefore, more research is needed in this area to clarify whether the accumulations of highly avid HCMV-specific CD8+T-cell populations are maintained at the detriment to their lower avid counterparts during latency and whether memory-inflated responses correspond to higher avidity populations.

4. CD8+T-cell co-stimulation

Additional information on the requirements by a CD8+T-cell that will inflate was provided by Arens and colleagues whose data indicated that stable vs. inflationary MCMV-specific memory CD8+T-cell populations require different co-stimulatory signalling with inflated CD8+T-cells not requiring CD28 co-interaction [131]. This implies that the stimulation of

memory-inflated CD8+T-cells vs initial priming of CD8+T-cell responses occur via differing mechanisms. It also fits with the $CD28^-$ phenotype described for inflated CMV CD8+T-cells.

5. Antigen presenting cell type *in vivo*

Evidence is now mounting that despite myeloid cells being the major latency site for HCMV, non-haematopoietic cells are responsible for directly presenting the CMV antigen to CD8+T-cells that ultimately inflate [132]. Torti et al. utilised the $Batf3^{-/-}$ murine model to investigate the role of cross-presenting DCs in the generation of memory-inflation [133]. These mice are unable to develop CD8α+, CD11b- and CD103+ DCs. Mice were infected with MCMV and the M38, M139, IE3 inflationary and M45 stable responses followed over time via flow cytometry. The results demonstrated that within the inflationary responses there are two distinct kinetic patterns; early inflation developing towards the M38 and m139 proteins and a second later inflation developing towards the IE-3 protein. However, the IE-3 inflation after the initial accumulation contracted and was later abolished compared to IE-3 inflationary CD8+T-cells within WT infected mice. This implicates the role of DCs in priming the IE-3 inflation but the M38 and m139 inflationary CD8+T-cell responses initiated via conventional priming.

Corroborating these findings was a second murine study by Torti and others [104]. The authors utilised a mouse model whereby non-haematopoietic cells lacked the expression of $H\text{-}2K^b$ which inflationary M38-specific CD8+T-cells are restricted through. Within the H-2KB deficient mice M38-inflation within the blood and peripheral tissues was lost. During latency, only WT mice demonstrated extensive M38 CD8+T-cell proliferation and this was within the lymph nodes where they presented with a $T_{CM}$ phenotype and M38-specific CD8+T-cells within the blood demonstrated low proliferation rates. They subsequently demonstrated that the dependence of memory-inflation on non-haematopoietic antigen presentation was a general phenomenon of MCMV inflationary CD8+T-cell populations towards IE-3 and m139. By utilising mice lacking $\beta_2$-microglobulin ($\beta_2M$) expression, except on DCs in the thymus, they demonstrated that IE-3 and m39 inflation was abrogated. This DC-restricted CD8+T-cell priming had little effect on typical M45 stable CD8+T-cell kinetics i.e. same percentage of

M45-CD8+T-cells within the periphery over time. This implicates DC cross priming as sufficient in initial CD8+Tcell generation and maintenance of stable CD8+T-cells but insufficient for the generation of memory-inflation. The same study also quantified MCMV genomes within splenic and lung non-haematopoietic vs haematopoietic cells during the time course of an MCMV infection. Larger quantities of the MCMV genome were present within the non-haematopoietic population until 28 days post infection. MCMV DNA decreased within the haematopoietic population from day 7 p.i to non-detectable levels 28 days p.i. This study speculates that during lytic replication MCMV is present within both cell types to prime initial CMV-specific CD8+T-cell responses but as latency is established only non-haematopoietic cells contain MCMV genomes to present during reactivation events.

Torti et al subsequently proposed a model for memory-inflation generation. LN-residing $T_{CM}$ M38-specific populations, when restimulated by non-haematopoietic cells during reactivation events, proliferate extensively and serve to replenish the peripheral $T_{EMRA}$ pool during MCMV reactivation.

Corroborating these findings, Redeker and colleagues quantified the levels of the MCMV genome in non vs. haematopoietic splenic cells and found that early during infection the genome is present in equal abundance in both cells types. As infection progresses the genome is predominantly situated within the non-haematopoietic population [3]. These studies therefore provide compelling evidence for the role of non-haematopoietic cells in driving memory-inflation via the presentation of CMV antigens during a CMV reactivation event.

Lastly, a second model for memory-inflation has been suggested that is dependent on CMV-specific CD8+T-cell exposure to antigen presented by non-haematopoietic cells such as endothelial cells with access to the blood supply [123]. Smith et al. demonstrated the stimulation of inflationary CD8+T-cells within LNs was dispensable for the maintenance of inflation after blocking CD8+T-cell regress from the LN. After treatment of mice with FTY720, the numbers of inflationary CD8+T-cells within the blood reduced little and retained the same

chronic stimulated phenotype. The M38-specific inflationary CD8+T-cells within mice that had migrated to peripheral tissues e.g. lungs and liver were present within areas that were accessible to the systemic circulation. Additionally, that the M38-specific inflationary CD8+T-cells residing within the spleen of FTY720 treated MCMV infected mice were associated with the red pulp and therefore in direct association with the blood supply.

6. Initial viral dose

Within healthy human donors, the magnitude of HCMV-specific responses documented varies between 0.1-5% for young donors and >10-40% within elderly donors [57, 58, 76, 77, 87]. Recently, Redeker et al. addressed the underlying mechanisms that may explain the variation in magnitude of the HCMV-specific CD8+T-cell responses [3]. Their initial hypothesis was based upon the assumption that the tissue initially infected by HCMV in any one person will have varying quantities of HCMV particle. It stated that the primary viral load a naïve individual receives impacts upon the magnitude of memory-inflation. Additionally the authors demonstrate that murine inflationary epitopes after a low dose inoculum elicit CD8+T-cell responses displaying stable $T_{CM}$ epitope kinetics and memory-inflation is absent. This was in comparison to high doses that elicited inflationary CD8+T-cells with $T_{EM}$ phenotypes. Thus, this study implicates an association between an increase in the initial viral loads and the development of $T_{EMRA}$ memory-inflated CD8+T-cell populations. This suggests that the size of the latently infected non-haematopoietic cell pool that is established during a primary HCMV lytic infection is a critical factor in generating CD8+T-cell memory-inflation. This may be by increasing the frequency of reactivation events and ultimately CD8+T-cell priming.

Taken together, there are two proposed scenarios for the maintenance of memory-inflation within the murine model (Fig-4). The first states that latently infected non-haematopoietic cells within secondary lymphoid organs, chronically present viral antigens directly to LN-residing CMV-specific $T_{CM}$ cells. These $T_{CM}$ are then able to differentiate into $T_{EM}$ cells and enter the periphery whereby they deal with the viral reactivation. The $T_{EM}$ cells do not

proliferate, accumulate systemically after viral reactivation clearance and eventually differentiate into $T_{EMRA}$ after lifelong chronic antigen encounter. The second scenario depicted by Smith et al. proposes that sources of antigen stimulation for inflationary CD8+T-cells are provided by the presentation of viral antigen by latently infected non-haematopoietic cells within both peripheral tissues and secondary lymphoid organs that have direct access to the blood supply e.g. red pulp of the spleen. These CD8+T-cells then patrol the periphery and peripheral tissues to control viral reactivation events. However, the common consensus within the literature is that it is non-haematopoietic cells that restimulate the inflationary CMV-specific CD8+T-cell population. Finally, haematopoietic cross-presentation is hypothesised as responsible for the initial priming and expansion of CMV-specific CD8+T-cells but non-haematopoietic presentation is required for accumulation/inflation [104, 118].

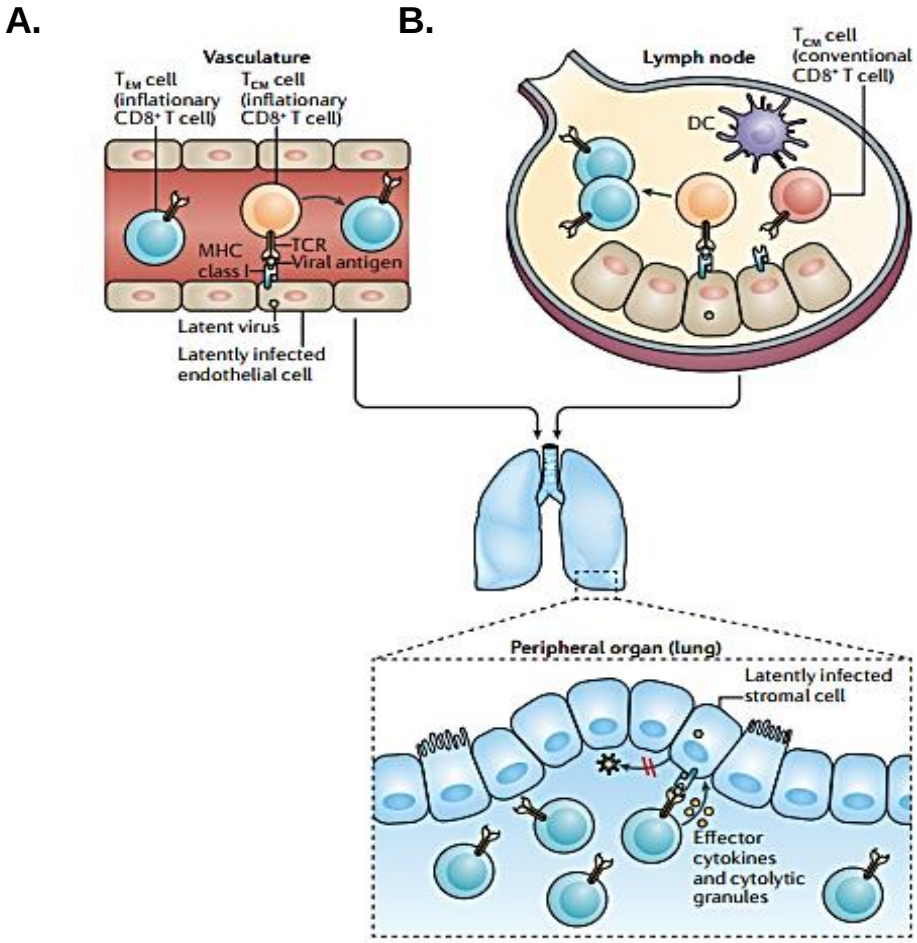


***Fig 4 - Models for the maintenance of HCMV memory-inflation by chronic antigen stimulation within the periphery or LN [93]. Permission to reuse within this thesis obtained from Nature Immunology. Licence number 3881380517852.*** During a reactivation event, CMV antigen, likely IE and E antigen derived, is presented by non-haematopoietic, cells either A) with access to the blood supply as hypothesised by Smith et al [123], or B) within the LN as hypothesised by Torti et al. [104]. This drives the differentiation of CMV-specific $T_{CM}$ to inflationary $T_{EM}$ and $T_{EMRA}$ with high cytotoxic effector functions. These inflationary $T_{EM}$ and $T_{EMRA}$ cells then migrate to and 'patrol' the periphery and peripheral tissues e.g. the lungs to exert their cytotoxic anti-viral effects and control reactivation events.

## 1.8 HCMV immune evasion

Despite the large CD8+ T response directed towards HCMV, the virus is able to avoid elimination and establish a lifelong latent infection characterised by sporadic reactivations [9]. This successful evasion is mainly attributed to the subversion of CD8+T-cell recognition of HCMV-infected cells. HCMV encodes an impressive array of immunomodulatory genes whose temporal expression i.e. infection phase dependent expression, interferes with the MHC-I antigen presentation pathway in multistep cascade [80] [48, 95]. The region of the viral genome best studied for MHC-I immune evasion is US2 through US11 (Table-1) (Fig-5). Louis Picker et al. demonstrated, within the context of the Rhesus model, that the US immunomodulatory genes are critical for superinfection of CMV to occur within a seropositive host by enabling evasion of the cytotoxic CD8+T-cell response [134].

The most extensively studied of the US gene encoded proteins are the US2 and US11 gene products that are expressed with E kinetics and function to redirect newly synthesised MHC-I molecules from the ER lumen to the cytoplasm. The US2/11 genes then trigger the proteasomal degradation of the MHC-I molecules [81]. The US2 protein binds to the MHC-I and utilises the Sec61 membrane complex to direct them to the cytosol [135]. The US11 protein is a type 1 membrane protein that transports the MHC-I to the cytosol where they are de-glycosylated by N-glycosylase before proteasomal degradation [136]. These proteins therefore hijack the host machinery that relocates misfolded host proteins or those requiring turnover, for degradation [135]. This MHC-I targeting has been shown to be of both a locus [137, 138] and allele specific manner [139] [140]. For example, both the US2 and US11 protein targets HLA-A/B alleles but HLA-C/G-alleles are resistant [137, 141] and that in particular, HLA-Cw*0702 alleles are less targeted by the US2 and US11 proteins [139, 140]. Importantly, US2 and US11 were shown by Hesse et al. to exert the largest effects on the reduction of MHC-I on the infected cell surface [142].

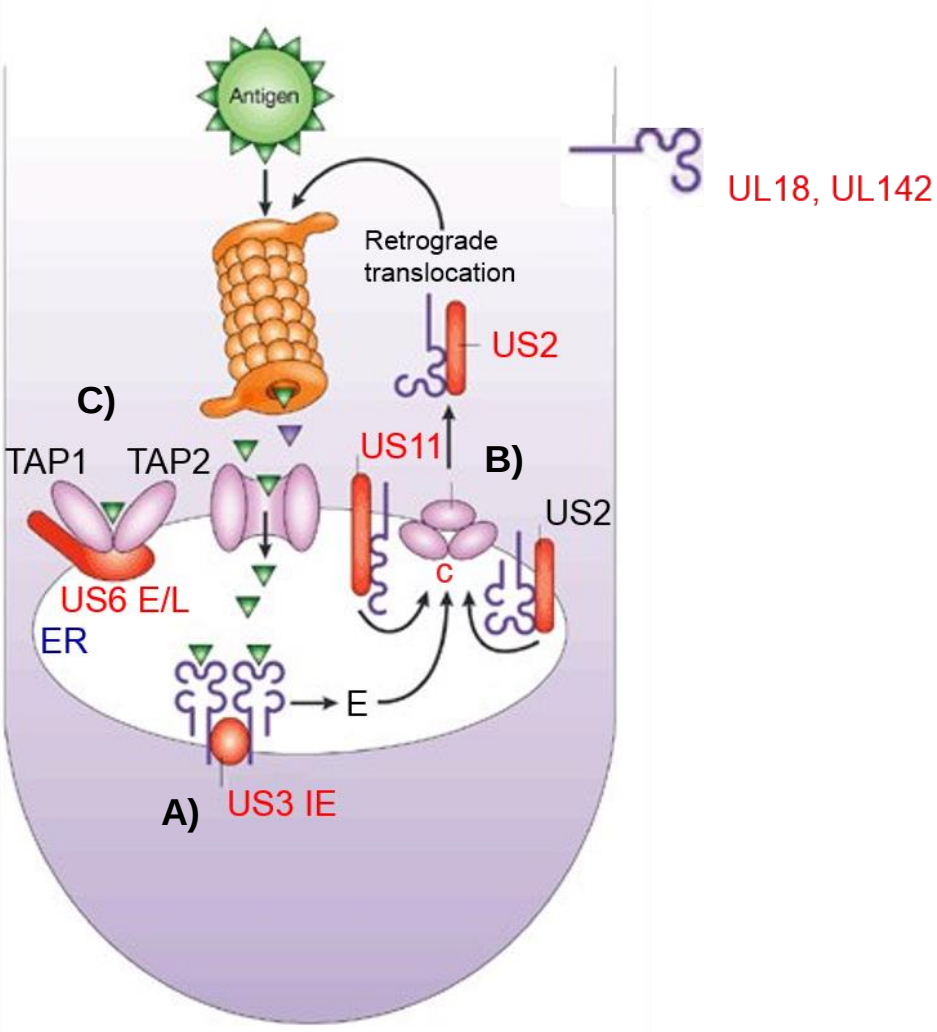


***Fig 5 – Modes of action of the human cytomegalovirus US2-11 immunevasin proteins [9].*** Permission to reuse content in this thesis obtained from Nature Immunology – Licence number 3882640385345. A) The US3 protein is expressed with IE kinetics. Its luminal domain functions to retain MHC-I molecules within the ER. B) The US2 and US11 proteins are expressed with E kinetics and facilitate the retrograde translocation of newly formed MHC-I molecules from the ER lumen to the cytosol via a 'translocon' pore complex consisting of Sec61 and TRAM [135]. Once in the cytosol they trigger the rapid degradation of the MHC-I molecules by the proteasome. The US11 protein remains in the ER whilst the US2 protein translocates with the bound MHC-I molecule to the cytosol. C) The US6 protein is expressed with E/L kinetics and prevents the formation of mature peptide:MHC-I complexes via preventing peptide translocation from the cytosol to the ER lumen by blocking the TAP transporter preventing ATP binding required for peptide translocation [143]. Overview of the US proteins is provided in Table-1.

Despite being expressed with IE kinetics (1-4 hours into infection), the US3 gene product has been reported to exert a minor overall effect on the total MHC-I surface down-regulation during an infection [142]. Ameres et al have demonstrated that this immunevasin is preferentially unable to target two HLA alleles; HLA-A3 and HLA-Cw*0702 ([140]. Both of whom are ligands for NK cell inhibitory receptors. US3 also functions to retain MHC-I within the ER by interacting with the tapasin chaperone to hold the MHC:US3 complex within the ER lumen. Additionally, the US3 protein interferes with MHC-II antigen presentation by blocking the invariant chain from associating with immature MHC-II [144].

US6 plays an important role in subverting MHC-I antigen presentation during the E/L phase of HCMV infection. US6 binds to the ER luminal domain of TAP1 preventing the translocation of peptide from the cytosol to the ER lumen. A TAP1 conformational change then results in the loss of ATP binding and mode of action [143, 145].

Last of the US2-11 gene products, the US10 protein can specifically target non-classical HLA-G alleles from an infected cell surface by targeting them for proteasomal destruction within the ER [146].

The pp65 and IE-1 proteins also play important roles in the evasion of CTL recognition (Table-1). The HCMV tegument proteins are recognised to have a dual role in the viral life cycle; fusion/entry into the host cell and modulation of the host immune response to incoming virus particles [147, 148]. The tegument phosphoprotein pp65, has been shown to prevent peptide-generation from the IE-1 viral transactivator [147-149] and therefore reduce the initial CD8+T-cell response to the virus. In addition to transactivating the viral genome, IE-1 has been identified as interfering with the IFN signalling pathway [150]. Huh and colleagues demonstrate the binding of IE-1 to the STAT2 protein enhances virus growth and prevents transcription of the IFN-β promoter via NF-κB. [151, 152]. Move or delete

***Table 1 – Immunevasion genes of HCMV and the MHC-I evasion functions of their encoded proteins***

| **Protein** | **Infection Phase** | **Immunomodulatory function** | **Reference** |
|---|---|---|---|
| US2 | E | Relocates MHC-I from the ER to the cytoplasm for degradation via the proteasome | [153] |
| US3 | IE | Retains MHC-I within the ER lumen | [154] |
| US6 | L | Prevents peptide translocation into the ER lumen via TAP | [145] |
| US11 | E | Relocates MHC-I from the ER to the cytoplasm for degradation via the proteasome | [136] |
| US10 | E | Delays MHC-I egress from the ER lumen, in particular HLA-G alleles | [155] |
| UL16 | E/L | Binds NK activating receptor ligands ULBPs | [156, 157] |
| UL18 | - | MHC-I homolog/NK evasion | [158] |
| UL40 | E | Up regulates cell surface expression of HLA-E molecules | [159] |
| pp65 | E and L | Prevents the generation of IE-1 antigenic peptides via IE-1 phosphorylation | [149] |
| gpUL142 | E | MHC-I homologue | [160] |

However, this viral-mediated MHC-I down-regulation poses a problem by reducing the inhibitory interaction of MHC-I to the inhibitory receptors present on NK-cells. Thus this may activate NK-cells via the 'Missing Self Hypothesis'. This hypothesis is based upon NK-cell activation being highly regulated via signals from both activating e.g. NKG2D and inhibitory receptors e.g. 'Killer Immunoglobulin Receptors' (KIRs) engaging their ligands on target cells [161]. Inhibitory receptors discriminate between infected and healthy host cells by the presence of inhibitory ligands such as MHC-I. Cells lacking MHC-I are therefore likely to be malignant or infected by viruses modulating the MHC-I antigen presentation pathway to avoid immune recognition. Equally, activating NK-cell receptors detect malignant or infected cells as their activating ligands are up-regulated by cells as a stress mechanism during

infection e.g. MICA/B [43]. In an effort to subvert this NK activation, CMV encodes for several immunomodulatory mechanisms that target NK-cells. These are carried out by the UL16, UL18, UL40, UL83, UL141 and the UL142 gene products [160].

UL18 is expressed in complex with $\beta_2$ microglobulin ($\beta_2$M) and has been shown to bind to an NK-cell inhibitory receptor at a higher affinity then MHC-I [160, 162], thus acting as an MHC-I homologue [158]. UL40 acts as an HLA-E allele up-regulator so that surface bound HLA-E may bind to the NK inhibitory receptor NKG2A [160]. NKG2D represents the most abundant NK-cell activating receptor whose seven ligands are up-regulated on the surface of cells when they become stressed or infected [163]. The ligands MICA/B have structural homology to the MHC-I molecules consisting of α1/α2 domains - they however do not bind peptides or associate with $\beta_2$M [163].

The HCMV-encoded UL16 protein preferentially targets NKG2D ligands MICA and ULB1/2/6 for down-regulation from the surface via ER retention within infected cells [157]. The gpUL142 protein has recently been discovered to down-regulate the activating ligand MICA [160].

Lastly, the UL40 gene which has interestingly been shown to up regulate MHC-I HLA-E alleles [160] which increases the interaction of UL40 with the NK inhibitory receptor NKG2A. This mechanism of NK evasion has also been reported for HIV infection [164].

Thus these few examples demonstrate the impressive array of both NK-cell and CD8+T-cell evasive mechanisms encoded by HCMV.

## 1.9 – Cross-presentation of CD8+T-cell HCMV antigens

In face of these numerous evasive mechanisms, a diverse CD8+T-cell response to HCMV is still generated; raising questions to how the CD8+T-cells are being primed *in vivo*.

Virus-specific CD8+T-cells become activated by host cells presenting peptide on their surface in the context of MHC-I. These host cells have acquired the antigen via the degradation of protein products from intracellular pathogens. Dendritic cells (DCs) are professional APCs that play an important role in the initiation of CD8+T-cell primary responses towards viral pathogens [165]. DCs present in the peripheral tissues, encounter and uptake Ag, undergo a maturation process when their 'pattern recognition receptors' (PRRs) are engaged. They then migrate to the lymph nodes (LNs) to present the processed antigen to naïve T-cells. [166]. It is currently debated how CD8+T-cell responses can be primed towards viral pathogens who evade the MHC-I antigen presentation pathway such as HCMV or are unable to infect DCs.

HCMV IE antigen-specific CD8+T-cells could be primed before the immunevasion mechanisms of the US gene region products can fully exert their effects. However, this direct priming is unlikely to occur for L antigen-specific CD8+T-cells whose peak expression occurs after the US2-11 proteins have affected the MHC-I pathway. In spite of this, HCMV-specific CD8+T-cell responses towards L antigens are detected ex vivo and are therefore being primed somewhere *in viv*o during WT infection. A phenomenon explaining this is 'Cross-presentation'.

Typically, exogenously acquired antigens are loaded onto MHC-II molecules for CD4+T-cell recognition on DCs, whilst intracellularly derived antigens are loaded onto MHC-I for CD8+T-cell recognition. It has become increasingly clear that DCs can also acquire the ability to uptake exogenous antigen and process these within the MHC-I pathway for presentation to CD8+T-cells. Cross-presentation therefore defines the mechanism by which naïve CD8+T-

cells are stimulated by peptide:MHC-I complexes on the surface of DCs that have acquired the antigen exogenously and processed it through their MHC-I pathway [167]. The DCs can acquire these exogenous antigens via the phagocytosis of apoptotic bodies derived from infected cells.

In the context of CMV, Snyder et al. studied the role of cross-presentation in the generation of CD8+T-cell responses in the murine model [114, 118, 168]. The authors generated a spread-defective MCMV strain deleted for glycoprotein L (gL). As a result the strain was able to undergo productive infection within the host cells it enters initially; however any progeny produced would subsequently lack the gL and be unable to enter any new host cells to initiate another round of infection**.** The ΔgL strain was used to infect mouse embryonic fibroblasts (MEFs) which were lacking expression of MHC-I and as such are unable to directly present MCMV antigen. These infected MEFs were then transferred into BALB/C mice. In the context of this model, MCMV-specific CD8+T-cell responses would only have been generated if the DCs were able to access exogenous MCMV-antigen from lysed MCMV-infected MEFs and present them in their surface MHC-I. The results demonstrated CD8+T-cell responses primed by the ΔgL mutant were almost identical in breadth and magnitude to the CD8+T-cell responses generated by the spread-efficient WT strain. This implicates the role of cross-presentation in the generation of MCMV-specific CD8+T-cell responses.

Several studies now clearly implicate cross-presentation as a major mechanism behind the initial priming of HCMV-specific CD8+T-cell responses and this has now been demonstrated for both the pp65 and IE-1 protein [169-171]. It would therefore be a reasonable argument that cross-presentation is also a key factor in the initial priming to HCMV antigens expressed after the US2-11 immunevasion proteins function in the viral lifecycle. However and importantly, DCs are permissible to CMV infection and direct presentation of CMV antigens acquired intracellularly during an infection by DCs may also play a role in CD8+T-cell

priming. However it has been demonstrated *in vitro* that the concerted action of the MCMV immunevasins can efficiently prevent the CD8+T-cell recognition of infected DCs [172]. If the same efficiency occurs *in vivo*, then it can be assumed that the majority of presentation to CMV-specific CD8+T-cells by DCs is likely by cross presentation.

## 1.10 – Contribution of HCMV to immune senescence within immunocompetent hosts

With regards to clinical importance, HCMV is now well established in causing severe mortality within immunocompromised patients due to uncontrolled viral replication resulting in organ damage.

Conversely, the implications of HCMV in immunocompetent individuals are now being investigated. The large accumulations of HCMV inflationary CD8+T-cells with age have led to the suggestion that HCMV is involved in the development of immunesenescence, vascular disease and even a reduced life span [173].

It is widely accepted that with age parameters of the host immune response decline and that this deterioration is most distinct within the CD8+T-cell compartment of the adaptive immune response. The main characterising feature of T-cell immune senescence is an increase in CD8+T-cells lacking the surface expression of $CD27^+$/$CD28^+$ molecules, increased $CD57^+$ expression and enhanced pro-inflammatory production [174].

Wikby et al. identified using longitudinal studies over a period of 20 years involving the Swedish HEXA131 (66 year old donors), OCTO (86-92 years of age) and the extended NONA (>90 years) cohorts a link between HCMV infection and early mortality. From these studies they developed a characteristic phenotype that was predictive of an increased risk of mortality known as the ‘Immune Risk Phenotype’ (IRP). They found this phenotype was already present in a HCMV-infected hexagenarians cohort [175-177]. It is not yet known how

representative or relevant the IRP may be to other HCMV-positive populations or ethnicity groups.

Memory-inflation has been linked to the inversion of the CD4+ to CD8+T-cell ratio due to the increase in CMV-specific CD8+T-cells within the total memory T-cell repertoire. Additionally, these inflated responses have been demonstrated as deriving from a few CD8+T-cell clones specific for dominant HCMV epitopes [76]. The oligoclonal expansions within elderly HCMV-positive individuals are hypothesised to dominate the CD8+T-cell repertoire and restrict the immunological space required for the development of primary immune responses.

Currently, a distinction remains to be made between the total effects of the large HCMV-specific T-cell responses and the effects of natural aging itself on the immune system. For example, it is as yet undetermined whether a decrease in the total naïve CD8+ T- cell pool in the elderly is directly associated with the expansion of the large HCMV-specific CD8+T-cell responses [6].

Despite initially being thought exhausted, inflated CMV-specific CD8+T-cell responses, in both the human and mouse model, have been established as polyfunctional (IFN-$\gamma^{+}$TNF-$\alpha^{+}$IL-2$^{+}$CD107a$^{+}$) in response to antigen [110, 178, 179]. Furthermore these CD8+T-cell responses remain cytotoxic producing both granzymeB and perforin [2]. Most importantly, that the CMV-specific CD8+T-cells retain this functionality with age [110, 180]. Overall the CMV-specific CD8+T-cell populations within the periphery have as such been speculated to influence the total inflammatory environment within the vasculature due to their high pro-inflammatory cytokine production (IFN-$\gamma^{+}$TNF-$\alpha^{+}$) [2]. Due to the unique expression of CX3CR1 on HCMV-specific CD8+T-cells, these polyfunctional CD8+T-cells have been demonstrated to migrate towards infected endothelium releasing their potent inflammatory cytokines causing endothelial damage *in vitro* [2]. CMV-specific CD8+T-cells could therefore induce cytolysis of infected endothelium during reactivation events causing direct

vasculature damage *in vivo* [2, 181]. As such, HCMV infection has been linked to reducing the life span of elderly individuals by up to 4 years due to cardiovascular disease, although the mechanisms are currently unclear [173].

## 1.11 - HCMV CD8+T-cell adoptive immunotherapy for the treatment of overt CMV disease

In both the HSCT and SOT setting, HCMV reactivation is a major cause of morbidity and mortality. Currently drugs are available for the treatment of CMV disease such as Acyclovir, Valacyclovir, Foscarnet, Ganciclovir and Valgancyclovir (review [182]). However the toxic side effects limits their use [182, 183] and it is currently debated whether to utilise these drugs in a prophylactic or therapeutic setting. Importantly, studies have linked the use of these drugs prophylactically as delaying the onset of CMV mediated disease to late time-points post-transplant and also enhancing the emergence of drug resistant CMV strains [184, 185]. Clinical studies are now focused on harnessing the CMV-specific CD8+T-cell response to control CMV reactivation in the post-transplant setting. The isolation of HCMV-specific CD8+T-cells from patients, expansion *ex vivo* and retransfer into the patients is known as ‘adoptive immunotherapy’.

Several preclinical murine models provided promising results in treating MCMV disease by the adoptive transfer of CD8+T-cells [186, 187] review [188]. An interesting finding from these studies was although all specificities transferred resulted in protection, those directed towards the murine IE-1/m123 were highly protective over others in preventing MCMV disease [187]. CMV-specific adoptive immunotherapy in HSCT transplant patients was first pioneered by Riddell at al. and Walter et al. who demonstrated the successful reconstitution of the CMV-specific CD8+T-cell immunity and safety of the approach [64, 189]. Several human clinical trials have since further demonstrated the safety of the methodology and effective antiviral activity [190-194].

Unfortunately, adoptive immunotherapy for CMV disease also has its limitations and is not common practice within the clinic. Problems arise if a donor is CMV seronegative or has low frequencies of circulating CMV-specific CD8+T-cells. Clearly in this situation pre-existing immunity is absent or CMV-specific CD8+T-cells difficult to isolate for expansion *in vitro*. The recent developments in the methodology for the TCR profiling from a single CD8+T-cell clone, has allowed for the transfer of previously established HCMV-specific CD8+ TCRs onto endogenous CD8+T-cells isolated from seronegative HSCT patients. This therefore allows for the generation of a HCMV-specific CD8+T-cell repertoire in a negative donor potentially undergoing primary infection. The efficacy of this method been demonstrated *in vitro* [195, 196] and within the murine model [8]. Currently, Phase I and II clinical trials are underway.

## 1.12 – Viral vaccine vectors

The fact that HCMV induces large $T_{EMRA}$ responses that persist for life, maintain their anti-viral functions and locate to peripheral tissues has facilitated research in using CMV as a vaccine vector. Both MCMV and HCMV are now being investigated for use as vectors to stimulate large CD8+T-cell population's specific for antigens derived from either infectious agents or malignancies.

Viral vectors represent gene delivery systems expressing genes of interest *in situ*. The advances in the field of molecular virology have established mechanisms for the genetic manipulation of viral genomes for vaccine development. Many infectious diseases have now been brought under successful control via the use of viral-based vaccines for example, polio, measles, smallpox and yellow fever. However many human viral pathogens remain a huge challenge for vaccination for instance, HIV and hepatitis C virus (HCV) due to their large genetic diversity and immune evasion mechanisms [197].

The use of viruses as a therapy delivery system raises several difficulties and ethical issues [198]. Firstly, one of the main concerns is the potential for the vaccine strain to revert to their pathogenic or virulent form followed by the spread to the unvaccinated population. Or additionally the vaccine strain may recombine with endogenous viruses already present in the vaccinated host. Secondly, the virus may render itself no longer antigenic therapeutically to the host immune system by deleting the inserted vaccine gene. In addition to safety issues, the extremely stringent safety procedures, long periods of scientific research and prior safety testing in animal models this makes the licensure for clinical trials within humans difficult.

Despite these difficulties, the natural biology of viruses provide them with advantages over the more common vector delivery systems such as bacteria and DNA. For example, their broad cell tropism, opportunity for genetic manipulation, host persistence and the induction of both humoral and cellular immunity make them ideal candidates as vectors [198]. Finally, viruses have evolved to utilise the host cell transcription machinery to express their own genes and therefore therapeutic or vaccine transgenes inserted into the viral genome.

As well as being used to vaccinate infectious diseases, viruses can be manipulated to express tumour antigen (TA) transgenes and therefore be used as a cancer therapy. Overall, investigations into viral-based cancer vaccines have shown that TA’s are more immunogenic when expressed as a whole transgene within a viral vector rather than within sub-peptide or protein based vaccines [199, 200]. Hence viruses can be genetically manipulated to tackle both infectious disease and malignancies.

## 1.13 – CMV based vaccine vectors developed by the 'Bacterial Artificial Chromosome' reverse genetic system

Research into the full pathogenic potential of CMV has been hampered due to a lack of methodology allowing the analysis of individual CMV protein function. With HCMV encoding for >160 antigenic proteins, the functions of many of these are still currently unknown. The development of the 'Bacterial Artificial Chromosome (BAC) reverse genetic system' represents a quick and reliable protocol introducing mutations within the CMV genome, introduced within *Escherichia coli* (*E. coli*), to define the functions of the mutated HCMV genes. The effects of these introduced mutations on the viral lifecycle are then first observed after infection of eukaryotic cells by analysing the phenotype of the resulting virus e.g. growth kinetics. The role of the protein can therefore be defined in the context of natural infection *in vivo* [201, 202]**.**

Viral BACs consist of a BAC DNA vector contained within the viral genome. A BAC vector contains; ~10Kb of bacterial DNA located on the *E. coli* circular fertility factor F (F-factor), two loxp sites, an origin of replication (for replication within bacterial cells), an antibiotic resistance marker, homologous regions of the viral gene to which the BAC is to be inserted and finally a Cre recombinase gene [201-203]. Once the BAC vector is inserted within the viral genome (via homologous recombination), the viral BAC is transformed into *E. coli* and plaques (or colonies) that have taken up the viral BAC identified via antibiotic resistance. Mutations can then be incorporated into the viral genomes, for example by site-directed mutagenesis facilitating pathogenesis studies. The genetically engineered viral-BAC DNA is then purified from the *E.coli* for transfection into eukaryotic cells and the production of infectious virus. The expression of the Cre recombinase and presence of the loxp sites allow for the exclusion of the BAC DNA from the viral genome when expressed within eukaryotic cells.

Viral BACs have now been widely used for the study of Herpesvirus pathogenesis (Reviewed [202, 204])**.** The first use of a Herpesvirus as an infectious BAC was developed by Messerle et al. utilising MCMV to determine the functions of individual CMV genes after their removal from the CMV genome. Currently, BACs have been developed for each human Herpesvirus excluding HHV-7 [202]. This has since facilitated a new era for their use as viral vaccine vectors via the insertion of foreign sequences by BAC technology [205]. For vaccination purposes, a recombinant CMV containing BAC DNA can then be modified by prokaryotic genetic e.g. homologous recombination, to insert the therapeutic gene of choice using the antibiotic marker to select for bacterial colonies containing the therapeutic gene insert.

The key characteristics of Herpesvirus infections include; lifelong persistence, sporadic reactivations and the induction of a large virus-specific $T_{EM}$ CD8+T-cell response [20] – making this an attractive virus to develop as a vaccine for the treatment of infectious diseases or cancer.

To examine the ability of MCMV to induce CD8+T-cell responses to non-CMV recombinant epitopes, Karer et al. developed recombinant MCMV-based viral vectors expressing either influenza peptide-epitopes or the LCMV glycoprotein using BAC technology [206]. The results demonstrated that CD8+T-cell responses in mice after WT influenza virus infection quickly reached 5% of the CD8+T-cell peripheral pool but contracted to a stable 0.5%. After mice were infected with recombinant MCMV expressing the NP influenza protein, NP-specific CD8+T-cell memory-inflation was observed up to 1.5% of the total CD8+T-cells. Similar results were observed with infection with Vaccinia Virus expressing the LMCV glycoprotein with a stable 0.4% of the total CD8+T-cell pool compared to an inflation reaching 1.3% after infection with recombinant MCMV expressing the glycoprotein.

A replication-competent MCMV-vector encoding an Ebola virus Zaire strain glycoprotein protected vaccinated mice from a lethal dose of the Ebola virus and induced long term

polyfunctional ($IFN^+/TNF^+$) Ebola-specific CD8+T-cell responses [207]. This recombinant-MCMV consisted of the Ebola glycoprotein gene inserted within the MCMV m157 protein and was designated MCMV/ZEBOV-NP. MCMV/ZEBOV-NP induced Ebola-specific CD8+T-cell responses at a mean of 2.88% of the total CD8+T-cell response within the blood of vaccinated mice. Additionally, longitudinal monitoring of the peripheral CD8+T-cell responses within vaccinated mice showed the inflation of the CD8+T-cell responses towards the Ebola glycoprotein from 0.79-3.08%. Thus these two studies indicate that inflationary CD8+T-cell responses can also be generated towards therapeutic genes inserted into a CMV-vector backbone using BAC technology.

Arguably the most successful use of a CMV-BAC was developed by Louis Picker and colleagues involving vectors of RhCMV expressing the Simian immunodeficiency virus (SIV) proteins Gag, Rev, Tat and Nef individually and deleted for the HCMV US2-11 gene homologues [13]. Vaccinated Rhesus monkeys demonstrated firstly, protection from both mucosal and intra-vaginal challenge of a highly pathogenic strain of SIV. Secondly suppression of the virus load to undetectable levels was observed after re-challenge [11] and lastly the elimination of the SIV virus over time within 50% vaccinated Rhesus monkeys [11]. Importantly, the vaccination of RhCMV seropositive monkeys with the RhCMV vectors, still provided protection from lethal SIV challenge demonstrating that the established RhCMV immune response was not detrimental to the vaccine-specific immune responses. Additionally, the authors found that the vaccine-specific CD8+T-cells are primarily directed towards peptides presented in the context of MHC-II rather than MHC-I and that the peptides are not derived from the typical immunodominant proteins of HIV previously described [12]. This implicates that the use of a CMV vector may advantageously allow for the development of CD8+T-cell responses to uniquely encoded peptide-epitopes within the vaccine antigen. Therefore compelling evidence is being presented for the use of cmv-based vectors to vaccinate against infectious diseases.

The potent ability of HCMV to induce large and persistent $T_{EM}$ which are important for epithelial mucosal immunity, the primary site for the majority of malignancies, also makes CMV an attractive platform for the vaccination of malignancies affecting the mucosa. Memory-inflated CD8+T-cell responses induced by the CMV vector towards vaccine TA inserts will theoretically be maintained for life and the acquisition of a $T_{EMRA}$ phenotype will equip the vaccine-specific CD8+T-cells with high cytotoxic potential. Importantly, the ability of CMV to superinfect hosts, the phenomenon whereby CMV is able to infect an established CMV seropositive host, will allow for the vaccination of CMV seropositive patients. As such these CMV vectors could be used for differing malignancies without losing efficacy. This may be achieved by the vaccination of patients with multiple vectors expressing differing TA's. HCMV a promising choice for the development of a vaccine-vector for cancer therapy.

Several laboratories have developed CMV as a vector for a cancer vaccine to target breast cancer, melanoma and prostate cancer [208, 209]. Klyushnenkova et al. developed two recombinant MCMV-based vaccines. The first expressing a MHC-II DR52b restricted peptide derived from the full length human prostate specific antigen (PSA) and the second expressing the full length protein. The authors then assessed the immunogenicity of these vaccines within a transgenic murine model expressing PSA as self-antigen restricted through MHC-II DR52b [209]. The results of these studies identified that both vaccines were able to induce specific CD8+T-cell responses that inflated over time. However, only the epitope-expressing vaccine was efficiently able to induce inflationary PSA specific CD8+T-cells after the mice were challenged with prostate tumour and these mice presented with delayed tumour growth. These results indicate that epitope structure within a CMV-based vaccine vector may determine the success of the tumour therapy.

Recently, Xu et al. developed both a replication competent and a replication-deficient recombinant MCMV-based vaccine vector expressing the TRP2 melanoma tumour antigen [208]. Those mice vaccinated with the replication competent MCMV-TRP2 and then

challenged 7 days later with B16-F10 melanoma cells did not develop malignancies and remained tumour free for >4 months post challenge. Interestingly, the replication deficient vector also induced comparable long term protective responses against tumour challenge– indicating that a live replicating CMV vaccine may not be required for efficacy.

A study by Snyder et al. inferred spread-deficient CMV strains, capable of a single cycle of replication after vaccination, as comparably immunogenic to the WT strain with CD8+T-cell memory-inflation still established [118]. Vaccination against infectious diseases within developing countries is restricted from widespread administration due to cost for booster vaccinations and medical equipment and training. CMV is a promising vaccine vector for these regions as a result of large immune responses generated towards CMV, and therefore the vector antigen, after a single dose. Utilising this advantage of CMV, Tierney et al. further manipulated by BAC technology the recombinant MCMV strain developed by Tsuda et al. termed MCMV/ZEBOV-NP, to instead express the nontoxic fragment C of the tetanus toxoid [210]. Their study demonstrated that the vector induced durable (>13 months) antibody responses after a single dose via the intraperitoneal route (I.P) within mice as measured by serum ELISAs. Additionally, vaccinated mice were protected from a lethal paralysing injection of tetanus toxin. The authors state that the MCMV/TetC vaccine construct therefore conferred an advantage over the current licenced formaldehyde inactivated vaccine which requires multiple doses.

In sum, these studies clearly demonstrate the ability of CMV vectors to induce durable and protective cellular and humoral immune responses to both infectious agents and cancer antigens.

## 1.14 –Cancer Testis Antigens (CTAgs)

The Cancer Testis antigens (CTAgs) are a recently characterised family of tumour associated antigens. CTAgs have restricted expression within healthy normal tissues but increased expression within immune privileged sites, such as the germ cells of the testis, trophoblasts of the placenta and are up-regulated in several malignancies [211, 212]. In health, these genes are expressed within the spermatogonia during proliferation and expression is progressively lost as the cells differentiate [212]. Since the discovery of the first CTAg termed 'Melanoma antigen-1' (MAGE1) in total 70 families of CTAgs and 140 protein members have been identified [213].

CTAgs are potentially promising antigens for the targeted therapy of several cancers due to their restricted expression on healthy tissues [211] and their expression on malignancies linked to poor outcome [214]. CTAgs have as such been the focus of several human clinical trials. This research study will focus on one particular CTAg – the 'New York Esophageal 1' protein.

## 1.15 New York Esophageal (NYESO1) CTAg

NYESO1 is a cytosolic CTAg discovered within a patient with esophageal cancer [215]. Along with a high number of other CTAgs, NYESO1 is positioned on chromosome Xq28 and encodes an mRNA of 180aa. This CTAg has been described as spontaneously inducing NYESO1-specific CD4/CD8+T-cell and antibody immune responses within 50% of patients with NYESO1 expressing malignancies [216] and is therefore thought to be highly immunogenic. The expression of NYESO1 has been detected in several malignancies such as head and neck cancer, melanoma, neuroblastoma and hepatocellular carcinoma [217]. These characteristics have focused the attention of cancer therapeutics on utilising NYESO1 to target multiple malignancies [217].

A few laboratories have utilised NYESO1 within the context of a viral vaccine vector for cancer therapy. Palmowski et al. generated a lentiviral vector expressing an HLA-A2-restricted NYESO1 epitope and tested its immunogenicity within mice [218]. The authors found that the injection of as few as 5 x $10^5$ NYESO1 expressing lentiviruses into the mice tail vein could establish a CD8+T-cell response directed towards NYESO1. The HIV-1 vectors used in the study were deleted for the Gag, Pol, Tat and Nef protein coding regions of HIV-1 and were therefore replication incompetent. However, even replication incompetent lentiviral vectors raise ethical issues such as risks of integration into the germ line.

A second laboratory conducted a Phase 1 clinical trial involving the generation of two viral vaccine vectors consisting of either; a recombinant fowlpox virus NYESO1 (rFNYESO1) expressing construct or a smallpox NYESO1 recombinant virus construct (VV-NYESO1). The immunogenicity and safety of these vaccines was assessed in 33 advanced disease stage patients with various malignancies including melanoma, ovarian, breast and prostate cancer [219]. The study detected NYESO1-specific CD8+T-cell responses in 19 patients after using a prime boost approach – VV-NYESO1 followed by the rFNYESO1. NYESO1-specific T CD8+T-cell clones recognised naturally processed NYESO1 antigen expressed on the surface of tumour cell lines indicating that the vaccines were priming NYESO1-specific CD8+T-cells that would be reactive towards tumours *in vivo*. With these successful results, the group of Jager et al. then performed a Phase II clinical trial with these vectors in 22 ovarian cancer and 25 melanoma patients following the same prime-boost based approach. The study found that NYESO1-specific CD4+ and CD8+T-cell responses correlated with tumour regression. The results implicate that prime/boost regimens combined with NYESO1-expressing viral constructs may induce robust NYESO1-specific CD8+T-cell responses within cancer patients.

Previous studies with NYESO1 vaccines have revealed that the form of the NYESO1 antigen that is administered impacts upon the immune response induced. Peptide vaccination with

NYESO1 induced NYESO1-specific CD8+T-cells that were of low affinity [219]. NYESO1 is known to induce spontaneous cytotoxic immune responses within NYESO1 expressing cancer patients [220]. These spontaneous immune responses were shown to have higher tumour reactivity than responses induced by peptide or full protein NYESO1 vaccines. Compared to peptide vaccination, the expression of the NYESO1 gene within viral vectors has been shown to effectively induce tumour reactive cytotoxic (CTL) CD8+T-cells [219] indicating that the use of viral vectors expressing the full NYESO1 antigen may correlate with long term tumour protection *in vivo.*

# AIMS

**Chapter 3 – Characterisation of the CD8+T-cell response to 'protected' epitopes identified using the RV798 strain of the virus**

This work will focus on the characterisation of CD8+T-cells directed towards HCMV epitopes that were identified utilising the RV798 strain by Stanley Riddell et al (Table-7, Chapter 3)[85]. This is to gain a greater understanding of the global HCMV-specific CD8+T-cell response. It has not been established the role that such HCMV CD8+T-cell responses directed towards these peptide-epitopes would play *in vivo* during a WT HCMV infection. It was hypothesised that they may have a different phenotypic profile to previously described CMV-specific CD8+T-cells characterised in the presence of the US2-11 proteins.

To begin to address the role of such CD8+T-cell responses *in vivo*, this investigation set out to;

1. Assess the magnitude to these protected epitopes between young (<70 years) vs older (>70 years) donors – i.e. do the $CD8^+$ T-cells accumulate with age.
2. Phenotypically characterise the *ex vivo* CD8+T-cell responses to the protected peptide by flow cytometry.
3. Identify whether these CD8+T-cell responses can efficiently kill peptide-loaded and HCMV infected targets *in vitro.*
4. Investigate which cell types infected with the WT (AD169) vs RV798 (ΔUS2-11) strains are able to present cognate antigen to specific CD8+T-cell clones i*n vitro* during infection with strains of the virus containing the WT US2-11 gene region (AD169 and Merlin) or deleted (RV798).
5. Assert whether these peptides can be cross presented to specific CD8+T-cells *in vitro*.

**Chapter 4 - identification and characterisation of HLA-C restricted memory-inflation**

Previous work in our lab observed large immunodominant responses to a peptide derived from the UL28 protein termed 'FRC' (Table-7/8) reaching upto 32% of a single older donors total CD8+T-cell repertoire producing IFN-γ and TNF-α in response to peptide stimulation. These CD8+T-cells increased significantly within the periphery of older donors. This research chapter aims to expand on the knowledge of the HLA-C CD8+T-cell repertoire directed towards HCMV.

In particular we wished to answer the following; is HLA-C memory-inflation restricted to UL28? Is HLA-C memory-inflation a general phenomenon of all HLA-C alleles? And do the expression kinetics of the HCMV peptide play a role in determining whether the peptide will inflate?

To answer these the following will be investigated;

1. Identify additional immunodominant HLA-C restricted HCMV-specific CD8+T-cell epitopes. A range of HLA-C restricted peptide-epitopes will be obtained from the literature in addition to epitopes identified by Stanley Riddell and colleagues (Table-7).
2. Determine the magnitude and frequency of the HLA-C restricted CD8+T-cell populations with the age of our donor cohort.
3. Phenotypically characterise the HLA-C restricted CD8+T-cell responses by flow cytometry
4. Functionally characterise HLA-C specific CD8+T-cell clones generated *in vitro.* In particular functional avidity, proliferation and killing capacity.
5. Investigate which cell types *in vivo* may be driving HLA-C mediated memory-inflation. To do this non vs haematopoietic cells will be infected *in vitro* and assessed for their ability to stimulate HLA-C restricted CD8+T-cell clones.

## Chapter 5 – Investigate the potential of 'memory-inflated' HLA-Cw*0702 for inclusion as an immunotherapy for HCMV mediated disease post-transplant

After further characterising the UL28 'FRC' HLA-Cw*0702-restricted populations (Chapter 4), these CD8+T-cells will be investigated for their potential development as an immunotherapy to treat overt HCMV disease in HSCT patients.

This will be done by;

1. Sequencing the TCR of a HLA-C restricted FRC-specific CD8+T-cell clone generated *in vitro*
2. Retrovirally transducing the TCR onto PBMCs obtained from a buffy coat preparation
3. Investigate the lytic ability of the transduced T-cells in recognising cognate peptide on peptide-loaded targets and HCMV infected target cells *in vitro*

## Chapter 6 - Characterisation of the CD8+T-cell response to 'cryptic' epitopes

In addition to the protected peptide-epitopes, the work by Riddell et al. also identified two cryptic peptide-epitopes that are translated in a non-canonical manner (Table-10). Cryptic CD8+T-cell peptide-epitopes have not, to our knowledge, been described for HCMV. Therefore the protective role of such CD8+T-cell populations is unknown. We aimed to determine how non-conventional peptide-epitopes generated from the HCMV virus will contribute towards the already large anti HCMV CD8+T-cell repertoire in healthy donors and if they could provide a protective role *in vivo*. It was hypothesised that the cryptic-specific CD8+T-cell responses may have a differing phenotype to those previously described for CMV-specific CD8+T-cells as a result of their unconventional generation.

This results section of this PhD investigation therefore aimed to;

1. Determine the frequency and magnitude of *ex vivo* CD8+T-cell responses directed towards the two cryptic peptide-epitopes 'RPW' and 'APD' within healthy individuals.
2. Phenotypically characterise cryptic epitope specific CD8+T-cell responses by flow cytometry.
3. Generate cryptic epitope-specific CD8+T-cell clones *in vitro* and determine whether they are able to recognise and lyse WT (AD169 and Merlin) HCMV infected cells *in vitro*.

## Chapter 7 – Develop a HCMV vaccine vector for the treatment of NYESO1 expressing malignancies

After analysing the ability of HCMV-specific CD8+T-cell populations to inflate and characterising their phenotype, we sought to manipulate the large CD8+T-cell responses induced by CMV towards malignancies. Therefore last in this PhD investigation, we aimed to direct CD8+T-cells towards NYESO1 expressing malignancies using a CMV-based vaccine vector.

To do this a vaccine vector based on a HCMV backbone will be generated to express the CTAg NYESO1 protein utilising BAC technology which will produce the recombinant HCMV-NYESO1 virus.

This will be achieved with the following;

1. In collaboration with Dr Richard Stanton (University of Cardiff) replacing the RL13 gene within a HCMV BAC (pALIIII – generated before this investigation by Dr Richard Stanton [221]) with the NYESO1 gene using recombineering genetics
2. Generating NYESO1-specific CD8+T-cell clones and testing their recognition of NYESO1 of both NYESO1 peptide-loaded target cells and during an *in vitro* infection of fibroblasts with HCMV-NYESO1
3. Test the cytotoxic (killing) ability of the NYESO1-specific CD8+T-cell clones against peptide-loaded and HMCV-NYESO1 infected fibroblasts *in vitro*

This was to give an indication of whether such a vaccine would be immunogenic towards the CD8+T-cell response.

# CHAPTER 2 - MATERIALS AND METHODS

## 2.1 Materials

***Table 2 – Materials used throughout the investigation***

| **Cell culture reagents** | **Company** |
|---|---|
| FCS | Gibco |
| 1X PBS | Dulba |
| 4% Para formaldehyde in PBS | Sigma |
| RPMI 1640 | Sigma |
| DMEM | Sigma |
| Optimem | Sigma |
| Penicillin/Streptamycin (P/S) | Gibco |
| Glutamine (Q) | Gibco |
| Saponin | Sigma |
| MACS Buffer (1X PBS, 0.5% BSA, 2mM EDTA) | In House |
| Fetal Calf Serum (FCS) | BioSera |
| Human Serum (HuS) | TCS |
| Lymphocyte Separation Media | Cedarlane |
| MLA144 cells and supernatant [222] | Cultures maintained in house |
| CFSE | Life technologies |

| | |
|---|---|
| Propidium Iodide | Thermo Fischer Scientific |
| CountBright Absolute Counting Beads | Life Technologies |
| CD4 Microbeads | Miltenyi Biotech |
| SOC media | Invitogen |
| **Culture Media** | **Components** |
| Culture media | RPMI 1640, 10% FCS, 1% P/S |
| T cell media | RPMI 1640, 30% MLA, 10% FCS, 1% HuS, 1% P/S, 50U/ml IL-2 |
| Cloning media | RPMI 1640, 10% FCS, 1% HuS, 1% P/S |
| **HLA class I typing PCR reagents** | **Company** |
| TDMH buffer | In house |
| BioTAQ DNA polymerase | Bioline |
| Ethidium Bromide | Sigma |
| 100bp ladder | Life Technologies |
| **IFN- γ ELISA reagents** | **Company** |
| NUNC maxisorp ELISA plates | Thermo Scientific |
| Anti IFN-γ | Thermo Scientific |
| Streptavidin | Sigma |
| Biotinylated anti Streptavidin | Thermo Scientific |
| TMB peroxidase substrate | Rockland |
| Blocking Buffer – 0.05% TWEEN, 1% BSA, 1X PBS | In House |

| | |
|---|---|
| Wash Buffer – 0.05% TWEEN, 1X PBS | In House |
| **CMV ELISA reagents** | **Company** |
| Carbonate-bicarbonate tablets | Sigma |
| Coating buffer (x1 capsule carbonate-bicarbonate in 25ml dd$H_20$) | In house |
| Dilution buffer (PBS, 0.05% Tween, 1% BSA) | In house |
| IgG conjugate (α-human IgG-HRP) | Southern Biotech |
| **Western blot reagents** | |
| NuPAGE 4-12% Bis-Tris gel | Invitrogen |
| NuPAGE MOPS SDS running buffer 20X | Invitrogen |
| Tropix CDR Star | Applied Biosystems |
| Blocking buffer | Applied Bioscience |
| Lysis buffer - 0.4M sodium 2-mercaptoethanesulfonate (MESNA), 125 mM Tris-HCl pH 6.8, 20% glycerol, 4% SDS, 0.004% bromophenol blue | In House |
| Developer film | Thermo Scientific |
| **Kits** | **Company** |
| Qiagen plasmid mini prep kit | Qiagen |
| Purelink HiPure plasmid maxiprep kit | Invitrogen |
| Endo free plasmid Maxi prep kit | Qiagen |
| SMARTer RACE 5'/3' Kit | Clontech |
| Genelute mammalian DNA miniprep kit | Sigma |

| | |
|---|---|
| RNeasy microRNA kit | Qiagen |
| QIAquick Gel Extraction Kit | Qiagen |
| IOTest® Beta Mark TCR V beta Repertoire Kit | Beckman Coulter |
| Gibson Assembly® Cloning Kit | NEB |
| Naïve CD8+T-cell isolation kit | Stem Cell Tech |
| MS column | Miltenyi Biotech |

***Table 3 – HLA primers used throughout the investigation [223].*** Primers used to type the HLA class I haplotype of HCMV seropositive donors. All primer sequences were obtained from [223].

| **Antigen** | **Forward primer sequence** | **Reverse Primer sequence** |
|---|---|---|
| HLA-A1 | 286F | 431R |
| HLA-A2 | 296F | 302R |
| HLA-A3 | 291F | 299R |
| HLA-A11 | 290F | 167R |
| HLA-B7 | 367R | 394R |
| HLA-B7 | 193F | 221R |
| HLA-B35 | 193F | 223R |
| HLA-B35 | 188F | 237R |
| HLA-B35 | 195F | 213R and 277R |
| HLA-B44 | 202F and 272F | 393R and 285R |
| HLA-B44 | 272F | 276R |
| HLA-B51 | 195F | 212R |
| HLA-B51 | 188F | 212R |
| HLA-B51 | 208F | 216R |
| HLA-B51 | 193F | 216R |
| HLA-Cw7 | 130F | 378R |
| HLA-Cw*0701 | 313F | 184R |
| HLA-Cw*0702, 0703 | 367F | 183R |
| HLA-Cw*0703 | 367F | 238R |
| HLA-Cw*1601 | 368F | 146R |
| HLA-Cw*1602 | 366F | 146R |
| Control forward primer | 210F | |
| Control reverse primer | | 211R |
| **HLA class I typing PCR mastermix (14 reactions)** | | |
| **Component** | **Volume (µL)** | |
| TDMH | 70.9 | |

| | | |
|---|---|---|
| Nuclease free H20 | 70 | |
| Control primer mix | 14 | |
| BIOTAQ DNA polymerase | 0.75 ( 5 units/µl) | |
| DNA | 140ng in 5µl | |
| **Primers for plasmid sequencing** | | |
| **Primer** | **Forward sequence** | **Reverse sequence** |
| M13F | GTAAAACGACGGCCAG | |
| M13R | | CAGGAAACAGCTATGAC |

***Table 4 – Antibodies used throughout the investigation***

| **HCMV peptide stimulation antibody panel;** | | | | |
|---|---|---|---|---|
| **Antigen** | **Fluorchrome** | **Company** | **Volume/100µl** | **Clone** |
| CD3 | Pacific Blue | eBioscence | 0.5µl | OKT3 |
| CD8 | PerCp-Cy5.5 | eBioscience | 2µl | RPA-T8 |
| IFN-γ | FITC | Biolegend | 2µl | 4S.B3 |
| TNF-α | Pe Cy7 | eBioscience | 1µl | MAb11 |
| IL-2 | PE | Biolegend | 10µl | MQ1-17H12 |
| **Viability Dye** | **Fluorchrome** | **Company** | **Volume/100µl** | |
| LIVE/DEAD Fixable Dead Cell Stain | Far Red fluorescent reactive dye | Invitrogen | 1µl of 1:100 dilution | |
| **Conventional phenotyping antibody panel;** | | | | |
| **Antigen** | **Fluorchrome** | **Company** | **Volume/100µl** | **Clone** |
| CD3 | Amcyan | BD Biosciences | 3µl | SK7 |
| CD8 | PerCp-Cy5.5 | eBioscience | 2µl | RPA-T8 |
| TNF-α | Pe | eBioscience | 3µl | MAb11 |
| CCR7 | FITC | R&D | 10µl | 150503 |
| CD27 | APC-Cy7 | eBioscience | 3µl | 0323 |
| CD28 | Pe-Cy7 | Biolegend | 1µl | 28.2 |
| CD45RO | PE-Texas red | Beckman Coulter | 3µl | UCHL1 |

| | | | | |
|---|---|---|---|---|
| CD45RA | AF700 | Biolegend | 0.5µl | H1100 |
| CD57 | APC | Biolegend | 0.5µl | HCD56 |
| **Viability Dye** | **Fluorchrome** | **Company** | **Volume/100µl** | |
| LIVE/DEAD Fixable Dead Cell Stain | Violet fluorescent reactive dye | Invitrogen | 1µl of 1:100 dilution | |
| **Cytotoxic phenotyping antibody panel;** | | | | |
| **Antigen** | **Fluorchrome** | **Company** | **Volume/100µl** | **Clone** |
| CD3 | Amcyan | BD Biosciences | 3µl | SK7 |
| CD8 | APC-Cy7 | Biolegend | 1µl | RPA-T8 |
| TNF-α | Pe | eBioscience | 3µl | MAb11 |
| CX3CR1 | PerCP-Cy5.5 | Biolegend | 5µl | 2A9-1 |
| NKG2D | PE Texas red | BD Horizon | 0.5µl | 1D11 |
| Perforin | Pe Cy7 | eBioscience | 2µl | δG9 |
| GranzymeB | APC | Biolegend | 2µl | GB11 |
| **Viability Dye** | **Fluorchrome** | **Company** | **Volume/100µl** | |
| LIVE/DEAD Fixable Dead Cell Stain | Violet fluorescent reactive dye | Invitrogen | 1µl of 1:100 dilution | |
| **Exhausted phenotyping antibody panel;** | | | | |
| **Antigen** | **Fluorchrome** | **Company** | **Volume/100µl** | **Clone** |
| CD3 | Amcyan | BD Biosciences | 3µl | SK7 |
| CD8 | APC-Cy7 | Biolegend | 1µl | RPA-T8 |

| | | | | |
|---|---|---|---|---|
| TNF-α | PE | eBioscience | 3µl | MAb11 |
| TIM3 | FITC | Biolegend | 5µl | F38-2E2 |
| PD-1 | BV421 | Biolegend | 5µl | EH12.2H7 |
| CD38 | Pe Cy7 | Biolegend | 5µl | HIT2 |
| **Viability Dye** | **Fluorchrome** | **Company** | **Volume/100µl** | |
| LIVE/DEAD Fixable Dead Cell Stain | Violet fluorescent reactive dye | Invitrogen | 1µl of 1:100 dilution | |
| | | | | |

**Table 5 – *HCMV pp65 and IE-1-derived CD8+T-cell peptide-epitopes derived from the pp65 and IE-1 proteins.*** The protein antigen, aa position within the protein antigen, peptide sequence (peptide name is denoted by the first three aa of the sequence), restricting HLA allele and kinetics of expression of the protein antigen are provided.

| CMV Antigen | Location in the Virion [224] | Function [224] | CTL Epitope | HLA Restricting Allele | Kinetics of Expression [225] |
|---|---|---|---|---|---|
| $UL44_{245-253}$ | Tegument | Tegument component, DNA processivity factor | **VTE**HDTLLY | A0101 | E |
| $UL83_{363-373}$ | Tegument | major tegument component, modulation of host cell immune response | **YSE**HPTFTSQY | A0101 | L |
| $UL123_{316-324}$ | IE-1 protein | viral transactivator | **VLE**EETSVML | A02 | IE |
| $UL83_{265-275}$ | Tegument | - | **RPH**ERNGFTVL | B0702 | L |
| $UL83_{417-426}$ | Tegument | - | **TPR**VTGGGAM | B0702 | L |

***Table 6 – DNA (purchased from Life Technologies) and peptides used in the generation of HCMV-NYESO1 and NYESO1-specific CD8+T-cell clones.*** The DNA sequence spanning the NYESO1 protein contained 80bp flanking homology to the HCMV RL13 protein.

| **Antigen** | **DNA name** | **DNA sequence** | **Company** |
|---|---|---|---|
| NYESO1 | NYESO1-RL13 insert for recombination | CAACACATGAAATTAAGTAACATATCTACCATGAAAT<br>ACAGCAAAGATATACTAATGTCTATCCATCCAATAG<br>CGGTACCATGCAGGCCGAGGGCAGAGGCACAGGC<br>GGATCTACTGGGGATGCTGATGGACCTGGCGGCC<br>CTGGCATTCCAGATGGCCCAGGCGGAAATGCTGGC<br>GGACCAGGCGAAGCTGGCGCTACAGGCGGAAGAG<br>GACCTAGAGGCGCTGGCGCCGCTAGAGCTTCTGG<br>ACCTGGGGGAGGCGCTCCTAGAGGACCTCATGGC<br>GGAGCTGCCTCTGGCCTGAATGGCTGCTGTAGATG<br>TGGCGCCAGAGGCCCCGAAAGCCGGCTGCTGGAA<br>TTCTACCTGGCCATGCCCTTCGCCACCCCCATGGA<br>AGCTGAGCTGGCCAGAAGAAGCCTGGCCCAGGAC<br>GCTCCTCCACTGCCTGTGCCAGGCGTGCTGCTGAA<br>AGAATTCACCGTGTCCGGCAACATCCTGACCATCC<br>GGCTGACAGCCGCCGACCACAGACAGCTGCAGCT<br>GAGCATCAGCAGCTGCCTGCAGCAGCTGTCCCTGC<br>TGATGTGGATCACCCAGTGCTTTCTGCCCGTGTTTC<br>TGGCCCAGCCTCCTAGCGGCCAGCGGAGATAATAT<br>GCACATCAATAAAATTTTTTATCTTTAGTCATTAATG<br>TTTGGGTGTGTTTATTCTGAGTTAATCACTTATAAGT<br>CGG | Life Technologies |
| **Antigen** | **HLA-restriction** | **Peptide sequence** | **Company** |
| NYESO1 | HLA-A2 | **SLL**MWITQV | GenScript |

### 2.1.1 Cell lines

Healthy lab donor fibroblasts (HLA-A1$^+$), Human fetal foreskin fibroblasts (HFFF2 purchased from Sigma Aldrich) (HLA-B7$^+$HLA-C$^+$) and MRC5 fibroblasts (HLA-A2$^+$HLA-B7$^+$HLA-Cw*0702$^+$ kindly provided by Dr Richard Stanton, School of Medicine, University of Cardiff or purchased from ATCC) were maintained in DMEM supplemented with 10% fetal calf serum (FCS), 1% penicillin/streptomycin (P/S) and 1% glutamine (Q). Epstein Barr virus (EBV) transformed B lymphoblastoid cell lines (LCLs) were generated *in vitro* by infecting peripheral mononuclear cells (PBMCs) with supernatant containing EBV strain B95.8 for 2 weeks in the presence of 200 ng/mL cyclosporine A. Following this, transformed LCLs were propagated in RPMI supplemented with 10% FCS and 1% P/S.

### 2.1.2 Virus Strains

The AD169 (3 x $10^8$ pfu/ml), RV798 – lacking the US2-11 viral gene region (1 x $10^8$ pfu/ml) and Merlin (RCMVIIII strain, 1 x$10^7$ pfu ml - kindly provided by Prof Gavin Wilkinson) viral strains used in this investigation were stored at -80$^o$C. The viral titre of stocks was determined by plaque assay of HFFF2 fibroblasts. Fibroblasts were infected with dilutions of virus from $10^{-5}$ to $10^{-10}$ for 4 hours followed by overlaying with 0.5% carboxymethylcellulose (CFC), 25% x2 concentrated DMEM and 25ml DMEM supplemented with 10% FCS and 1% P/S. After 2 weeks at 37$^o$C the average number of plaques per well was determined and the viral titre calculated as the average of the last dilution where plaques could still be observed.

### 2.1.3 Study cohort

A total of 55 young and 35 older (categorised as <70 and >70 years respectively) healthy HCMV seropositive healthy subjects were investigated in this study (age, sex and HLA class I genotype - Appendix table 1 and 2). The recruitment of healthy older and younger participants was approved by the Solihull ethics committee study ref 14/WM/1254. Written and informed consent was taken prior to participation.

# 2.2 Methods

## 2.2.1 Preparation of Peripheral blood Mononuclear Cells (PBMC's) from healthy donor blood

PBMCs were isolated from whole blood by density gradient centrifugation. Seropositive blood was collected into 10ml 'BD Heparin Vacutainer Tubes' (BD Biosciences), diluted 1:1 with RPMI and layered onto 15ml of lymphoprep. This was centrifuged at 680xg for 30 minutes at 22$^{o}$C with the brakes off. The lymphocytes were aspirated off the interface between the lymphoprep and plasma/RPMI. The lymphocytes were washed twice with 30ml of RPMI and centrifuged at 840xg for 10 minutes at 22$^{o}$C to remove the excess lymphoprep. Following this cells were counted on a haemocytometer. For cryopreservation, the pellet was resuspended in freezing medium containing 70% RPMI, 20% FCS and 10% DMSO with between 5-10 x $10^6$ cells transferred per cryovial. Cryovials were transferred to a -80$^{o}$C freezer overnight (O/N) within a controlled chilling rate 'Mr Frosty Freezing Container' (Thermo Fisher Scientific) after which they were stored long term in liquid nitrogen.

## 2.2.2 Determination of CMV serostatus

Serum from donors recruited to the investigation was tested by an ELISA for the presence of anti-CMV IgG to determine the donors CMV serostatus. Mock and HCMV lysate generated from infected fibroblasts, used as the negative and positive fractions for the IgG in serum samples to bind to, were generated prior to the start of this investigation by Miss Jusnara Begum and Dr Annette Pachnio.

- Day 1

Both mock and CMV lysate were diluted at 1/4000 in coating buffer (Table-2) and 50µl of each dilution added per well in triplicate of a NUNC MAXISORP ELISA plate (Table-2). The plate was left O/N at 4$^{o}$C.

- Day 2

The ELISA plate was washed three times in 200µl wash buffer (Table-2). A standard curve was generated by a ½ dilution series in dilution buffer from 1:0.244 to 1:1000. The serum samples were diluted 1/60 in dilution buffer and 10µl added to wells on the washed ELISA plate containing 90µl dilution buffer (final dilution of the serum samples = 1/600). The plate was incubated for 1 hour at room temperature (RT). Following incubation, the plate was washed a further three times and 100µl per well of a 1:8000 dilution of the IgG conjugate (Table-2) in dilution buffer added. The plate was left to incubate for 1 hour at RT then washed a further three times. The addition of 100µl TMB substrate (Table-2) for 15 minutes at RT was followed by the addition of 100µl 1M HCL to stop the colour reaction. Lastly, the absorbance of the plate was read at 450nm and results calculated in Graphpad prism 6. Donors with CMV titres above 10 were considered CMV positive.

### 2.2.3 HLA class I typing of seropositive donor PBMCs

DNA was extracted from donor PBMCs using the 'GenElute mammalian DNA miniprep kit' according to the manufacturer's guidelines (Table-2). The primers used for the specific HLA Class I alleles and the concentrations used are provided in Table-3 [223]. The reactions were conducted in a total of 13µL (Table-3) and all sequences of the primers used can be found in [223]. Reactions were run with the following PCR programme;

- an initial denaturing step of 96$^{o}$C for 1 minute,
- 5 cycles of; 96$^{o}$C for 25 seconds, 70$^{o}$C for 4 seconds and 72$^{o}$C for 45 seconds,
- 21 cycles of; 96$^{o}$C for 25 seconds, 65$^{o}$C for 50 seconds and 72$^{o}$C for 45 seconds
- 4 cycles of; 96$^{o}$C for 25 seconds, 55$^{o}$C for 60 seconds and 72$^{o}$C for 120 seconds.

Products of the PCR reaction were then run on a 1% agarose gel (Ethidium Bromide 1µL/20mL of agarose, Table-2) by electrophoresis for 60 minutes. PCR bands were visualised by UV light.

### 2.2.4 Stimulation of PBMCs with HCMV-derived peptides

To assess HCMV-specific CD8+T-cell responses, PBMCs were stimulated with HCMV peptide. PBMCs were thawed in culture medium and counted. 1 x $10^6$ cells per stimulation were used in a total volume of 500µl culture medium in FACS tubes. Relevant peptide was added to the tubes at a final concentration of 1µg/ml. 'Staphylococcus enterotoxin B' (SEB) served as a positive control (final concentration 0.2mg/ml) and one tube was left unstimulated (negative control). 0.5µl of Brefeldin A (BfA) was added to all tubes to block cytokine secretion to allow their measurement by flow cytometry (section 2.2.5). The tubes were incubated at 37ºC, +5% $CO_2$ for 6 hours before staining for surface antibodies (section 2.2.5).

### 2.2.5 Intracellular cytokine staining (ICS)

Following 6 hours peptide stimulation, activated CD8+T-cells were detected by ICS. PBMCs were washed once in PBS and centrifuged at 840xg at 10ºC for 5 minutes – all subsequent wash steps were conducted with these conditions. The supernatant was removed and PBMCs were stained with antibodies in 100µl PBS. First, 1µl of viability dye (Table-4) was added to the tubes and left to incubate for 15 minutes RT in the dark before one wash in PBS and one wash in MACS buffer. After the addition of surface antibodies, the tubes were left to incubate for 15 minutes at 4ºC in the dark after which they were washed once in MACS buffer. To fix the cells, 100µl of 4% PFA was added and cells incubated for 15 minutes at RT in the dark. The PFA was washed off once with MACS buffer and cells were permebilised by the addition of 100µl of 0.5% saponin. After 5 minutes, the intracellular antibodies were added to the tubes and left to incubate for 30 minutes at RT in the dark. A final wash step after incubation was conducted in MACS buffer and the cells analysed on the LSR II (BD Biosciences). A minimum of 100 000 events was acquired per sample tube and 50 000 events for control tubes. Unless indicated, all LSR II data was analysed in Kaluza 1.3 software (Beckman Coulter).

### 2.2.6 TCR Vβ staining

To determine the oligoclonality of the HCMV-specific CD8+T-cell responses, PBMCs of seropositive donors were stained to determine TCR Vβ usage with a flow cytometry repertoire kit from Beckman Coulter (Table-2) following 6 hours peptide stimulation (1µg/ml final concentration) at 37ºC. Cells were surface stained at 4ºC with CD8 PerCP-Cy5.5 (eBiosciences), CD3 PB (eBiosciences) and the TCR Vβ repertoire kit according to the manufacturers guide and APC LIVE/DEAD Fixable dye for 15 minutes. Cells were then washed once in PBS (540xg rpm, 5 minutes). Cells were stained intracellularly for TNF-α, as described in 2.2.5, to identify activated HCMV-specific CD8+T-cells. Cells were then acquired on the LSR II with a minimum of 100 000 live events recorded.

### 2.2.7. CD8+T-cell cloning

To isolate CD8+T-cells specific for the HCMV peptides used in this study, PBMCs of donors with identified CD8+T-cell populations to the HCMV peptide were subjected to peptide stimulation followed by an IFN-γ secretion assay (Miltenyi Biotech) and a limiting dilution.

#### 2.2.7.1 IFN-γ capture assay

PBMCs were CD4 depleted using microbeads as per the manufacturers guide (Table-2) and stimulated with the relevant peptide (final concentration 1µg/ml) for 3 hours to induce the activation and IFN-γ production of specific CD8+T-cells. These were enriched for by IFN-γ-capture for limiting dilution cloning.

i) IFN-γ catch reagent labelling

After the 3 hour stimulation, cells were washed three times in RPMI culture medium (10% FCS, 1% P/S). The supernatant was completely removed and the pellet resupsended in 70µl of cold MACS buffer and 30µl of catch reagent added per $10^7$ PBMCs. These were then incubated on ice for 5 minutes.

ii) Secretion of IFN-γ

10ml of warm RPMI culture media (10% FCS and P/S) was added to the cells which were incubated at 37$^{o}$C on a rotator for 45 minutes to allow the binding of secreted IFN-γ to the catch reagent on the cell surface.

iii) Detection of IFN-γ

Cells were washed with 15ml cold MACS buffer and centrifuged at 840xg for 10 minutes at 4$^{o}$C. The cell pellet was resuspended in 70µl MACS buffer and 30µl per $10^7$ PBMCs of PE conjugated IFN-γ detection antibody added. The cells were then incubated at 4$^{o}$C for 10 minutes in the dark.

iv) Magnetic labelling

Cells were washed in MACS buffer at 840xg for 10 minutes at 4$^{o}$C and the pellet resuspended in 120µl MACS buffer and 30µl per $10^7$ of anti-PE microbeads added followed by incubation for 20 minutes at 4$^{o}$C in the dark.

v) Magnetic separation

Unbound anti-PE microbeads were washed off in MACS buffer at 840xg for 10 minutes at 4$^{o}$C. The pellet containing the magnetic labelled cells was resuspended in 500µl cold MACS buffer, applied to an MS column (Miltenyi Biotech Table-2) and collected in a fresh FACS tube. The number of specific CD8+T-cells obtained were counted on a haemocytometer.

**2.2.7.2 Limiting Dilution Cloning**

PBMCs isolated from Buffy preparations were Phytohaemagglutinin (PHA) treated (final concentration 10µg/ml) for 1 hour before irradiation with 4000 rads – these served as a cytokine feeder layer in the cloning procedure to support the survival and proliferation of the specific CD8+T-cells. HLA-class I matched LCLs were peptide-pulsed (1 µg/ml final concentration) for 1 hour at 37$^{o}$C before also being irradiated with 4000 rads to prevent proliferation – these served as APCs. The Buffy's/LCLS were washed three times in RPMI

culture medium. For the limiting dilution cloning, 10 plates (96 –well round bottom) with 0.3 T-cells/well and 10 plates with 3 T-cells/well for each specificity were subsequently prepared. Per 10 cloning plates, 100ml of cloning mixture (Table-2) consisted of; 100 x $10^6$ Buffy cells, 10 x $10^6$ LCLs, CD8+T-cells at a total of 0.3 or 3 T cells/well. 100µl/well of this preparation was plated out on day 1. The limiting dilution cultures were supplemented on day 3 with 100µl/well T-cell media (60% MLA Table-2), and left at 37$^o$C for 14 days.

**2.2.7.3 Assessment of peptide specificity by IFN-γ ELISA**

14 days after cloning, expanded wells were tested for HCMV peptide specificity. For this, 50µl of the CD8+T-cells was taken from the expanded wells and co-cultured with 1 x $10^4$ peptide-pulsed or DMSO-pulsed autologous LCL in duplicate at 37$^o$C O/N.

ELISA plates were coated overnight (O/N) with anti IFN-γ (50µl per well of a 1µg/ml dilution,, Thermo Scientific Table-2). The following day, ELISA plates were blocked for 1 hour in 150µl/well of blocking buffer (Table-2) at RT. Plates were washed three times in wash buffer (Table-2) and 50µl supernatant from the overnight co-cultures was added to the relevant wells. The IFN-γ standard (20000 to 0 IFN-γ pg/ml) was also added to the plates at this point in duplicate. The plates were left to incubate for 2 hours at RT and after incubation washed six times in wash buffer. A second biotinylated antibody that binds IFN-γ was then added to the wells with 50µl per well of a 0.25µg/ml dilution and left to incubate for 1 hour at RT. After incubation, plates were washed six times in wash buffer and 50µl/well of a 5µg/ml dilution of streptavidin added (1:1000 in wash buffer, stock 5mg/ml) for 30 minutes at RT. The excess streptavidin was washed off and 50µl TMB peroxidase substrate (Table-2) added and the colour reaction allowed to develop for up to 30 minutes. The reaction was then stopped by the addition of 1M hydrochloric acid and the plate absorbance was measured at 450nm.

Specific clones were transferred to and propagated on 24 well plates for further use in *in vitro* assays and cryopreservation. The clones were maintained in 2ml T-cell media (Table-

2) with the addition of 1 x $10^6$ PHA treated, irradiated Buffy cells and 1 x $10^5$ peptide-pulsed, irradiated LCLs every 14 days.

### 2.2.8 CFSE proliferation assays

PBMCs were stained with 1μM 'Carboxyfluorescein succinimidyl ester' (CFSE) (Life Technologies) in 100μL PBS for 10 minutes at 37°C before quenching the excess dye for 10 minutes at 4°C in RPMI media (10% FCS, 1% P/S). 1 x $10^5$ CFSE labelled PBMCs were co-cultured for 7 days at 37°C with 2.5 x $10^4$ γ-irradiated LCLs, which had been peptide-pulsed for 1 hour at 37°C prior to co-culture, on a 96 well plate. Non peptide-pulsed LCLs and SEB-stimulated PBMCs were included as a negative and positive control. After 7 days, PBMCs were surface stained with CD3-pacific blue (eBioscience) and CD8-PerCP-Cy5.5 (eBioscience) for 15 minutes at 4°C and the number of $CFSE^{low}$ events recorded on the LSR II (BD Biosciences). For HCMV-specific CD8+T-cell clones, the same protocol was followed; however, analysis on an LSR II occurred after 24-72 hours co-culture.

### 2.2.9 CD8+T-cell clone recognition of cognate peptide on HCMV infected fibroblasts

To assess the ability of HCMV-specific CD8+T-cell clones to recognise cognate antigen during a productive infection of fibroblasts *in vitro*, clones were co-cultured O/N with HCMV-infected fibroblasts followed by an IFN-γ ELISA. 1 x $10^4$ healthy lab donor fibroblasts (HLA-$A1^+$) or MRC5 fibroblasts (HLA-$A2^+$HLA-$B7^+$HLA-$Cw*0702^+$) depending on the HLA restriction of the CD8+T-cell clone in question were plated per well, of a 96-well plate and left to adhere O/N. Fibroblasts were infected with AD169, Merlin or RV798 the following day at an MOI of 5 and left for 6, 12, 24, 48, 72, 96 and 120 hours. At the indicated time-points, 10000 specific CD8+T-cells were added and co-cultured O/N at 37°C. The following day, 50μL of the supernatant was used in an IFN-γ ELISA (described in section 2.2.7.3). Specific CD8+T-cell clones were also added to uninfected fibroblast as a negative control, and to wells without fibroblasts as an effector only negative control. As a positive control, specific

CD8+T-cells were added to fibroblasts that had been peptide-pulsed for 1 hour at 37ºC with the relevant peptide. All conditions were tested in triplicate.

### 2.2.10 CD8+T-cell recognition of HCMV infected monocytes

To assess the ability of CD8+T-cell clones to recognise cognate antigen during a productive infection of monocytes *in vitro*, clones were co-cultured overnight with HCMV infected monocytes followed by an IFN-γ ELISA. PBMCs of donors with the identified CD8+T-cell population in question were plated at a density of 2 x $10^6$ per well of a 24 well plate for a minimum of 3 hours at 37ºC. After 3 hours, the monocyte layer was trypsinised and plated at 1 x $10^4$ per well of a v-bottom 96-well plate. Monocytes were infected with the Merlin strain at an MOI of 5 and recognition determined 6-120 hours p.i as described in section 2.2.9 after an O/N co-culture with 10000 CD8+T-cell clones.

### 2.2.11 CD8+T-cell killing assays

The ability of HCMV-specific CD8+T-cell clones to kill peptide-loaded target cells was assessed *in vitro* using CFSE cell tracker dye coupled with the membrane impermeable cell viability dye 'Propidium Iodide' (PI). Target cells were labelled with CFSE as described previously (section 2.2.8). CD8+T-cell clones were co-cultured O/N at 37ºC with peptide-loaded, (1µg/ml final concentration, 1 hour 37ºC) CFSE labelled LCL target cells at 1:1, 2:1, 5:1 and 10:1 effector: target ratios on a 96-well v-bottom plate to allow cell: cell contact. The target cell numbers were maintained at 0.5 x $10^4$ cells to allow the accurate quantification of viable cell loss. Following overnight co-culture, all cells were transferred to a FACs tube, washed in MACS buffer at 540xg for 5 minutes and resuspended in 100µl PBS. Immediately before acquisition of events on the LSR II, 1µL of PI (Table-2) and 12.5µL (equating to 13500 beads total) of CountBright absolute beads (Life technologies Table-2) were added to the cells. 100 000 events were recorded per sample tube and a negative control of O/N co-culture (1:1 ratio) with DMSO-pulsed LCLs was included.

To calculate CD8+T-cell killing, the following equation was used (as per manufacturers guide (CountBright absolute beads, Life technologies Table-2);

**Cells/µl** = [number of CFSE POSITIVE/PI negative cell events/number of bead events]*[assigned bead count of the lot/volume sample in µl]

**% specific lysis** = 100 - ([cells/µl of sample]/ [cells/µl of DMSO control]*100)

For the analysis of the specific cell lysis of HCMV infected fibroblasts 0.2 x $10^4$ fibroblasts target cells were maintained and the CD8+T-cell clone effector numbers were modified accordingly. 10 000 events were recorded per sample tube and a peptide-pulsed fibroblast tube was included as a positive control.

### 2.2.12 – Measurement of CD25 upregulation after co-culture of HCMV CD8+T-cell clones with HCMV infected fibroblasts

To analyse the activation of HCMV-specific CD8+T-cell clones after recognising cognate antigen during a WT (Merlin) infection of fibroblasts, clones were subjected to CD25 staining by flow cytometry. 1 x $10^4$ fibroblasts were seeded onto a flat bottom 96 well plate O/N and the following day infected with the RCMVIIII Merlin strain at an MOI of 0.05. After 72 hours, CD8+T-cell clones were removed from the infected monolayer and subjected to flow cytometric analysis as described in section 2.2.5 using CD8 PerCP-Cy5.5 (e Biosciences), CD3 PB (eBiosciences), the CD25 PE (Biolegend) and APC LIVE/DEAD Fixable dye (Invitrogen).

### 2.2.13 Measurement of surface HLA alleles on HCMV infected fibroblasts

To evaluate the levels of surface HLA class I alleles on the surface of fibroblasts during a productive HCMV infection, fibroblasts were stained with the W6/32 (anti-HLA-ABC, BD Biosciences) or DT9 (anti-HLA-C – kindly provided by Dr Veronique Braud Institute of Molecular and Cellular Pharmacology, Sophia Antipolis, Valbonne). 1 x $10^4$ HFFF2 (HLA-A11+HLA-B35$^+$HLA-Cw2$^+$HLA-Cw4$^+$HLA-Cw7$^+$) MRC5 (HLA-A2$^+$HLA-B7$^+$HLA-Cw*0702$^+$)

fibroblasts were plated onto 96 well plates and left to adhere O/N. Fibroblasts were then infected with either AD169 or RV798 at an MOI of 5. After 3, 6, 12, 24, 48, 72, 96 and 120 hours p.i, cells were trypsinised and washed in PBS (535xg, 5 minutes) before surface staining with the monoclonal antibodies. DT9 stained fibroblasts were then washed in PBS before staining with a secondary α-mouse FITC-conjugated antibody (Sigma) Cells were then analysed on an LSR II and data processed using BD Facs DIVA software 8.0 (BD Biosciences)

### 2.2.14 CD8+T-cell clone TCR sequencing

For the investigation of a HLA-Cw*0702-restricted HCMV-specific TCR as a potential immunotherapy, the TCR of specific CD8+T-cell clones was sequenced using the 'SMARTer RACE 5'/3' Kit from Clontech'. This kit allowed the amplification of the complete 5' sequence of the TCR α/β chains of HCMV-specific CD8+T-cell clones.

i. Primer design

Gene specific primers (GSPs) for the constant region of human α and β TCR chains were designed and contained 15bp homology (GATTACGCCAAGCTT) sequence at the 3'-end to allow the amplified PCR fragment to be cloned into the pRACE vector for subsequent sequencing.

ii. Generation of cDNA for fusion into RACE vector

Firstly, the TCR α and β chain genes were amplified from cDNA generated after RNA extraction and a PCR reaction using the GSPs. A minimum of 2 x $10^6$ specific CD8+T-cell clones were centrifuged at 540xg for 5 minutes. RNA was extracted from the CD8+T-cell clone pellet using the RNeasy microRNA kit from Qiagen according to the manufacturers guide. cDNA was generated from RNA following the 'SMARTer RACE 5'/3' kit' manufacturers guidelines. The only deviation from the full protocol was the setup of 2 identical reactions - one each for the α and β chain. Full protocol can be obtained from http://www.clontech.com/GB/Products/cDNA_Synthesis_and_Library_Construction/RACE_R

apid_Amplification_of_cDNA_Ends/5_Prime_RACE_and_3_Prime_RACE?sitex=10030:22372:US

iii. Characterisation of the cDNA products

The α and β TCR chain PCR reaction products were electrophoresed on a 1% agarose gel and the DNA from the bands extracted using the 'QIAquick Gel Extraction Kit' from Qiagen following the manufacturers guidelines.

iv. Cloning of the cDNA products into the pRACE vector for sequencing

The following pRACE reaction mixture was incubated for 15 minutes at 50ºC (50% of the specified volumes in the manufacturers guide);

- 0.5µl Linearized pRACE vector
- 2.5µl gel-purified cDNA product (section iii)
- 1µl In-fusion HD mastermix

A total of 2.5µl of the pRACE reaction mixture was used to transform 50µl of Stellar competent cells (Table-2) in a 15ml tube on ice for 30 minutes, followed by heat shocking the cells for exactly 45 seconds at 42ºC. Cells were recovered on ice for 2 minutes and a total of 497.5µl SOC media (Table-2) added – this was then incubated in a shaking rotator (200rpm) for 1 hour at 37ºC. The resulting culture was then spread O/N on LB + ampicillin plates (final concentration 100µg/ml). Colonies were picked the following day into 5ml LB broth + ampicillin (final concentration 100µg/ml) and the pRACE plasmid with the FRC TCR insert isolated using the 'Qiagen plasmid mini prep kit' using the manufacturer's guidelines.

V. Sequencing the pRACE vector products

50ng of pRACE plasmid and M13F sequencing primer (Table-2) in a total volume of 11µl was sequenced using the University of Birmingham Genomics service. Sequencing results were analysed using Chromas and TCR α and β sequences determined using the IMGT/V-Quest online sequence aligner tool http://www.imgt.org/IMGT_vquest/share/textes/

## 2.2.15 Generation of a TCR construct for transduction of CD8+T-cells

Once the TCR sequence of the CD8+T-cell clone was known, the α and β sequences were inserted into the myeloproliferative sarcoma virus-derived vector pMP71 plasmid vector (a kind gift from Dr Christopher Baum, Hannover Medical School, Germany) as an individual sequence. The TCR sequences of the α and β chains (obtained in section 2.2.14) were entered into the ensemble website (http://www.ensembl.org/index.html**)** and the start codon of the α and β variable chain sequences were identified. This allowed for the identification of the full length V(D)J region for both the α and β chain. A transgene was then designed which added the constant regions of both chains to their respective V(D)J fragments, and each chain was separated by a 2A linker sequence (Fig-6). The 2A linker allowed for the cleaving of the α and β chains once transcribed within transduced T-cells. The sequences of the TRAC1 and TRBC1 constant regions used which include an extra cysteine allowing for an enhanced αβ folding.

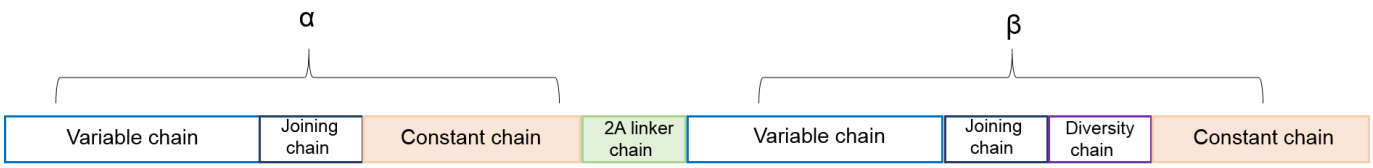


***Fig 6 – Schematic sequence of the TCR for codon optimisation and ordered from IDT GBlocks.***

This sequence was codon optimised and ordered from IDT GBlocks., The resulting DNA 'GBlocks' were inserted into the pMP71 plasmid via the 'Gibson assembly method' [226] using the 'Gibson assembly kit' (Table-2 NEB) as per the manufacturers guidelines. The resulting plasmid was transformed into TOP10 competent bacteria (Table-2) and plated O/N on LB + ampicillin (final concentration 100µg/ml). Picked colonies were grown in 5 ml LB + ampicillin (final concentration 100µg/ml) O/N and the plasmid isolated using the Qiagen plasmid mini prep kit following the manufacturer's guidelines. Plasmids were sequenced to ensure that the FRC TCR had folded correctly and the sequence was intact. Plasmids with

the correct insert were selected for generating stocks and isolated using the 'Endofree plasmid maxi prep kit' (Table-2) as per the manufacturer's guidelines.

### 2.2.16 TCR transduction of CD8+T-cells from buffy coats

After the insertion of the TCR into the pMP71 plasmid, this construct was used to transfect phoenix amphotropic cells and in turn used to transduce T-cells obtained from a buffy coat to test the potential immunotherapy *in vitro* [227].

- Day 0

Phoenix cells were thawed from liquid nitrogen and plated into a T75cm$^2$ tissue culture flask 48 hours before they were to be transfected with the TCR/pMP71 construct.

- Day 1

Once 50% (minimum) confluent, phoenix cells were resuspended in a flask with 11ml of fresh DMEM (10% FCS, no P/S) and co-transfected with the TCR/pMP71 construct (final concentration 5.5µg) and pPCL-ampho packaging vector (5.5µg final concentration, NovusBio). The pCL-Ampho packaging vector was included to maximize recombinant–retrovirus titers.

Prior to the transfection, the FRC-TCR/pMP71 and pCL-Ampho vectors were incubated for 10 minutes with 28µg PEI (Sigma) in 1ml of OPTIMEM for 10 minutes at RT. For transfection, this DNA:PEI complex was then added to the flask of phoenix cells for 12 hours at 37$^o$C.

Retroviral based vectors require cell division for efficient infection and integration of T cells. Therefore transduction efficiency is dependent on the activation of the T cells prior to transduction [228]. PBMCs isolated from buffy preparations were stimulated with 2µg (final concentration) α-CD28 (Milteyni Biotech), 1µg (final concentration) α-CD3 OKT3 (eBioscience) and 600 IU IL-2 O/N at 37$^o$C. A non-tissue culture treated plate was coated with 3ml per well of retronectin (30ng/ml, clontech) O/N at 4$^o$C.

- Day 2

After the 12 hour transfection, the supernatant in the phoenix cell flask was replaced with fresh DMEM (10% FCS, no P/S) and the cells allowed to secrete pMP71/FRC expressing retrovirus into the supernatant for 24 hours.

- Day 3

After 24 hours, the TCR/pMP71-retroviral supernatant was harvested, centrifuged at 535xg for 5 minutes, filtered through a 0.45µM filter and was then ready for use in a transduction.

The rectronectin coated plate was washed once with 3ml PBS before blocking for 1 hour at RT with 3ml of PBS + 2% BSA. This was then washed with 3ml PBS and 3ml of the TCR/pMP71-retroviral supernatant added per positive transduction well. Mock transduced supernatant was added to mock transduced wells and served as a negative control. The plate was centrifuged at 32$^{o}$C for 2 hours at 2288xg to ensure the viral construct was attached to the retronectin on bottom of the plate.

The stimulated buffy PBMCs were washed twice in DMEM (10% FCS, no P/S) at 1600rpm for 5 minutes and 4 x10$^{6}$ cells resuspended in 4 ml DMEM (10% FCS, no P/S).

Once the viral supernatant had been centrifuged onto the plate for 2 hours, the supernatant was removed and the activated PBMCs were added to the TCR/pMP71-retroviral coated wells. The plate was centrifuged immediately at 535xg rpm for 5 minutes to ensure the T-cells contacted the pMP71/FRC-containing retrovirus particles.

### 2.2.17 Generation of a HCMV vaccine vector with an NYESO1 insert by recombineering – in collaboration with Dr Richard Stanton, University of Cardiff

The recombineering of the pALIIII HCMV BAC was accomplished using SW102 bacteria that contain a viral phage expressing the lamba red genes that are expressed when the bacteria are placed at 42ºC. These genes mediate homologous recombination and are switched off at 32ºC. Full protocol kindly provided by Dr Richard Stanton at http://medicine.cf.ac.uk/media/filer_public/2013/09/13/recombineering_merlin_bac-7.pdf. Dr Richard Stanton inoculated SW102 bacteria containing the pALIIII HCMV BAC into 5ml of LB broth that contained a final concentration of 12.5µg/ml (same final concentration throughout) Chloramphenicol overnight at 32ºC. The following day, Dr Richard Stanton inoculated 0.5ml of the overnight culture into fresh 25ml LB both + chloramphenicol and allowed to reach an $OD_{600}$. Bacteria were transferred to a 50ml falcon tube by Miss Louise Hosie (completed the work from now on excluding plating the bacteria, under Dr Richard Stanton's direct guidance) and the lamda red proteins within the bacteria induced via incubation at 42ºC for 15 minutes before transfer to ice for 20 minutes. Bacteria were pelleted at 1087xg for 5 minutes and resuspended in 1ml of ice cold dd$H_20$ before the addition of a further 25ml and centrifugation repeated. This wash step was repeated once more and the pellet resuspended in the residue dd$H_20$. The SW102's were transferred to a cuvette cooled to 4ºC and kept on ice for 5 minutes. 5µL of NYESO1 DNA (purchased from Life Technologies and includes the DNA sequence of the full NYESO1 protein flanked either side with 80bp homology to the RL13 HCMV protein, Table-6) was added to the bacteria which were then electroporated at 250V and recovered for 5 minutes in 5ml LB broth at 32ºC for 4 hours. After the recovery period, bacteria were spread onto LB plates + sucrose + X-gal + IPTG and left for 36 hours at 32ºC. Positively BAC transfected colonies (white opaque) were then picked in 5ml LB broth + chloramphenicol O/N before isolating the BAC via a mini prep of the colonies and sequencing for the correct NYESO1 insertion. Additionally, DNA obtained from the mini plasmid preparations of colonies containing the HCMV-NYESO1 BAC were

restriction digested for 2 hours at 37ºC (10µl plasmid, 7µl $H_20$, 1µl HinDIII) and run on a gel O/N (16 hours) on a 0.8% agarose gel. Confirmation that the insert had not disrupted the BAC structure and had recombined correctly was provided by comparison to the parental BAC pALIIII digestion [221] and sequencing of plasmids (University of Birmingham, Genomics Services) using the M13F/R primers (Table-3). Two plasmids that had correctly recombined NYESO1 inserts were selected for generating DNA stocks for stable transfection of fibroblasts by inoculating 5ml LB broth containing chloramphenicol with 100µL of the residual mini preparation colonies at 32ºC. After 8 hours the entire culture was inoculated into fresh 500ml LB + chloramphenicol O/N at 32ºC and maxi prepped using the 'Purelink HiPure plasmid maxiprep kit' (Table-2). For the stable transfection of fibroblasts to generate viral stocks, 2 x $10^6$ HFFF2s were electroporated with 30ng of maxi prepped HCMV-NYESO1 DNA. Electroporated cells were recovered on tissue culture-treated 10$cm^2$ dishes until plaques could be observed. At this point, the entire monolayer was trypsinised and inoculated into 2 x $10^6$ uninfected HFFF2s and transferred into a T150$cm^2$ tissue culture flask in 20ml DMEM culture media. Once plaques could be observed, viral supernatant was removed and replaced with fresh DMEM culture media. The 20ml of the viral supernatant was used to inoculate two flasks of uninfected HFFF2s to confirm viral progeny production by observing more plaques and to increase the final viral stock pfu. Once plaques could be observed in the newly infected flasks, over the next 21 days, the viral supernatant from the four flasks was removed, frozen at -80ºC and replaced with fresh DMEM culture media. At the end of the 21 day period, viral supernatant was centrifuged at 15337xg for 2 hours in ultracentrifugable GSA Sorvall bottles at 4ºC. The viral pellet was resuspended in 2ml DMEM culture media and 100µL of virus stocks transferred to cryovials and stored at -80. The viral titre of the stocks was determined by plaque assay as described in section 2.1.2.

### 2.2.18 Generation of NYESO1-specific CD8+T-cell clones from healthy donors

NYESO1-specific CD8+T-cell clones were generated to test the immunogenicity of the HCMV-NYESO1 *in vitro* as published [229]. Immature monocytes were isolated from buffy

coats of healthy donors by plating 2 x $10^6$ PBMCs per well of a 24 well plate for a minimum of 3 hours to allow monocytes to adhere. After adhering, monocytes were trypsinised from the bottom of the plate, transferred to a fresh 24 well plate and differentiated to dendritic cells (DCs) over 4 days via the addition of 'Granulocyte macrophage colony-stimulating factor' (GMCSF) (800IU/ml, Peprotech) and IL-4 (10ng/ml, Peprotech) in RPMI media. DCs were then matured O/N with IFN-γ (100IU/ml) and LPS (10ng/ml) to induce CD44 and CD88 expression. The DCs were peptide-pulsed for 10 days with a HLA-A2-restricted NYESO1 peptide **SLL**MWITQC (aa position 157-165) [336-338] and co-cultured with autologous naïve CD8+T-cells (isolated from the same buffy coat and cryostored on the same day as the monocytes) (Table-2, Stem Cell Tech). After this 10 day co-culture, 50% of the DCs and CD8+T-cell co-culture was restimulated twice with γ-irradiated buffys and peptide-pulsed HLA-A2+ LCLs. After the second restimulation, CD8+T-cells were sorted based on CD137 expression (Miltenyi Biotech) and $CD137^+$ CD8+T-cells subjected to limiting dilution as described in 2.2.7.2 The remaining 50% were restimulated a third time after a further 14 days and subjected to an IFN-γ catch assay (Miltenyi Biotech) and limiting dilution as described in 2.2.7.2. Expanded wells after 14 days were tested for peptide specificity as described in section 2.2.7.3. The recognition of HCMV-NYESO1 infected HLA-$A2^+$ MRC5 fibroblasts after an O/N co-culture was determined as described in section 2.2.9. The specific lysis of NYESO1 peptide-pulsed HLA-$A2^+$ LCLs and HCMV-NYESO1 infected MRC5 fibroblasts (MOI 5) after 24 hours was conducted as in section 2.2.11 but with 35000 and 10000 events recorded on an LSR II respectively.

### 2.2.19 Statistics

All statistics were computed in Graphpad Prism 6 using non parametric tests. Specific statistical tests are indicated in figure legends. Statistical significance was defined as a p-value of <0.05 (*), <0.01 (**), <0.001(***) and <0.0001 (****).

# CHAPTER 3

# CHARACTERISATION OF THE CD8+T-CELL RESPONSE TO ‘PROTECTED’ EPITOPES IDENTIFIED USING THE RV798 STRAIN OF CMV

# Chapter 3 - Introduction

During chronic infection, the HCMV-specific CD8+T-cell response can occupy on average 10%, reaching >20%, of the total circulating CD8+T-cell repertoire with age [87, 100, 107, 230]. These expanded accumulations have a distinctive $T_{EMRA}$ phenotype ($CCR7^{-}$ $CD45RA^{+}CD27^{-}CD28^{-}$) and display high cytotoxicity [87, 108, 231]. It has since been realised that this current view of the CMV-specific CD8+T-cell immune response, which is based upon a restrictive set of immunodominant epitopes from the pp65 and IE-1 protein, is incomplete and vastly underestimating the global CD8+T-cell response. Further complicating the matter is the presence of the immunomodulatory US2-11 encoded proteins that interfere with the MHC-I pathway. Within infected fibroblasts these have been demonstrated to dampen the cytotoxic CD8+T-cell response to infected cells [232].

A study by Gold et al. identified a novel peptide-epitope derived from the murine M45 protein using a strain of MCMV deleted for the immunomodulatory m152 protein [233]. Specific CD8+T-cell responses to this peptide were found *in vivo* despite the peptide not being presented *in vitro* during a fibroblast infection with the WT m152 virus. However, this may not represent the global priming abilities of all cell types permissible to CMV *in vivo* and may be a feature of fibroblasts. Therefore, our view of the global CD8+T-cell targets towards HCMV has additionally may have been hampered by the restricted use of fibroblasts as the staple cell line for CMV infection *in vitro*. As such, important and potentially immunodominant CD8+T-cell responses *in vivo* may yet remain undetected.

To address this, studies using both, synthetic peptide libraries derived from either 14 HCMV proteins or the entire HCMV genome [230, 234] have shed light into the global HCMV CD8+T-cell response within healthy chronically infected individuals. These studies extended the range of known HCMV antigens able to elicit CD8+T-cell responses from pp65 and IE-1 including; US2, US3, US6 US11, UL16, and UL18.

Two critical studies prior to the start of this research investigation utilised a mutant strain of HCMV deleted for the main US immunomodulatory genes (US2-S11) termed RV798

(generated by Jones et al. [83]). The studies hypothesised that the absence of the immunevasin region allowed for the surface presentation of potentially all antigenic targets of the virus. A study in our research lab identified that the CD8+T-cell response directed towards HCMV increased up to 10 fold upon removal of the US2-11 genes (RV798 infection) compared to the presence of the WT US2-11 region (AD169 infection). This was indicated by IFN-γ production after incubation of AD169 vs RV798 infected APCs with PBMCs. The work identified novel CD8+T-cell responses to additional CD8+T-cell antigens e.g. IE-2 [84].

The research group of Dr Stanley Riddell, also utilised the RV798 virus strain of CMV to identify novel targets of the HCMV CD8+T-cell response [82]. Via incubation of PBMCs from chronically infected donors with RV798 infected APCs, the research group isolated CD8+T-cell clones and mapped the specificities to proteins of the virus using single CMV deletion mutant strains. Specificity was determined by loss of recognition by CD8+T-cell clones towards cells infected with the CMV mutant – indicating the deleted protein contained the cognate peptide. Through this work, novel HCMV peptides were identified and the sequences of 16 were kindly provided to our research group by Prof Stanley Riddell (Table-7). These epitopes were derived from a range of HCMV antigens and from all phases of the virus life cycle (IE-L). Furthermore within this study, Riddell et al demonstrated that these antigens were not recognised by the same CD8+T-cell clones during a WT AD169 infection of fibroblasts *in vitro*. These peptides were as such termed ‘protected epitopes’ by our research group as it was hypothesised they were ‘shielded’ from the CD8+T-cell clones *in vitro* during a WT infection due to the actions of the US2-11 gene region products. It was further hypothesised that the CD8+T-cell responses to these *in vivo* may be initially generated by cross-presentation due to the US2-11 gene region interfering with their direct presentation to the immune response.

It has not yet been determined whether these novel peptide-epitopes (Table-7) identified by Manley et al. could be directly presented to the CD8+T-cell immune response *in vivo* during a WT HCMV infection - when the immunevasive US2-11 gene products are able to interfere

with MHC-I processing. Or additionally, whether such CD8+T-cell responses could play a protective role in removing virally infected cells *in vivo*.

This investigation aimed to characterise the *ex vivo* responses to these peptides in terms of kinetics of expression, phenotype and recognition of cognate antigen during a WT (US2-11) infection of cells *in vitro*. Of particular importance is our access to the Birmingham '1000 Elders' cohort of healthy donors that are aged 60 years or over allowing us to analyse how the *ex vivo* CD8+T-cell responses change with age. It was also hoped to distinguish between 'stable' vs 'inflationary' HCMV epitopes within this peptide cohort as has been previously identified for MCMV and whether memory-inflation is restricted to immunodominant peptides derived from the pp65 and IE-1 proteins.

# Chapter 3 - Results

## 3.1 - *Ex vivo* responses to 'protected' HCMV epitopes are frequently detected in chronically infected healthy individuals

Due to the protection of these peptides from the immune response *in vitro*, it was theorised that their specific CD8+T-cell responses *in vivo* may differ to those generated against previously researched HCMV epitopes e.g. pp65-derived 'NLV' (Table-5). The characteristics of the protected peptide-epitopes are provided in Table-7. They are derived from a wide range of HCMV antigens including; UL16, UL17, UL23, UL24, UL28, UL33, UL36, UL52, UL56, UL84, UL105, UL122 and US23. They also have diverse functions, are expressed across all phases of the viral lifecycle IE-L and importantly restricted through HLA-A, -B and –C alleles.

The first aim of this investigation was to characterise the magnitude and kinetics of the *ex vivo* CD8+T-cell responses generated *in vivo* towards the 'protected epitopes' within healthy seropositive donors. These CD8+T-cells populations were analysed for changes in magnitude with age. Donors were therefore categorised into younger (YD <70 years) or older (OD >70 years) groups. To achieve this, PBMCs were screened for *ex vivo* CD8+T-cell responses indicated by intracellular cytokine production (IFN-γ, IL-2 and TNF-α) in response to 6 hours peptide stimulation. As positive and negative controls, PBMCs from the same donors were stimulated with SEB or media only (gating strategy of the ICS protocol is provided in Fig-7). The negative control background cytokine production ranged from 0.01-0.22% of the total CD8+T-cells. In all cases this was subtracted from the peptide stimulated sample tube (data not shown). Throughout this investigation, donors were only screened for CD8+T-cell responses if they presented with the HLA type appropriate to the HLA-restriction of the peptide in question. Responding CD8+T-cells to the HLA-A/-B and –C 'protected' epitopes were previously detected in an MRes study in our research group (L.Hosie MRes, University of Birmingham, 2013). This work seeks to first extend this work by analysing the kinetics to these CD8+T-cell epitopes in a larger donor cohort. As such, 54 young and 37

elderly HCMV infected healthy donors aged between 23-96 years of age (donor description provided in appendix table 1-3 and 4-6 for YD and OD donors respectively), were screened.

**Table 7 – *HCMV 'protected' CD8+T-cell peptide-epitopes***. Protected epitope sequences (*) kindly provided by Dr Stanley Riddell (Some peptides unpublished data, others [85] investigated their processing). The protein antigen, aa position within the protein antigen, peptide sequence (peptide name is denoted by the first three aa of the sequence), restricting HLA allele, kinetics of expression and function of the protein antigen (if known) that the peptides are derived from are provided

| CMV Antigen | Location in the Virion [224] | Function [224] | CTL Epitope | HLA Restricting Allele | Kinetics of Expression [225] |
|---|---|---|---|---|---|
| $UL69_{569-578}$ | Tegument | cell-cycle arrest (G1 - S) transport of unspliced RNA from nucleus | **RTD**PATLTAY* | A0101 | E/L |
| $UL105_{715-723}$ | | proposed helicase and primase activity, DNA replication | **YAD**PFFLKY* | A0101 | E/L |
| $UL84_{3-11}$ | | Phosphoprotein with a suggested role in DNA-synthesis | **RVD**PNLRNR* | A0301 | L |
| $UL36_{51-60}$ | Matrix or tegument | inhibitor of caspase activity (apoptosis) | **RSA**LGPFVGK* | A1101 | E |
| $UL16_{162-170}$ | Glycoprotein | NK cell evasion | **YPR**PPGSGL* | B0702 | E |
| $UL17_{12-21}$ | Capsid | | **RPR**HCRLEML* | B0702 | E/L |
| $UL52_{349-358}$ | Matrix or tegument | unknown | **SPS**RDRFVQL* | B0702 | L |
| $UL36_{78-88}$ | - | - | **HPF**GFVEGPGF* | B3501 | E |
| $UL122_{466-475}$ | IE2 protein tegument | replication, inhibition of apoptosis | **NEG**VKAAWSL* | B4403 | IE |
| $UL56_{503-511}$ | Matrix or tegument | involved in DNA encapsidation | **DAR**SRIHNV* | B5101 | E/L |
| $US23_{65-73}$ | Matrix or tegument | unknown | **IPH**NWFLQV* | B5101 | n/a |
| $UL36_{7-21}$ | - | - | **TLM**AYGCIAIRA GDF* | B5101 | E |
| $UL23_{34-42}$ | Tegument | unknown | **WPK**DRCLVI* | B5101 | E/L |
| $UL28_{327-335}$ | Tegument | | **FRC**PRRFCF* | Cw0702 | IE |
| $UL33_{120-128}$ | | putative chemokine receptor (G-coupled receptor) | **SYR**STYMIL* | Cw0702 | L |
| $UL24_{120-134}$ | Tegument | | **YLC**CQTRLAFV GRFV* | Cw1601 | L |

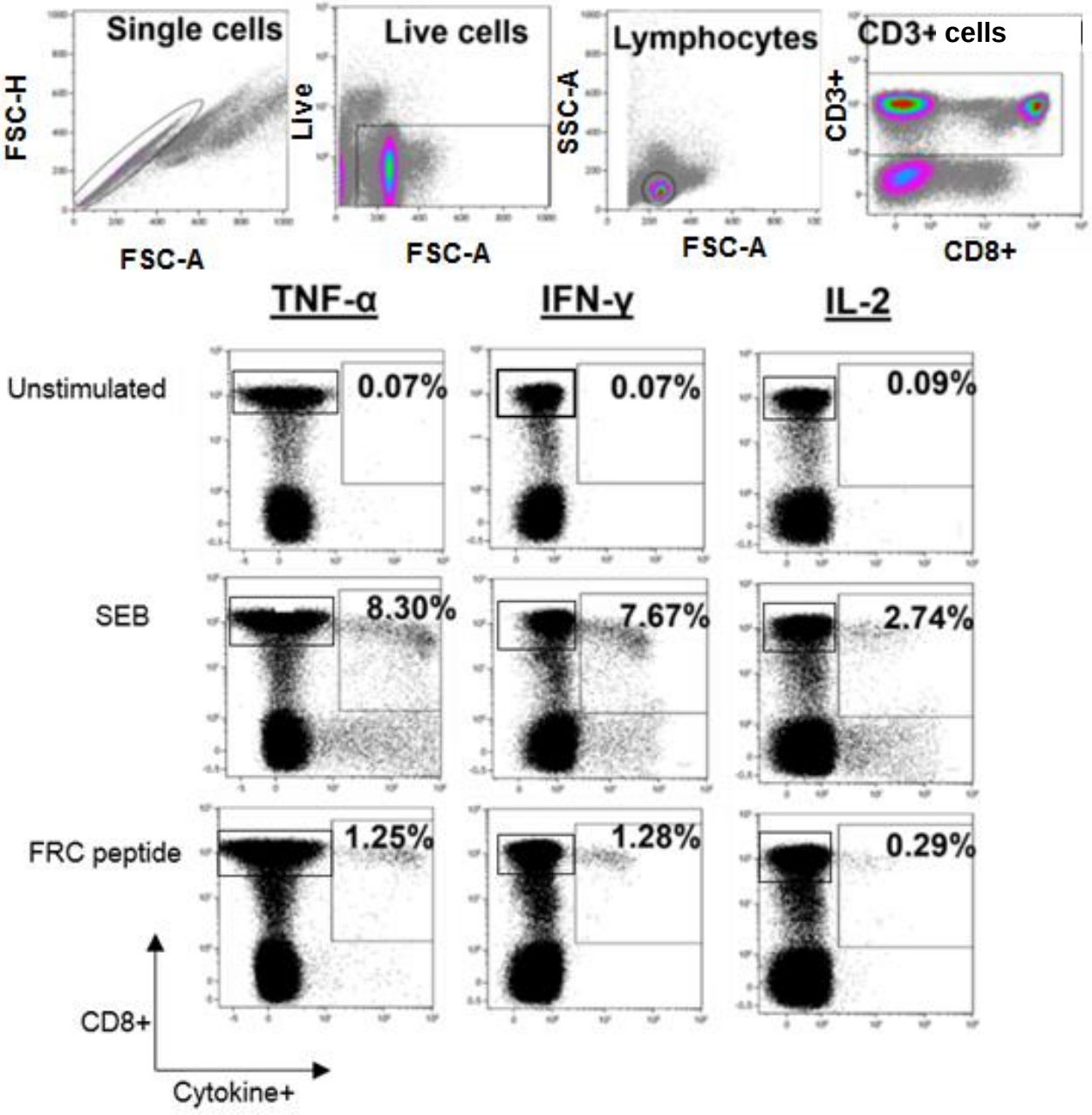


***Fig 7 – Gating strategy to identify activated CD8+T-cell populations following HCMV peptide stimulation.***
PBMCs from HCMV seropositive donors were stimulated with HCMV peptide (final concentration 1µg/ml) for 6 hours. Single, live, CD3+CD8+ lymphocytes were gated on sequentially within Kaluza 1.3 software (Beckman Coulter). Cytokine producing CD8+T-cells were then identified in the gated CD8+ population. The cytokine gate was placed using the SEB stimulated control to identify the downregulation of CD8+ after stimulation. Any cytokine positive cells below this gate were considered background CD4+ cytokine producing cells. The percentages represent the percentage of activated CD8+T-cells producing cytokine as a percentage of the totalCD8+T-cell population. In all cases, the percentages shown have had the unstimulated control percentages subtracted.

Overall, 12 out of the 16 peptides (Table-7) induced specific CD8+T-cell populations (Fig-8/9) restricted through HLA-A/-B and –C producing cytokines. The peptides that did not elicit CD8+T-cell responses in this cohort were the HLA-B51-restricted peptides (n = 13). In all cases, the HCMV-specific CD8+T-cell populations were largely Th1 like – producing large amounts of IFN-γ and TNF-α. As has been previously described, the CMV-specific CD8+T-cell populations produced little IL-2 (compared to the magnitude of IFN-γ and TNF-α production) (Fig-9) [235]. The CD8+T-cell IFN-γ and TNF-α production elicited by the peptides were of similar magnitudes (Fig-8/9). All averages and the raw ICS response results are provided in appendix tables 1-6. Fig-9A demonstrates the positive and negative spread of the CD8+T-cell responses obtained in all donors against the individual peptides. Fig-9B demonstrates the mean of the positive CD8+T-cell responses obtained against each individual peptide.

Both the HLA-A and –B-restricted peptides elicited significant CD8+T-cell responses (Fig-8 and 9A/B). The CD8+T-cell responses against the HLA-A peptides ranged from 0.02-5.65% of the total peripheral CD8+T-cell pool producing cytokine and remained at a stable percentage with age i.e. between donors < vs >70years (Fig-9A/B). The UL69-derived RTD and UL105a-derived YAD epitopes elicited the most frequent HLA-A-restricted CD8+T-cell responses (Table-7) - 30% (9/30) and 33% (10/30) donors respectively (Fig-9A/B) which did not increase significantly with age. The RTD-specific CD8+T-cell responses producing IFN-γ and TNF-α ranged from 0.02%-1.00% (IFN-γ) and 0.02%-1.24% (TNF-α) of the total CD8+T-cell response (Fig-8, 9A/B). These CD8+T-cell responses remained at an average of 0.28% (IFN-γ) or increased from 0.28%-0.43% (TNF-α) between the <70 vs >70 donor categories (Fig-8, 9A/B). The YAD-specific responses producing IFN-γ and TNF-α ranged from 0.02%-0.28% (IFN-γ) and 0.02%-0.91% (TNF-α) of the total CD8+T-cell response. These CD8+T-cell responses increased from an average of 0.12%-0.15% (IFN-γ) and 0.24%-0.34% (TNF-α) between the <70 vs >70 donor categories (Fig-8, 9A/B) but was not significant. The IL-2 production with age of the RTD- and YAD-specific CD8+T-cell responses remained almost

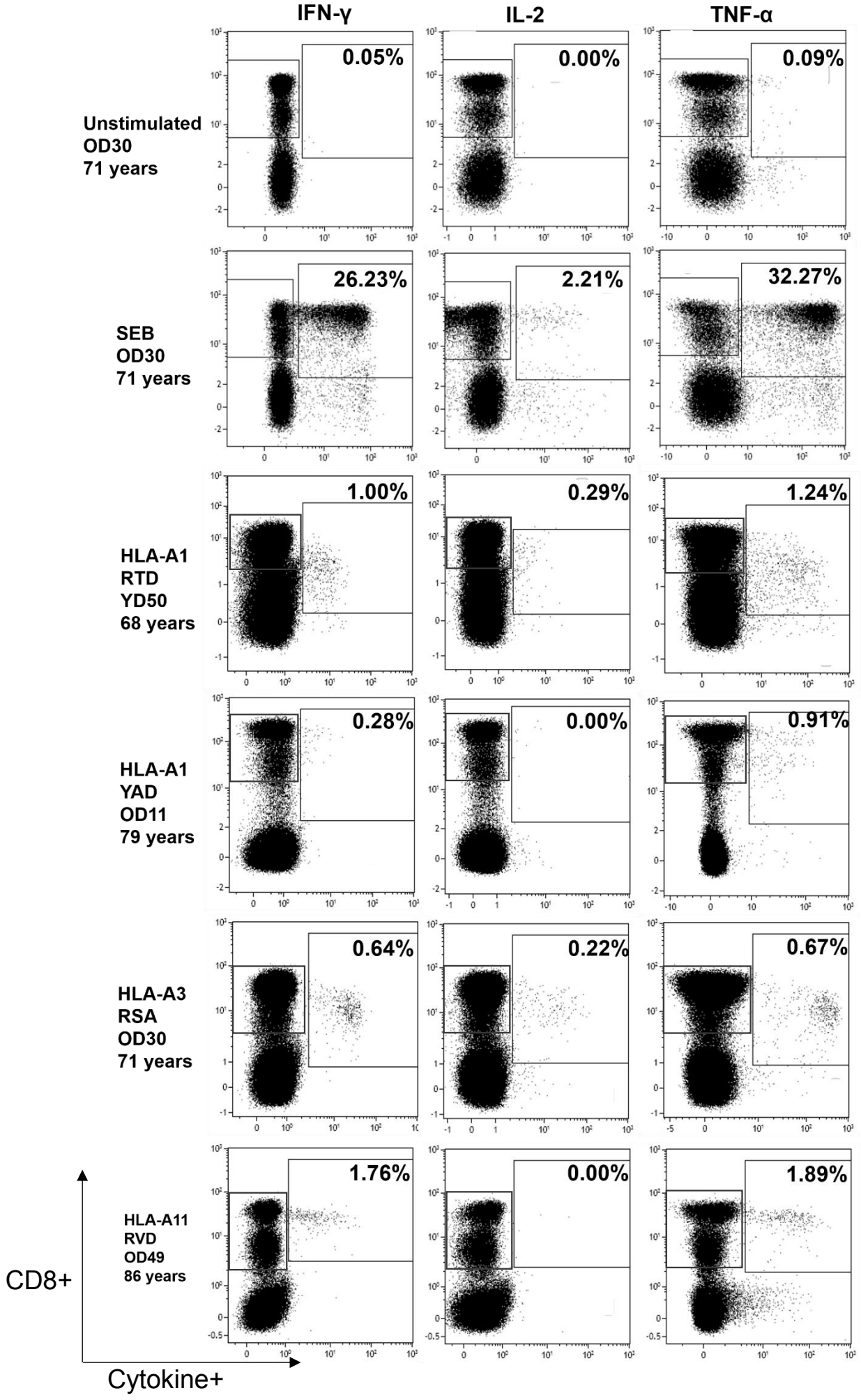
IFN-γ
IL-2
TNF-α
Unstimulated
OD30
71 years
0.05%
0.00%
0.09%
SEB
OD30
71 years
26.23%
2.21%
32.27%
HLA-A1
RTD
YD50
68 years
1.00%
0.29%
1.24%
HLA-A1
YAD
OD11
79 years
0.28%
0.00%
0.91%
HLA-A3
RSA
OD30
71 years
0.64%
0.22%
0.67%
HLA-A11
RVD
OD49
86 years
1.76%
0.00%
1.89%
CD8+
Cytokine+

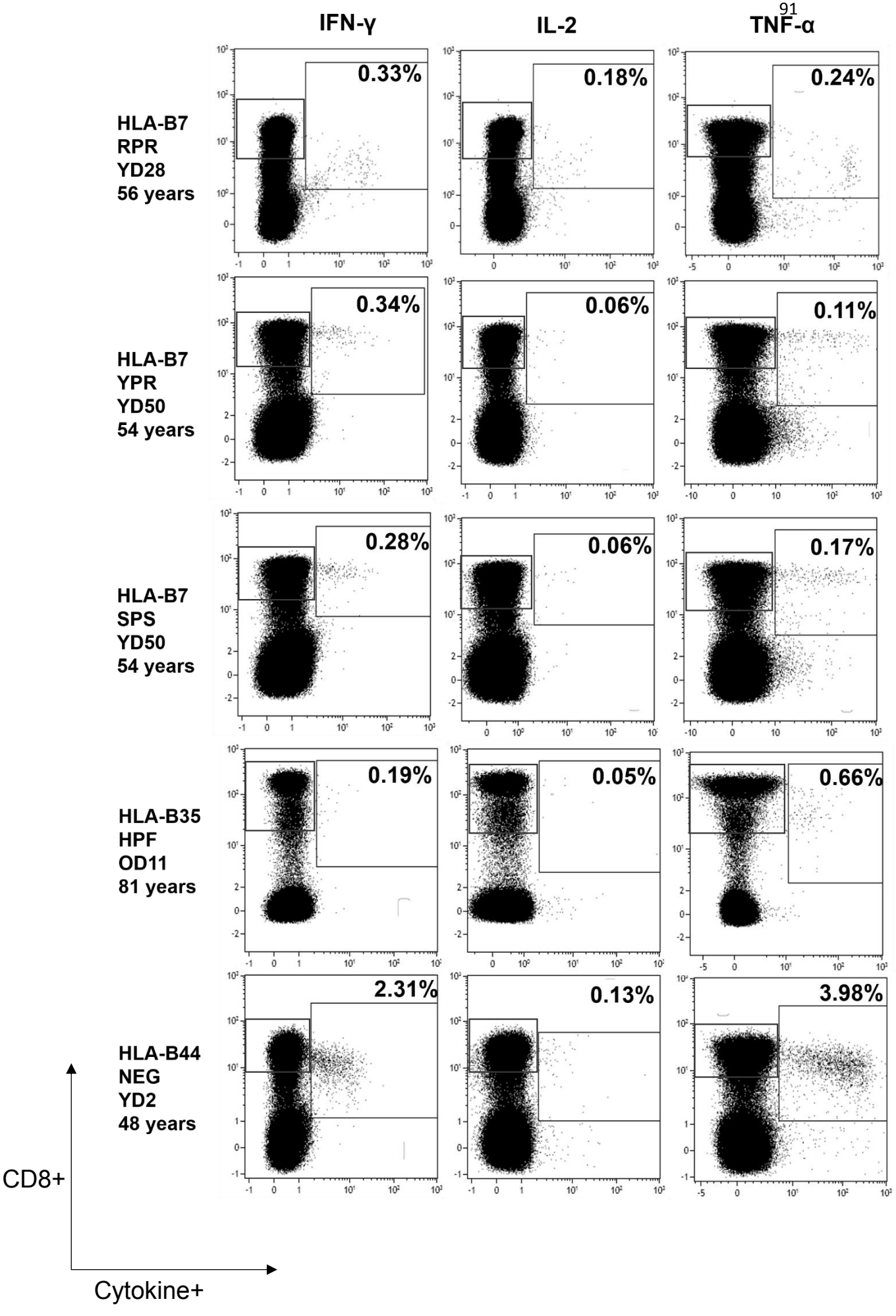
IFN-γ
IL-2
TNF-α
HLA-B7
RPR
YD28
56 years
0.33%
0.18%
0.24%
HLA-B7
YPR
YD50
54 years
0.34%
0.06%
0.11%
HLA-B7
SPS
YD50
54 years
0.28%
0.06%
0.17%
HLA-B35
HPF
OD11
81 years
0.19%
0.05%
0.66%
HLA-B44
NEG
YD2
48 years
2.31%
0.13%
3.98%
CD8+
Cytokine+

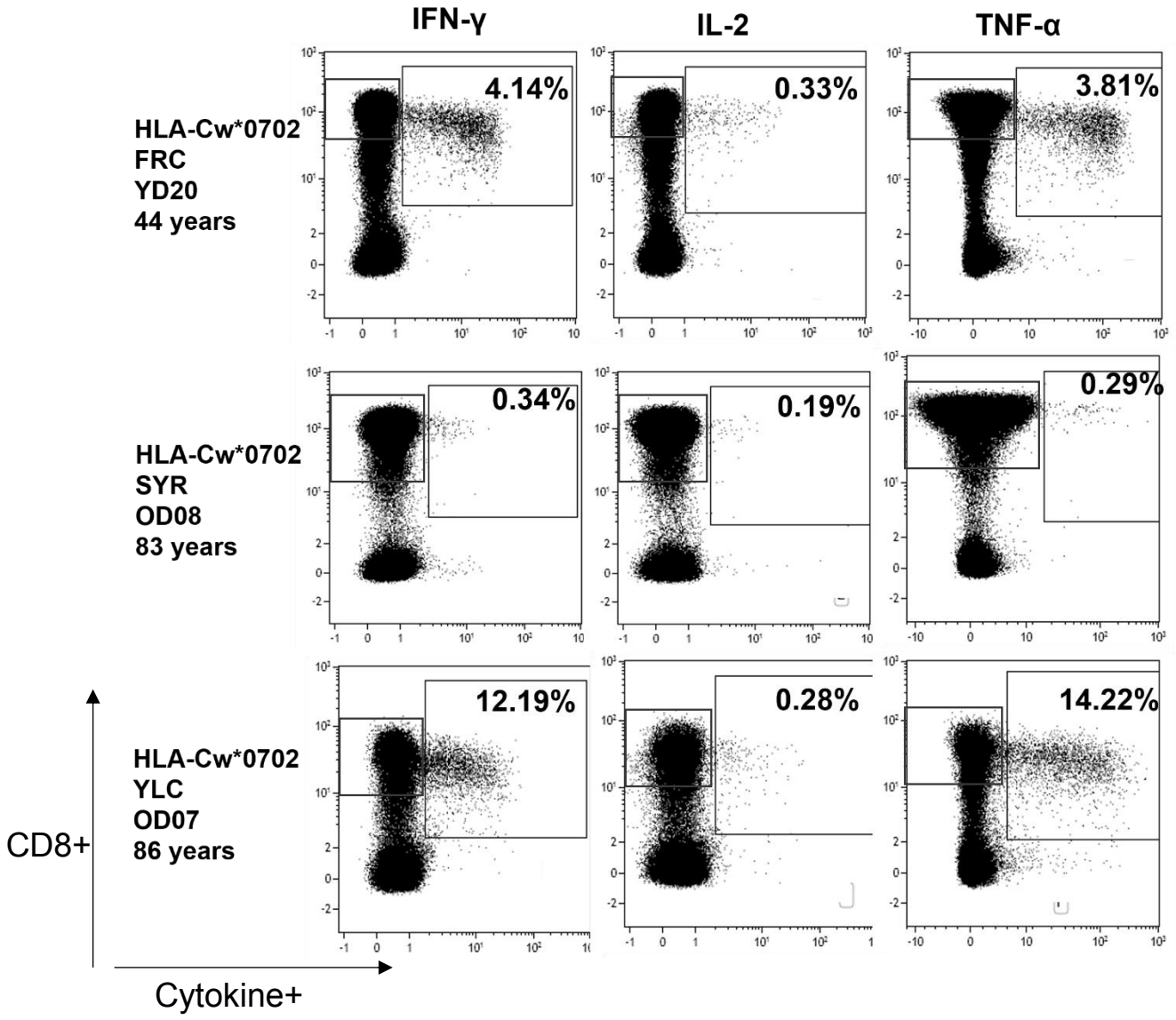


***Fig 8 – Ex vivo CD8+T-cell responses to the 'protected' HCMV epitopes within healthy seropositive individuals.*** PBMCs from HCMV seropositive donors were stimulated with HCMV peptide (final concentration 1µg/ml) for 6 hours followed by intracellular staining for IFN-γ, IL-2 and TNF-α to identify specific CD8+T-cell responses. The flow plots represent representative dot plots for each of the protected peptides to which specific CD8+T-cell responses were detected. The IFN-γ, IL-2 and TNF-α production are given in the left to right hand columns respectively. Unstimulated negative and SEB positive controls are provided in the top and second row respectively. In each case the HLA-restriction, peptide name, donor ID (appendix tables 1 and 4) donor age are provided on the left hand side of the plots. All data was analysed in Kaluza 1.3 software (Beckman Coulter). The percentages represent the percentage of activated CD8+T-cells producing cytokine of the total CD8+T-cell population. In all cases, the percentages shown have had the unstimulated control percentages subtracted.

identical (Appendix Table-2, 5). The UL84-derived HLA-A3-restricted RVD peptide elicited the single largest HLA-A-restricted response at 5.65% IFN-γ and 4.69% TNF-α in one donor of 52 years. The HLA-A11-restricted UL36-derived RSA peptide also elicited stable CD8+T-cell responses with age with an average remaining at 0.27% (IFN-γ) or increasing 0.21-0.26% (TNF-α) of the total CD8+T-cell response between the <70 vs >70 year categories.

The CD8+T-cell responses elicited by the HLA-B-restricted peptides were either smaller (average 0.04% IFN-γ, 0.02% IL-2 and 0.05% TNF-α) than those elicited by the HLA-A, or not present (HLA-B51-restricted peptides DAR, IPH, TLM and WPK peptides, n = 13, Fig-8, 9A/B). These also did not demonstrate a significant increase in size with age. The largest HLA-B-restricted response was elicited by the UL122 (IE-2 viral trans activator) derived NEG peptide at 2.31%, 0.13% and 3.98% of the total CD8+T-cell pool producing IFN-γ, IL-2 and TNF-α respectively within a donor of 48 years.

In comparison to the HLA-A/-B-restricted peptides, a HLA-Cw*0702-restricted CD8+T-cell epitope termed 'FRC', derived from the UL28 HCMV protein, was identified to elicit an average of 2.63% IFN-γ, 0.24% IL-2 and 2.44% TNF-α producing CD8+T -cells of the total CD8+T-cell pool within younger donors (<70 years)(Fig-9A/B). This epitope-specific CD8+T-cell pool increased to an average of 8.24% IFN-γ, 0.85% IL-2 and 10.37% TNF-α producing CD8+T-cells in older donors (>70 years)(Fig-9B). The FRC peptide also induced the highest frequency of responses in this donor cohort with 70% (28/40) of donors responding with IFN-γ and TNF-α CD8+T-cell production after FRC stimulation ranging from 0.03-32.25% and 0.03-31.07% of donors total CD8+T-cell pool respectively (Fig 9A/B). Interestingly, the FRC-peptide elicited higher percentages of CD8+T-cells producing IL-2 than the HLA-A/-B-restricted peptides (albeit a much lower magnitude than IFN-γ/TNF-α (0.03-4.23%) (Fig-9B). Lastly, the magnitude of both IFN-γ and TNF-α production induced by the FRC peptide increased significantly between donors <70 vs >70 years of age (Fig-9B)(Investigated in Chapter 4).

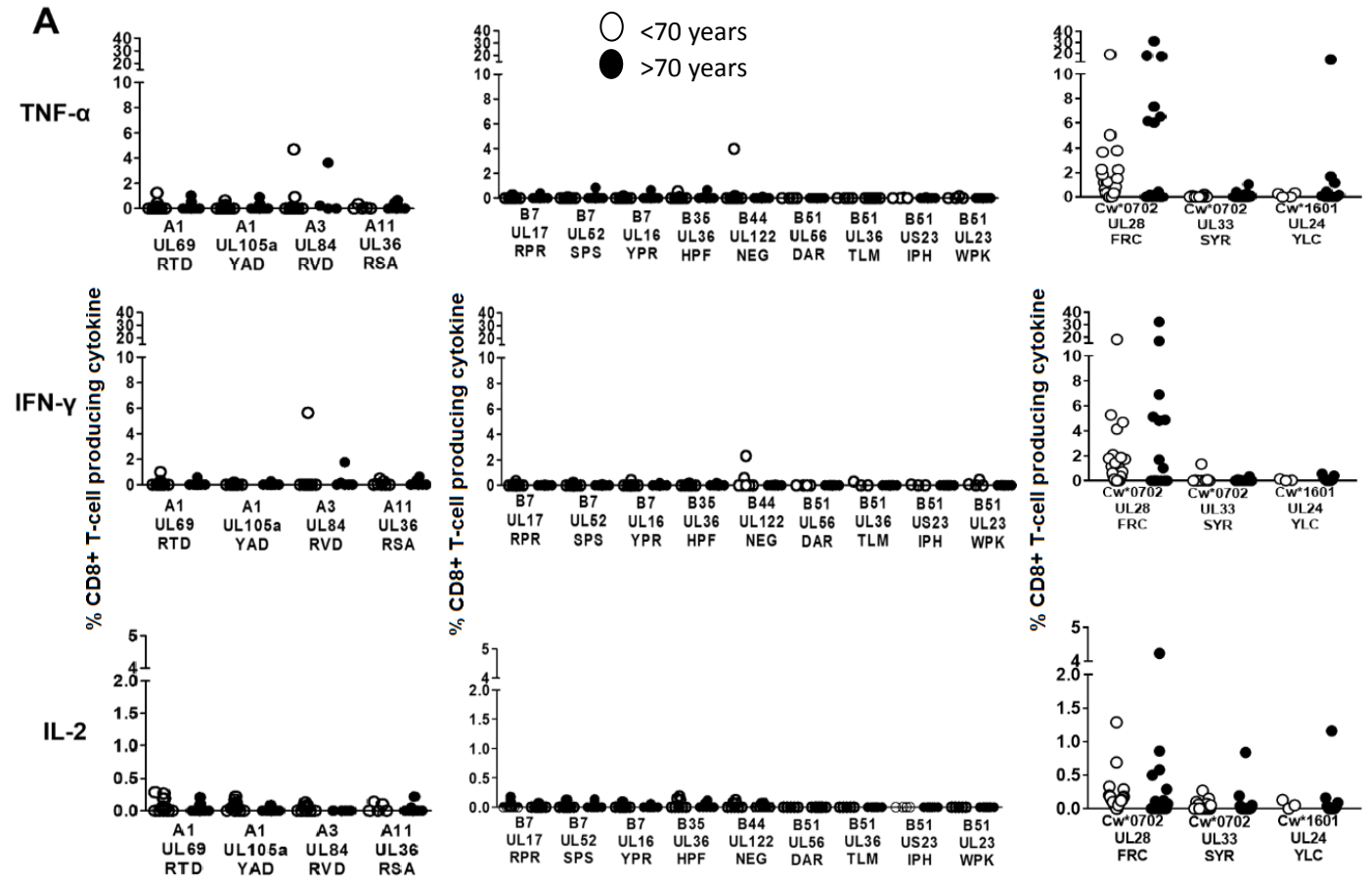
A
TNF-α
IFN-γ
IL-2
% CD8+ T-cell producing cytokine
<70 years
>70 years
A1 UL69 RTD
A1 UL105a YAD
A3 UL84 RVD
A11 UL36 RSA
B7 UL17 RPR
B7 UL52 SPS
B7 UL16 YPR
B35 UL36 HPF
B44 UL122 NEG
B51 UL56 DAR
B51 UL36 TLM
B51 US23 IPH
B51 UL23 WPK
Cw*0702 UL28 FRC
Cw*0702 UL33 SYR
Cw*1601 UL24 YLC

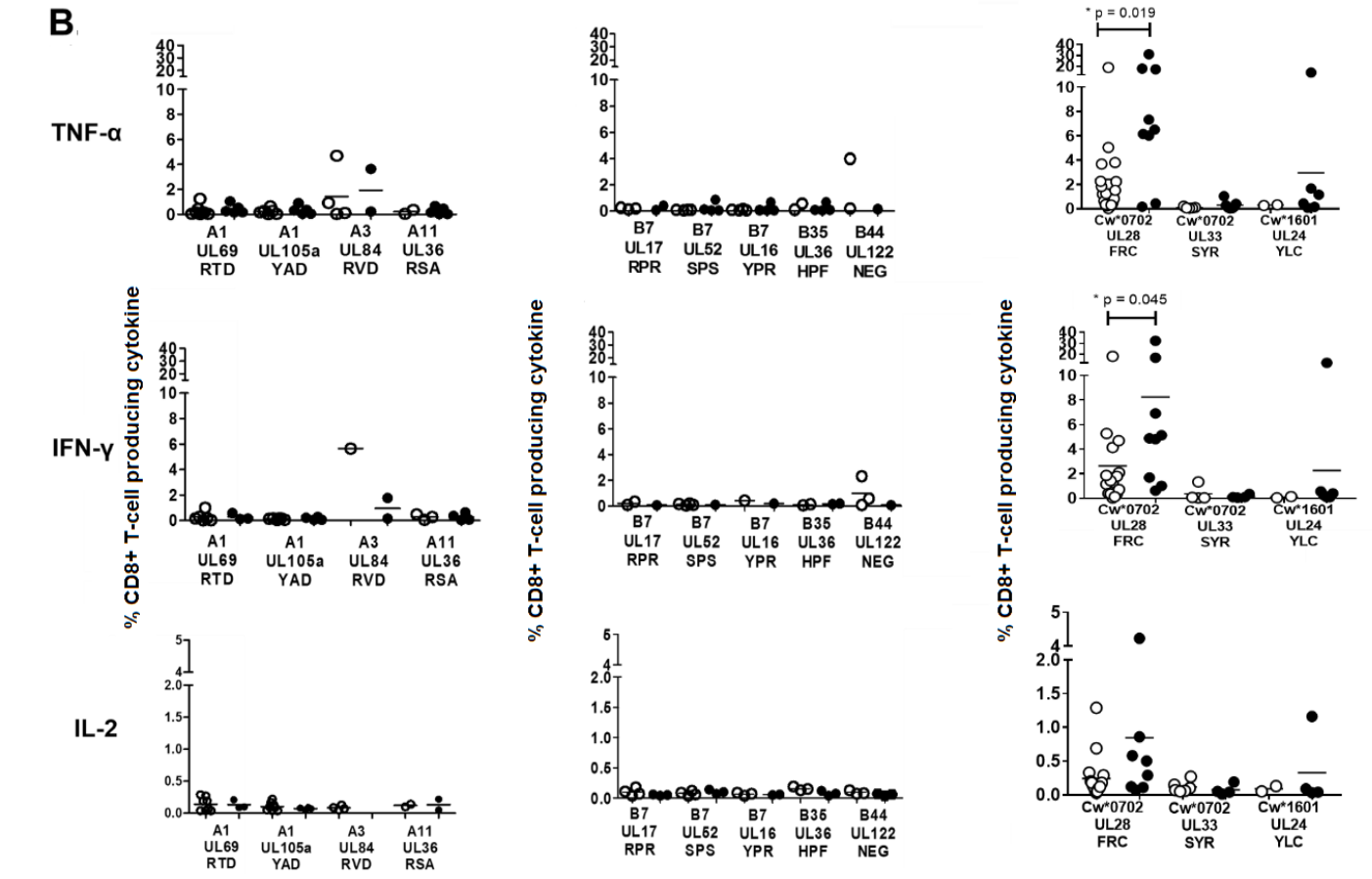
B
TNF-α
IFN-γ
IL-2
% CD8+ T-cell producing cytokine
* p = 0.019
* p = 0.045
A1 UL69 RTD
A1 UL105a YAD
A3 UL84 RVD
A11 UL36 RSA
B7 UL17 RPR
B7 UL52 SPS
B7 UL16 YPR
B35 UL36 HPF
B44 UL122 NEG
Cw*0702 UL28 FRC
Cw*0702 UL33 SYR
Cw*1601 UL24 YLC

***Fig 9 – Summary of the ex vivo responses detected against the 'protected' peptides producing IFN-γ, IL-2 and TNF-α***. PBMCs from HCMV seropositive donors were stimulated with HCMV peptide (final concentration 1µg/ml) for 6 hours followed by intracellular staining for IFN-γ, IL-2 and TNF-α to identify specific CD8+T-cell responses. Younger (<70 years) vs older (>70 years) donors were screened for ex vivo CD8+T-cell responses to the protected CD8+T-cell peptides. The open circles represent donors <70 years of age. Black circles represent donors >70 years of age. A) Summary of all negative and positive CD8+T-cell responses specific for the protected peptides detected in young vs older donors. The TNF-α, IFN-γ and IL-2 production elicited by the peptides are provided in the top, middle and bottom rows respectively. The HLA-A, -B and –C restricted peptides are provided in the left, middle and right hand columns respectively. B) Summary of the positive CD8+T-cell responses detected towards the protected peptides within young vs older donors. Lines represent mean of all positive CD8+T-cell responses obtained for each protected peptide. The TNF-α, IFN-γ and IL-2 production elicited by the peptides are provided in the top, middle and bottom rows respectively. The HLA-A, -B and –C restricted peptides are provided in the left, middle and right hand columns respectively. Statistical significance was obtained using multiple Mann Whitney tests in Graphpad Prism 6 with * as a p-value < 0.05.

It must be noted that statistical significance of the FRC-specific CD8+T-cell populations was observed after conducting multiple Mann Whitney tests between the <70 and >70 donor cohorts and could be a result of statistical chance. Any statistics obtained using multiple comparisons will be herein stated within figure legends.

CD8+T-cell responses to a further two HLA-C-restricted epitopes (HLA-Cw*0702-restricted UL33-derived SYR and HLA-Cw*1601-restricted UL24-derived YLC – Table-7) were detectable in 25% (8/32) and 62% (8/13) donors respectively ranging from 0.04%-0.34% and 0.04%-1.16%. The YLC-specific CD8+T-cell responses did increase with age, however, these were not significant and in large due to one large YLC response of 12.19% IFN-γ, 1.16% IL-2 and 14.22% TNF-α within a single donor of 86 years (Fig-9B and appendix tables-1-6) The SYR-specific CD8+T-cell TNF-α production increased slightly with age (0.06%-0.17%) but again was not significant.

The US2-11 gene region products therefore do not prevent the *in vivo* induction of a primed CD8+T-cell response to novel peptide-epitopes that were identified utilising the RV798 mutant. In addition, an immunodominant CD8+T-cell response was detected in this cohort specific for a HLA-C-restricted HCMV-specific CD8+T-cell epitope termed 'FRC' derived from the UL28 protein that is expressed in the IE phase of the HCMV lifecycle.

## 3.2 – The phenotypic characterisation of the *ex vivo* 'protected' peptide specific CD8+T-cell populations by flow cytometry

Previous studies have demonstrated that the *ex vivo* CD8+T-cell memory phenotype between CD8+T-cell populations specific for a range of differing HCMV antigens, including UL83 (pp65), UL82 (pp71), UL123 (IE-1), UL122 (IE-2), UL99, UL28, UL48, US29, US32, UL55 (gB), and US3 are not significantly different to each other [236]

Next in the investigation we wished to phenotypically characterise the CD8+T-cell responses to the protected peptides identified in the absence of the US1-11 gene region. It was hypothesised that during a WT (US2-11 gene region intact) infection they may be infrequently presented to the immune system. Resulting in a CD8+T-cell population with a less differentiated phenotype.

The RTD, YAD and FRC peptides were selected for MHC-I tetramers to be obtained from the NIH tetramer facility. They were the most frequent HLA-A and HLA-C responses respectively and would allow a comparison between a 'stable' vs 'immunodominant' peptide. Unfortunately, despite the efforts of both our laboratory and the NIH tetramer facility an FRC MHC-I tetramer could not be obtained. Therefore all the protected peptide-specific CD8+T-cell responses were phenotyped after ICS to identify specific cells by TNF-α production (phenotype gating strategy provided in Fig-10).

CD8+T-cell responses specific for the HLA-A1-restricted RTD and YAD, HLA-A3-restricted RSA, HLA-B44-restricted NEG, HLA-Cw*0702-restricted FRC and SYR and lastly HLA-Cw*1601-restricted YLC peptides were subsequently phenotyped after 6 hours peptide stimulation (Fig-11) (Table-7).

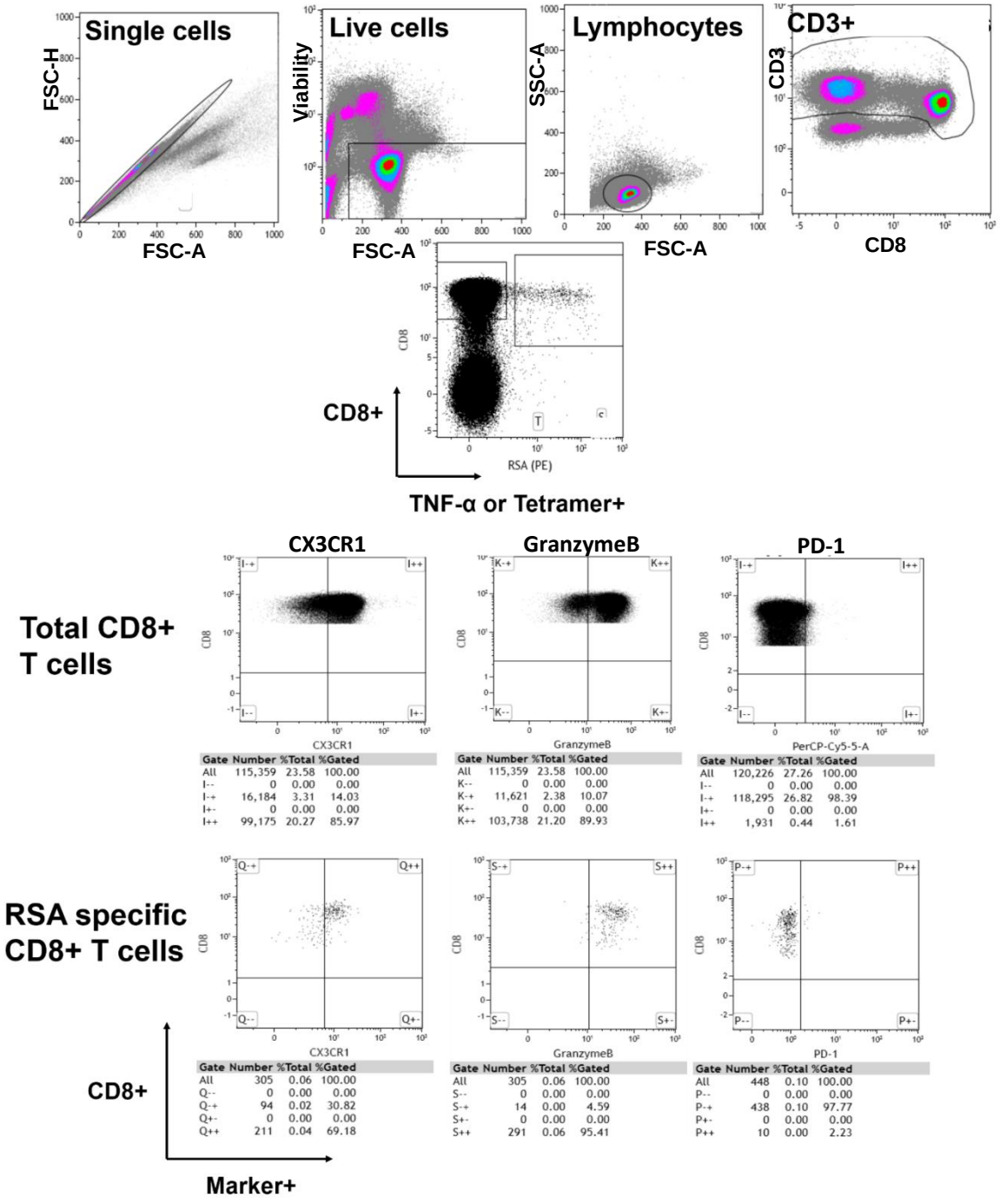


***Fig 10 – Gating strategy of the phenotypical analysis of ex vivo HCMV-specific CD8+T-cell responses by ICS after peptide stimulation.*** The expression of single cell phenotypic markers was assessed on epitope-specific CD8+T-cells after peptide stimulation. PBMCs from HCMV seropositive donors were stimulated with HCMV peptide (final concentration 1µg/ml) for 6 hours followed by intracellular staining for TNF-α to identify specific CD8+T-cell responses and allow phenotypic characterisation. PBMCs were stained with the antibody panels outlined in Table-4. Single, viable, $CD3^{+}CD8^{+}$ lymphocytes were sequentially gated on prior to the analysis of phenotypic marker expression. Gates for single markers were placed using the total CD8+T-cell population ($CD3^{+}CD8^{+}$) to identify negative vs positive populations for the marker in question. The same gate was then applied to the epitope specific CD8+T-cells. Included here is an example of HLA-A3-restricted RSA-specific cells after peptide stimulation for 6 hours, and representative dot plots demonstrating CX3CR1, GranzymeB and PD-1 expression.

The CD8+T-cells were investigated for the expression of several phenotypic markers. Firstly, the T-cell homing marker CCR7 in combination with the CD45 isoforms – CD45RA and CD45RO - were included within the analysis. This allowed the characterisation of the CD8+T-cell responses into memory CD8+T-cell subset compartments [108, 237].

The T-cell co-stimulatory markers CD27 and CD28 were used to determine the antigen differentiation status of the CD8+T-cell responses The loss of these molecules is an indicator of a larger proliferative history of the CD8+T-cell and typically indicates a T-cell further down the differentiation pathway i.e. late antigen differentiated [70, 238].

Cytotoxicity markers perforin, granzymeB, and NKG2D were also investigated. This was to assess the cytotoxic potential these CD8+T-cells possess upon antigen encounter. Additionally, the activation state of the CD8+T-cells was analysed by the inclusion of the CD38 marker.

The exhaustion T-cell markers PD-1 and TIM3 were included. This was to assess whether the protected-peptide specific CD8+T-cells were functionally exhausted *in vivo*.

Lastly, CMV-specific CD8+T-cells have been identified as having a unique high expression of the CX3CR1 fractalkine receptor hypothesised to home these T-cells to the endothelium [2, 72]. This marker was therefore also included within the analysis.

### 3.2.1 – Single cell marker expression

First, the expression of single cell markers was analysed on the protected peptide-specific CD8+T-cell responses (Fig-11). Overall, there were distinct phenotypic patterns based upon the HLA restriction of the CD8+T-cell responses and between epitope specificities) (Fig-11). However, no significance difference was obtained when looking at the expression of single cell markers – due in part to one HLA-B-restricted CD8+T-cell response being phenotyped (Fig-11).

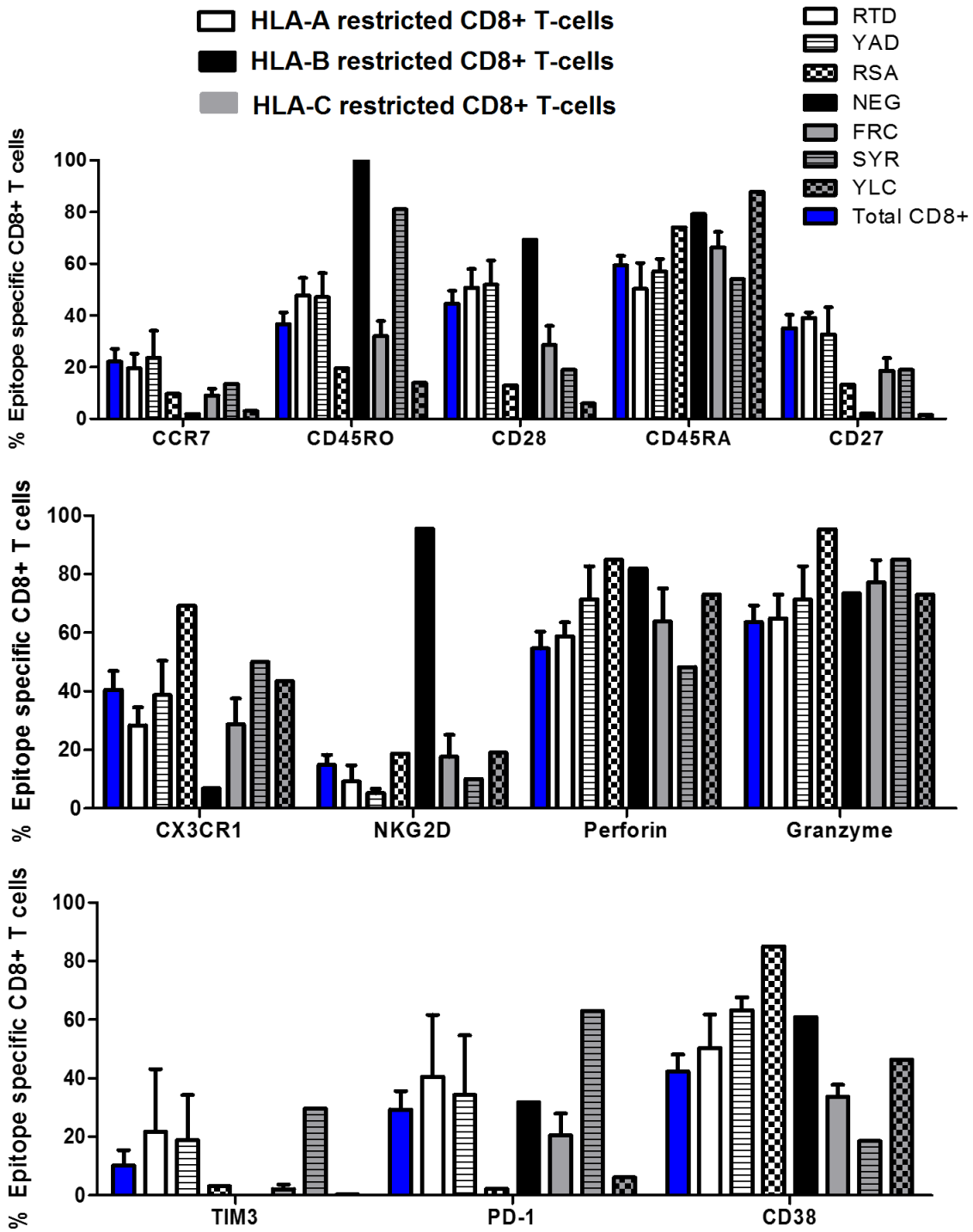


***Fig 11 – Ex vivo phenotype of protected peptide specific CD8+T-cell responses determined by flow cytometry after peptide stimulation and ICS.*** The expression of single cell markers on the HCMV-specific CD8+T-cells was assessed. PBMCs from HCMV seropositive donors were stimulated with HCMV peptide (final concentration 1µg/ml) for 6 hours followed by intracellular staining for TNF-α to identify specific CD8+T-cell responses and allow phenotypic characterisation. PBMCs were stained with the antibody panels outlined in Table-4. Graphs represent the single marker *ex vivo* phenotype of the individual HCMV protected peptide-specific CD8+T-cell populations. Epitope-specific CD8+T-cell responses identified by ICS – gating strategy provided in Fig-7. HLA-A-restricted CD8+T-cell responses are indicated by white or white patterned bars, HLA-B-restricted CD8+T-cell responses indicated by the black bar and HLA-C-restricted CD8+T-cell responses by grey or grey patterned bars. The blue bars represent the average *ex vivo* phenotype of the total CD8+T-cell responses excluding epitope-specific CD8+T-cells n =17. Bars represent mean and those without error bars n = 1. Error bars represent SEM. RTD and YAD n = 3 and 4. FRC n = 9.

Therefore next the phenotypic results were pooled depending upon whether the CD8+T-cell responses were HLA-A, -B or –C-restricted. When the *ex vivo* CD8+T-cell responses were pooled statistical significance was obtained with regards to the expression of single surface markers. Clear patterns between the HLA-A and –C-restricted CD8+T-cells emerged (Fig-12).

The pooled HLA-A CD8+T-cell responses, compared to the -B and –C restricted, presented with the following overall phenotype (Fig-12);

**$CCR7^{High}CD54RO^{Low}CD45RA^{Low}/CD28^{High}CD27^{High}/CX3CR1^{High}NKG2D^{low}Perforin^{high}GranzymeB^{high}Tim3^{High}PD\text{-}1^{High}CD38^{High}$.** The expression of the CD27/CD28 co-stimulatory molecules is indicative that the HLA-A responses are of an earlier antigen driven differentiated phenotype with a lower proliferative history.

The HLA-B-restricted NEG-specific CD8+T-cell response, compared to the –A and –C restricted, presented with the following phenotype (Fig-12);

**$CCR7^{neg}CD45RO^{high}CD45RA^{high}/CD28^{high}CD27^{Neg}/CX3CR1^{low}NKG2D^{High}Perforin^{high}GranzymeB^{high}/Tim^{Neg}\text{-}Pd\text{-}1^{High}CD38^{high}$**

Indicative that the HLA-B NEG-specific response is of an intermediate antigen driven phenotype as defined by Appay et al [70], having downregulated CD27 and having high cytotoxicity indicated by NKG2D expression. The co-expression of CD45RA/RO has identified T-cells in an intermediary transitional state [239].

The pooled HLA-C-restricted CD8+T-cell responses, compared to the –A and –B restricted, presented with the following phenotype (Fig-12);

**$CCR7^{low}CD45RO^{Low}CD45RA^{high}/CD28^{Low}CD27^{Low}/CX3CR1^{High}NKG2D^{low}Perforin^{high}GranzymeB^{high}/Tim3^{low}PD\text{-}1^{High}CD38^{Low}$.**

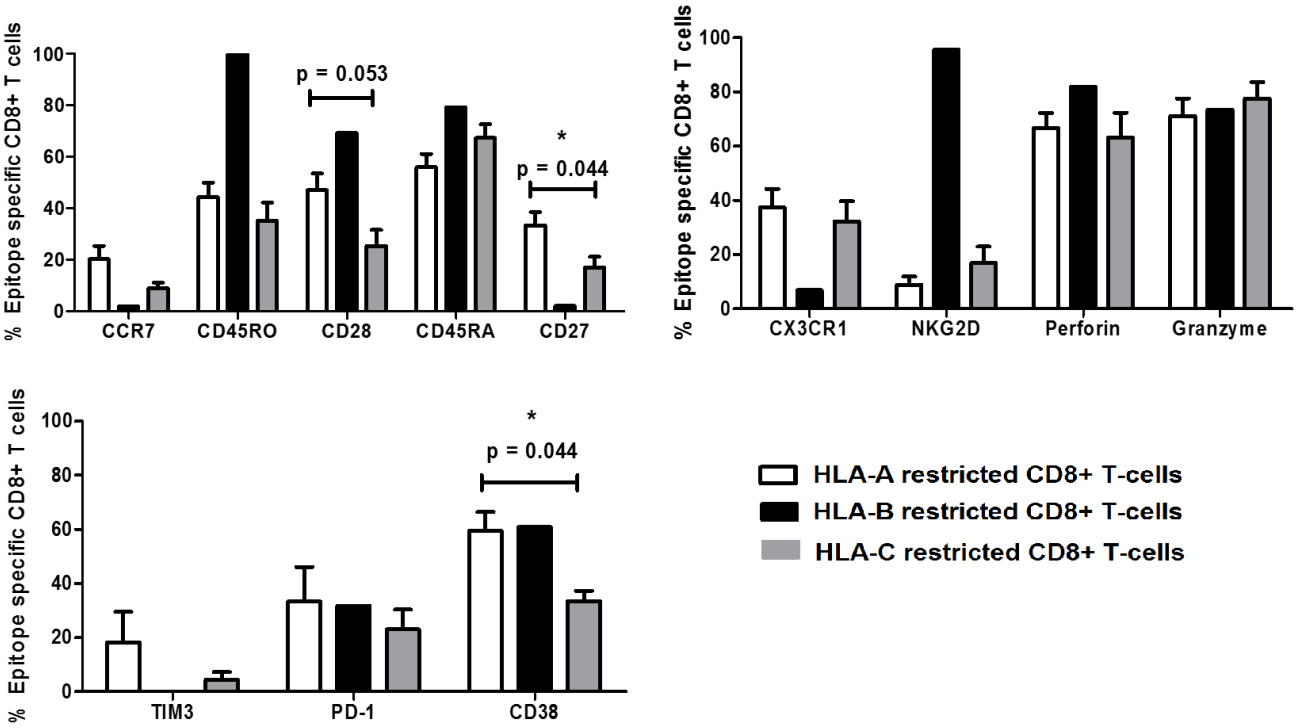


***Fig 12 – The ex vivo phenotype of the protected peptide CD8+T-cell populations when characterised based upon HLA-A, -B or –C-restriction.*** The expression of single cell markers on the pooled HCMV-specific CD8+T-cells was assessed categorised on HLA-restriction. PBMCs from seropositive donors were stimulated with HCMV peptide (final concentration 1µg/ml) for 6 hours followed by intracellular staining for TNF-α to identify specific CD8+T-cell responses and allow phenotypic characterisation. PBMCs were stained with the antibody panels outlined in Table-4. The phenotypes obtained for the individual epitope-specific CD8+T-cell responses obtained in Fig-11 were pooled deepening on whether the CD8+T-cells were HLA-A, -B or –C restricted. The bars represent the mean expression of that particular marker within the pooled CD8+T-cell responses and error bars SEM. The pooled HLA-A CD8+T-cell responses included the HLA-A1 RTD and YAD and HLA-A11 RSA-specific CD8+T-cells, n = 7. The HLA--B consisted of the NEG-specific CD8+T-cell responses, n = 1. The pooled HLA–C CD8+T-cell responses include the FRC-, SYR- and YLC-specific CD8+T-cells, n = 11. Those without error bars represent n = 1. Statistical significance was obtained using multiple Mann Whitney tests in Graphpad 6 with a p value < 0.05.

The HLA-C CD8+T-cells expressed significantly lower levels of CD27 compared to the HLA-A-restricted CD8+T-cells (p = 0.044, Fig-12). The HLA-C CD8+T-cells also expressed lower levels of CD28 compared to the pooled HLA-A responses (p = 0.053) (Fig-12). Interestingly, the HLA-C restricted responses had a significantly lower expression of the CD38 activatory marker despite a phenotype suggestive of frequent antigen encounter (Fig-12).

This is indicative that the HLA-C-restricted responses are of a later antigen driven differentiation phenotype compared to the HLA-A-restricted populations [70]. This $T_{EMRA}$ phenotype is suggestive of memory-inflated CD8+T-cell populations described previously within the murine model [105, 240].

3.2.2 – Memory CD8+T-cell compartment

In the murine model, stable CD8+T-cell responses have been identified as belonging to the $T_{CM}$ compartment and inflationary to the $T_{EMRA}$. After observing that the HLA-C CD8+T-cell populations displayed a more overall $T_{EMRA}$ like phenotype ($CCR7^{low}CD45RO^{+}CD28^{low}CD45RA^{high}CD27^{low}$) compared to HLA-A-restricted, it was next identified what CD8+T-cell memory compartments they occupy. In this section $T_N$ (naïve like profile), $T_{CM}$, $T_{EM}$ and $T_{EMRA}$ were identified as $CCR7^{+}CD45RA^{+}$, $CCR7^{+}CD45RA^{-}$, $CCR7^{-}CD45RA^{-}$ and $CCR7^{-}CD45RA^{+}$ respectively (gating strategy is provided in Fig-13A).

First, the CCR7 vs CD45RA expression was analysed on the individual HCMV-specific CD8+T-cell responses. The HLA-Cw*1601-restricted SYR, and HLA-A1-restricted YAD- and RTD-specific CD8+T-cell populations contained the largest populations of $T_N$ CD8+T-cells (10.81%, 11.21% and 7.60% respectively) (Fig-13B).

The HLA-A1-restricted RTD and YAD CD8+T-cell responses consisted of the largest percentage of $T_{CM}$ (identified as $CCR7^{+}CD45RA^{-}$) at 12.48% and 12.52% respectively, followed by the HLA-A11-restricted RSA-specific CD8+T-cell response at 6.42% of the total epitope-specific CD8+T-cell response (Fig-13B).

The HLA-Cw*0702 SYR-specific CD8+T-cell population was comprised of the largest percentage of $T_{EM}$ (identified as $CCR7^{-}CD45RA^{-}$) at 37.84% (Fig-13B).

The HLA-Cw*0702-restricted FRC-, HLA-A11-restricted RSA-, HLA-B44-restricted NEG- and HLA-Cw*1601-restricted YLC-specific CD8+T-cell responses comprised the largest percentage of $T_{EMRA}$ (identified as $CCR7^{-}CD45RA^{+}$) at 58.59%, 66.86%, 74.34% and 82.48% of the total epitope-specific CD8+T-cell response respectively (Fig-13B).

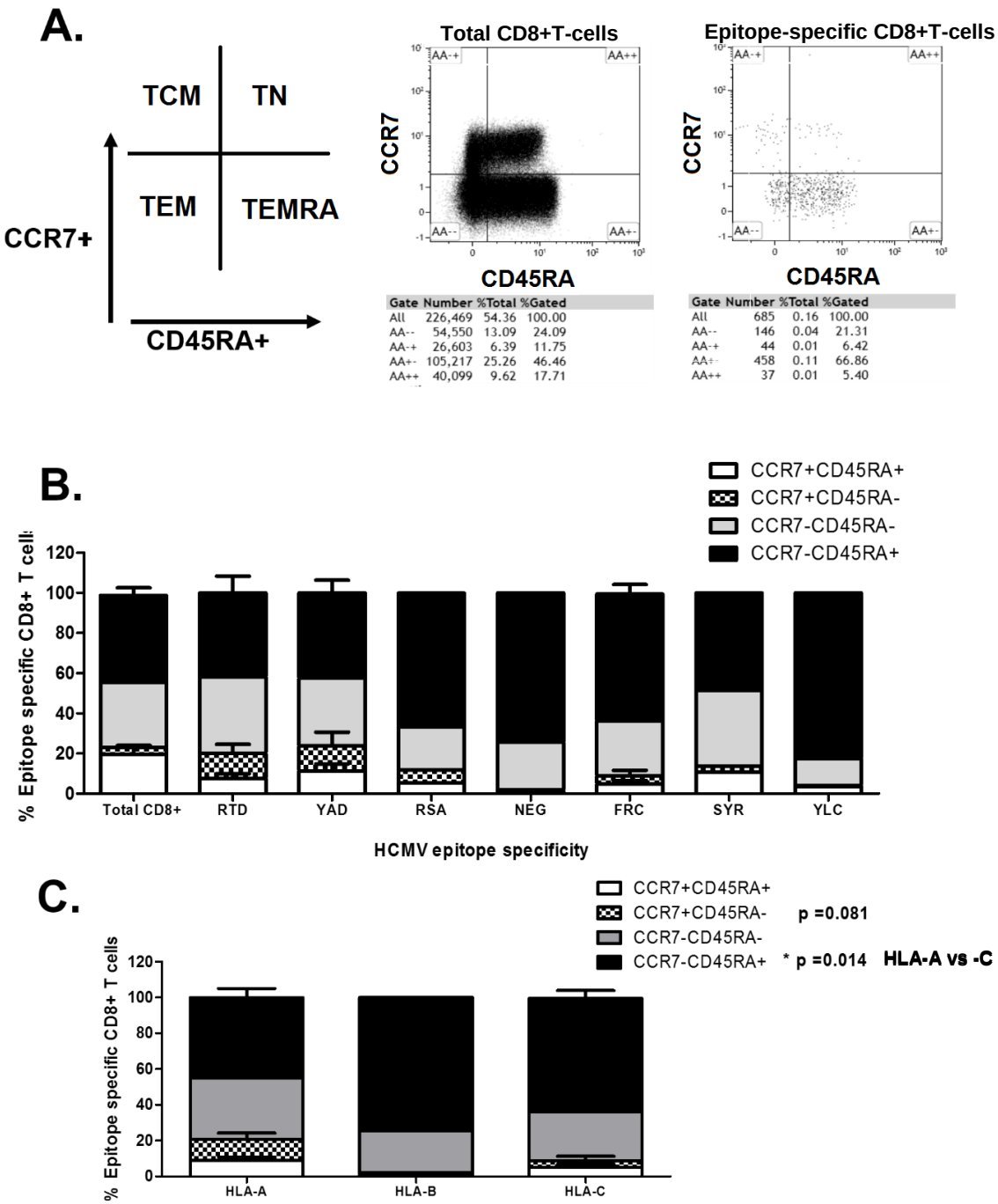


***Fig 13 – CCR7 vs CD45RA memory phenotype of the ex vivo CD8+ protected peptide-epitope responses as detected by flow cytometry after peptide stimulation and ICS.*** The memory compartment phenotype of HCMV-specific CD8+T-cells was assessed by CCR7 vs CD45RA expression. PBMCs from seropositive donors were stimulated with HCMV peptide (final concentration 1µg/ml) for 6 hours followed by intracellular staining for TNF-α to identify specific CD8+T-cell responses before phenotypic characterisation. PBMCs were stained with the antibodies outlined in Table-4. A) Gating strategy for identifying the distinct CD8+T-cell memory compartments in Kaluza 1.3 software (Beckman Coulter). CD3+CD8+T-cells and then epitope-specific cells were gated upon in a hierarchal manner as outlined in Fig-7. CD45RA+, CCR7+ CD8+T-cells were identified in the total CD8+T-cell population (left hand flow plot) and this gate applied to the epitope-specific CD8+T-cells (right hand flow plot). B) Summary of the CCR7 vs CD45RA memory phenotype of the individual protected epitope-specific CD8+T-cell responses C) Summary of the CCR7 vs CD45RA memory phenotype of the pooled CD8+T-cell responses to the protected peptides based on their HLA-A, -B, or –C-restriction. The pooled HLA-A-restricted CD8+T-cell responses included the HLA-A1-restricted RTD and YAD and HLA-A11-restricted RSA-specific CD8+T-cells, n = 7. The HLA-B-restricted consisted of the NEG-specific CD8+T-cell responses, n = 1. The pooled HLA–C-restricted CD8+T-cell responses include the FRC-, SYR- and YLC-specific CD8+T-cells, n = 11. B/C) Bars represent mean and error bars SEM. Those without error bars n = 1. RTD N =4, YAD n = 3, FRC n = 9. Statistical significance was conducted in Graphpad prism 6 using multiple Mann Whitney tests with * as a p value < 0.05.

Next, the CCR7 vs CD45RA expression was analysed on the pooled HLA-A- vs –B vs –C-restricted CD8+T-cell populations. The pooled HLA-C CD8+T-cell responses had a significantly decreased proportion of $T_{CM}$ ($CCR7^{+}CD45RA^{-}$) at 5.17% than the pooled HLA-A-restricted responses at 8.96% (Fig-13C). In addition they had a significantly increased percentage of $T_{EMRA}$ CD8+T-cells ($CCR7^{-}CD45RA^{+}$) compared to the pooled HLA-A-restricted CD8+T-cell population - 64.18% vs 44.84% ($p = 0.014$). The pooled HLA-C CD8+T-cell populations also had a decrease in the fraction of $T_{CM}$ compared to the HLA-A ($CCR7^{+}CD45RA^{-}$) ($p = 0.081$) (Fig-13C). Thus corroborating the earlier observation that the HLA-C-restricted CD8+T-cells are of a general $T_{EMRA}$ phenotype whilst the HLA-A-restricted CD8+T-cells display a $T_{CM}$ phenotype (Fig-12).

3.2.3 – Antigen differentiation status

Next we utilised the categorisation method of CD8+T-cells in differing differentiation statuses defined by Appay et al. whereby the acquisition of a $CD27^{-}CD28^{-}$ phenotype represents a late antigen differentiated memory CD8+T-cell, $CD27^{+}CD28^{-/}CD27^{-}CD28^{+}$ an intermediate and $CD27^{+}CD28^{+}$ a CD8+T-cell early in the differentiation pathway [70].The association of a progressively more antigen differentiation status, indicated by the loss of CD27/CD28, has also been identified as an indicator of increased history of proliferative capacity [238].

The CD27 vs CD28 expression was first analysed on the individual HCMV-specific CD8+T-cell populations (gating strategy is provided in Fig-14A). The HLA-Cw*-0702-restricted FRC-specific CD8+T-cell populations had a significant decrease in the percentage of early differentiated CD8+T-cells ($CD27^{+}CD28^{+}$) compared to the HLA-A1-restricted RTD-specific CD8+T-cell populations (13.06% vs 31.83% respectively, p = 0.016, Fig-14B). The RTD-specific and YAD-specific CD8+T-cell populations comprised the largest proportion of early differentiated CD8+T-cells at 31.83% and 28.32% respectively (Fig-14B).

The HLA-B44-restricted NEG- and HLA-Cw*0702-restricted SYR-specific CD8+T-cell populations had the largest populations of $CD27^{-}CD28^{+}$ intermediate differentiated T-cells at 66.80% and 62.16%. The HLA-A11-restricted RSA, HLA-Cw*0702-restricted FRC and HLA-Cw*1601-restricted YLC populations had the largest percentage of late differentiated CD8+T-cells at 84.38%, 60.74% and 93.23% respectively (Fig-14B).

The CD27 vs CD28 expression was then subsequently interpreted when the CD8+T-cell responses were pooled into HLA-A, -B or –C-restriction categories. When the CD8+T-cell populations were pooled, the HLA-C restricted CD8+T-cells had a significantly decreased percentage of early differentiated CD8+T-cells at 9.28% compared to the HLA-A-restricted responses at 27.93% (Fig-14C). The HLA-B-restricted response was largely formed of $CD27^{-}CD28^{+}$ CD8+T-cells (66.8%) indicative of an intermediate phenotype [70].

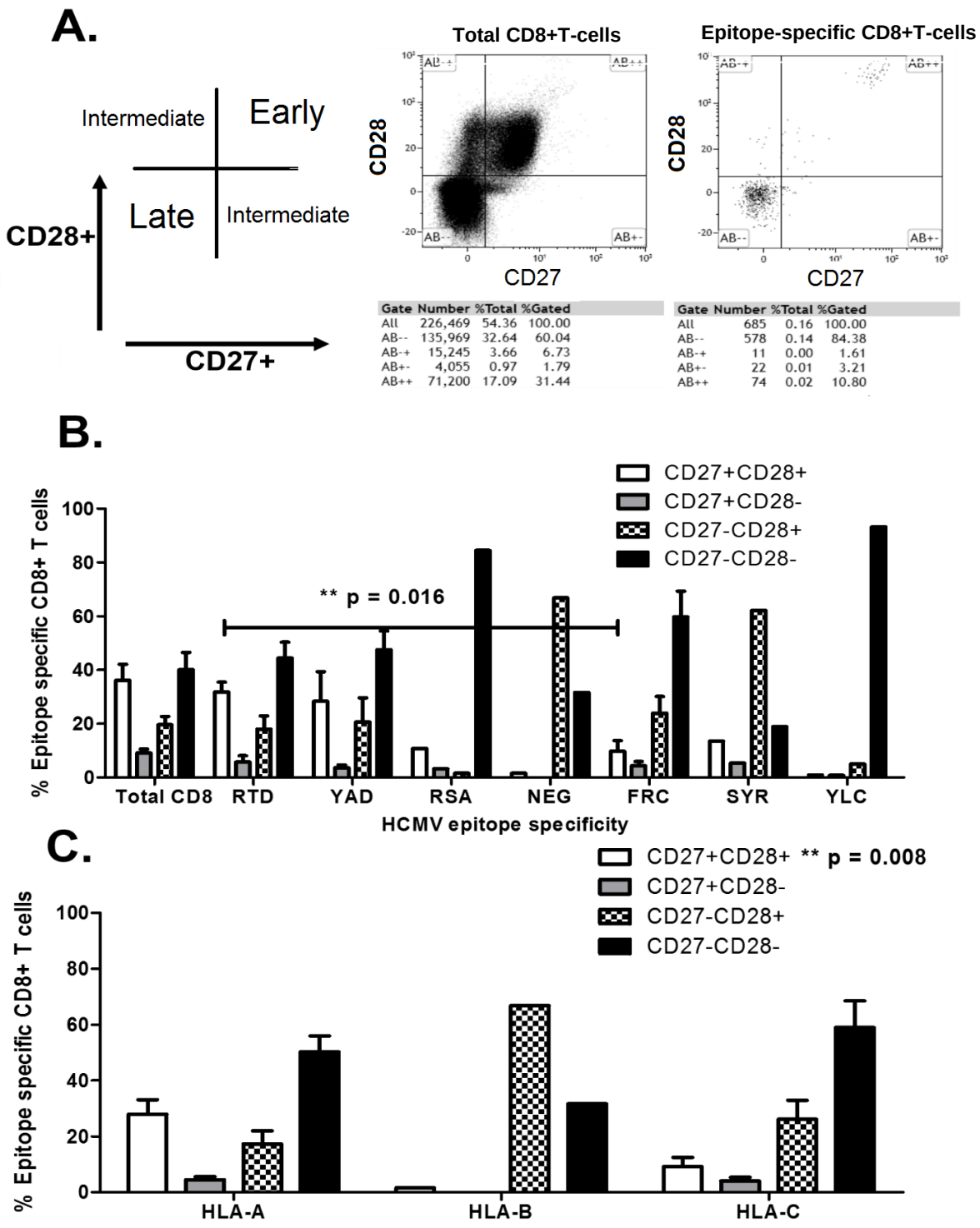


**Fig 14 – Antigen differentiation status of the ex vivo CD8+T-cell responses specific for the protected peptides.** The CD27 vs CD28 antigen differentiation status of HCMV-specific CD8+T-cells was assessed. PBMCs from seropositive donors were stimulated with HCMV peptide (final concentration 1µg/ml) for 6 hours followed by intracellular staining for TNF-α to identify specific CD8+T-cell responses before phenotypic characterisation. PBMCs were stained with the antibodies outlined in Table-4. A) Gating strategy used in Kaluza 1.3 software to identify early (CD27+CD28+), intermediate (CD27+, CD28-, CD27-CD28+) or late (CD27-CD28-) antigen differentiated epitope-specific CD8+T-cells. The CD8+ population was gated on as described in Fig-7. The CD27 and CD28 gate was placed using the total CD8+T-cell population (left hand flow plot) and then placed upon the epitope-specific CD8+T-cells (right hand flow plot) B) Summary of the stages of the antigen differentiated CD8+T-cell populations detected for all individual HCMV epitope-specific CD8+T-cell responses determined by CD27 vs CD28 expression. RTD N =4, YAD n = 3, FRC n = 9. Those without error bars n = 1 C) Summary of the antigen differentiation status detected within the pooled protected epitope-specific CD8+T-cell responses based upon HLA-A, -B or –C-restriction. The pooled HLA-A-restricted CD8+T-cell responses included the HLA-A1-restricted RTD and YAD and HLA-A11-restricted RSA-specific CD8+T-cells, n = 7. The HLA-B-restricted consisted of the NEG-specific CD8+T-cell responses, n = 1. The pooled HLA–C-restricted CD8+T-cell responses include the FRC-, SYR- and YLC-specific CD8+T-cells, n = 11. B/C) Bars represent mean and error bars SEM. Those without error bras n = 1. Statistical significance was obtained Graphpad Prism 6 with ** as a p value < 0.005 using multiple Mann-Whitney tests.

Lastly, in comparison to the HLA-A-restricted, the HLA-C-specific CD8+T-cells comprised a slightly larger percentage of late differentiated CD8+T-cells (Fig-14C) (50.24% compared to 58.94%).

Altogether, the memory phenotype and differentiation status data suggests the HLA-A-restricted CD8+T-cells are a lesser antigen differentiated $T_{CM}$ phenotype and the HLA-B-restricted of an intermediate differentiated phenotype. The HLA-C-specific CD8+T-cell populations were of a later differentiated $T_{EMRA}$ phenotype. This was largely due to the majority of responses phenotyped being specific to the HLA-Cw*0702-restricted FRC peptide. To ensure this late differentiated phenotype is a general feature of HLA-C-restricted CD8+T-cell populations, more donors and HLA-C peptide specific populations should be phenotyped.

**3.3 - Direct and cross presentation of the HCMV 'protected' peptides**

Antigens expressed during the L phase of the lifecycle are less likely to be directly presented when the US2-11 gene region products have also been expressed. However, CD8+T-cell responses against antigens expressed during the E-L stages of the viral lifecycle have been identified [58]. Thus, this indicates a role of cross-presentation in priming CD8+T-cells to the full antigenic repertoire of HCMV *in vivo* or implicates direct presentation by a cell type in which the US2-11 proteins cannot exert their immunomodulatory effects.

During the identification of these protected peptides during an RV798 (ΔUS2-11) infection, specific CD8+T-cell clones were unable to recognise these peptides during a WT infection *in vitro* of fibroblasts when the US2-11 gene region was present [82]. Manley et al. looked for recognition of these peptides at 24 and 48 hours post infection during AD169 and RV798 infection of APCs respectively. This raises the question to how these responses are generated *in vivo*. The first explanation could be that the peptides are presented directly to the immune response prior to the US2-11 gene products being able to impair MHC-I presentation. This may be before the 24 hours p.i. time-point during an AD169 infection that Manley et al. investigated. A second explanation is that cell types other than fibroblasts *in vivo* may be more efficient at presenting these protected peptides. A third explanation could be cross-priming of the CD8+T-cells by DCs.

This section aimed to identify if these peptides can be presented directly to specific CD8+T-cell clones by two different cell types during a productive infection *in vitro* – i.e. IE to L time-points. Furthermore it also sought to demonstrate the ability of DCs to cross present these peptide-epitopes to specific CD8+T-cell clones *in vitro*.

HLA-A1-restricted RTD and YAD-specific CD8+T-cell clones were first generated from the PBMCs of HCMV infected donors (YD4 and YD5 for RTD and YAD respectively)(Appendix tables 1 to 3) by isolating $CD8^+$ T cells producing IFN-γ after 3 hours peptide-stimulation using an IFN-γ secretion assay (Miltenyii Biotech, Table-2). These CD8+T-cells were then plated out on 96 well plates via a limiting dilution assay and maintained in culture for 14 days

with peptide-loaded LCL target cells. CD8+T-cell clone specificity was determined by IFN-γ ELISA of expanded wells. Examples of some of the specific CD8+T-cell clones obtained are provided in Fig-15.

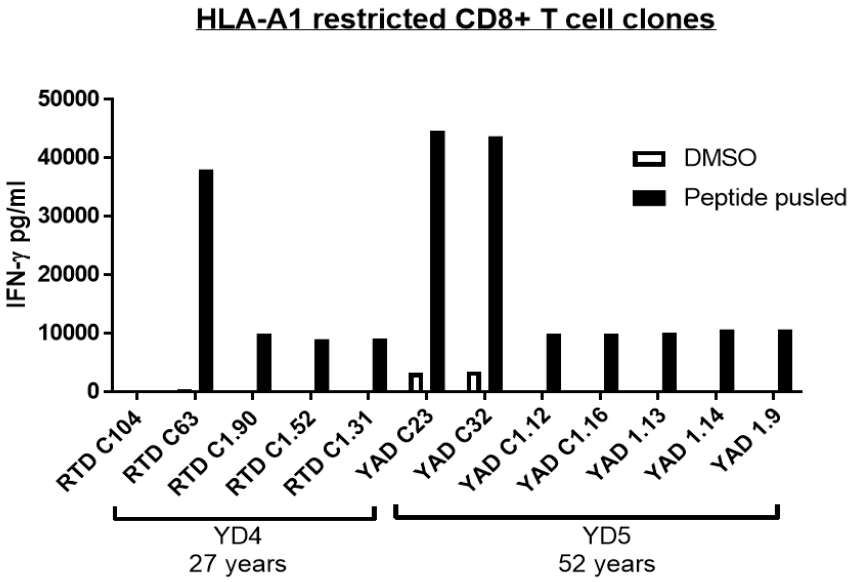


***Fig 15 – Generation of HLA-A1-restricted HCMV protected epitope specific CD8+T-cell clones in vitro.*** Specific CD8+T-cell clones for the UL69-derived RTD and UL105a derived YAD peptide were generated *in vitro* by isolating CD8+T-cells after 3 hours peptide stimulation of PBMCs with ether the RTD or YAD peptides by an IFN-γ catch assay (Miltenyi Biotech). This was followed by a limiting dilution. The PBMCs selected had previously identified ex vivo CD8+T-cell responses to the peptides in question. The graph demonstrates the representative IFN-γ production of RTD and YAD-specific CD8+ example clones determined by ELISA after O/N co-culture of the CD8+T-cell clones with DMSO control loaded (white bars) or peptide-loaded LCLs (black bars).

The functional avidity of the specific clones was subsequently determined via a peptide dilution assay (Fig-16). Clones were co-cultured O/N with HLA-matched peptide-loaded LCLs followed by an IFN-γ ELISA. The LCLs were loaded with a range of peptide concentrations from 50pg-50μg ($10^{-11}$-$10^{-5}$ $\log_{10}$M). Clones specific for the pp65-derived HLA-A2-restricted NLV peptide were generated by Dr Miriam Ciaurriz and Dr Annette Pachnio. These were kindly provided for the *in vitro* assays in this investigation.

The RTD-specific clones had an avidity range of 0.25μg-0.5μg (average $10^{-7}$ $\log_{10}$M) and the YAD-specific CD8+T-cell clones 0.025μg-0.25μg (average $10^{-8}$ $\log_{10}$M) (Fig-16). This was comparable to the avidity range of the NLV-specific clones of 0.025μg-0.25μg (average $10^{-8}$ $\log_{10}$M, Fig-16).

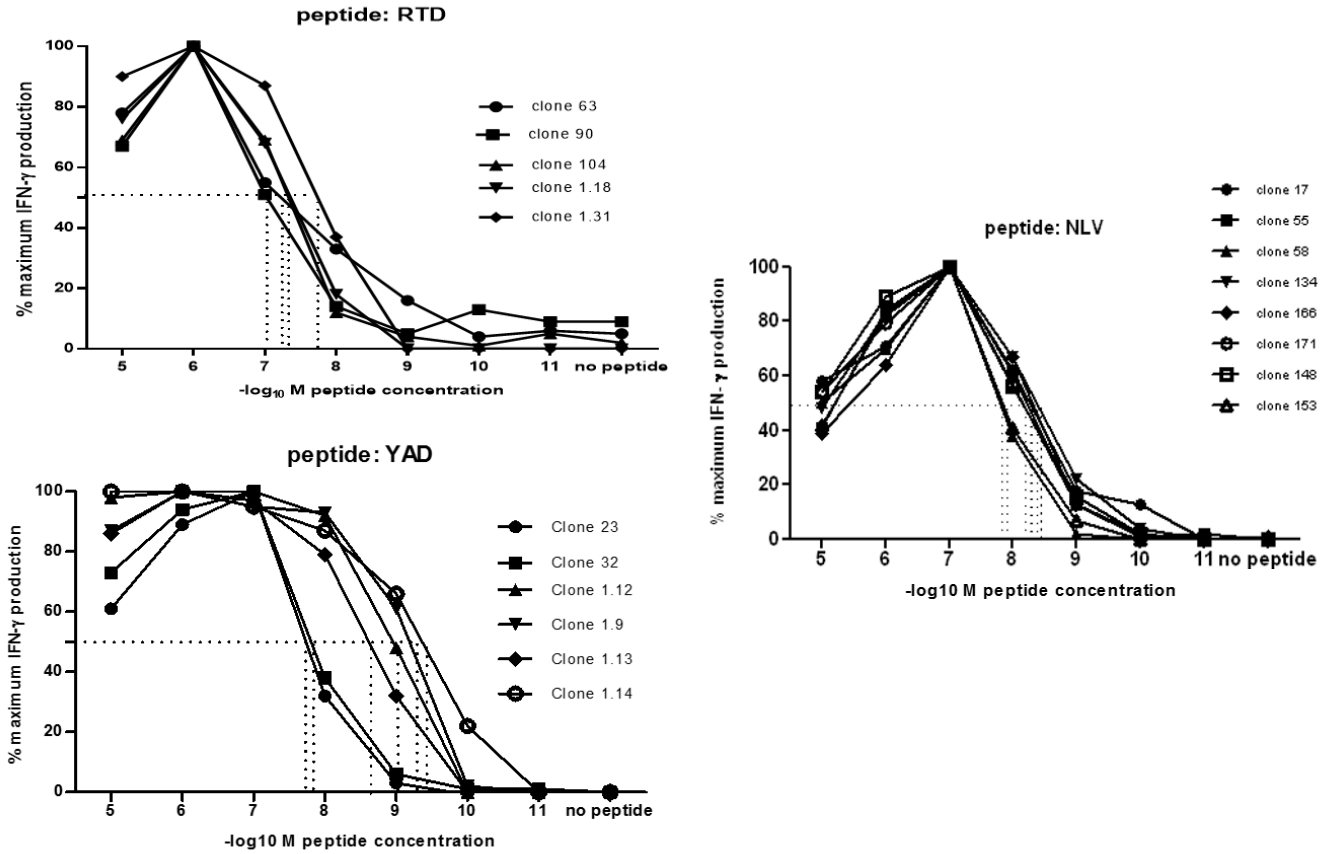


***Fig 16 – Functional avidity of Specific CD8+T-cell clones for the UL69-derived RTD and UL105a derived YAD peptides vs pp65-specific CD8+T-cell clones.*** Graphs demonstrate the functional peptide avidity ($EC_{50}$) of the RTD (top) and YAD (bottom) and NLV-specific (right) CD8+T-cell clones. $EC_{50}$ was determined as the concentration of peptide that induced the 50% maximal IFN-γ production. Specific CD8+T-cell clones were generated *in vitro* by an IFN-γ catch assay (Miltenyi Biotech) after 3 hours peptide stimulation assay of PBMCs with previously identified CD8+T-cell responses to the peptides in question followed by a limiting dilution.. CD8+T-cell clones were co-cultured O/N with LCLs loaded with peptide concentrations ranging from 50μg to 50pg followed by an IFN-γ ELISA. NLV-specific CD8+T-cell clones generated by Dr Miriam Ciaurriz, University of Birmingham, UK. Each curve represents an individual clones and dashed lines represent the $EC_{50}$ of the individual clone.

The RTD and YAD-specific CD8+T-cell clones were then used to test for the ability to recognise cognate peptide that is naturally processed during infection with CMV strains containing the WT US1-11 gene region (AD169 and Merlin) *in vitro* (Fig-17). This was compared to CD8+T-cell recognition during an RV798 infection lacking this region as a positive control due to their method of identification with the RV798 strain. The recognition of haematopoietic (monocytes) vs non-haematopoietic (fibroblasts) was also compared as non-haematopoietic cells have been implicated as either the initial priming cell type or cell type driving memory-inflation respectively.

The HLA-A1-restricted CD8+T-cell clones specific for the RTD and YAD peptides had differing recognition profiles depending upon the kinetics of expression of the protein from which they are derived (Fig-17).

During an AD169 infection of HLA-A1$^{+}$ healthy donor human fibroblasts, the E-L-expressed UL69-derived RTD peptide, which is also present within the incoming virion particle, was recognised by specific clones at IE-L time-points of an infection (6-72 hours) (Fig-17). The E-L-expressed, UL105a-derived YAD peptide that is not present within the incoming virus particles was recognised by specific CD8+T-cell clones at E-L to L times of an AD169 fibroblast infection (48-72 hours p.i) (Fig -17).

Both the RTD- and YAD-specific clones released a larger magnitude of IFN-γ at all time-points of a RV798 infection of the same fibroblasts compared to the level released during an AD169 infection (Fig-17).

As the AD169 strain is able to only infect fibroblasts *in vitro* as a result of mutations that are quickly acquired during passaging [241], the Merlin strain was used to analyse recognition of infected monocytes. Interestingly, recognition of the RTD peptide was lost at IE-E (6-24 hours p.i.) time-points of a monocyte infection. A small IFN-γ production was elicited at 24 and 72 hours p.i (Fig-17). The recognition of the YAD peptide during a Merlin infection of monocytes followed the same recognition profile as that in AD169 infected fibroblasts (48-72 hours p.i.) but at a lower magnitude of IFN-γ production (Fig-17).

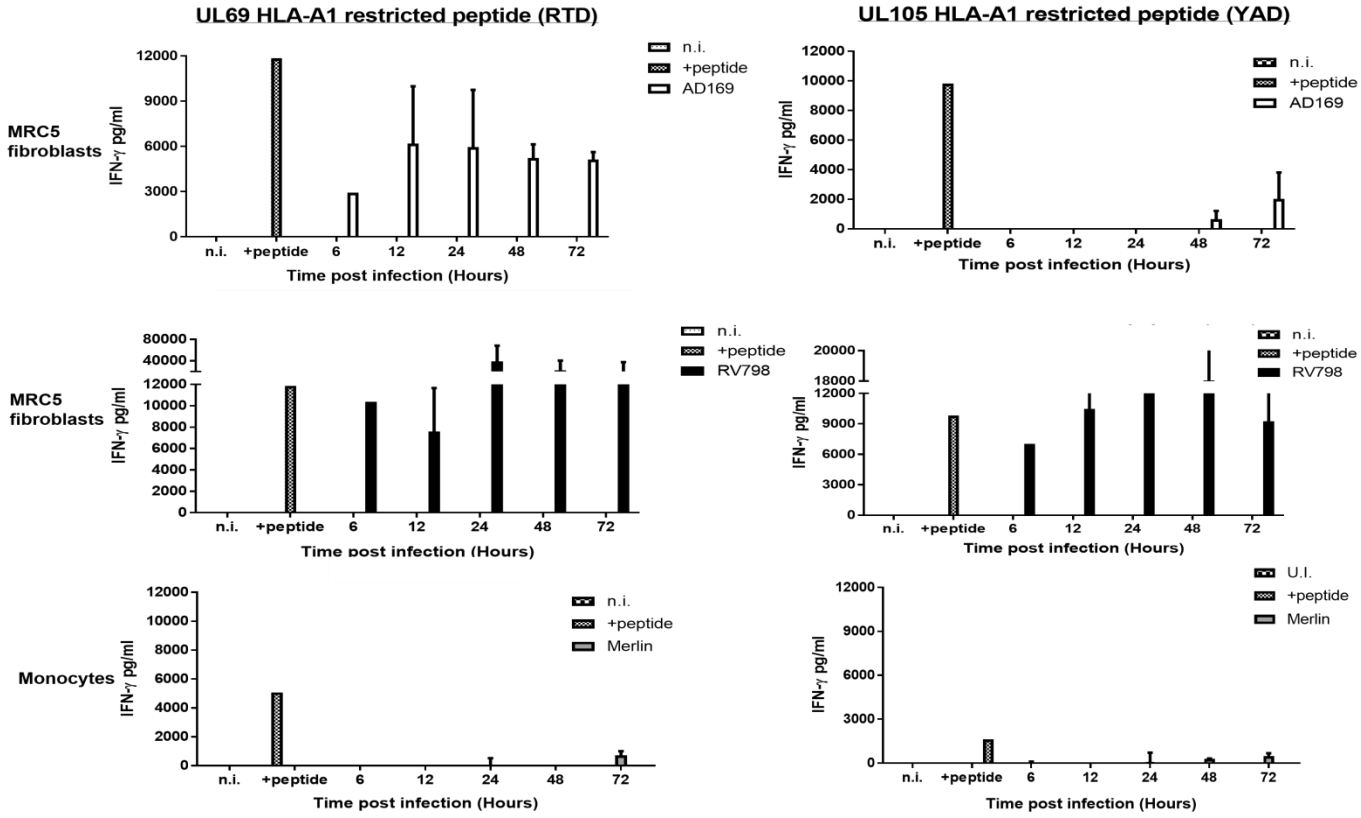


***Fig 17 – Recognition of fibroblasts and monocytes by HLA-A1-restricted HCMV-specific CD8+ T cell clones during a productive infection in vitro.*** The recognition of naturally processed and presented HLA-A1 RTD and YAD peptide during a HCMV infection was analysed by the incubation of 6-72 hour infected fibroblasts O/N with CD8+T-cell clones. Positive recognition was determined by IFN-γ release into the supernatant detected by IFN-γ ELISA. HLA-A1+ healthy human donor fibroblasts were infected with wither AD169 (top row) or RV798 (middle row) for 6-72 hours at an MOI of 5. Monocytes isolated form the PBMCs of donors with previously identified *ex vivo* CD8+T-cell responses were infected with the Merlin strain (bottom row) for 6-72 hours at an MOI of 5. At each time-point infected cells were incubated with 10 000 RTD- (left column) or YAD-specific (right column) CD8+T-cell clones. Bars represent the mean IFN-γ production in pg/ml per time-point by specific CD8+T-cell clones and error bars SEM. n = 1-5 per time-point for fibroblasts and n = 2 for monocytes.

To determine whether the RTD and YAD peptides could be cross presented by DCs, a protocol developed by Mr Calum Forrest (University of Birmingham) was conducted in a collaboration (Fig-18).

DCs were isolated from PBMCs from donors previously identified to have *ex vivo* CD8+T-cell responses to these peptides. The DCs were differentiated over a period of 4 days with IL-4 and GM-CSF and fed with antigen for 2 hours with either HCMV AD169 infected fibroblast lysate or mock infected fibroblast lysate (Dr Annette Pachnio and Miss Jusnara Begum, University of Birmingham UK). This was followed by the addition of R848 and Poly(I:C) for 24 hours. Following maturation, DCs were co-cultured with RTD- or YAD-specific HCMV-

specific CD8+T-cell clones O/N (16 hours) at an effector: target ratio of 10:1. An IFN-γ ELISA of the supernatant was conducted to determine CD8+T-cell activation (Fig-18). Positive and negative controls included the co-culture of CD8+T-cells with peptide or mock lysate. An additional negative control was provided by the culture of CD8+T-cells only O/N. NLV-specific clones were included in the assay as the pp65 peptide has been demonstrated within the literature to be cross presented to DCs *in vitro* [169, 170].

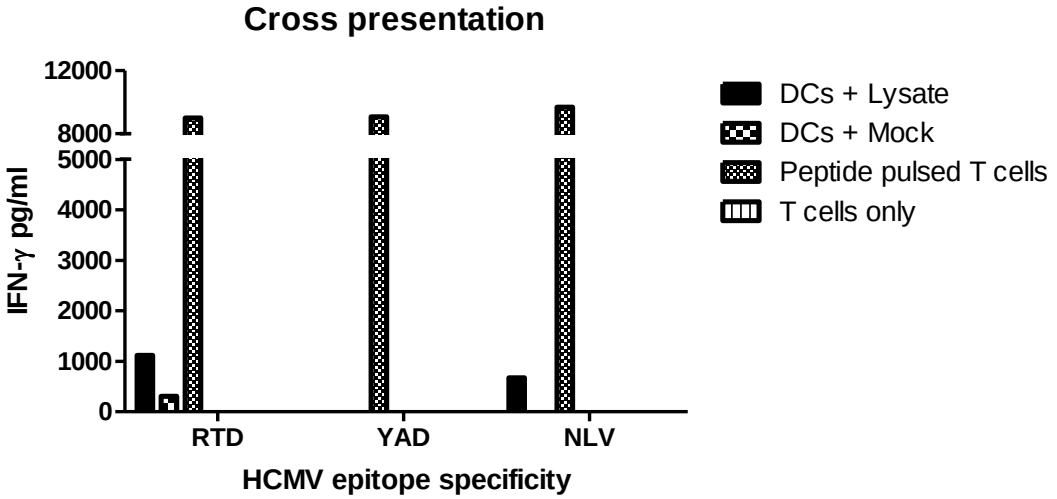


***Fig 18 – Cross presentation of the HCMV protected epitopes.*** The cross presentation of UL69-derived RTD and UL105a-derived YAD peptides to specific CD8+T-cell clones *in vitro* was investigated. DCs from donors with previously identified CD8+T-cell responses to the peptide in question were isolated, differentiated and fed with HCMV AD169 fibroblast lysate for 2 hours at 1:1 ratios and then 24 hours with 4ug/ml R848 and 20ug/ml Poly(I:C). This was followed by co-culture with HCMV-specific CD8+ T cell clones for 16 hours. For positive and negative controls, CD8+T-cell clones were co-cultured with peptide or mock lysate. An additional negative control was provided by the culture of CD8+T-cell clones alone O/N. Positive cross-priming of the specific CD8+T-cells by the DCs was identified by IFN-γ production and therefore CD8+T-cell activation. n = 1. Bars represent the IFN-γ production elicited by the CD8+T-cell clones into the supernatant.

Both peptide derived from HCMV proteins that are present within the infectious virion – UL69 and pp65 – were cross presented by DCs to CD8+T-cell clones (Fig-18). Both of these protein antigens would be present within the HCMV lysate as they are present within infectious virions. The UL105a protein is not present within the infectious virion as it forms part of the HCMV DNA helicase complex [242, 243] and was not cross presented to the HCMV-specific CD8+T-cell clones.

# Chapter 3 summary

This work undertook the first functional and phenotypical characterisation of the *ex vivo* CD8+T-cell responses to 16 CD8+T-cell peptide-epitope targets, identified and kindly provided by Dr Stanley Riddell.

The identification of these peptide targets was achieved via infection of APCs with the RV798 strain of the virus, which is deleted for the WT US2-11 immunomodulatory gene region. CD8+T-cell clones were generated *in vitro* that recognised targets presented during the RV798 infection and their specificity subsequently mapped to individual proteins using single knock out strains of the virus. The abrogation of CD8+ recognition identified the HCMV antigen specificity. These peptide-epitopes were derived from the UL16, UL17, UL23, UL24, UL28, UL33, UL36, UL52, UL56, UL84, UL105, UL122 and US23 HCMV proteins.

As the peptide targets were initially discovered in the absence of the US2-11 region, it was unknown whether the peptide-epitopes *in vivo* are naturally presented on the surface of cells infected with a WT strain e.g. AD169 with an intact US2-11 region or are cross-presented to the CD8+T-cell response. They were subsequently termed ‘protected’ peptides.

Frequent *ex vivo* CD8+T-cell responses were identifiable to the HLA-A, -B and –C-restricted targets within healthy, latently infected donors. A total of 54 younger (<70 years) and 37 older (>70 years) donors were screened for *ex vivo* CD8+T-cell responses to these ‘protected’ peptides. The specific CD8+T-cell responses were identified after peptide stimulation of seropositive donor PBMCs with the protected peptides followed by ICS for IFN-γ, IL-2 and TNF-α production.

What became clear was that the magnitude of the elicited CD8+T-cell responses differed depending upon the HLA-restriction.

The HLA-C-restricted targets elicited the largest *ex vivo* CD8+T-cell responses, (Table-7). These CD8+T-cell responses were dominated by those elicited by the HLA-Cw*0702-restricted UL28-derived FRC peptide-epitope which also induced the most frequent CD8+T-

cell responses of the protected epitope cohort (28/39 donors). These CD8+T-cell responses demonstrated marked inflationary kinetics with age between donors <70 and >70 years of age. These could reach 32% of an 86 year old donor's total peripheral CD8+T-cell pool producing IFN-γ. Interestingly, a second protective epitope 'SYR' also restricted through HLA-Cw*0702 derived from the UL33 protein did not demonstrate the same memory-inflation kinetics with age. However the SYR peptide did induce a large CD8+T-cell response within a donor of 86 years that totalled 12.19% and 14.22% of the total CD8+T-cell response producing IFN-γ and TNF-α respectively.

The HLA-A-restricted protected peptide-epitopes elicited responses of a significant size detectable in a large percentage of donors. In particular, the HLA-A1-restricted UL69-derived RTD, and UL105a-derived YAD epitopes elicited CD8+T-cell IFN-γ and TNF-α production that remained remarkably stable with age.

The HLA-B-restricted protected peptide-epitopes elicited infrequent or undetectable CD8+T-cell responses. The largest was elicited by a HLA-B44-restricted, IE UL122 (IE-2) derived epitope NEG at 3.94% of the total CD8+T-cell population producing TNF-α. However this was within a single donor.

When the phenotype of the *ex vivo* CD8+T-cell populations directed towards the protected epitopes were characterised, they were found to be cytotoxic (indicated by intracellular perforin/granzymeB expression) and display varying levels of activation (CD38) and inhibitory/exhaustion (TIM3/PD-1) markers.

Additionally, when the phenotypic results obtained for the CD8+T-cell responses were categorised based upon the HLA-restriction of the eliciting peptide, these displayed differing memory phenotypes and antigen differentiation status. The total HLA-C-restricted CD8+T-cell populations were more antigen differentiated, indicated by a significant decrease in the number of $CD27^{+}CD28^{+}$ and an increase in $CD27^{-}CD28^{-}$ CD8+T-cells. Additionally, the HLA-Cw*0702 FRC-specific CD8+T-cell populations consisted of $T_{EMRA}$ CD8+T-cells

(identified as $CCR7^{-}CD45RA^{+}$) - indicative of the phenotype associated with memory-inflated populations [105, 240]. HLA-A-restricted responses contained larger percentages of $T_{CM}$ ($CCR7^{+}CD45RA^{-}$) CD8+T-cells and consisted of a larger proportion of early and intermediate differentiated CD8+T-cell populations ($CD27^{+}CD28^{+}$, $CD27^{-}CD28^{+}$/$CD27^{+}CD28^{-}$). This is indicative of the phenotype associated with stable CD8+T-cell memory populations [70].

Specific CD8+T-cell clones to two of the protected peptides RTD and YAD were generated *in vitro* and their ability to recognise naturally processed antigen on the surface of infected cells was assessed. The clones were demonstrated to recognise peptide that is directly presented on the surface of either fibroblasts or monocytes that are infected with the AD169 and Merlin CMV strains respectively *in vitro*. An important finding from this section was the demonstration that a UL69-derived protected peptide-epitope can be cross presented to specific CD8+T-cell clones by DCs incubated with AD169 HCMV infected cell lysate after 16 hours (O/N) co-culture.

The CD8+T-cell responses to these newly characterised peptides can demonstrate *ex vivo* phenotypes similar to those previously reported for inflationary HCMV-specific CD8+T-cell populations that are highly differentiated [71]. However, the CD8+T-cell responses directed to HCMV HLA-A-restricted peptides can also present with an earlier T-cell phenotype that have been previously identified in individual's undergoing primary HCMV infection and stable CD8+T-cell populations in the mouse model [68, 105, 106]. This work additionally demonstrated that there may still be undiscovered immunodominant epitopes of HCMV and that the peripheral HLA-C restricted CD8+T-cell repertoire directed towards HCMV is both greatly underestimated and under researched.

# CHAPTER 3 DISCUSSION

## Identification of frequent CD8+T-cells to epitopes identified during an RV798 infection

Human Cytomegalovirus has a broad tropism *in vivo* infecting both haematopoietic and non-haematopoietic tissues [241, 244]. This coupled with the different priming routes (direct vs cross presentation) [169-171] and the phenomenon of memory-inflation creates a complex picture of the global CD8+T-cell immunity to this virus. For this reason it is important that the focus of CMV CD8+T-cell research is moved away from utilising the pp65 and IE-1 proteins as representative antigens. Previous work has determined CD8+T-cell epitopes from a range of CMV antigens [58, 82, 84, 230]. This range includes the pp28, pp50, gH, gB, US2, US3, US6, UL18 and IE-2 proteins. Additionally, a total global analysis of the HCMV CD8+T-cell repertoire found 151 of 213 (70%) examined HCMV ORFs elicited $CD4^{+}$ or CD8+T-cell responses [230]. However the kinetics and phenotype of such responses have not yet been determined extensively.

Work by the research group of Stanley Riddell identified previously uncharacterised CD8+T-cell epitopes of HCMV which are derived from antigens across the lifecycle (IE-L) and restricted through HLA-A, -B and -C alleles ([82] Table-7). These were identified using the RV798 virus and were termed ‘protected’ epitopes by our research group. The data presented here has characterised the *ex vivo* CD8+T-cell responses to these peptides. The US2-11 gene products, whom function to dampen the cytotoxic CD8+T-cell response to CMV infected cells, do therefore not prevent the initial generation of a diverse CD8+T-cell repertoire to these peptides. This repertoire is directed against several antigens across all phases of the viral lifecycle including UL16, UL17, UL24, UL28, UL33, UL36, UL52, UL84, UL105, and UL122 restricted through HLA-A, -B and –C.

**HLA-restriction of a HCMV CD8+T-cell epitope may play a role in the resulting phenotype of the CD8+T-cell response**

This research identified differing magnitudes of CD8+T-cells directed towards the 16 peptide-epitopes characterised in this work when the age of our donor cohort was considered. Understanding the functionality and phenotype of such CD8+T-cells and how this alters with age will address whether they are different to previously identified CD8+T-cell responses for example those directed towards the pp65 protein. Additionally, it may provide a distinction between whether epitopes derived from HCMV can elicit inflationary vs stable CD8+T-cell responses that have been characterised in the murine model [88, 105].

The HLA-B-restricted CD8+T-cell peptides elicited CD8+T-cells that were infrequent or absent (HLA-B51-restricted peptides derived from the US23, UL56 and UL23 proteins) within seropositive donors. The HLA-A-restricted peptides, in particular the UL69-derived RTD and UL105a-derived YAD peptides, elicited frequent CD8+T-cell responses that remained at similar magnitudes within the periphery with age. Lastly, the HLA-C-restricted peptide-epitopes elicited the largest magnitudes of CD8+T-cell responses producing IFN-γ and TNF-α. In particular, a HLA-Cw*0702-restricted UL28-derived peptide-epitope termed FRC induced CD8+T-cell responses that ranged from 0.03-32.25% and 0.03-31.07% producing IFN-γ and TNF-α respectively. This increased significantly with the age of our donor cohort. Therefore a distinction was made between HCMV epitopes in this peptide cohort that elicit stable and inflationary CD8+T-cell responses between the younger and older donors in our study. The following of the CD8+T-cell responses longitudinally within donors was not conducted within this study and should be a focus of future research to identify the point when FRC-specific CD8+T-cells begin to inflate. To determine that the HLA-Cw*0702-restricted FRC responses increased with age whereas the HLA-A1 restricted did not, multiple Mann Whitney tests were conducted between the <70 and >70 year cohorts. A limitation of this work therefore arises in that significance may have arisen by statistical chance. In order to correct for this, a larger donor cohort should be screened for these CMV-

specific CD8+T-cell responses to increase the statistical power to allow a multiple comparison corrections, such as Bonferroni, to be applied to the analysis to ensure the significance still holds.

A second limitation of this work was the availability of tetramers for the HLA-Cw*0702 restricted FRC peptide. MHC-I tetramers for the UL69- and UL-105a-derived RTD and YAD peptides were obtained from the NIH Tetramer facility. However both our research group and the NIH could not correctly refold HLA-Cw*0702 FRC monomers. It was therefore decided to phenotype all epitope-specific CD8+T-cell responses after peptide stimulation to ensure consistency between the epitope-specific CD8+T-cell responses. However, by utilising peptide stimulation followed by ICS, this likely underestimated the size of the epitope-specific CD8+T-cell population as MHC-I tetramer detection is highly sensitive. Using peptide stimulation may also have missed epitope-specific CD8+T-cells that do not produce cytokines that were investigated i.e. IL-4 or IL-10. These would be detectable using MHC-I tetramers which bind to specific CD8+T-cells regardless of effector function. Furthermore, MHC-I tetramer staining would detect very low affinity CD8+T-cells that peptide stimulation may leave undetected [245].

This work identified $CCR7^{+}CD45RA^{+}$ epitope-specific CD8+T-cells after 6 hours peptide stimulation. It is debated within the literature whether true naïve CD8+T-cells will respond to TCR engagement after 6 hours. Naïve CD8+T-cells have been documented to rapidly produce IFN-α and TNF-α in response to a primary viral infection but lack anti-viral function [246, 247]. MHC-I tetramer staining would address whether the $CCR7^{+}CD45RA^{+}$ T-cells represent early differentiated memory CD8+T-cells that have been newly recruited to the peripheral epitope-specific CD8+T-cell population or indeed true naïve populations.

Despite these limitations, the ICS method used provided a functional readout that MHC-I tetramer detection would be unable to provide – only functional cells will respond to the peptide with cytokine production. In summary, it would be ideal to compare the MHC-I tetramer phenotype vs the activated CD8+T-cell phenotype after peptide stimulation of the

same epitope-specific populations. This would provide a true determination of the size and diversity of the population with regards to T-cell subsets and affinity. It will additionally provide a functional read out/indication of anti-viral capacity.

Subsequently after ICS, this work delineated that the HCMV-specific CD8+T-cell responses directed towards the 'protected' epitopes differ in their *ex vivo* CD8+T-cell phenotype depending on their HLA-restriction. HLA-A-restricted protected peptides elicited CD8+T-cell responses with an overall earlier antigen differentiated phenotype. This was denoted by a larger percentage of $CD27^{+}CD28^{+}$ and $CCR7^{+}CD45RA^{-}$ populations compared to HLA-C-restricted populations and a HLA-B-restricted CD8+T-cell population [238]. However, of the 11 responses phenotyped, 9 were specific for the HLA-Cw*0702-restricted FRC peptide. These phenotypic results may therefore represent a phenomenon of this particular CD8+T-cell population. A third limitation of this work therefore presents itself in the low n numbers phenotyped for particular epitope-specific CD8+T-cell populations. This was a result of low numbers of donors available after the initial screening for CD8+T-cell responses to these newly characterised CMV peptides. A larger range of HLA-C peptides and larger donor cohort should as such be phenotyped to extend this phenotypic observation to a more general CMV-specific HLA-C-restricted CD8+T-cell population.

However, the phenotype of individual HLA-A-restricted RTD/YAD-specific 'stable' vs HLA-C FRC-specific 'inflationary' CD8+T-cell populations corroborated the phenotypic data identified in murine studies [88, 105]. Stable CD8+T-cell responses are known to present with a $T_{CM}$ phenotype – and inflationary a $T_{EMRA}$ phenotype [105]**.**

It is now known that the HCMV U2-11 encoded immunevasins do not uniformly target all HLA alleles with the same efficacy i.e. HLA-A, –B and –C alleles are targeted for degradation to differing magnitudes [137, 139-141]. For example a study has implicated US2 as being able to target HLA-A, HLA-G and the majority of HLA-B alleles for degradation *in vitro* [141]**.** Conversely, the remaining HLA-B alleles e.g. HLA-B7, and HLA-C alleles appear to be exempt from US2-mediated degradation [141]. In particular relevance to this

investigation, Ameres et al. identified US3 as having no impact on HLA-Cw*0702 surface expression [140]. They additionally showed that the US2 and US11 proteins had a minor effect on CD8+T-cell clone recognition of HLA-Cw*0702 peptides *in vitro* – translating to target cell lysis [139].

Therefore it is a possibility that the HLA-restriction of a HCMV peptide is important in determining the frequency with which a HCMV peptide is presented to the CD8+T-cell response. Each cell type permissible to CMV infection may require a unique concerted mode of action by the US2-11 immunevasin proteins depending upon the HLA haplotype of the cell. In particular, within cell types that the US2-11 proteins are unable to exert their effects due to a particular HLA haplotype, allows the increased presentation of particular HLA-restricted peptides. This may determine how often the resulting CD8+T-cell population encounters the cognate peptide.

These findings from the literature may provide a plausible explanation for the phenotypic data obtained in this study for the HLA-C CD8+T-cell responses - specifically, the HLA-Cw*0702 FRC-specific CD8+T-cells. HLA-Cw*0702 alleles may remain on the cell surface during an infection of a cell type in which the US2/3 and 11 proteins are unable to target these alleles efficiently for degradation. This may lead to the more frequent presentation of the HLA-Cw*0702-restricted FRC peptide-epitope over the HLA-A-restricted peptides. As this peptide is expressed with IE kinetics, it is more likely to be presented during a reactivation event before CD8+T-cell elimination of the reactivating virus [225, 248]. Ultimately, the FRC-specific CD8+T-cell population will develop a highly antigen driven phenotype e.g. $CD27^{-}CD28^{-}CD45RA^{+}$ and the initial CD8+T-cell pool may accumulate.

However within this investigation an additional HLA-Cw*0702-restricted peptide termed SYR derived from the UL33 protein did not also elicit CD8+T-cell responses that increased with age. The SYR peptide is expressed with L kinetics during the viral life cycle (Table-7). Infrequent non-inflating CD8+T-cell populations were detected towards a second IE-expressed UL123 (IE-2)-derived HLA-B44-restricted peptide termed ‘NEG’ (Table-7).Clearly,

as individual factors, the HLA-restriction and IE kinetics of the peptide-epitope in question do not solely explain whether a CD8+T-cell response will inflate.

**Direct vs cross presentation of the 'protected' peptide-epitopes**

It is unknown how the CD8+T-cells to these 'protected' epitopes are generated initially *in vivo* if they were identified using the RV798 virus. During a WT infection *in vivo*, the US2-11 gene region products are likely to interfere with the direct presentation of these peptides to the CD8+T-cell response and could support the theory of cross presentation as an initial mechanism of priming. Cross presentation is hypothesised to be vital in the generation of cytotoxic CD8+T-cell responses during a primary infection with WT (US2-11 gene region present) HCMV despite a vast array of MHC-I immunomodulatory proteins [169, 171, 249]. However, it remains unknown to what extent the US2-11 gene region products are able to prevent CMV antigen presentation within all cell types permissible to CMV *in vivo*. It is possible that these responses are primed *in vivo* by direct presentation from an infected cell type e.g. endothelium or epithelium in which the US2-11 proteins cannot interfere with the MHC-I presentation pathway as efficiently as observed within fibroblasts *in vitro.*

It is also likely that these CD8+T-cell responses could be primed before the US2-11 gene region products can exert their full immunomodulatory effects. Supporting this is a study by Thom et al. [250]. The analysis of cell types permissible to MCMV infection within the salivary gland of infected mice led to the identification that CMV preferentially targets non-epithelial cells early during a primary infection [250]. Furthermore, that MHC-I antigen presentation interference is incomplete within this cells during this phase. This resulted in a time during infection whereby CMV-specific CD8+T-cells could detect MCMV antigen. Therefore, the 'protected' peptides identified by Riddell at al. could also be primed in this manner during a primary infection with HCMV.

To begin to address the mechanisms by which these CD8+T-cells can be primed, specific CD8+T-cell clone recognition of the RTD and YAD peptides (Table-7) during an AD169 (WT

US2-11 gene region) infection of fibroblasts *in vitro* indicated by IFN-γ production was assessed. The recognition profile was fitting with the expression kinetics of the protein from which the RTD and YAD peptides are derived from. The RTD peptide is derived from the UL69 protein that is part of the incoming infectious virion and is expressed with E kinetics [225, 251]. As such the RTD peptide was recognised at IE-L time-points of the assay as it may be immediately available for MHC-I processing. The YAD peptide is derived from the UL105a protein, part of the helicase complex, not associated with the mature virion and expressed with E-L kinetics [225, 242]. The YAD peptide was recognised only at E-L time-points of the assay. HCMV peptide-epitopes that were identified in the absence of the US2-11 gene region can as such be efficiently presented to CD8+T-cells directly during a primary *in vitro* infection of fibroblasts. It is well known that CMV rapidly mutates upon infection of fibroblasts *in vitro* to loose genetic regions that are required for entry into cell types other than fibroblasts [241]. Additionally, it has been extensively reported that the US2-11 gene region immunomodulatory protein products can efficiently interfere with the MHC-I presentation pathway within fibroblasts *in vitro* [252]. Therefore, these CD8+T-cell recognition experiments should be conducted within cell types more relevant to the virus tropism *in vivo* e.g. endothelial cells. In these cells it is not yet known how efficiently the US2-11 proteins can interfere with the MHC class I presentation pathway but they are known to harbour HCMV genomes [253].

This work then confirmed that the UL69-derived RTD peptide can also be cross presented *in vitro* to specific CD8+T-cell clones by DCs that have had access to UV-inactivated HCMV cell lysate. This was at levels consistent with pp65-derived NLV cross presentation. However, the UL105a-derived YAD peptide-epitope was not cross-presented to specific CD8+ T cell clones within this time frame (16 hours). This likely reflects the differences in the anatomical location of the HCMV antigens. The UL69 protein could be accessible within the lysate to the DCs for efficient processing and allow the presentation of the RTD peptide during the 16 hours incubation time-point. Hence, the protected peptides could theoretically

be presented to the immune system by both direct and cross presentation *in vivo*. However this was conducted once with a single specific clone and should be repeated.

**Future research**

The non-inflating e.g. UL69-derived RTD vs inflationary e.g. UL28-derived FRC CD8+T-cell populations require further characterisation with regards to phenotype and functionality (investigated in detail in chapter 4). This could shed light on the mechanism behind why one CD8+T-cell population inflates whilst the other remains stable. Importantly, the knowledge of HLA-C-restricted CMV epitopes and their specific CD8+T-cell populations should be extended to clarify if this inflation is a phenomenon of additional HLA-C-restricted peptides or specific to the UL28-derived FRC peptide. Finally, the maintenance of HLA-C alleles on HCMV infected cells *in vitro* with the WT US2-11 gene region present should be analysed and whether this is a driving factor in a HLA-C CD8+T-cell population inflating.

# CHAPTER 4

# IDENTIFICATION AND CHARACTERISATION OF CMV HLA-C-RESTRICTED MEMORY-INFLATION

- **Project 1: HLA-C CD8 T-cells dominate the peripheral anti-HCMV CD8+T-cell response**

- **Project 2: The phenotype and functionality of memory-inflated HLA-C CMV CD8 T-cells**

- **Project 3: Antigen driven stimulation of HLA-C-specific T-cells as a potential mechanism for inflation**

# Chapter 4 - Introduction

The role of HLA-C-restricted CD8+T-cell populations during viral infections has been poorly researched compared to HLA-A/-B-restricted populations. HLA-A and B alleles are more polymorphic and therefore able to present a more diverse repertoire of antigens to the immune response [254, 255]**.** Additionally, HLA-C alleles have a much lower surface expression of HLA-C alleles, compared to HLA-A and –B alleles. HLA-C-restricted CD8+T-cells have therefore previously been considered infrequent and their antiviral activity poorly understood [256]. Further complicating matters is the fact that HLA-C alleles are commonly inherited together with HLA-B alleles (termed linkage disequilibrium) making the distinction between HLA-C- and HLA-B-restricted CD8+T-cell populations hard to achieve. Yet prominent HLA-C CD8+T-cell populations have been documented within viral infections such as CMV, HIV, HCV and EBV [256-258] and the presence of these HLA-C CD8+T-cell populations linked to the resolution of such viral infections [259, 260].

HLA-A- and –B-restricted CD8+T-cell populations have been extensively studied in HCMV infection in particular towards the pp65 and IE-1 proteins, whereas HLA-C-restricted CD8+T-cells have been poorly investigated. One reason for this, is the linkage disequilibrium of HLA-B and HLA-C alleles has led to the mistaken identification of HCMV HLA-C-restricted peptides as HLA-B. For example, the HLA-Cw*0702-restricted CRV peptide was initially identified and characterised as HLA-B7-restricted [261]. Furthermore, a HLA-B8-restricted peptide QIK initially characterised by Elkington et al. [58] has recently also been identified as presented in HLA-Cw6 [262]. [139, 261, 262]. It is entirely plausible that there are currently still HLA-C-restricted HCMV peptides that have yet to be identified and characterised correctly.

Viruses efficiently target MHC-I molecules for degradation and surface down-regulation to avoid recognition by cytotoxic CD8+T-cells. However, this poses a problem for virally

infected cells by exposing them to NK cell attack. MHC-I molecules play a dual role in both activating the adaptive immune response and dampening the innate NK cell response [263]. HIV-1 was the first virus discovered to have evolved mechanisms (in particular the Nef protein) to regulate the specificity of which MHC-I alleles are down-regulated from the infected cell surface. The NEF protein was discovered to leave HLA-C alleles on infected cell surfaces, which are inhibitory receptors for NK cells, but downregulate HLA-A/-B which are vitally important for activating cytotoxic CD8+T-cells [264] [265].

Ex *vivo* HCMV-specific CD8+T-cell responses in this work to a HLA-Cw*0702-restricted epitope FRC (Table-7) were observed to reach upto 32% of the total peripheral CD8+T-cell response in donors (Chapter 3) [76, 82, 84]. Previously, immunodominant responses to a HLA-Cw*0702-restricted peptide derived from the UL122 (IE-1) protein ‘CRV’, have been documented by Ameres et al. reaching magnitudes of 2.97-4.48% of the total peripheral CD8+T-cell pool. Ameres et al. demonstrated that the HLA-C CRV-specific CD8+T-cell responses exceeded those derived from a second immunodominant protein pp65 (HLA-B7 TPR) and other IE-1 targets (HLA-A2-restricted VLE) within the same seropositive donors [139]. CD8+T-cell clones specific for the CRV peptide were efficiently able to lyse infected cells whereas the killing by clones specific for other IE-1-derived HLA-A/B-restricted targets was inhibited [139]. The authors explain the possibility that HLA-Cw*0702 alleles are exempt from HCMV-mediated MHC-I surface down-regulation as has been recently proposed [139]. Ameres et al. postulate that as HLA-Cw*0702 is known to be a ligand for the NK cell inhibitory receptors, HLA-Cw*0702 alleles may remain on the surface as an evasive NK-cell mechanism. This would allow large accumulations of virus-specific CD8+T-cells to be generated.

HCMV reactivation within a cohort of HSCT transplant patients was reported to upregulate inhibitory NK cell receptors on CD8+T-cells [266]. This implicates HCMV infection as resulting in changes of HLA-C alleles on host immune cells. Furthermore, a proteomics

study of CMV-infected fibroblasts by Weekes et al. identified the delayed down-regulation of HLA-Cw2 and HLA-G alleles compared to HLA-A11, - A24 and HLA-E [225]. This window of opportunity where the HLA-C alleles are still present on an infected cell surface represents a time when HLA-C-restricted CD8+T-cell populations could efficiently control viral reactivation events and re-stimulate the initial CD8+T-cell pool.

HLA-C-restricted CD8+T-cells can seemingly represent a large proportion of the HCMV CD8+T-cell repertoire in some seropositive individuals and may play an important part of viral reactivation and latency control *in vivo*. Altogether this evidence suggests that the HLA-C CD8+T-cell response in viral infections, and in particular HCMV, as greatly under researched. Furthermore that HLA-C-restricted peptides represent a source of previously uninvestigated immunodominant epitopes of HCMV.

# Chapter 4 – Results

# Project 1: HLA-C CD8 T-cells dominate the anti-HCMV CD8+T-cell response

## 4.1 HLA-C-restricted CD8+T-cell responses dominate the periphery of donors over the CD8+T-cell responses restricted through HLA-A and HLA-B

After identifying and phenotyping frequent *ex vivo* CD8+T-cell responses specific for a panel of epitopes identified during a RV798 ΔUS2-11 infection it became increasingly clear that a HLA-C-restricted peptide elicited significantly differing CD8+T-cell responses. This was with regards to kinetics and phenotype to those specific for HLA-A-restricted peptides identified in the same panel (Fig-8/9, 12-14). The HLA-Cw*0702-restricted UL28-derived FRC-specific CD8+T-cell populations were of a significantly later antigen driven phenotype compared to the phenotype of the HLA-A-restricted RTD CD8+T-cell populations (Fig-13/14). Strikingly the immunodominant responses to the HLA-Cw*0702-restricted FRC peptide were observed that increased significantly with age (Fig-8/9).

It was next investigated whether this HLA-C-restricted memory-inflation was a common feature of HCMV HLA-C-restricted peptides or a phenomenon of the UL28-derived HLA-Cw*0702-restricted FRC peptide. Therefore, to further characterise the overall contribution of HLA-C-restricted CD8+T-cell populations to the total HCMV-specific CD8+T-cell repertoire, a panel of HLA-C-restricted CD8+T-cell peptides was obtained from the literature (Table-8)

The panel of additional HLA-C-restricted peptides obtained from the literature consisted of peptides with a variety of restricting HLA-C alleles and were either derived from the pp65 or IE-1 protein (Table-8). As such, the HLA-C-restricted peptides from either the pp65 or IE-1 protein had differing kinetics of expression. It was therefore also investigated whether HLA-C mediated memory-inflation, if observed against other peptides, was spread across phases of the lifecycle.

***Table 8 – HLA-C-restricted peptides used in the investigation.*** *identified by Stanley Riddell et al.. The protein antigen, aa position within the protein antigen, peptide sequence (peptide name is denoted by the first three aa of the sequence), restricting HLA allele, kinetics of expression that the peptides are derived from are provided.

| HCMV Antigen | Amino acid location | Peptide sequence | HLA-C restriction | Kinetics of expression [225] | Reference [84, 139, 262, 267] |
|---|---|---|---|---|---|
| pp65 | 7-15 | **RCP**EMISVL | Cw1 | L | [262] |
| pp65 | 341-349 | **QYD**PVAALF | Cw4 | L | [262] |
| IE-1 | 88-96 | **QIK**VRVDMV | Cw6 | IE | [262] |
| IE-1 | 305-313 | **LSE**FCRVL | Cw0702 | IE | [267] |
| IE-1 | 309-317 | **CRV**LCCYVL | Cw0702 | IE | [84, 139, 267] |
| UL28 | 327-335 | **FRC**PRRFCF | Cw0702 | IE | * |
| UL33 | 120-128 | **SYR**STYMIL | Cw0702 | L | * |
| pp65 | 294-302 | **VAF**TSHEHF | Cw12 | L | [262] |
| UL24 | 120-134 | **YLC**CQTRLAFVGRFV | Cw1601 | L | * |

Some of the donors who were previously screened for the protected epitope responses were then screened for CD8+T-cell populations specific for these HLA-C peptides. Additionally, when the same donors presented with the correct HLA type, also screened for CD8+T-cell responses to well-known and documented immunodominant peptides derived from the pp65 (HLA-A2 NLV, HLA-B7 RPH, HLA-B7 TPR), IE-1 (HLA-A1 YSE, HLA-A2 VLE) and pp50 (HLA-A2 VTE) proteins as a comparison (Table-5). PBMCs were peptide stimulated for 6 hours followed by intracellular cytokine staining for IFN-γ, IL-2 and TNF-α production to identify activated specific CD8+T-cell responses, as described previously (Fig-7).

Strikingly, even when pooled CD8+T-cell responses to HLA-A/-B-restricted immunodominant peptides were included within the analysis (Table-5), the pooled HLA-C-restricted responses in our donor cohort dominated those restricted through HLA-A and –B (Fig-19).

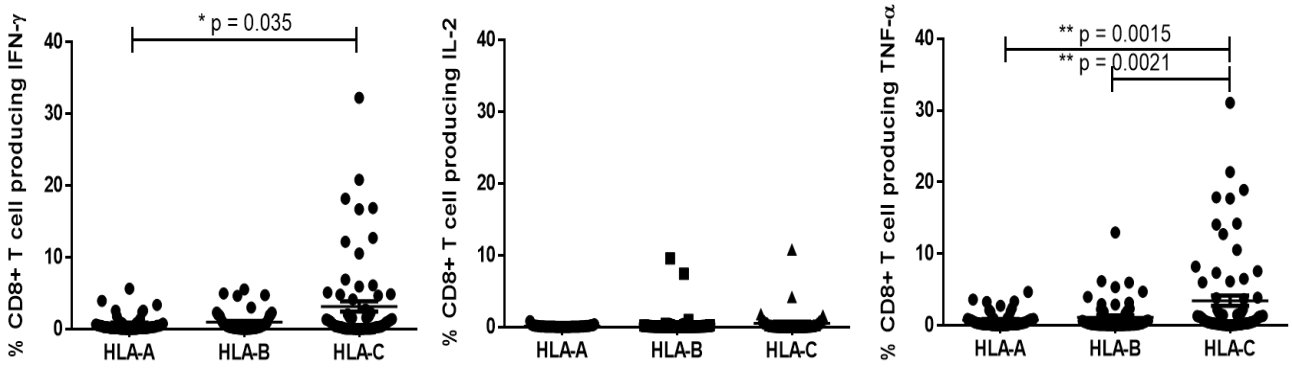


***Fig 19 – Dominance of CMV HLA-C restricted CD8+T-cell populations within the CD8+T-cell repertoire of the study cohort.*** **.** PBMCs from seropositive donors were stimulated with HCMV peptide (final concentration 1µg/ml) for 6 hours followed by intracellular staining for TNF-α, IFN-γ and IL-2 to identify specific CD8+T-cell responses. PBMCs were stained with the antibodies outlined in Table-4. A) Summary of the *ex vivo* CD8+T-cell responses detected towards the HLA-C-restricted peptide-epitopes vs HLA-A/-B-restricted conventional immunodominant peptide-epitopes derived from the pp65 and IE-1 proteins – see Table-5 and -8 for full peptide-epitope details. The IFN-γ, IL-2 and TNF-α production are provided in the left, middle and right hand graphs respectively. Statistical significance was obtained in Graphpad Prism 6 using Mann Whitney test and * as a p value < 0.05 and ** < 0.01.

## 4.2 - Identification of HLA-Cw*0702-restricted CD8+T-cell populations that display marked memory-inflation with age

The kinetics of the individual HLA-C-restricted CD8+T-cell responses between young (<70 years) vs older (>70 years) was next analysed. CD8+T-cell responses to a HLA-Cw*12-restricted peptide 'VAF' derived from pp65 and therefore produced with L kinetics ranged from 0.27%-1.83% of the total CD8+T-cell producing cytokines (Fig-20, n = 3). This did not accumulate.

A pp65-derived HLA-Cw*4-restricted peptide QYD peptide elicited 1 response of 0.03% IFN-γ and 0.02% TNF-α in 3 donors, and a pp65-derived HLA-Cw*1-restricted peptide RCP elicited no responses in two donors (data not shown). However due to low n numbers on account of the HLA type of the donors conclusions cannot be drawn from these peptides.

The IE-1-derived HLA-Cw6-restricted peptide QIK elicited responses in 6/6 donors ranging from 0.07-2.74% of the total CD8+T-cell pool (Fig-20). However, the responses did not display memory-inflation kinetics with age and on average induced 0.51%, 0.44% and 0.43% CD8+T-cells IFN-γ, IL-2 and TNF-α and of the total CD8+T-cell pool.

As previously mentioned, the L-expressed HLA-Cw*1601-restricted peptide YLC elicited one large CD8+T-cell response in an elderly donor at 12.19% of the total CD8+T-cell response producing TNF-α (n = 13, Fig8-9, 20). In all other donors YLC elicited smaller responses ranging from 0.04% to 1.16% and did not increase significantly with age.

Two of the HLA-C-restricted peptides, 'CRV' and 'LSE' also elicited CD8+T-cell populations that demonstrated striking memory-inflation with age as was observed with the UL28-derived FRC peptide (Fig-20/21). These were also HLA-Cw*0702-restricted, derived from the IE-1 protein and therefore expressed with IE kinetics.

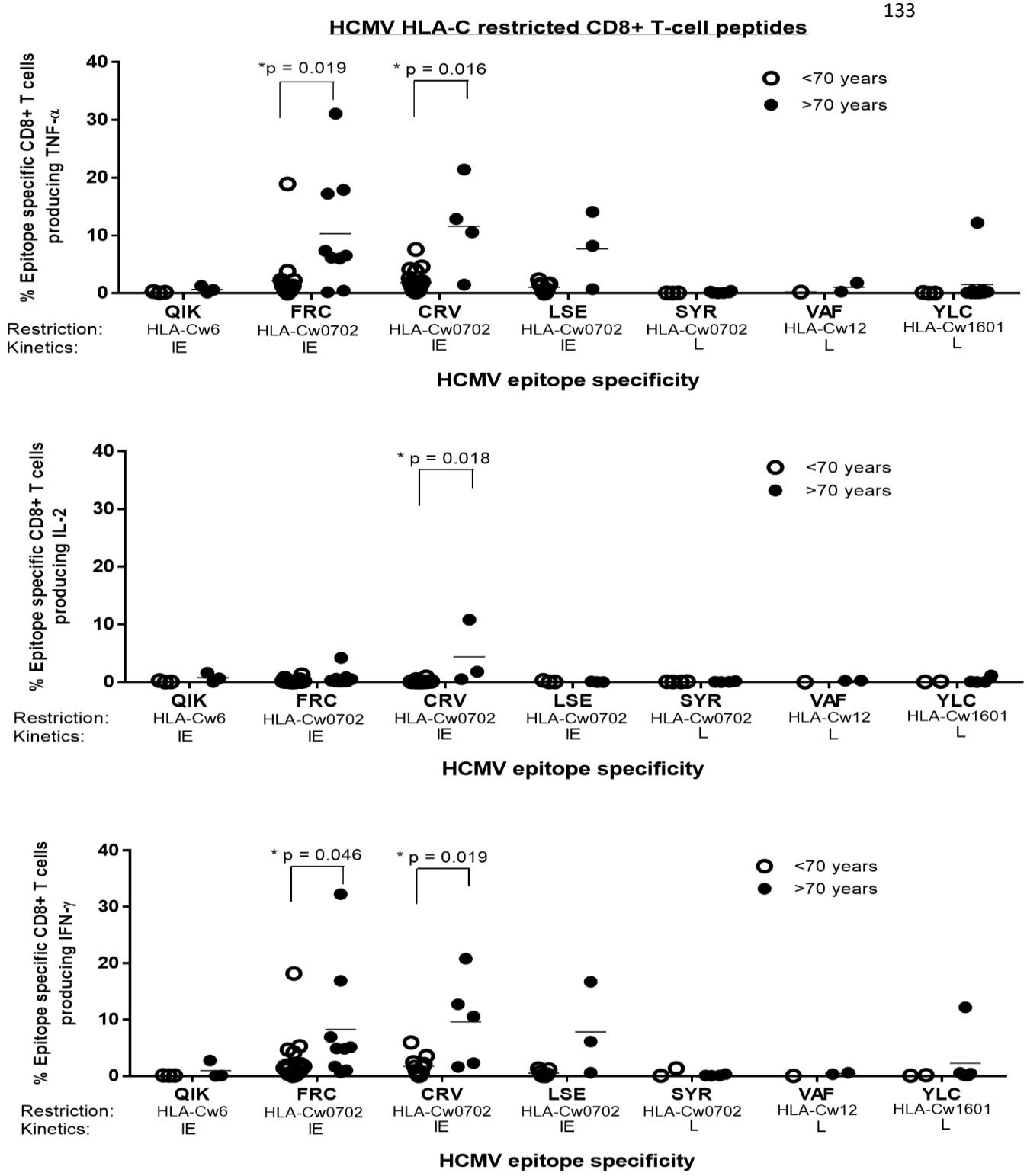


***Fig 20 –*** S***ummary of the ex vivo CD8+T-cell responses elicited by HLA-C restricted HCMV peptides with age.*** HCMV seropositive donors were screened with a panel of HLA-C-restricted peptides to identify potential immunodominant epitopes. PBMCs from seropositive donors were stimulated with HCMV peptide (final concentration 1µg/ml) for 6 hours followed by intracellular staining for TNF-α (top graph), IL-2 (middle graph) and IFN-γ (bottom graph), to identify specific CD8+T-cell responses. White circles represent donors <70 years of age and black circles >70 years of age. Each circle represents an individual donor. Statistical significance was obtained using multiple Mann Whitney tests in Graphpad prism 6 between the <70 and >70 year category with * as a p value < 0.05. n = 3 – 39 donors depending on the peptide.

The dominant HLA-Cw*0702 CD8+T-cell responses were also frequent being detected in 75% (16/21) and 85% (13/15) of donors tested for the CRV and LSE peptides respectively (Fig-20, 22-23). The *ex vivo* CD8+T-cell responses detected against the CRV peptide ranged from 0.08%-20.83% (IFN-γ), 0.03%-10.81% (IL-2) and 0.21%-21.43% (TNF-α) of the total CD8+T-cell pool (Fig-20, 22). These CD8+T-cell responses increased significantly from an average of 1.51% IFN-γ, 0.13% IL-2, 1.70% TNF-α within donors <70 years of age to 9.60% IFN-γ, 4.38% IL-2, 10.02% TNF-α within donors >70 years of age of the total CD8+T-cell pool responding (Fig-20, 22).

The *ex vivo* CD8+T-cell responses directed against the LSE peptide ranged from 0.36%-16.40% (IFN-γ), 0.06%-0.32% (IL-2) and 0.36%-14.09% (TNF-α) of the total CD8+T-cell pool (Fig-20, 23). These CD8+T-cell responses increased, trending to significance in part due to low n numbers in the >70 years cohort (n = 3), from an average of 0.56% IFN-γ and 0.86% TNF-α within donors <70 years of age to 7.80% IFN-γ and 5.92% TNF-α within donors >70 years of age of the total CD8+T-cell pool responding (Fig-20, 23). The IL-2 production decreased from 0.07% to 0.05% on average of the total CD8+T-cell pool in donors <70 vs >70 years of age.

Interestingly, as also mentioned previously (Fig-9) the CD8+T-cell responses elicited by a third HLA-Cw*0702-restricted peptide SYR, expressed with L kinetics, were smaller ranging from 0.04% to 1.34%, less frequent (6/31, 19% donors) and did not change in magnitude with age (Fig-20).

Therefore, HLA-C mediated memory-inflation was observed specifically towards peptides presented through HLA-Cw*0702 and was further restricted to peptides derived from antigens with IE expression kinetics. These three HLA-Cw*0702-restricted CD8+T-cell populations were then investigated more extensively.

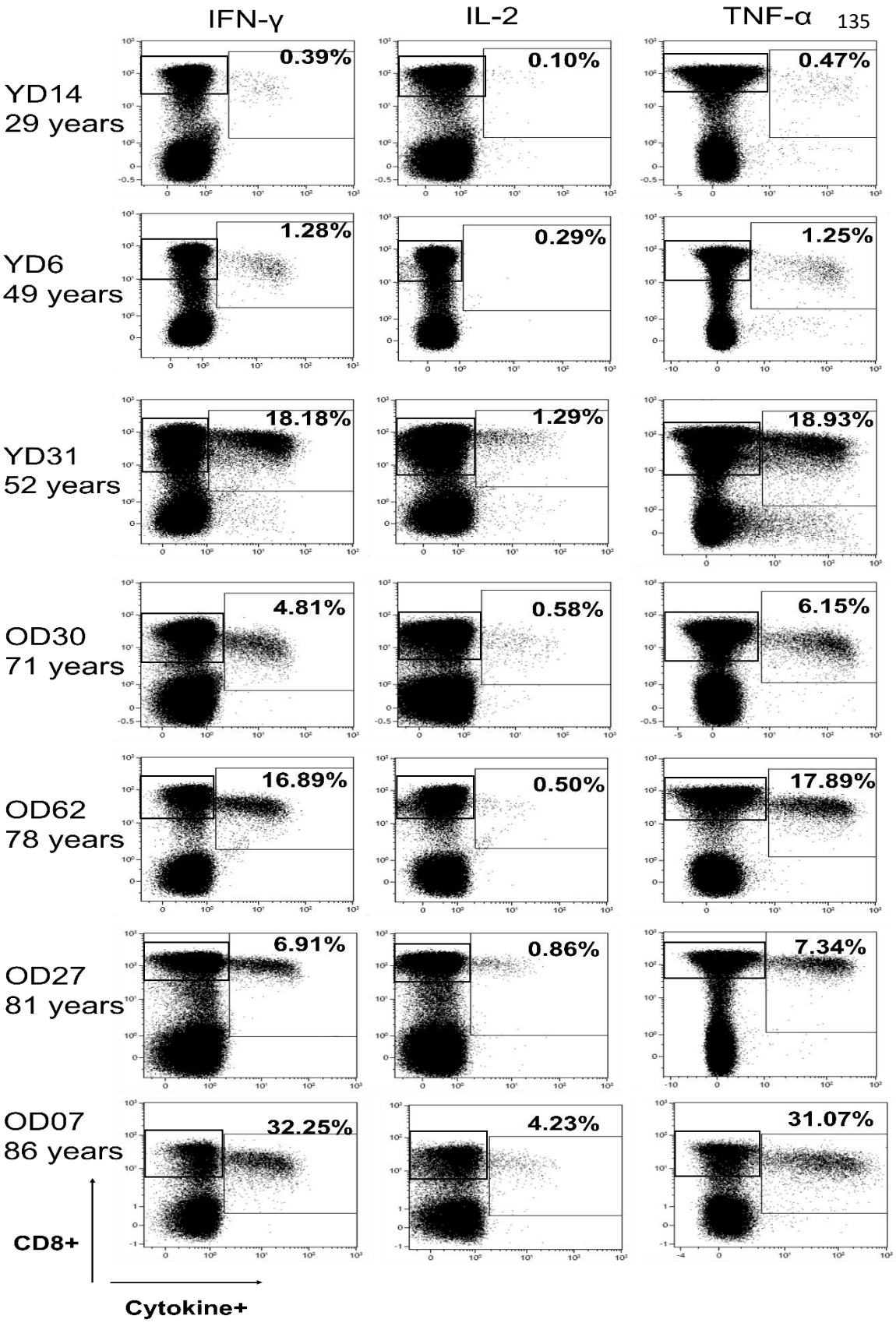


***Fig 21 – Representative dot plots of the ex vivo CD8+T-cell responses against the HLA-Cw*0702 UL28-derived FRC peptide with age.*** PBMCs from seropositive donors were stimulated with the FRC peptide (final concentration 1µg/ml) for 6 hours followed by intracellular staining for IFN-γ (left column), IL-2 (middle column) and TNF-α (right column) to identify specific CD8+T-cell responses. The age of the donor is provided on the left hand side of the plots. Each row represents the cytokine production in that individual donor. Data was analysed in Kaluza 1.3 software. The size of the epitope-specific CD8+T-cell response is provided on the plots defined as the percentage of cytokine positive CD8+T-cells of the total CD8+T-cell response. In all cases, the percentages shown have had the unstimulated control percentages subtracted.

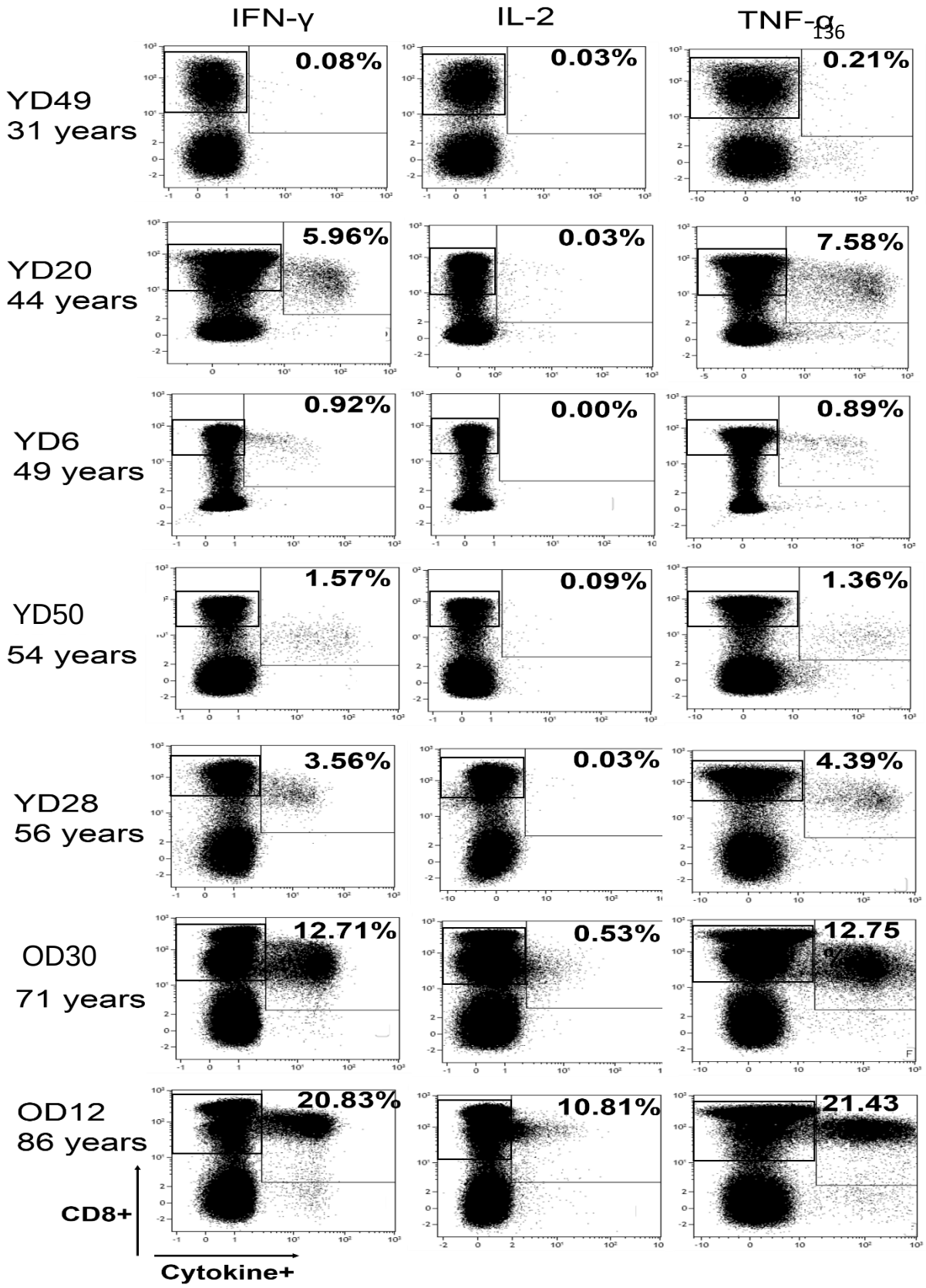


***Fig 22 – Representative dot plots of the ex vivo CD8+T-cell responses against the HLA-Cw*0702 IE-1-derived CRV peptide with age.*** PBMCs from seropositive donors were stimulated with the CRV peptide (final concentration 1µg/ml) for 6 hours followed by intracellular staining for IFN-γ (left column), IL-2 (middle column) and TNF-α (right column) to identify specific CD8+T-cell responses. The age of the donor is provided on the left hand side of the plots. Each row represents the cytokine production in that individual donor. Data was analysed in Kaluza 1.3 software. The size of the epitope-specific CD8+T-cell response is provided on the plots defined as the percentage of cytokine positive CD8+T-cells of the total CD8+T-cell response. In all cases, the percentages shown have had the unstimulated control percentages subtracted.

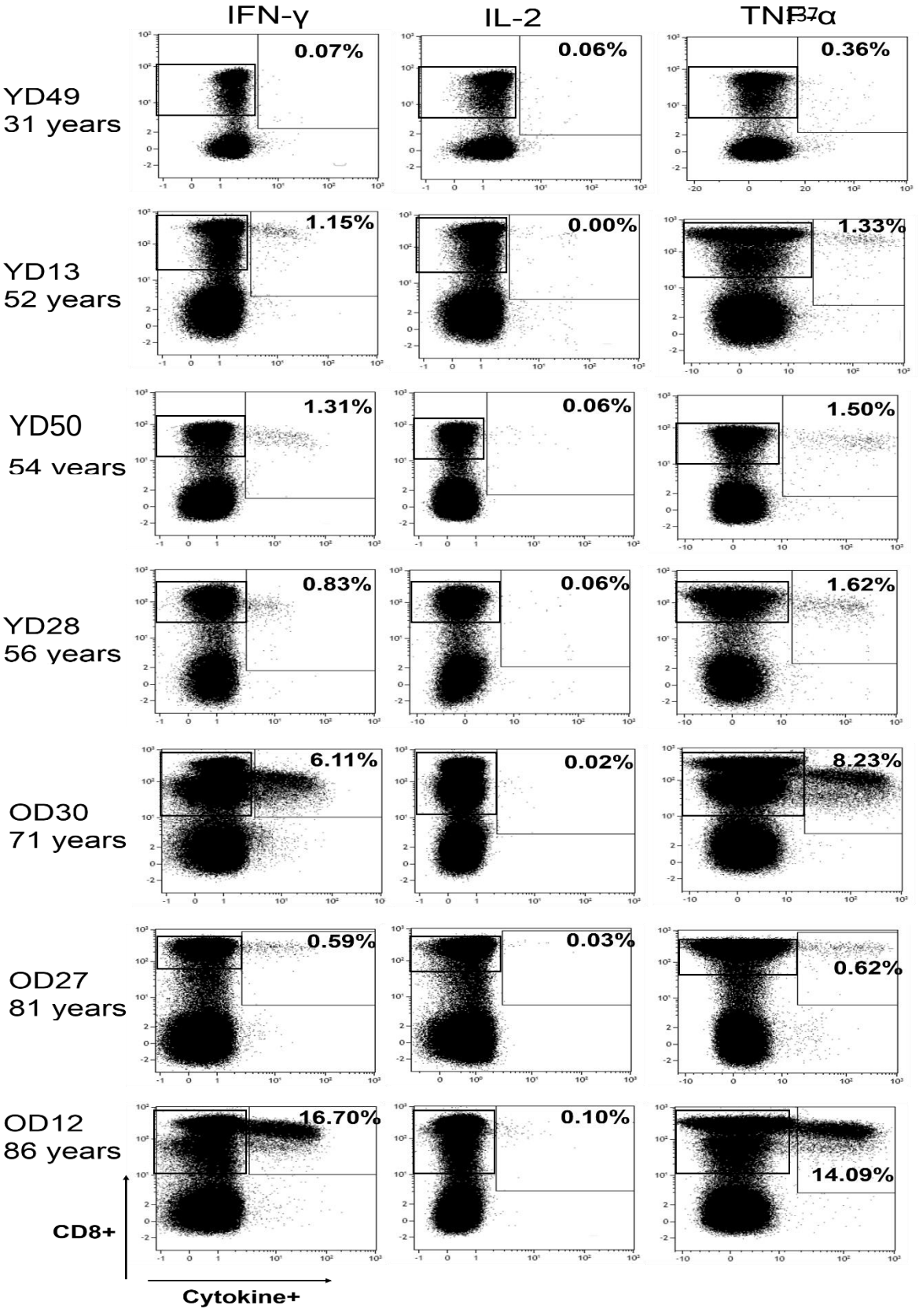


***Fig 23 – Representative dot plots of ex vivo CD8+T-cell responses against the HLA-Cw*0702 IE-1-derived LSE peptide with age.*** PBMCs from seropositive donors were stimulated with the LSE peptide (final concentration 1µg/ml) for 6 hours followed by intracellular staining for IFN-γ (left column), IL-2 (middle column) and TNF-α (right column) to identify specific CD8+T-cell responses. The age of the donor is provided on the left hand side of the plots. Each row represents the cytokine production in that individual donor. Data was analysed in Kaluza 1.3 software. The size of the epitope-specific CD8+T-cell response is provided on the plots defined as the percentage of cytokine positive CD8+T-cells of the total CD8+T-cell response. In all cases, the percentages shown have had the unstimulated control percentages subtracted.

**4.3 - Kinetics of HLA-Cw*0702 HCMV mediated CD8+T-cell memory-inflation with age**

The striking immunodominance of the HLA-Cw*0702 CD8+T-cell responses that was already present in younger age led to the further investigation of the kinetics of this memory-inflation with increment decades of the HCMV infected donors.

The HLA-Cw*0702-restricted FRC, CRV and LSE peptides elicited IFN-γ and TNF-α production that significantly correlated with age by spearman's rank correlation (Fig-24A). Additionally, the average increment in the epitope-specific populations each decade from 20 to 100 years was calculated. On average the FRC-, CRV- and LSE-specific CD8+T-cell populations increased within the periphery of our donor cohort per decade at a rate of 1.41%, 2.35% and 1.30% producing IFN-$\gamma^+$ respectively and 1.93%, 2.45% and 1.04% producing TNF-$\alpha^+$ respectively. The age where the largest increase in the HLA-Cw*0702 CD8+T-cell populations was observed was between the ages of 80-100 years (Appendix Fig-1). Interestingly, when the FRC-specific CD8+T-cell responses within males vs females were correlated with age, the female population exhibited a significant increase in the number of CD8+T-cells producing IFN-γ (0.30%-32.25%) and TNF-α (0.18%-31.07%) respectively with age (Fig-24D). However this may represent a larger proportion of our elderly cohort being female (Appendix tables 1-6).

To assess the overall contribution of the HLA-Cw*0702-restricted CD8+T-cell responses within individual donors to the total CD8+T-cell repertoire, where two or more of the HLA-Cw*0702 epitope specific responses were present within an individual donor, these were summed (Fig-24B/C). The summed HLA-Cw*0702 populations ranged from a remarkable 0.54%-39.41% producing IFN-γ, 0.16%-11% producing IL-2 and 0.54%-53.23% producing TNF-α of the total CD8+T-cell pool within donors aged 23 to 86 years of age (Fig-24B/C). These summed responses displayed marked inflation with increasing age of the donor (Fig-24B). On average the summed responses increased significantly between donors <70 vs >70 years of age 4.76%-28.69% producing IFN-γ, IL-2 0.58%-5% and 5.15-32.88% producing TNF-α (Fig-24C)

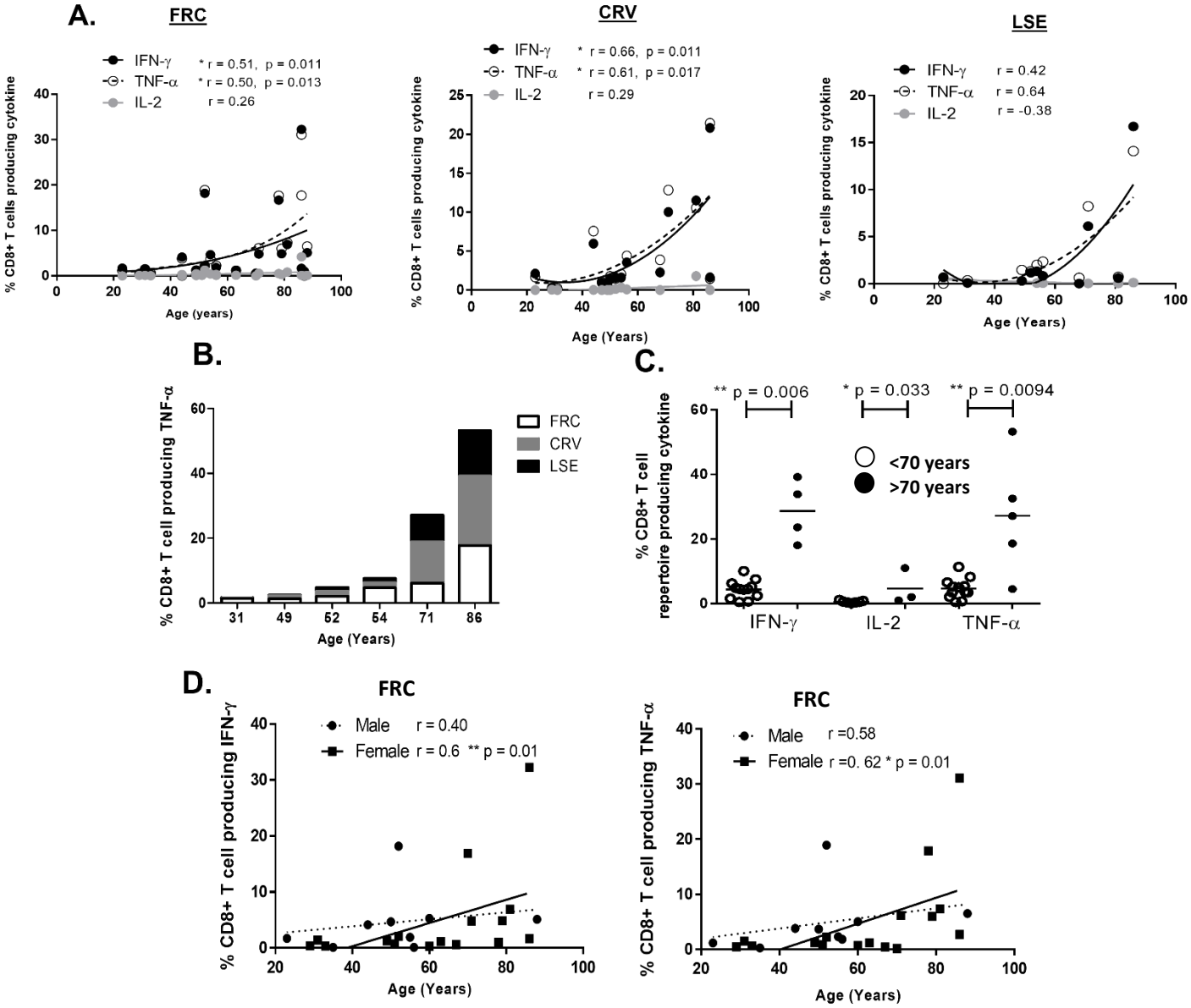


***Fig 24 – Kinetics of HLA-Cw*0702-restricted memory-inflated CD8+T-cell populations with age.*** The kinetics of the HLA-Cw*0702 HCMV CD8+T-cell populations were analysed with the age of the donor cohort. PBMCs from seropositive donors were stimulated with HCMV peptide (final concentration 1µg/ml) for 6 hours followed by intracellular staining for IFN-γ, IL-2 and TNF-α to identify specific CD8+T-cell responses. A) Magnitude of the cytokine production elicited by the HLA-Cw*0702 peptides correlated with age. Spearman's rank correlation of the magnitude of cytokine production elicited by the FRC- (left), CRV- (middle), and LSE-specific (right) CD8+T-cells with the age of the donors in our cohort. Each circle represents the percentage of the total CD8+T-cell response elicited by the peptide in question. Lines represent a polynomial curve to represent the data trend. B) The sum percentage of the FRC-, CRV- and LSE-specific CD8+T-cell populations within individual representative donors where all three HLA-Cw*0702 populations were present. C) Summary of the totalled percentage of all three HLA-Cw*-0702 CD8+T-cell populations within individual donors. White circles represent donors <70 years and black circles represent donors >70 years. Statistical significance was obtained via Mann Whitney in Graphpad Prism 6 with ** as a p-value of < 0.005 D) Correlation of the IFN-γ (left) and TNF-α (right) production elicited by the UL28-derived FRC peptide with age in males (dotted line) vs females (black lines). Lines represent linear regression. In A/D) Statistical significance was obtained by spearman's rank correlation and C) multiple Mann-Whitney tests in Graphpad prism 6 with * and ** as p-values of <0.05 and <0.01.

## 4.4 - HLA-Cw*-0702 mediated memory-inflation dominates individual CD8+T-cell memory compartments of older seropositive donors

After observing that these populations dominated the total peripheral CD8+T-cell pool of both young and older individuals, it was next determined to what extent the HLA-Cw*0702 CD8+T-cell responses comprised of the individual memory CD8+T-cell compartments.

PBMCs of donors with *ex vivo* HLA-Cw*0702 CD8+T-cell responses were phenotyped for CCR7 vs CDR45RA expression by flow cytometry to identify; $T_N$ ($CCR7^+CD45RA^+$), $T_{CM}$ ($CCR7^+CD45RA^-$), $T_{EM}$ ($CCR7^-CD45RA^-$) and $T_{EMRA}$ ($CCR7^-CD45RA^+$) memory populations after 6 hours HLA-C peptide stimulation (gating strategy provided in Fig-25A). To identify the HLA-Cw*-0702 peptide responding CD8+T-cells within each compartment, these individual memory populations were then analysed for TNF-α producing CD8+T-cells (Fig-25C). To do this, the gate utilised to identify the HLA-C-specific CD8+T-cells within the total CD8+T-cell population (TNF-α gate Fig-25B) was placed upon the $T_N$, $T_{CM}$, $T_{EM}$ and $T_{EMRA}$ populations as demonstrated in Fig-25C. .

Within a representative individual younger donor, the FRC-specific HLA-Cw*0702-restricted CD8+T-cell response (Fig-24B) comprised up to 0.88%, 1.89%, 1.61% and 5.15% of the total $T_N$, $T_{CM}$, $T_{EM}$ and $T_{EMRA}$ memory compartments respectively (Fig-25C). These FRC-specific CD8+T-cells increased within the same memory compartments of a representative older individual donor of 86 years to 1.50%, 13.5%, 24.13% and 22.71% respectively (Fig-25D).

When summarised, the HLA-Cw*0702-restricted populations accounted for on average 2.32%, 4.69%, 6.03% and 7.76% of the total $T_N$, $T_{CM}$, $T_{EM}$ and $T_{EMRA}$ memory compartments respectively within our younger donor cohort <70 years of age (Fig-25E). This increased dramatically within our elderly cohort >70 years of age to 4.57%, 12.23%, 21.14 & and 20.11% respectively (Fig-25E).

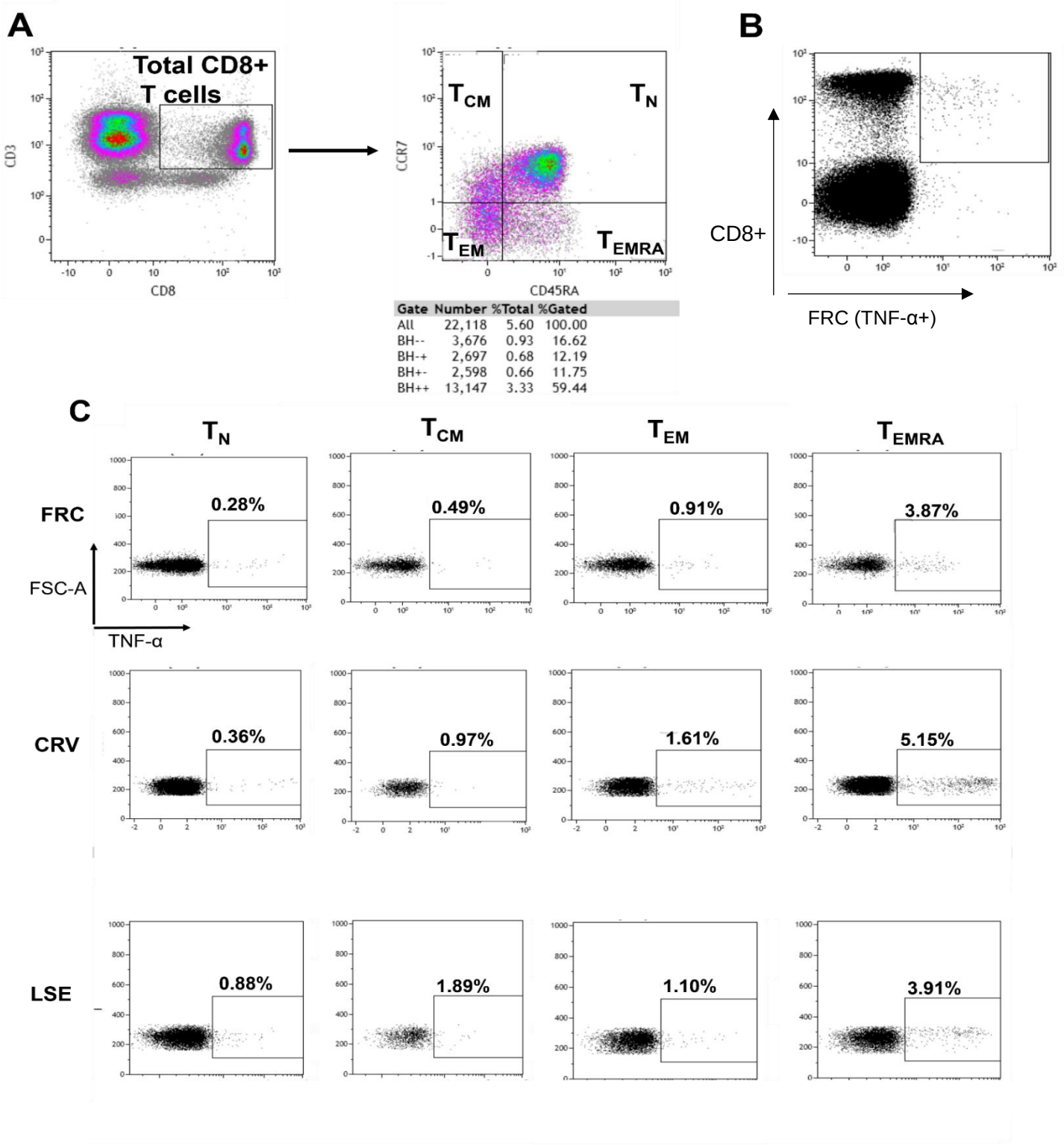


**Fig 25 - Percentage of the memory CD8+T-cell compartment comprised of the HLA-Cw*0702 inflated HCMV-specific CD8+T-cell response.** PBMCs from seropositive donors were stimulated with HLA-C HCMV peptide (final concentration 1µg/ml) for 6 hours followed by staining with CCR7 vs CD45RA and intracellular staining for TNF-α to identify specific CD8+T-cell responses. TNF-α positive cells within the CCR7 vs CD45RA gates was then analysed A) Gating strategy to identify memory CD8+T-cell memory compartments. The CCR7 vs CD45RA gates were first applied on the CD8+T-cell population to identify the memory compartments and the TNF-α was applied to these compartments. B) The FRC-specific CD8+T-cell response used in this gating strategy example in YD13 of 52 years. The percentage values shown have the unstimulated TNF-α production value subtracted C) Representative dot plot demonstrating the percentage of the memory CD8+T-cell compartments occupied by the FRC- (top row), CRV- (middle row) and LSE-specific (bottom row) CD8+T-cell populations in the $T_N$ (left column), $T_{CM}$ (second column), $T_{EM}$ (third column) and $T_{EMRA}$ (last column) memory CD8+T-cell compartments of the total CD8+T-cell population. Within each memory gate identified in A, the TNF-α positive gate was applied on the individual memory compartments. This indicated the percentage of HLA-C-specific CD8+T-cells within that compartment. The percentage of HLA-C epitope-specific CD8+T-cells within each compartment are indicated on the plots.

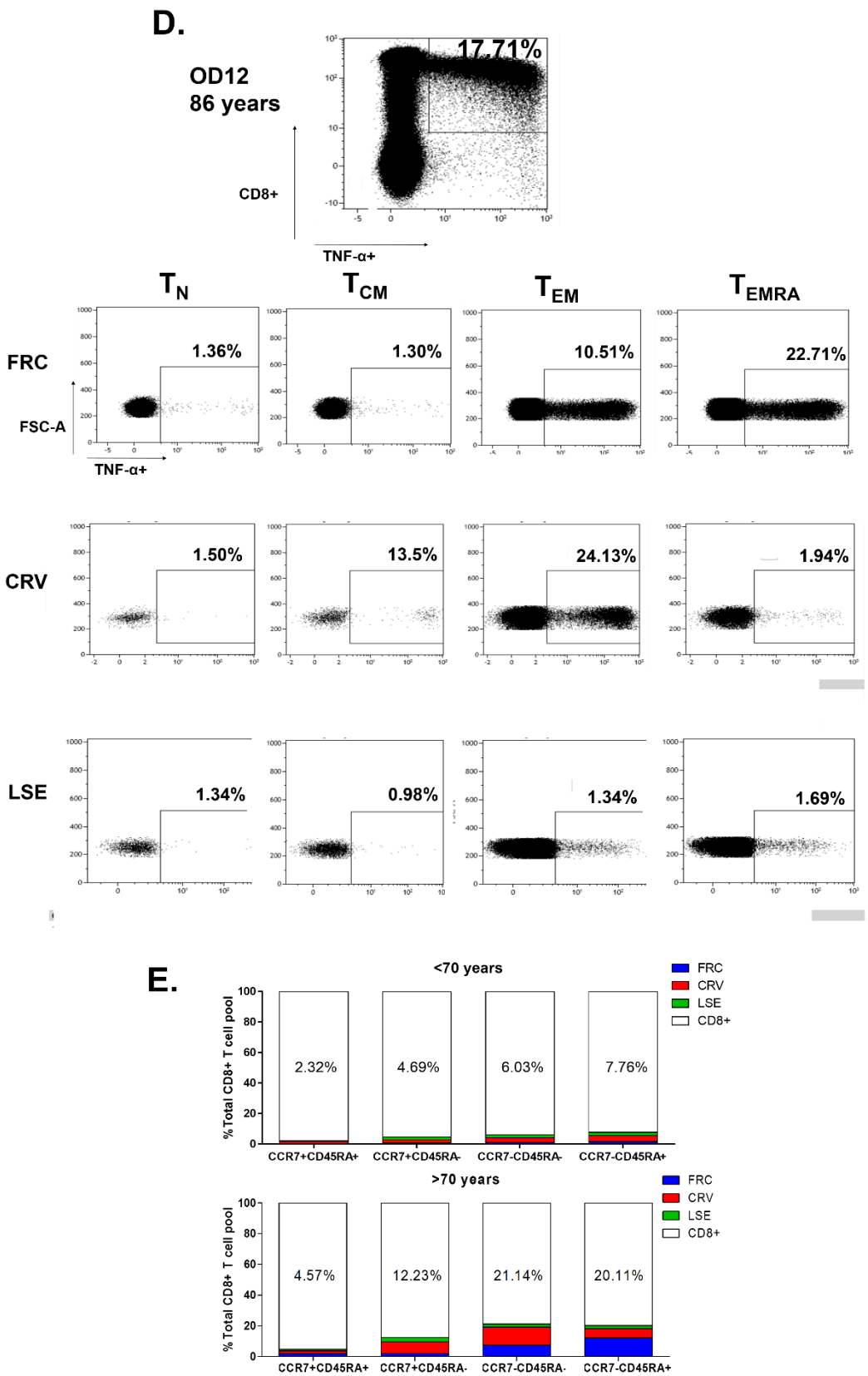


***Fig 25 continued - percentage of the memory CD8+T-cell compartment occupied by the HLA-Cw*0702 inflated HCMV-specific CD8+T-cell responses*** D) Representative dot plots demonstrating the percentage of the HLA-Cw*0702 inflated CD8+T-cell responses comprising the individual memory CD8+T-cell compartments within an older donor of 86 years. The top plot demonstrates the FRC-specific population within the older donor used in the example. The percentage of the FRC-, (top row) CRV- (bottom row) and LSE-specific (bottom row) populations in the $T_N$ (left column), $T_{CM}$ (second column), $T_{EM}$ (third column) and $T_{EMRA}$ (last column). The percentage of HLA-C epitope-specific CD8+T-cells within each compartment are indicated on the plots. The percentage values shown have the unstimulated TNF-α production value subtracted E) Summary of the percentage of the three HLA-Cw*0702 CD8+T-cell populations comprising the individual memory compartments within YD (top) vs OD donors (bottom). For <70 year category, n = 4, 4 and 3 for FRC- CRV- and LSE-specific CD8+T-cell responses. For >70 year category n = 4, 3 and 3 for the FRC-, CRV- and LSE-specific CD8+T-cell responses.

The four compartments were occupied by similar percentages of the LSE-specific CD8+T-cell populations between <70 vs >70 years. However the percentage within the $T_{CM}$ compartment increased slightly from 1.76%-2.72% (Fig-25E).

The memory compartment occupied by the largest percentage of CRV-specific CD8+T-cell populations was the $T_{EMRA}$ compartment in younger donors at 4.02% which switched to the $T_{EM}$ compartment at 11.68% within older donors (Fig-25E).

In both the <70 vs >70 year donors, the memory compartment comprised of the largest FRC-specific CD8+T-cell populations was the $T_{EMRA}$ compartment that increased from 1.65%-12.02% with age (Fig-25E).

To conclude this section, the HLA-Cw*0702 can dominate the $T_{EM}$ and $T_{EMRA}$ compartments with age. Suggesting that they are chronically driven by antigen.

# Chapter 4

## Project 1 Summary

This work has identified three remarkably immunodominant CD8+T-cell populations that are restricted through HLA-Cw*0702 and specific for IE-derived antigen. The largest populations were observed against a UL28-derived peptide termed 'FRC', followed by two populations specific for IE-1-derived peptides termed 'CRV' and 'LSE'. These HLA-C populations remained the most immunodominant CD8+T-cell responses when donors were also screened for the conventional immunodominant pp65/IE-1-derived HLA-A1, -A2 and –B7 restricted VTE, VLE, YSE, NLV, RPH and TPR peptides.

Individual CD8+T-cell responses to the FRC, CRV and LSE peptides reached a maximum of 31.07%, 21.43% and 12.75% producing TNF-α within individual donors of the total peripheral CD8+T-cell repertoire respectively. Notably, these HLA-Cw*0702-restricted populations when summed exceeded over 56% of an individual's total peripheral CD8+T-cell pool. Impressively, the HLA-Cw*0702-restricted CD8+T-cells comprised on average almost 8% of a younger donor cohorts $T_{EMRA}$ compartment which increased dramatically to almost 21% in donors aged >70 years. The FRC-specific CD8+T-cells could reach an impressive 22.71% of the $T_{EMRA}$ pool within a donor of 86 years. Remarkably, the summed HLA-Cw*0702 CD8+T-cells also comprised significant proportions of the $T_N$, $T_{CM}$ and $T_{EM}$ compartments reaching averages of 4.57%, 12.23%, 21.14 respectively within older donors

This HLA-C memory-inflation was found to be confined to CMV peptides that are HLA-Cw*0702-restricted and expressed during the viral life cycle with IE kinetics. This was supported by non-inflating CD8+T-cell populations observed in this investigation towards; the IE-1-derived HLA-Cw6-restricted QIK peptide, the L-expressed UL33-derived HLA-Cw*0702-restricted SYR peptide and lastly HLA-C-restricted peptides derived from the L-expressed pp65 protein.

# Project 2 – Phenotype and functionality of memory-inflated HLA-C CMV CD8 T-cells

## 4.5 - The cytokine polyfunctionality of HLA-Cw*0702 CD8+T-cell populations alters with age, response size and differs significantly to other HCMV-specific CD8+T-cell populations

HCMV CD8+T-cell memory-inflated populations have previously been identified as increasing their polyfunctionality with both the age of the donor and as the size of the specific CD8+T-cell response increases [110, 268]**.** Large populations of pp65-specific CD8+T-cell populations have been identified as accumulations of enhanced polyfunctional populations with age – indicated by IFN-γ, IL-2, TNF-α, CD107a and perforin expression - compared to younger individuals with smaller pp65-specific CD8+T-cell populations [110].

Next, the cytokine polyfunctionality of the HLA-Cw*0702-restricted CD8+T-cell responses was analysed with the age of the donors (between <70 and >70 years) and the size of the epitope-specific responses. This cytokine polyfunctionality was also compared to that of other HCMV-specific CD8+T-cell populations. This was in order to determine whether polyfunctional CD8+T-cells preferentially accumulated within the HLA-Cw*0702 populations with age.

To do this, boolean bimodial parameter analysis was applied within the Kaluza 1.3 software (gating strategy provided in Fig-26) and then the novel polyfunctionality index algorithm devised by Larsen et al. [funky cell software [269] was utilised to determine the percentage of the epitope-specific T-cells producing any combination of IFN-γ, IL-2 and TNF-α.

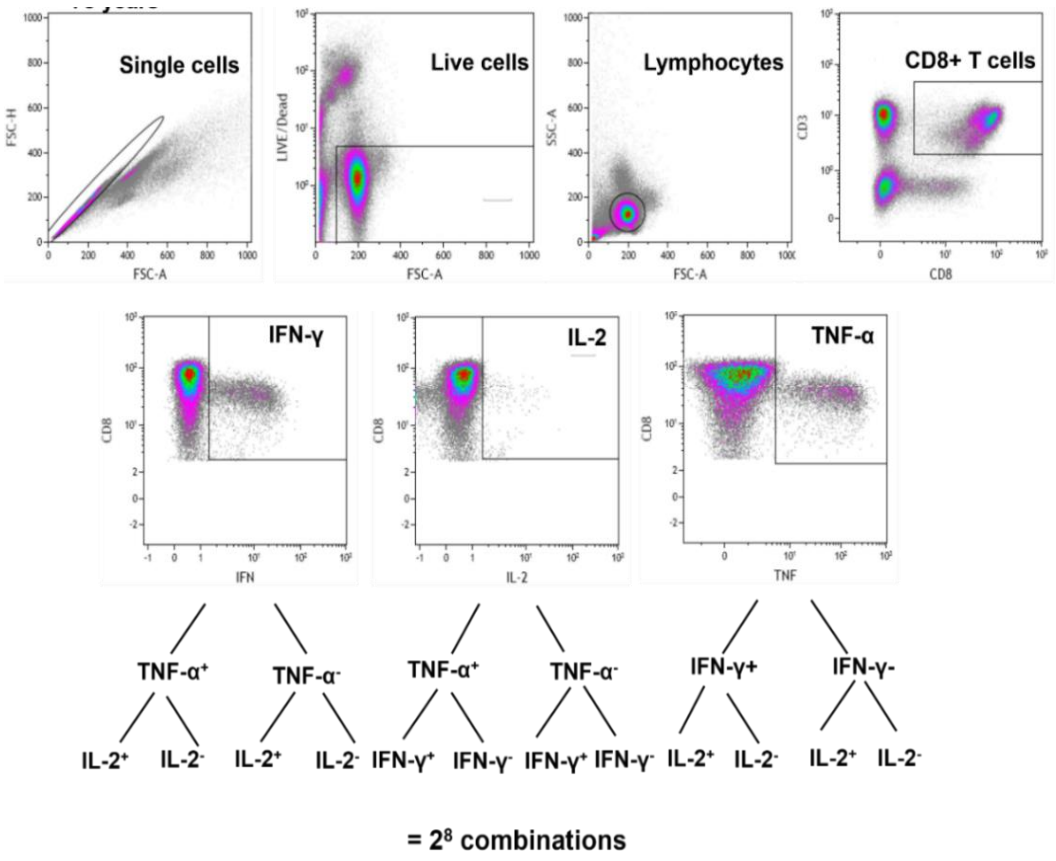


***Fig 26 – Gating strategy for Boolean cytokine polyfunctionality analysis in Kaluza 1.3 software.*** Determination of the percentage of HCMV-specific CD8+T-cells producing combination of the IFN-γ, IL-2 and TNF-α cytokines. PBMCs from HCMV seropositive donors were stimulated with HCMV peptide (final concentration 1µg/ml) for 6 hours. Single, live, CD3+CD8+ lymphocytes were gated on sequentially within Kaluza 1.3 software (Beckman Coulter) as outlined in Fig-7. Cytokine producing CD8+T-cells were then identified in the gated CD8+ population. A positive gate for each cytokine function was placed on the total CD8+T-cells. Within the Kaluza software, Boolean gates for the $2^8$ combinations of cytokine production were manually generated and the numbers of cells within each combination were then inputted into 'Funkycell' software [269]. The resulting polyfunctional output - the percentage of cells within each cytokine combination and the polyfunctionality index - were generated into graphical format within Graphpad Prism 6.

4.5.1 – Cytokine polyfunctionality between donors <70 vs >70 years of age

The production of IFN-γ, IL-2 and TNF-α cytokines in any combination by individual CD8+T-cells within the total HLA-Cw*0702 epitope-specific CD8+T-cell populations was evaluated after peptide stimulation between donors <70 vs >70 years of age.

There were two general trends that were observed between the age categories.

The first; within older donors the number of individual HLA-Cw*0702 epitope-specific CD8+T-cells producing the pro-inflammatory cytokines IFN-γ and TNF-α increased compared to younger donors (CRV; 69%-86% and LSE; 38%-51%, Fig-27A/C). The FRC-specific CD8+T-cell population retained an equal proportion of individual CD8+T-cells producing both IFN-$\gamma^{+}$TNF-$\alpha^{+}$ between the age categories (70%, Fig-27A/C).

The second trend; within older donors the number of individual HLA-Cw*0702 CD8+T-cells producing IL-2 was decreased (Fig-27A/C).

CRV-specific CD8+T-cells producing IL-2 as their single cytokine were not present in donors >70 years of age. LSE-specific CD8+T-cells producing IL-2 in combination with TNF-α were not present within donors >70 years of age. Finally, FRC-specific CD8+T-cells producing IL-2+IFN-γ or IL-2/+TNF-α were not present in donors >70 years of age (Fig-27A/C).

Despite these trends, no significant differences in cytokine production was obtained between the young vs older categories.

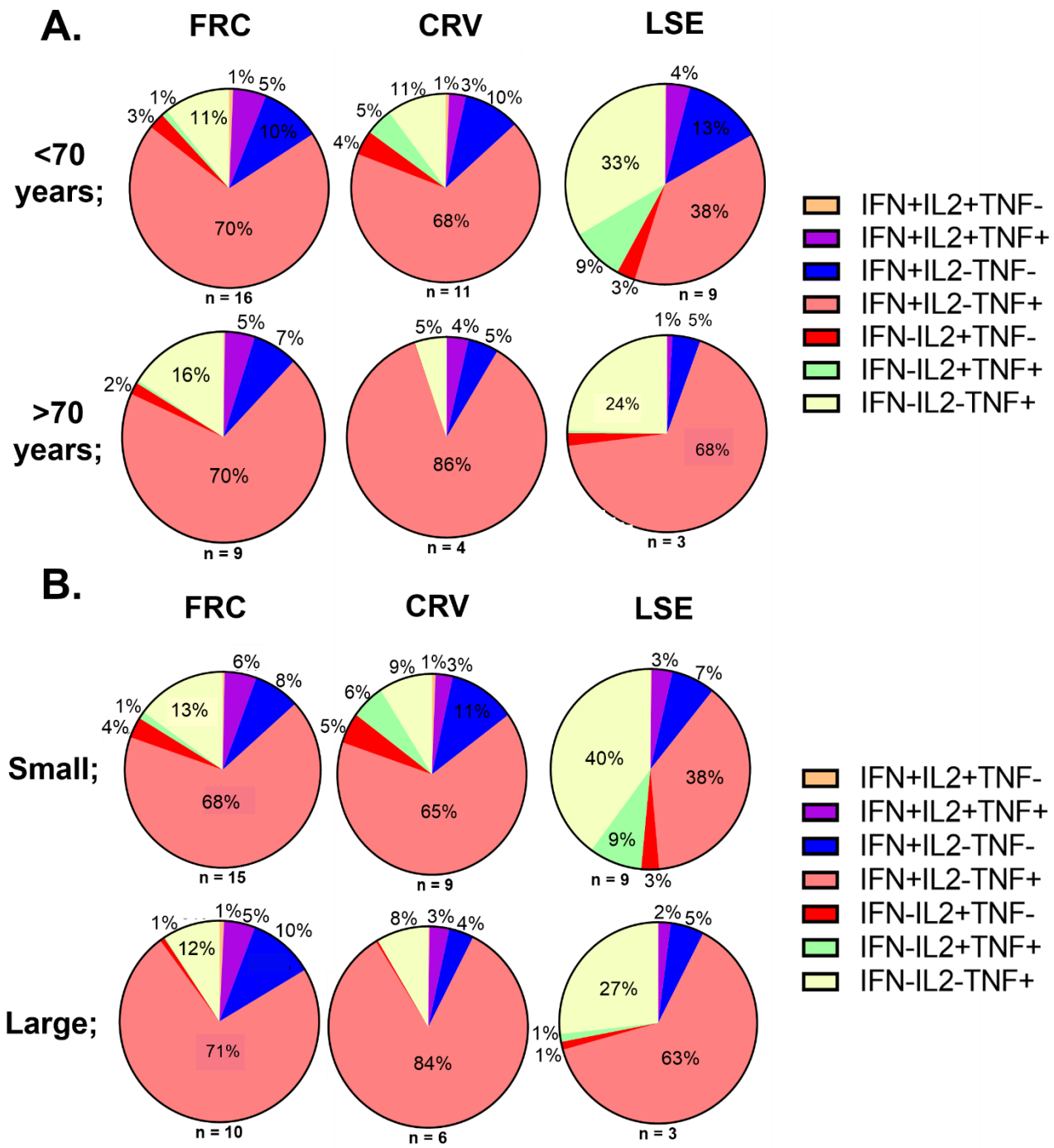


***Fig 27 – Cytokine polyfunctionality profiles of the HLA-Cw*0702-restricted inflated responses with age and response size***. The proportion of HLA-Cw*0702-restricted CD8+T-cells producing combinations of IFN-γ, IL-2 and TNF-α after peptide stimulation. PBMCs from seropositive donors were stimulated with HLA-C HCMV peptide (final concentration 1µg/ml) for 6 hours followed by intracellular staining for IFN-γ, IL-2 and TNF-α to identify specific CD8+T-cell responses. Cytokine polyfunctionality profiles were determined as outlined in Fig-26. A) Average cytokine polyfunctionality profiles of the FRC- (left), CRV- (middle) and LSE-specific (right) HLA-Cw*0702-restricted responses between the <70 (top) and >70 year (bottom) donor category. The percentages provided per pie slice represent the percentage of epitope-specific CD8+T-cells producing the cytokine combination B) Average cytokine polyfunctionality profile of the FRC- (left), CRV- (middle) and LSE-specific (right) HLA-Cw*0702-restricted responses between small (top) vs large (bottom) epitope-specific response sizes. The HLA-Cw*0702-specific CD8+T-cell populations were categorised as small or large if they were <2% or > than 2% of the total CD8+T-cell response responding to peptide. The n numbers are provided below the pie charts. Statistical significance was analysed by a Kruskall-Wallis test in Graphpad prism 6 of the cytokine combination categories between <70 vs >70 year donor categories with * as a p-value of <0.05.

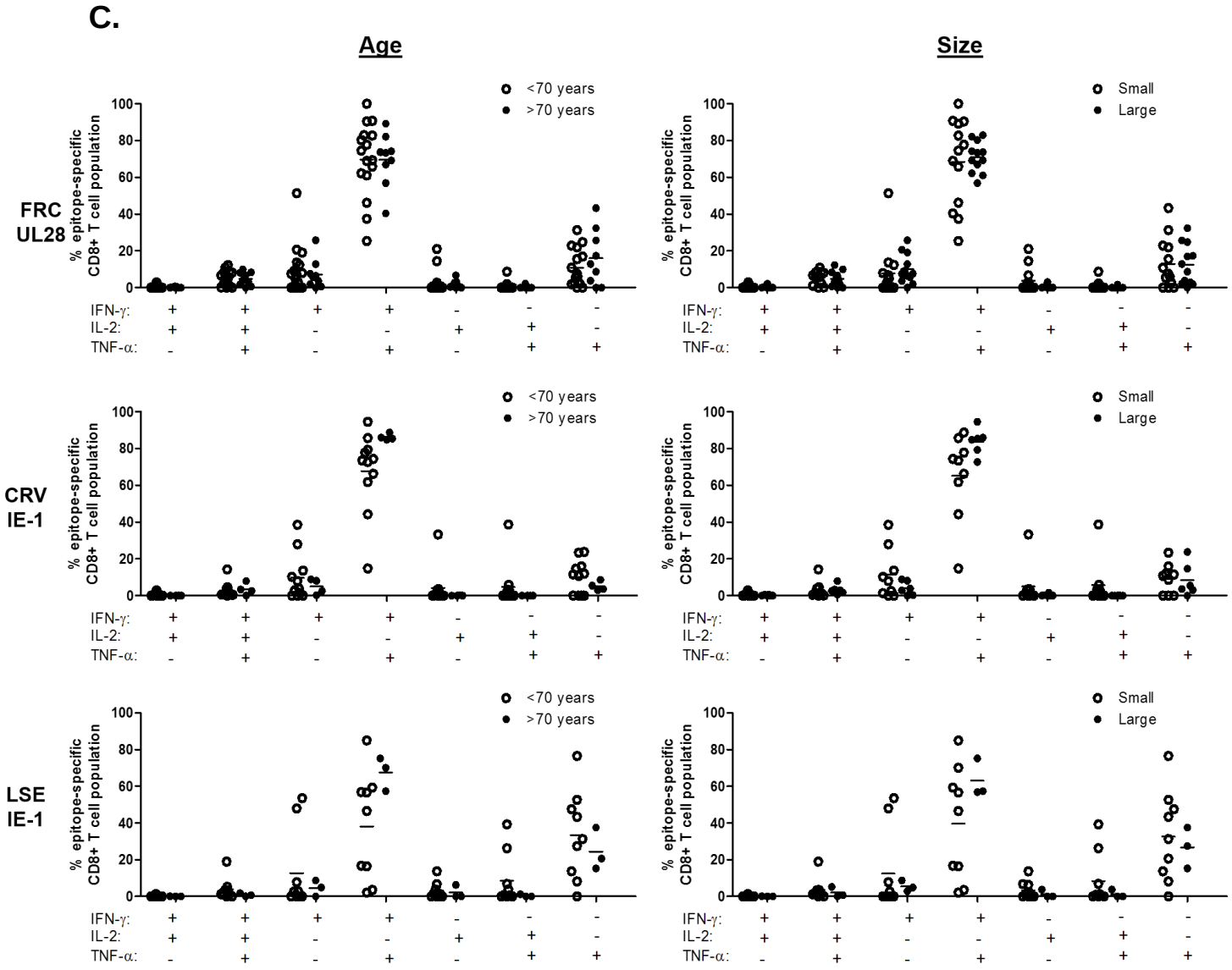


***Fig 27 continued – Cytokine polyfunctionality profiles of the HLA-Cw*0702-restricted inflated responses with age and response size***. C) Summary of the cytokine polyfunctionality profiles of the FRC (top row), CRV (middle row) and LSE (bottom row) HLA-Cw*0702-specific CD8+T-cell responses in donors <70 vs >70 years (left hand column, white vs black circles respectively) and in small vs large epitope specific CD8+T-cell responses (right hand column, white vs black circles respectively). The small and large categories are defined as in B). The cytokine polyfunctionality was determined for all HCMV-specific CD8+T-cell populations as described in Fig 26. Each circle represents the percentage of the epitope-specific CD8+T-cell population producing that combination of cytokines in an individual donor.

4.5.2 – Cytokine polyfunctionality between small vs large epitope-specific CD8+T-cell populations

The cytokine polyfunctionality was then analysed when the HLA-Cw*-0702 CD8+T-cell populations were categorised depending on the epitope-specific CD8+T-cell response size. These were defined as; small <2% vs large >2% of the total CD8+T-cell response based upon the values selected by Chiu et al. [110].

Similar trends to that observed with age (section 4.5.1) were also detected; reductions in the production of IL-2 but increased IFN-γ/TNF-α production.

The proportion of HLA-Cw*0702-restricted CD8+T-cells producing IFN-$\gamma^+$TNF-$\alpha^+$ but not IL-2 increased as the *ex vivo* magnitude of the HLA-Cw*0702 CD8+T-cell populations also increased (FRC; 68%-71%, CRV; 68%-84% and LSE; 38%-63%) (Fig-27B/C).

As the size of the HLA-Cw*0702 populations increased the number of individual CD8+T-cells producing IL-2 as their single cytokine decreased (FRC; 4%-1%, CRV; 5%-<1% and LSE; 3%-1% between small vs large categories).

The proportion of FRC-and CRV-specific CD8+T-cells producing IL-$2^+$ in combination with TNF-$\alpha^+$ was lost within larger epitope populations (Fig-27B/C).

The proportion of LSE-specific CD8+T-cells producing IL-$2^+$ in combination with IFN-$\gamma^+$ decreased from 9%-1% as the epitope-specific population increased (Fig-27B/C).

Despite these trends, no significant difference in cytokine production was obtained between the small vs large epitope-specific CD8+T-cell population categories.

4.5.3 – Cytokine polyfunctionality of HLA-Cw*0702 CD8+T-cells vs HLA-A-restricted HCMV CD8+T-cell populations

Next the HLA-Cw*-0702 CD8+T-cell population cytokine polyfunctionality was compared to that of CD8+T-cell responses specific for the immunodominant pp65-derived peptide NLV peptide (Table-5) or the HLA-A1-restricted peptides RTD and YAD characterised in this study (Chapter 3, Table-7).

The overall trend observed was that the HLA-A1 restricted CD8+T-cell populations consisted of more CD8+T-cells producing IL-2 than the HLA-Cw*0702 or NLV-specific CD8+T-cell populations.

The RTD-/YAD-specific CD8+T-cell responses consisted of the largest proportion of individual CD8+T-cells capable of producing IFN-$\gamma^+$IL-$2^+$TN$F^+$ (19% and 22% respectively Fig-28A/C).

The HLA-Cw*0702 FRC and CRV populations consisted of a significantly larger proportion of individual CD8+T-cells producing both IFN-$\gamma^+$TNF-$\alpha^+$ but not IL-2 compared to the YAD HLA-A1-restricted CD8+T-cell populations (Fig-28A/C).

NLV-specific CD8+T-cells also had a larger percentage of individual CD8+T-cells producing both IFN-$\gamma^+$TNF-$\alpha^+$ but not IL-2 compared to the YAD-specific CD8+T-cell response (Fig-28A/C).

Next the cytokine polyfunctionality was assessed taking into account the average ‘mean fluorescence intensity’ (MFI) of the TNF-α staining obtained for the HCMV-specific CD8+T-cell populations. This is indicative of how many cytokine molecules on a per cell basis a CD8+T-cell is producing.

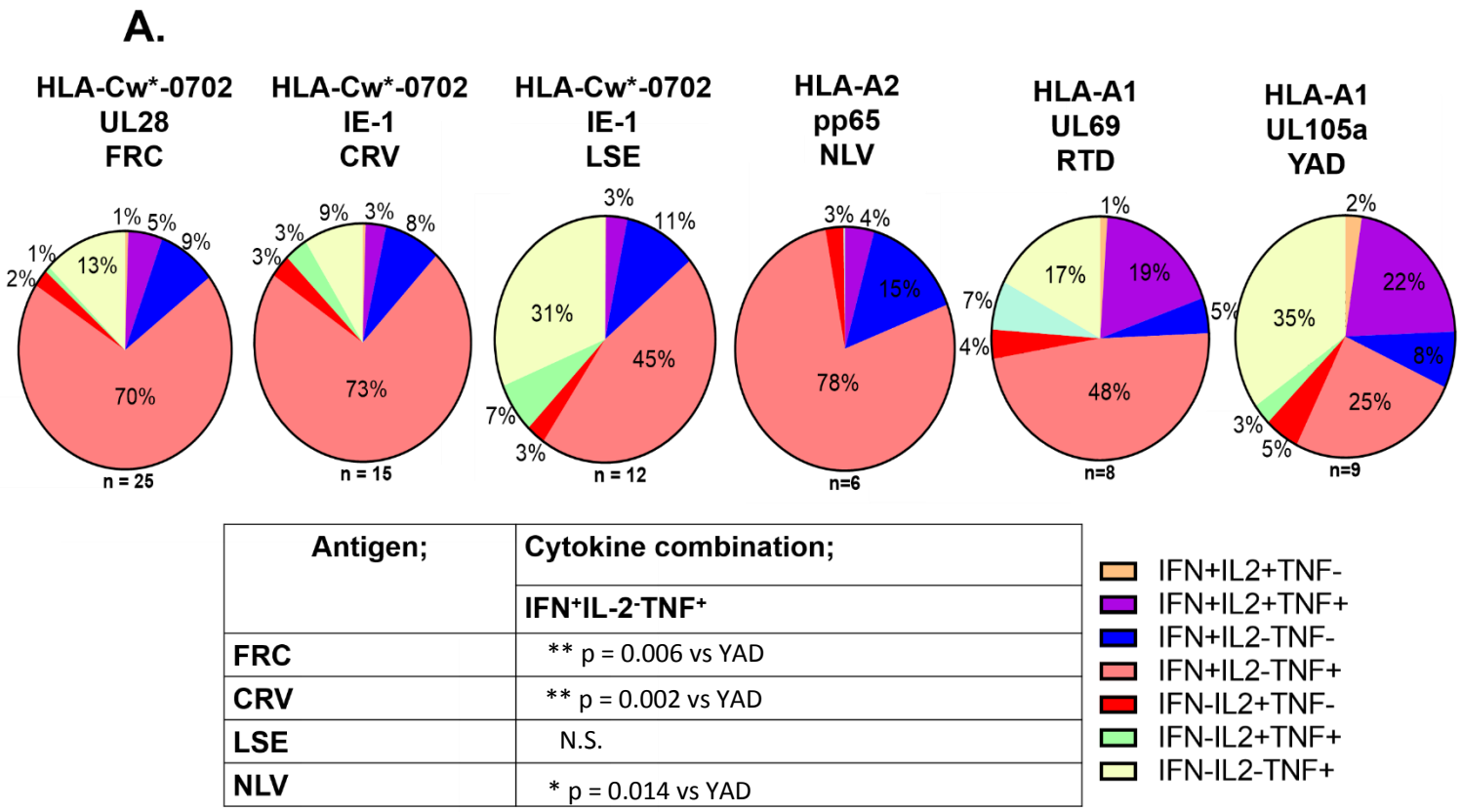


| Antigen; | Cytokine combination; |
|---|---|
| | IFN⁺IL-2⁻TNF⁺ |
| FRC | ** p = 0.006 vs YAD |
| CRV | ** p = 0.002 vs YAD |
| LSE | N.S. |
| NLV | * p = 0.014 vs YAD |

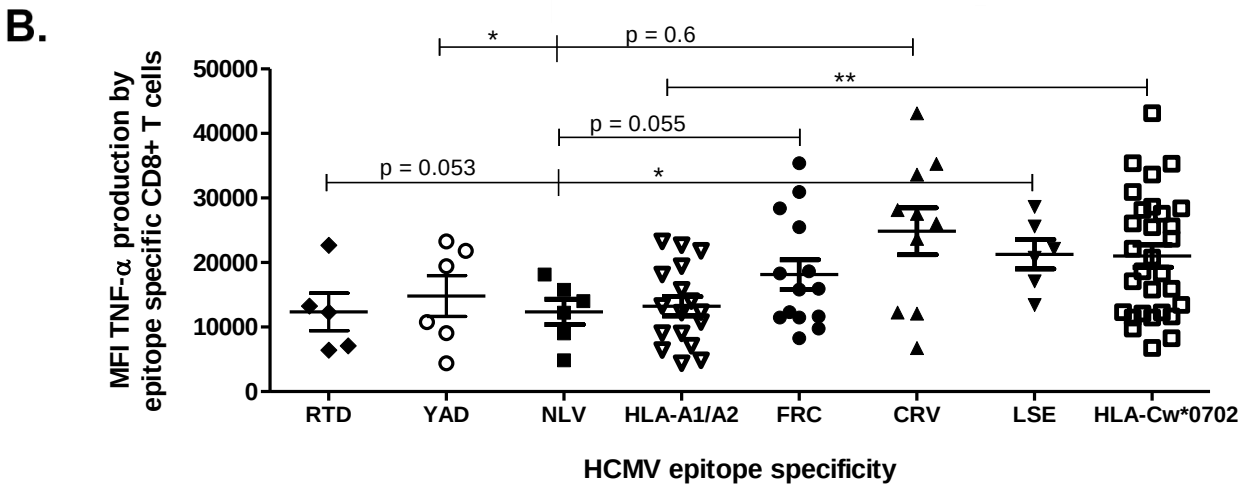


***Fig 28 – Cytokine polyfunctionality and cytokine MFI of the inflated HLA-Cw*0702-restricted HCMV-specific populations vs HCMV-specific CD8+T-cell populations that are HLA-A-restricted.*** The cytokine polyfunctionality profile of the HLA-Cw*0702-restricted CD8+T-cell populations was compared to the profiles of HLA-A-restricted HCMV-specific CD8+T-cell populations. PBMCs from seropositive donors were stimulated with HCMV peptide (final concentration 1µg/ml) for 6 hours followed by intracellular staining for IFN-γ, IL-2 and TNF-α to identify specific CD8+T-cell responses A) The cytokine polyfunctionality profile of HLA-C and HLA-A-restricted HCMV-specific CD8+T-cell responses. The cytokine polyfunctionality was determined for all HCMV-specific CD8+T-cell populations as described in Fig 26. The percentages represent the percentage of epitope specific-CD8+T-cells producing the cytokine combination. Statistical significance was determined by Kruskall Wallis test in Graphpad Prism 6 with Dunn corrections applied * as a p value < 0.05 and ** < 0.01. B) Mean fluorescence intensity (MFI) of the total TNF-α produced by HCMV-specific CD8+T-cell populations after 6 hours HCMV peptide stimulation. The summed HLA-A-restricted CD8+T-cell responses include RD/YAD/NLV and the pooled HLA-Cw*0702 include FRC/CRV/LSE. Lines represent mean and errors bars SEM. Statistical significance was determined using multiple Mann Whitney tests in Graphpad Prism 6 with * as a p values < 0.05 and ** < 0.01.

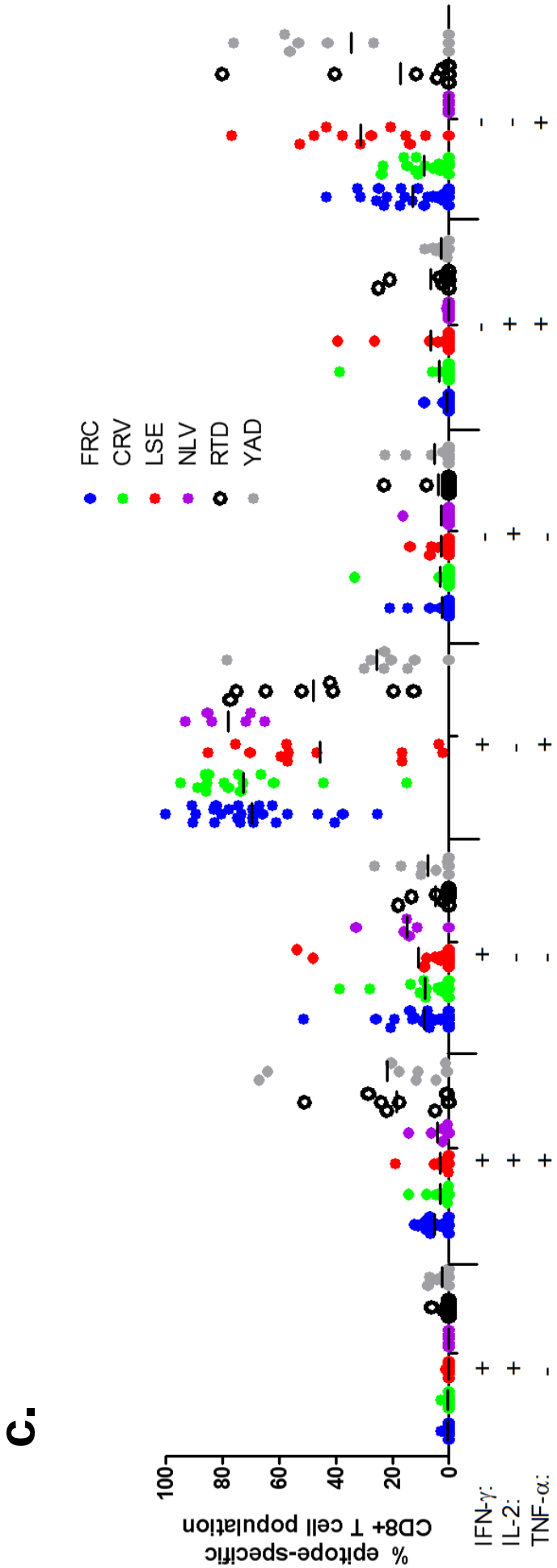


***Fig 28 continued – Cytokine polyfunctionality and cytokine MFI of the inflated HLA-Cw*0702-restricted HCMV-specific populations vs HCMV-specific CD8+T-cell populations that are HLA-A-restricted.*** C) Summary of the cytokine polyfunctionality profiles of the FRC (blue), CRV (green) and LSE (red) HLA-Cw*0702-specific CD8+T-cell responses vs HLA-A1 RTD (white), HLA-A1 YAD (grey) and HLA-A2 (pink) specific CD8+T-cell responses. The cytokine polyfunctionality was determined for all HCMV-specific CD8+T-cell populations as described in Fig 26. Each circle represents the percentage of the epitope-specific CD8+T-cell population producing that combination of cytokines in an individual donor.

The CRV- and LSE-specific CD8+T-cells produced TNF-α with a significantly increased MFI over RTD- and NLV-specific CD8+T-cells (Fig-28B). When the CD8+T-cell responses were pooled based upon their HLA-restriction, the summed HLA-Cw*0702 CD8+T-cell responses produced TNF-α with a significantly increased MFI over the HLA-A-restricted HCMV-specific CD8+T-cell responses (Fig-28B). The MFI of the TNF-α produced by FRC-specific CD8+T-cells trended to significance over the cytokine produced by NLV-specific CD8+T-cells ($p = 0.055$, Fig-28B).

Overall, this is suggestive that the HLA-Cw*-0702-restricted populations are producing more TNF-α cytokine molecules on a per cell basis over HLA-A-restricted HCMV-specific CD8+T-cell populations, including immunodominant NLV-specific populations. The MFI of the IFN-γ production was not significantly different (data not shown).

Statistical significance in Fig-28B was obtained by multiple comparison testing so it must be noted the possibility that significance was obtained by chance. More donors should be screened for these *ex vivo* CD8+T-cell responses to allow for statistical corrections to be applied.

To summarise, the HLA-Cw*-0702-restricted populations consisted of larger percentages of CD8+T-cells capable of producing both the pro-inflammatory cytokines IFN-γ and TNF-α whilst decreasing the percentage producing IL-2. This was as both age and size of the epitope-specific CD8+T-cell populations increased. Additionally, the HLA-Cw*0702 CD8+T-cell populations displayed a cytokine polyfunctionality profile similar to NLV-specific CD8+T-cell populations whom have been identified as both inflationary and highly differentiated [71]. Finally, the total HLA-Cw*0702 CD8+T-cell populations produced less IL-2 than the HLA-A1 RTD- and YAD-specific CD8+T-cell populations. In total, this supports the previous phenotype data where the FRC-specific HLA-Cw*0702 responses were later differentiated and expressed lower levels of CD28 compared to RTD/YAD-specific CD8+T-cells (Chapter 3). CD8+T-cells later in the differentiation pathway are $CD28^-$ and as such produce less IL-2 [270].

## 4.6 - The *ex vivo* phenotype of HLA-Cw*0702 CD8+T-cell populations become increasingly antigen differentiated and increase their cytotoxic potential with age

Memory-inflated CMV-specific CD8+T-cell populations are widely documented as being of a highly differentiated $T_{EMRA}$ phenotype associated with the acquisition of high cytotoxic and effector function [105, 237, 271]. Previously the *ex vivo* FRC-specific CD8+T-cell populations were phenotyped via flow cytometry for memory phenotype and cytotoxic markers (Chapter 3, Fig-12-14). The CRV- and LSE-specific CD8+T-cell populations were therefore next phenotyped utilising the same method of peptide stimulation followed by intracellular cytokine staining by flow cytometry. The same panel of phenotypic markers used to characterise the FRC-specific CD8+T-cells was investigated; CCR7, CD45RA, CD45RO, CD27, CD28, CX3CR1, NKG2D, perforin, granzymeB, CD38 and PD-1. The HLA-Cw*0702 CD8+T-cell populations were then analysed for phenotypic changes with age, in particular; memory subset distribution, antigen differentiation status and cytotoxic potential.

### 4.6.1 Single cell marker expression

First, the expression of single cell markers on the HLA-Cw*0702 CD8+T-cells was correlated with age (Fig-29).

The HLA-Cw*0702-restricted populations increased the expression of cytotoxic molecules with age (Fig-29). The intracellular perforin expression increased significantly for the summed HLA-Cw*0702 CD8+T-cell populations (range 29.17%-96.99%). The perforin expression by the FRC- and CRV-specific CD8+T-cell populations correlated significantly with the age of our donor cohort (range 20.63%-99.84%, 13.64%-99.60% respectively). The LSE-specific CD8+T-cells also increased intracellular perforin production with age (range 40.84%-98.62%) ($p = 0.06$) (Fig-29). The granzymeB expression was higher than perforin expression within younger donors and only increased significantly with age for CRV-specific CD8+T-cell populations (range 36.30%-99.07%) (Fig-29).

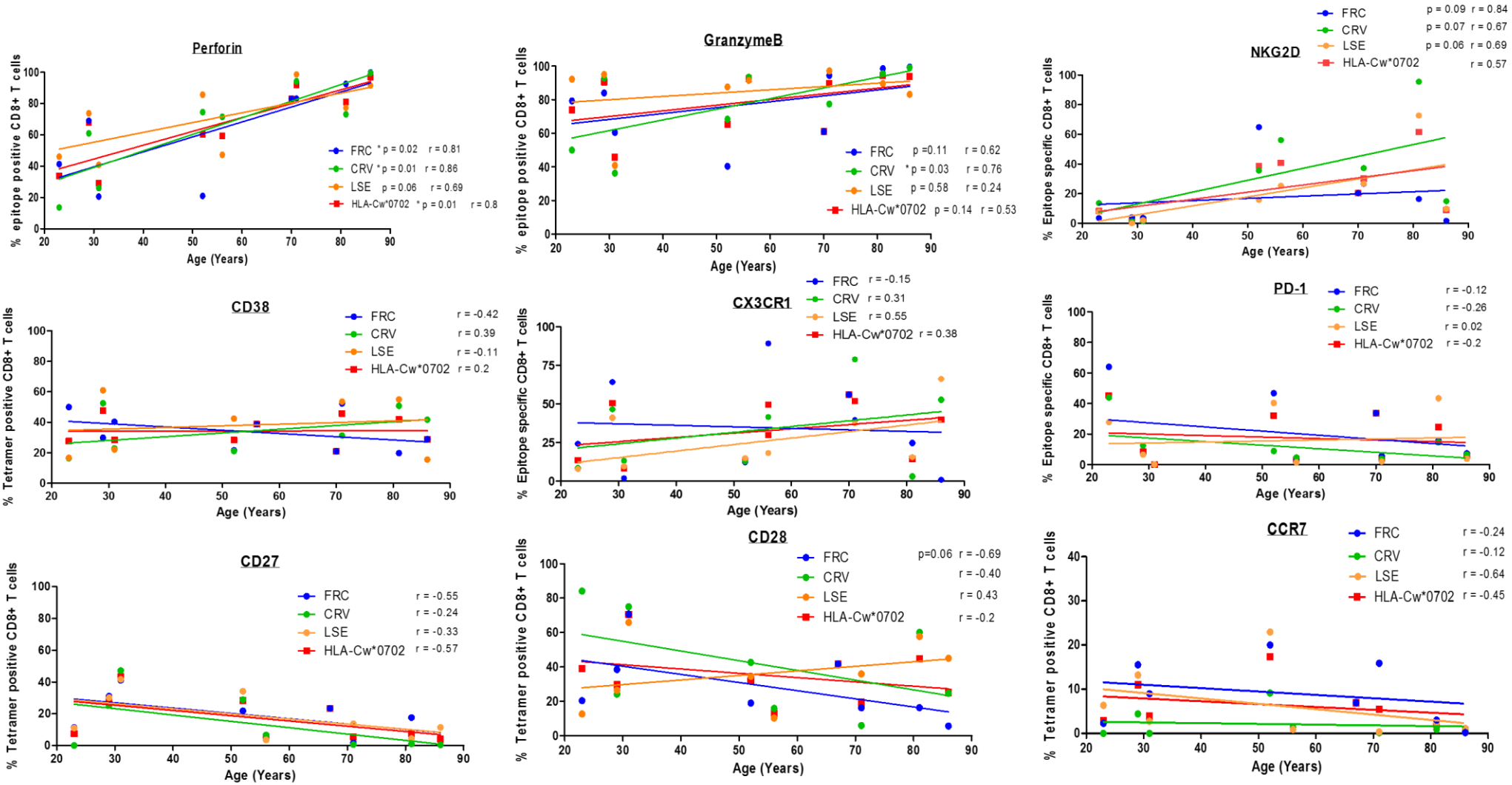


***Fig 29 – Phenotype of the ex vivo HLA-Cw*0702-restricted CD8+T-cell responses determined by flow cytometry correlated with age.*** The expression of single cell markers was analysed on the HLA-Cw*0702 CD8+T-cells and correlated with age. PBMCS of donors with known HLA-Cw*0702 populations were peptide stimulated with the HLA-C peptides for 6 hours. PBMCs were then stained with the antibodies outlined in Table-4 followed by intracellular cytokine staining for TNF-α to identify the specific CD8+T-cell populations before phenotypic characterisation. The correlation of perforin, granzymeB, NKG2D, CD38, CX3CR1, PD-1, CD27, CD28 and CCR7 expression with the age of our donor cohort. Statistical significance was obtained by spearman's rank correlation in Graphpad Prism 6. Lines represent linear regression. Red lines represent the linear regression of the summed HLA-Cw*0702 CD8+T-cell population values for that particular marker.

Interestingly, the FRC-, CRV- and LSE-specific CD8+T-cell responses increased NKG2D expression with age ($p = 0.09$, 0.07 and 0.06 respectively, average summed HLA-Cw*0702 response range 1.73%-61.54%, Fig-29). NKG2D is an activating receptor for NK cells that on CD8+T-cells acts a co-stimulatory molecule and is expressed when the CD8+T-cell has been recently activated to enhance pro-inflammatory cytokine production [272]. A second activatory marker CD38, was maintained at similar levels with age – summed HLA-Cw*0702 CD8+T-cell response range 20.93%-47.79%, Fig-29).

Concurrent to the observed increase in cytotoxicity markers, there was a trend for the inflated HLA-Cw*0702 CD8+T-cell populations to decrease PD-1 expression with age (summed HLA-Cw*0702 response range 45.21%-0.00%, Fig-29).

The HLA-Cw*0702-restricted responses exhibited a progressive increase of the endothelial fractalkine receptor CX3CR1 within elderly individuals (summed HLA-Cw*0702 8.07%-55.93%, CRV-specific CD8+T-cells 8.33%-78.83% and LSE-specific CD8+T-cells 7.69%-66.13%, Fig-29). The FRC-specific CD8+T-cell populations demonstrated a small decrease with age (range 0.87%-89.22%, Fig-29).

The FRC- and CRV-specific CD8+T-cells displayed a $CD27^{mid}CD28^{mid}$ phenotype that progressed to $CD27^{low}CD28^{low}$ with age (Fig-29) The LSE-specific CD8+T-cell populations differed with an increase in CD28 expression with age (Fig-29). All three HLA-Cw*0702 epitope-specific CD8+T-cell populations decreased CCR7 when correlated with the age of the donor cohort (ranges; FRC 0.18%-20%, CRV 0%-9.15% and LSE 0.34%-22.94%, Fig-29).

4.6.2 - Memory phenotype compartment

To determine what memory compartment the HLA-Cw*0702 responses were occupying and how this altered with age, CCR7 vs CD45RA expression was evaluated. This memory phenotype was analysed between <70 vs >70 year donor cohorts (Fig-30A). With age, the FRC-specific population significantly decreased the proportion of $T_N$ ($CCR7^+CD45RA^+$) CD8+T-cells (6.92%-0.61%) and increased the proportion of $T_{EMRA}$ ($CCR7^-CD45RA^+$) CD8+T-cells (p = 0.06, 49.62%-69.75%, Fig-30A). The CRV-specific CD8+T-cells comprised a larger percentage of $T_{EM}$ ($CCR7^-CD45RA^-$) CD8+T-cells within the total epitope-specific population with age (34.93%-52.34%). The CRV-specific CD8+T-cell population also decreased the proportion of $T_{EMRA}$ ($CCR7^-CD45RA^+$) CD8+T-cells with age (62.73%-46.43%). The total LSE-specific CD8+T-cell population significantly decreased in the percentage of $T_N$ ($CCR7^+CD45RA^+$) CD8+T-cells (6.86%-0.40%) with a concomitant increase in the percentage of $T_{EM}$ ($CCR7^-CD45RA^-$) CD8+T-cells with age (31.85%-45.76%, Fig-30A).

4.6.3 – Antigen differentiation status

The antigen differentiation status of the HLA-Cw*0702 CD8+T-cells and how this altered with age was determined using CD27 vs CD28 expression. This was analysed between <70 vs >70 year donor cohorts (Fig-30B). The total FRC-specific population decreased the percentage of early differentiated ($CD27^+CD28^+$) (20.54%-3.72%), and increased the percentage of late differentiated ($CD27^-CD28^-$) CD8+T-cell populations (43.7%-83.04%, p = 0.06, Fig-30B). The CRV-specific CD8+T-cell populations exhibited the same trends in early (16.28%-3.08%) and late differentiated CD8+T-cells (46.37%-67.14%) (Fig-30B). The LSE-specific CD8+T-cell populations had a significant increase in CD8+T-cells within the intermediate $CD27^-CD28^+$ compartment with age coupled with a decrease in the $CD27^+CD28^+$ early differentiated compartment (15.84%-3.38%). This parallels with the increase of CD28 expression with age (Fig-29).

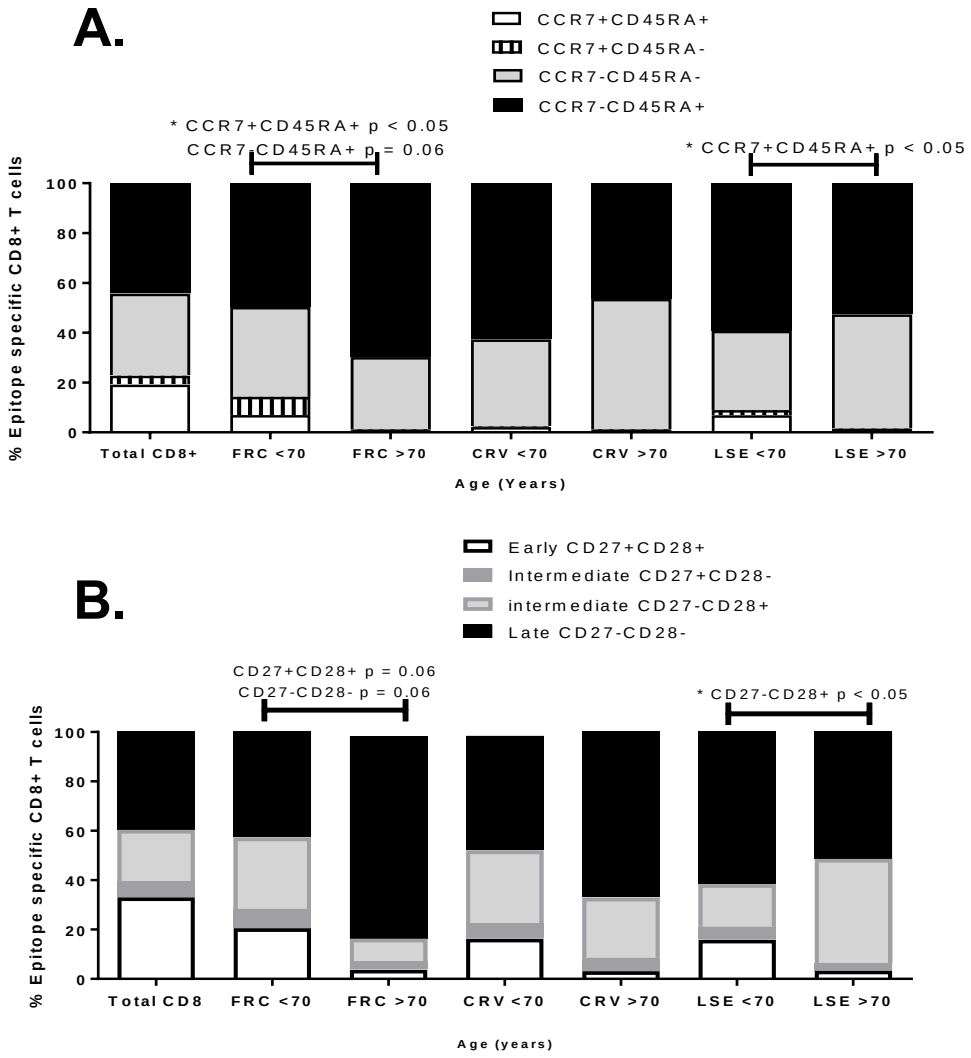


***Fig 30 – Memory phenotype and antigen differentiation status of the ex vivo HLA-Cw*0702-restricted CD8+T-cell responses with age*** The HLA-Cw*0702-restricted CD8+T-cell populations were analysed for CCR7 vs CD45RA expression and CD27 vs CD28 expression between donors <70 vs >70 years of age. PBMCS of donors with known HLA-Cw*0702 populations were stimulated with the HLA-C peptides for 6 hours followed by intracellular cytokine staining for TNF-α to identify the specific CD8+T-cell populations A) Memory phenotype of HLA-Cw*0702-restricted populations between donors <70 or >70 years of age determined as $T_N$ CCR7+CD45RA+, $T_{CM}$ CCR7+CD45RA-, $T_{EM}$ CCR7-CD45RA- and $T_{EMRA}$ CCR7-CD45RA+ by flow cytometry. Gates were applied as outlined in Fig-13 B) Antigen differentiation status of the HLA-Cw*0702 populations between donors <70 or >70 years of age determined as early (CD27+CD28+), intermediate (CD27+CD28- or CD27-CD28+) and late (CD27-CD28-) by flow cytometry. Gates were applied as outlined in Fig-14 In A/B statistical significance was determined by using multiple Mann Whitney tests in Graphpad Prism 6 with * as a p-value <0.05. n = 4-5, 5, 5 for FRC, CRV and LSE <70 years category. n = 4, 3 and for FRC, CRV and LSE >70 years category.

To summarise this section, the inflated HLA-Cw*0702 CD8+T-cell responses increased their cytotoxic potential with age whilst displaying a decrease in the T-cell exhaustion marker PD-1 and upregulating the NKG2D receptor – a marker of recent activation/co-stimulation. Additionally the FRC-specific CD8+T-cell population progressed to a $T_{EMRA}$ and later antigen driven phenotype with age – decreasing CCR7, CD27 and CD28 expression.

## 4.7 - Inflated HLA-Cw*0702 populations become increasingly antigen differentiated and cytotoxic as the size of the epitope specific CD8+T-cell response increases

We demonstrated that the HLA-Cw*0702 populations alter their phenotype with age towards a more $T_{EMRA}$ memory phenotype i.e. increase in cytotoxic molecules and decrease in CCR7 and CD27 expression (Section 4.6). Additionally, this study showed that the HLA-Cw*-0702 populations alter their polyfunctionality with regards to cytokine production based upon age and the epitope-specific CD8+T-cell response size (Section 4.5). Subsequently in this investigation, the *ex vivo* phenotype of the HLA-Cw*0702 CD8+T-cell populations were interpreted as the epitope-specific population accumulated. In particular their memory subset distribution and antigen differentiation status. The phenotypic markers used previously – CCR7, CD45RA, CD45RO, CD27, CD28, CX3CR1, NKG2D, perforin, granzymeB, CD38 and PD-1 – were investigated. The epitope size categories were defined as small (<2%) and large (>2%) of the total CD8+T-cells responding to peptide by cytokine production.

### 4.7.1 – Single marker expression

First the expression of single markers was correlated with the size of the HLA-Cw*0702 epitope-specific CD8+T-cell response. As the size of the TNF-α producing HLA-Cw*0702 CD8+T-cell populations increased, a concomitant increase in perforin and granzymeB (CRV-specific CD8+T-cell perforin expression *p = 0.046, Fig-31). Converse to what was observed with age (Fig-29), there was a trend to decrease NKG2D expression as the FRC-specific populations increased but, however, trended to increase for the CRV- and LSE-specific CD8+T-cell populations (Fig-31). The CX3CR1 expression increased with the size of the CRV- and LSE-specific CD8+T-cells but decreased for FRC-specific (Fig-31). CD38 expression was maintained with the size of FRC- and CRV-specific CD8+T-cell populations (Fig-31). As was confirmed with age, there was a trend to reduce PD-1 expression as the HLA-Cw*0702 populations accumulated (Fig-31). The largest FRC-specific CD8+T-cell response phenotyped (17.22% of total CD8+T-cells producing TNF-α – OD12) displayed an

exaggerated $T_{EMRA}$ phenotype with the highest; perforin/granzymeB but lowest CD27/CD28/CCR7 expression and also lost NKG2D and CXC3R1 expression.

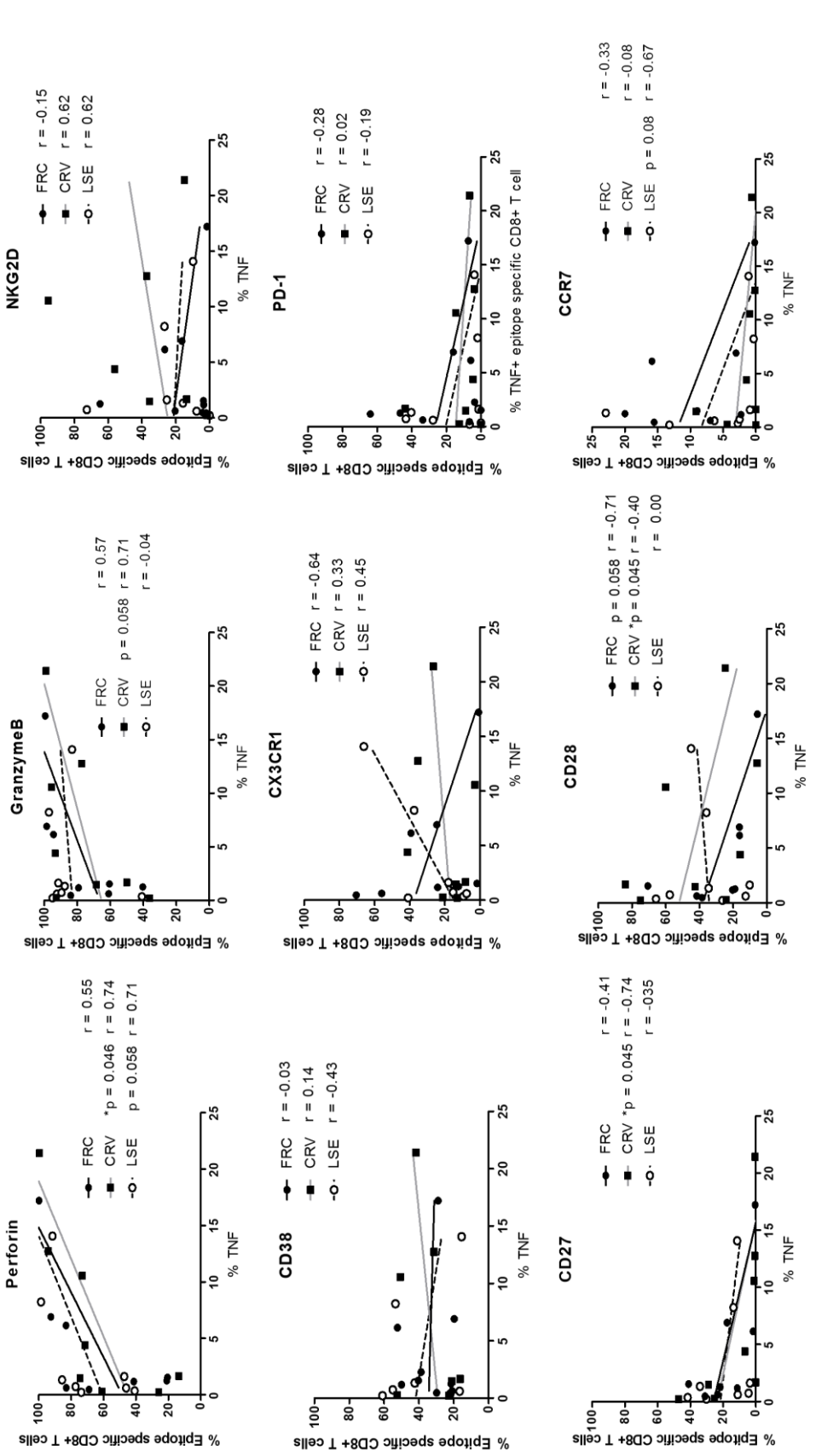


***Fig 31 – The ex vivo CD8+T-cell phenotype of HLA-Cw*0702 CD8+T-cell populations as the size of the epitope specific CD8+T-cell response increases determined by flow cytometry.*** The expression of single cell markers was analysed on the HLA-Cw*0702 CD8+T-cells and correlated with the size of the epitope-specific CD8+T-cell response. PBMCS of donors with known HLA-Cw*0702 populations were peptide stimulated with the HLA-C peptides for 6 hours. PBMCS were then stained with the antibodies outlined in Table-4 and intracellular cytokine staining for TNF-α to identify the specific CD8+T-cell populations before phenotypic characterisation. The correlation of perforin, granzymeB, NKG2D, CD38, CX3CR1, PD-1, CD27, CD28 and CCR7 expression with size of the epitope-specific CD8+T-cell response. The size of the epitope-specific response is indicated by the percentage of CD8+T-cells producing TNF-α in response to peptide stimulation of the total CD8+T-cell response. Statistical significance obtained by speaman's rank correlation in Graphpad Prism 6. Lines represent linear regression.

4.7.2 – Memory phenotype compartment

To evaluate whether the HLA-C CD8+T-cells occupied different memory compartments as the epitope-specific CD8+T-cell populations accumulated, CCR7 vs CD45RA expression was analysed between the small (<2%) and large (>2%) epitope-specific responses.

As was evidenced with age (Fig-30A), the FRC-specific populations reduced the number of $T_N$ ($CCR7^+CD45RA^+$) and increased the number of $T_{EMRA}$ ($CCR7^-CD45RA^+$) CD8+T-cells between the small vs large epitope-specific size categories (average 5.09%-0.71% and 54.13%-74.23% respectively, Fig-32A).

The CRV-specific CD8+T-cell responses significantly increased the number of $T_{CM}$ ($CCR7^+CD45RA^-$) CD8+T-cells between small vs large responses but these remained a small percentage of the total epitope-specific population (average 0.08%-0.79%, Fig-32A). The CRV-specific CD8+T-cell responses also maintained similar levels of $T_{EM}$ ($CCR7^-CD45RA^-$ average 40.73%-42.19%) and $T_{EMRA}$ ($CCR7^-CD45RA^+$ average 57.10%-56.14%) CD8+T-cells with size (Fig-32A).

The LSE-specific CD8+T-cell response contained a larger percentage of $T_{EM}$ (average 34.87%-43.67%) and decreased proportion of $T_N$ (average 5.77%-0.043%) within the large epitope-specific population category. The LSE-specific CD8+T-cell population maintained a small $T_{CM}$ population with size (average 1.71%-1.77%) (Fig-32A).

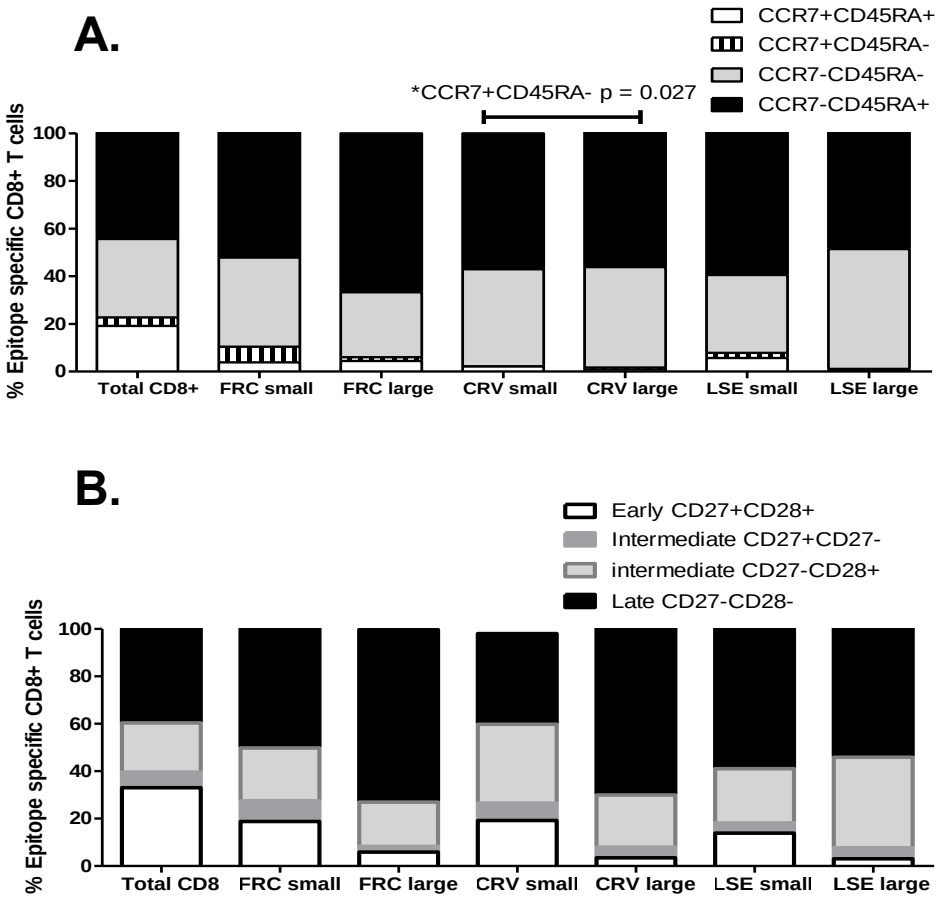


***Fig 32 - The memory phenotype and antigen differentiation status of the ex vivo HLA-Cw*0702 CD8+T-cell populations as the size of the epitope-specific CD8+T-cell response increases.*** The HLA-Cw*0702-restricted CD8+T-cell populations were analysed for CCR7 vs CD45RA expression and CD27 vs CD28 expression between small (2%) vs large (>2%) epitope-specific CD8+T-cell populations. PBMCS of donors with known HLA-Cw*0702 populations were peptide stimulated with the HLA-C peptides for 6 hours followed by intracellular cytokine staining for TNF-α to identify the specific CD8+T-cell populations. PBMCs were subjected to antibody staining with the panels provided in table 4. A) Memory phenotype of the HLA-Cw*0702 populations between small <2% vs large >2% CD8+T-cell populations responding to peptide stimulation. Determined as $T_N$ CCR7+CD45RA+, $T_{CM}$ CCR7+CD45RA-, $T_{EM}$ CCR7-CD45RA- and $T_{EMRA}$ CCR7-CD45RA+ by flow cytometry. B) Antigen differentiation status of the HLA-Cw*0702 populations between small <2% vs large >2% CD8+T-cell populations responding to peptide stimulation. Determined as early (CD27+CD28+), intermediate (CD27+CD28- or CD27-CD28+) and late (CD27-CD28-) by flow cytometry. Statistical significance was determined in Graphpad Prism 6 via using multiple Mann Whitney Tests with * as a p-value <0.05. n = 14, 10 and 6 for FRC, CRV and LSE small categories. n = 12, 5 and 2 for FRC, CRV and LSE large categories.

4.7.3 – Antigen differentiation status

Lastly, the antigen differentiation status of the HLA-Cw*0702 CD8+T-cells was evaluated with size. This was to indicate whether the HLA-C CD8+T-cells were accumulations of late differentiated CD8+T-cells with a history of high proliferation rates [70, 238].

The total FRC-specific CD8+T-cells dramatically increased the percentage of late differentiated CD8+T-cells within larger populations (average 54.87%-81.28%, Fig-32B).

The CRV-specific CD8+T-cells also largely increased the number of late differentiated CD8+T-cells ($CD27^{-}CD28^{-}$ average 38.23%-70.09%, Fig-32B).

The LSE-specific CD8+T-cell response increased the percentage of intermediate differentiated ($CD27^{-}CD28^{+}$) CD8+T-cells while decreasing early differentiated (CD27+CD28+) T-cells as the population accumulated (Fig-32B).

Altogether, the *ex vivo* phenotype of HLA-Cw*-0702 CD8+T-cell populations became more antigen differentiated and increased their cytotoxic potential (perforin+granzymeB+) as the size of the epitope-specific CD8+T-cell response increased. The FRC-specific had the largest increase in both the $T_{EMRA}$ and late differentiated compartments within older donors and larger epitope-specific populations. The total LSE-specific CD8+T-cell population demonstrated the smallest proportions of late differentiated $T_{EMRA}$ CD8+T-cells in both older donors and larger accumulated epitope-specific CD8+T-cell populations.

## 4.8 – HLA-Cw*0702-restricted CD8+T-cell populations display a later differentiated $T_{EMRA}$ phenotype compared to HLA-A-restricted HCMV-specific CD8+T-cells

The *ex vivo* memory phenotype and antigen differentiation status of the HLA-Cw*0702 CD8+T-cells was compared to that of HLA-A-restricted HCMV-specific CD8+T-cells. All three HLA-Cw*0702 CD8+T-cell populations were comprised of a significantly lower proportion of early $CD27^+CD28^+$ CD8+T-cells compared to NLV and RTD-specific CD8+T-cells (Fig-33B). All three HLA-Cw*0702 populations had an increased percentage of $T_{EMRA}$ CD8+T-cells (Fig-33A) compared to RTD-specific populations. As such, the HLA-Cw*0702-restricted populations represented CD8+T-cells that were more antigen differentiated compared to other HCMV-specificities (Fig-33).

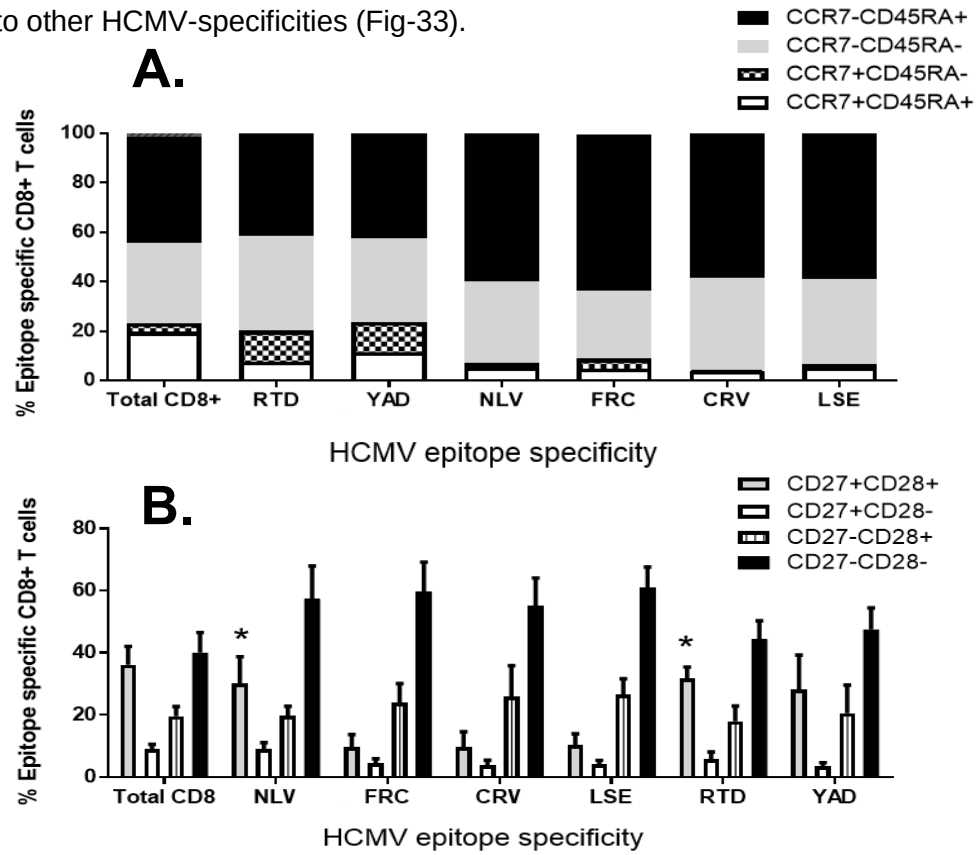


***Fig 33 – Memory phenotype and antigen differentiation status of ex vivo HCMV-specific HLA-Cw*0702-restricted CD8+T-cells vs HLA-A-restricted CD8+T-cell*** The CCR7 vs CD45RA and CD27 vs CD28 expression on HLA-Cw*0702 restricted CD8+T-cell populations was compared to HLA-A-restricted HCMV CD8+T-cell populations. PBMCS of HCMV seropositive donors populations were peptide stimulated for 6 hours followed by intracellular cytokine staining for TNF-α to identify the specific CD8+T-cell populations. A) Memory phenotype of the HCMV-specific CD8+T-cell populations determined as $T_N$ CCR7+CD45RA+, $T_{CM}$ CCR7+CD45RA-, $T_{EM}$ CCR7-CD45RA- and $T_{EMRA}$ CCR7-CD45RA+ by flow cytometry. B) Antigen differentiation status of the HCMV-specific populations determined as early (CD27+CD28+), intermediate (CD27+CD28- or CD27-CD28+) and late (CD27-CD28-) by flow cytometry. Bars represent mean and error bars SEM. Statistical significance represents significance in the percentage of early (CD27+CD28+) CD8+T-cells within the FRC-, CRV- and LSE-specific HLA-Cw*0702 CD8+T-cell populations compared to the NLV- and RTD-specific CD8+T-cell populations respectively determined by using multiple Mann Whitney tests in Graphpad prism6. * = a p value <0.05. n = 8, 8, 8, 4, 4 and 6 for FRC, CRV, LSE, RTD, YAD and NLV respectively.

## 4.9 - HLA-Cw*0702-restricted CD8+T-cell clones display high functional avidity

The next step in this investigation was to assess the anti-viral functionality of the inflated HLA-Cw*0702 CD8+T-cells *in vitro* to indicate their efficacy in controlling viral infections *in vivo*. We first aimed to assess their avidity for their cognate antigen.

Specific CD8+T-cell clones were generated *in vitro* from PBMCs of HCMV seropositive donors with previously identified HLA-Cw*0702 populations. This was conducted by an IFN-γ secretion assay (Miltenyi Biotech) after 3 hours peptide stimulation followed by limiting dilution assays. The specificity of the CD8+T-cell clones were determined by IFN-γ ELISAs (Fig-34A). FRC-specific clones were generated from donors YD6/YD13 and CRV- and LSE-specific clones from donor YD13 (Fig-34A).

The avidity of the HLA-Cw*0702 clones was then assessed after O/N co-culture with peptide-loaded LCLs with concentrations ranging from 50pg-50μg. The $EC_{50}$ avidity of individual clones was calculated as the concentration of peptide that induced the 50% maximal IFN-γ production. This was compared to the HLA-A1 RTD/YAD- and HLA-A2 NLV-specific CD8+T-cell clones generated in Chapter 3 Fig-15/16. This allowed a comparison of CD8+T-cell clones specific for 'inflationary' HLA-Cw*0702 epitopes to the NLV epitope that has been identified as both immunodominant and inflationary in the literature [87, 273, 274]. Additionally this allowed a comparison to the RTD/YAD peptide-epitopes that were identified to elicit stable CD8+T-cell responses with age (Chapter 3, Table-7).

The avidity of both the FRC- and CRV-specific HLA-C-restricted clones was determined to range from 50pg-0.025μg (Fig 34B). This was significantly increased over RTD-, YAD- and NLV-specific CD8+T-cell clones (RTD-specific 0.25μg-0.5μg, YAD-specific 0.025μg-0.25μg and NLV-specific 0.025μg-0.25μg, Chapter 3, Fig-16 and Fig-34C). The $EC_{50}$ of the LSE-specific polyclonal line was determined to be 50pg (Fig-34B).

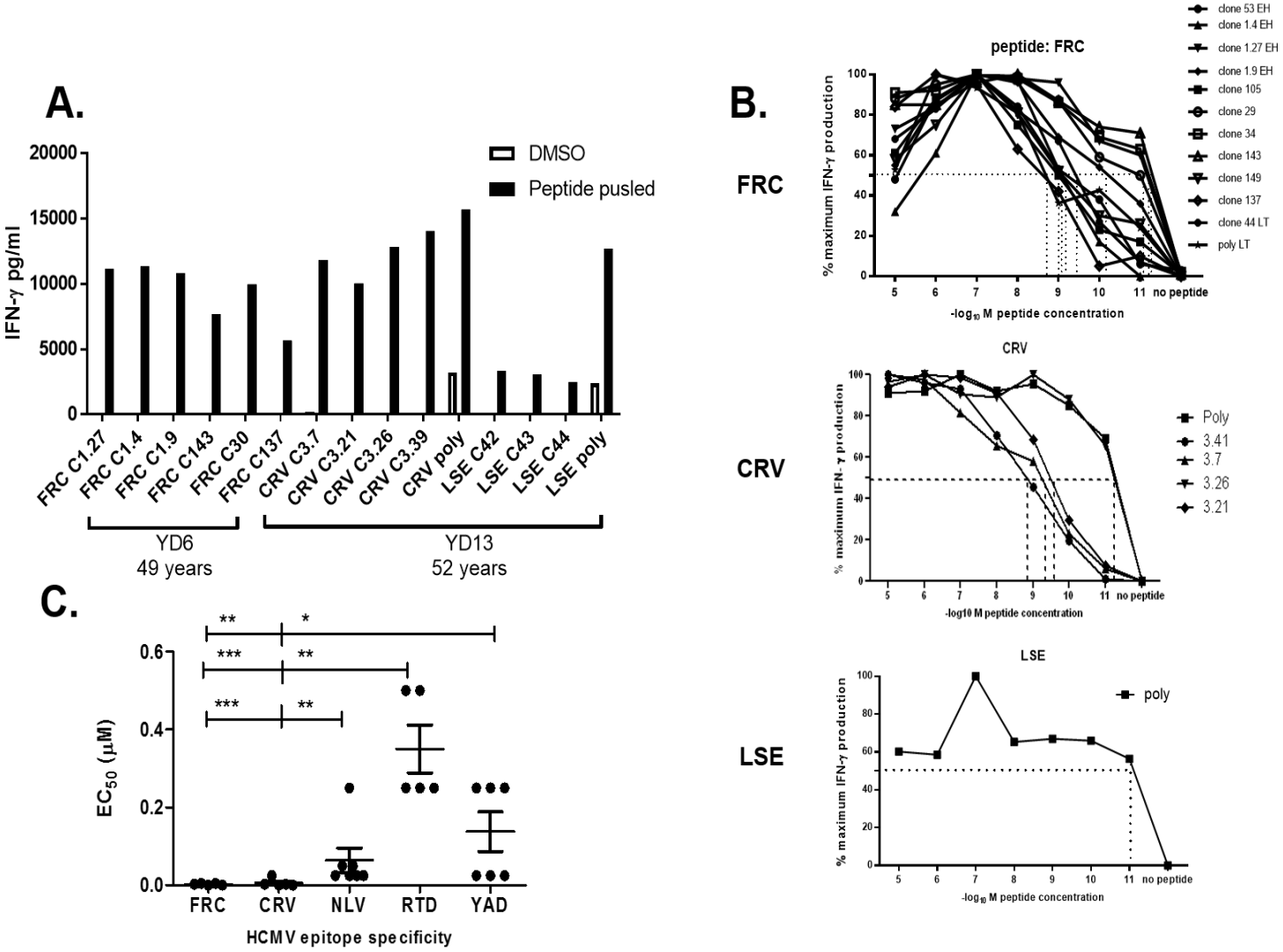


***Fig 34 – Generation of HLA-Cw*0702-restricted HCMV-specific CD8+T-cell clones in vitro and determination of their functional avidity.*** Specific CD8+T-cell clones for the UL28-derived FRC and UL122/IE-1-derived CRV and LSE peptides were generated *in vitro* by an IFN-γ catch assay (Miltenyi Biotech) following 3 hours peptide stimulation assay of PBMCs with previously identified CD8+T-cell responses to the peptides in question and a limiting dilution assay. The $EC_{50}$ avidity of individual clones was calculated as the concentration of peptide that induced the 50% maximal IFN-γ production. A) Representative IFN-γ production of some example clones determined by ELISA after O/N co-culture of CD8+T-cell clones with DMSO control loaded (white bars) and peptide-loaded LCLs (black bars). B) Functional peptide affinity assay of the FRC (top), CRV (middle) and LSE (bottom) CD8+T-cell clones. CD8+T-cell clones were co-cultured O/N with LCLs loaded with peptide concentrations ranging from 50μg to 50pg followed by an IFN-γ ELISA. The dashed lines represent the $EC_{50}$ of the individual clones. **C**) Summary $EC_{50}$ values obtained for CD8+T-cell clones specific for HCMV-specific epitopes. Statistical significance was obtained via Mann Whitney test in Graphpad Prism 6 with * as a p-value < 0.05, ** < 0.005, *** < 0.0005.

## 4.10 - Killing of peptide-loaded and infected fibroblasts *in vitro* by HLA-Cw*0702-restricted CD8+T-cell clones

Throughout this investigation, the inflated HLA-Cw*0702 CD8+T-cell populations have been proven to be exceptional candidates for their inclusion within immunotherapy to treat CMV disease in the post HSCT setting. This is based on their high avidity, maintenance into older age and high cytotoxic potential (intracellular perforin and granzymeB production). A CD8+T-cell response maintained into older age could provide lifelong protection from CMV reactivation events offering an advantage in the adoptive immunotherapy setting for post-HSCT patients. However, for these CD8+T-cell populations to be successful after adoptive transfer, they need to be efficient in killing and therefore removing virally infected cells *in vivo*.

The capability of HCMV HLA-C-specific CD8+T-cell clones to kill peptide-loaded targets *in vitro* was evaluated and compared to clones specific for the pp65-derived NLV peptide or the UL69/UL105a-derived RTD/YAD peptides. HCMV-specific CD8+T-cell clones were cultured with CFSE-labelled peptide-loaded HLA-matched LCLs O/N followed by staining with Propidium Iodide (PI). This allowed the analysis of the percentage of CFSE POSITIVE target cells that were PI negative and therefore still viable after incubation with the CD8+T-cell clones (gating strategy provided in Fig-35A).

All clones tested were efficiently able to kill peptide-loaded targets after an O/N incubation at 1:1 to 10:1 effector:target ratios. The NLV-specific followed by the YAD-specific clones had the highest percentage of specific cell lysis (range 95.99%-98.80%) (Fig-35B). The CRV-specific clones demonstrated the lowest specific lysis (average range 17.99%-71.78%) (Fig-35B). The FRC-specific CD8+T-cell clones lysed specific cells ranging from 59.00%-90.11%. (Fig-35B) (n = 2 CRV, FRC, NLV and n =1 RTD/YAD). It should be noted that the killing efficiency may be clone dependent in this assay and not completely representative of the entire epitope-specific CD8+T-cell population or *in vivo* killing capacity. Additionally, the *in vitro* culture conditions may also influence the killing capacity of the clones. Therefore this

should be repeated with a greater range of CD8+T-cell clones. The important finding is that the HLA-Cw*0702 CD8+T-cell clones can efficiently lyse peptide-loaded target cells *in vitro*.

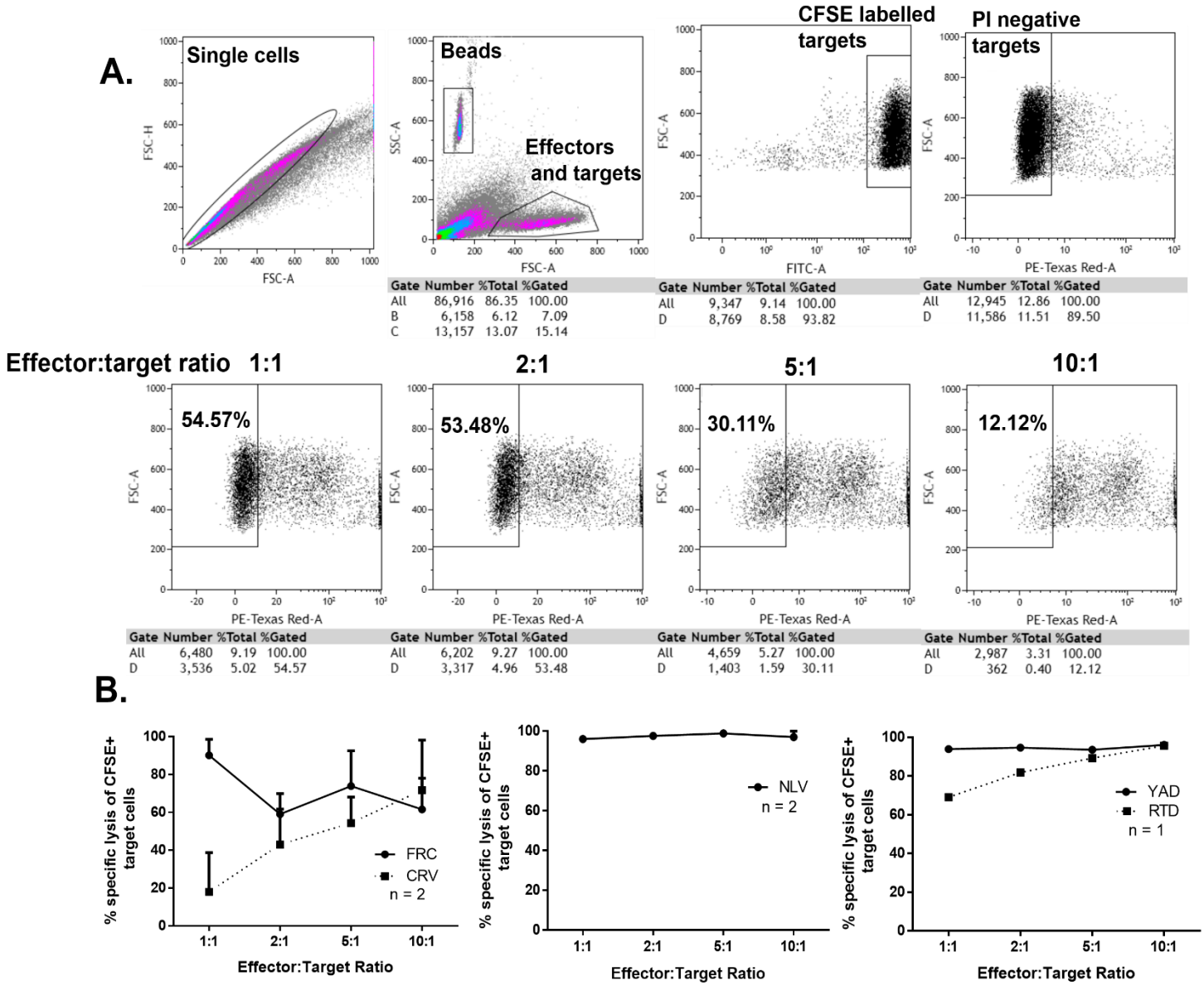


***Fig 35 – HCMV-specific CD8+T-cell clone killing of peptide-loaded target cells.*** The ability of HCMV CD8+T-cell clones to specifically lyse HCMV infected cell targets was assessed. A) Gating strategy for identifying the number of CFSE positive, PI negative 'viable' peptide-loaded target cells remaining after incubation with HCMV CD8+T-cell clones a 1-10:1 effector: target ratios O/N. Single cells, effector and target cells were gated upon. To differentiate between effector and targets, peptide-loaded LCLs were stained with CFSE prior to incubation with the effectors. CFSE positive, PI negative targets were then gated upon within the DMSO-pulsed LCL control tubes. The PI negative gate was then applied to the CFSE positive targets cells within 1:1, 2:1, 5:1 and 10:1 sample tubes. Lastly, a gate was placed around the counting beads (Life Technologies). The percentage specific cell lysis was calculated as indicated in the materials and methods and as per manufacturer's guidelines when using the counting beads. B) Summary of the percentage specific lysis of the HLA-C FRC and CRV (left graph), HLA-A2 NLV (middle graph) and HLA-A1 RTD and YAD-specific (right graph) CD8+T-cell clones.

After observing the efficient removal of peptide-loaded targets by the HCMV-specific CD8+T-cell clones, next their ability to lyse HCMV infected target cells during an *in vitro* infection was evaluated. This was to give an accurate idea of their ability to recognise and kill infected cells presenting naturally processed antigen. MRC5 fibroblasts were infected at a low MOI of 0.05 with the Merlin strain for 24 hours followed by co-culture with either FRC-, CRV or NLV-specific CD8+T-cell clones at 1-10:1 effector to target ratios for a further 48 hours (Fig-36A/B). The CD8+T-cell clones were subsequently removed from the monolayer and characterised for the upregulation of the activatory marker CD25 by flow cytometry (Fig-36B). As a negative control CD8+T-cell clones were incubated with an uninfected fibroblast monolayer. The background CD25 levels from this negative control were subtracted from the values obtained with CD8+T-cells incubated with the Merlin infected monolayer. The Merlin strain was selected as it is a clinical isolate and therefore a more physiological representation of a CMV infection *in vivo* (review [241]).

All CD8+T-cell clones were activated after incubation with Merlin infected MRC5 cells indicated by CD25 upregulation (Fig-36B). The CRV- and FRC-specific clones from the 10:1 ratio had increased upregulation of CD25 compared to NLV-specific clones (43.97%, 53.92% and 11.32% CD25 positive CD8+T-cell clones respectively) (Fig-36B).

Subsequently, the levels of specific cell killing was quantified using AD169 infected fibroblasts which had been previously optimised in our research group. An FRC-specific CD8+T-cell clone was able to specifically lyse up to 80% of AD169 infected fibroblasts *in vitro* at 12 and 24 hours p.i at 1:1 to 10:1 effector to target ratios (range 66.58% to 82.10% 12 hours and 70.69% to 81.47% 24 hours, Fig-36C). The FRC-specific clone also produced IFN-γ, detected by ELISA after incubation with 12 and 24 hour infected AD169 fibroblasts (data not shown). To conclude, FRC-specific CD8+T-cell clones upon positive recognition, engagement of antigen and production of effector molecules such as IFN-γ, induce subsequent death of infected cell targets. This provides premise for developing the FRC-specific CD8+T-cell population as an immunotherapy for HCMV mediated disease.

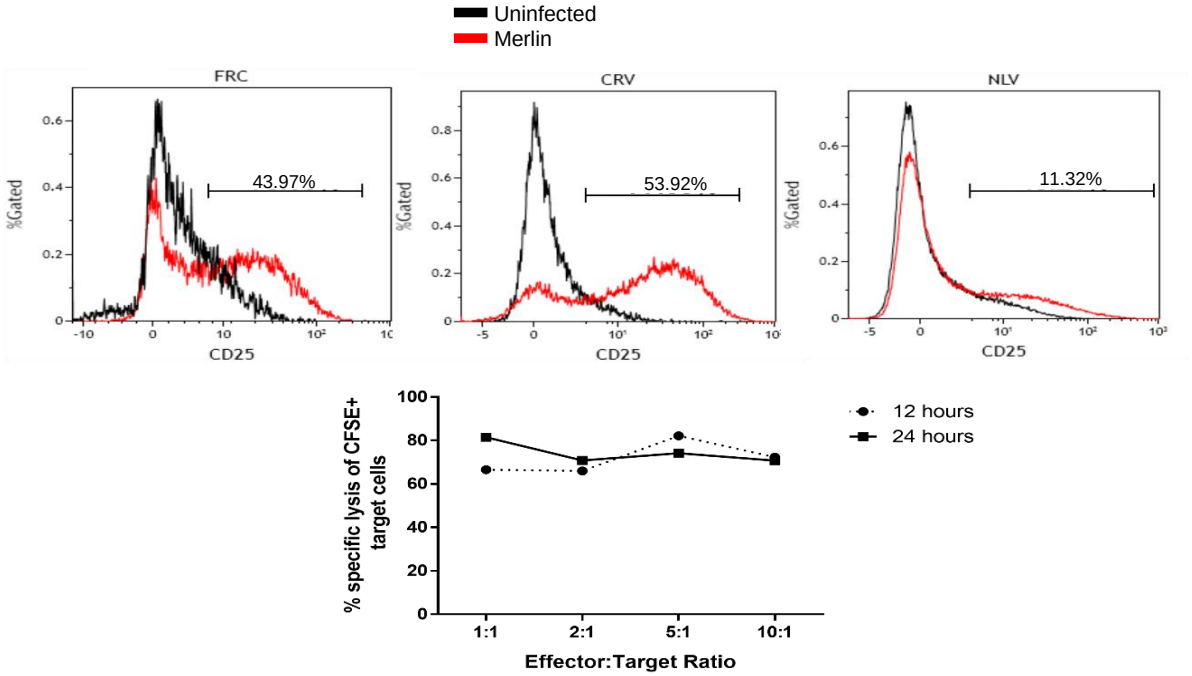


***Fig 36 – CD8+T-cell killing of AD169 infected targets and CD25 upregulation on activated CD8+T-cell clones.*** HCMV-specific clones were evaluated for their ability to disrupt a HCMV-infected monolayer *in vitro* and upregulate the CD25 activatory marker A) CD25 upregulation on FRC- (left), CRV- (middle) and NLV-specific (right) CD8+T-cell clones after 48 hours incubation with Merlin infected MRC5 cells compared to clones incubated with uninfected fibroblasts. CD8+T-cells were removed from the monolayer and subjected to CD25 antibody staining and flow cytometric analysis B) Specific cell lysis of AD169 infected MRC5 fibroblasts after 12 and 24 hours pi by an FRC-specific CD8+T-cell clone. Percentage of specific lysis was determined as outlined in Fig 35 and materials and methods.

# CHAPTER 4

## Project 2 Summary

The *ex vivo* phenotype of HCMV-specific HLA-Cw*0702 CD8+T-cell populations were characterised and found to alter when both the age of the donor and the size of the epitope-specific CD8+T-cell responses increased. The HLA-Cw*0702 FRC-specific populations presented with a large increase in the percentage of CD8+T-cells further down the differentiation pathway ($CD27^-CD28^-$). Importantly, increases in the proportion of $T_{EM}$ and $T_{EMRA}$ within the FRC-specific HLA-Cw*0702 CD8+T-cell populations was also observed within older donors and large epitope-specific accumulations. The cytotoxic potential of the HLA-Cw*0702-restricted CD8+T-cells within larger epitope-specific CD8+T-cell populations and older donors significantly increased – indicated by perforin and granzymeB expression. The same T-cells appeared more activated with age with an increased NKG2D expression and maintenance of CD38. The percentage of HLA-Cw*0702-restricted CD8+T-cells capable of producing both pro-inflammatory cytokines IFN-γ and TNF-α was increased within large accumulations and age, while the proportion of CD8+T-cells producing IL-2 was lost. This complemented the progressive loss of CD28 required for IL-2 production. Additionally, the FRC- and CRV-specific HLA-Cw*0702 CD8+T-cell populations were comprised of significantly more $IFN\text{-}\gamma^+TNF\text{-}\alpha^+$ double-producing CD8+T-cells compared to the HLA-A1-restricted YAD-specific CD8+T-cell populations. The latter were more capable of producing IL-2. The functionality of the HLA-Cw*0702 CD8+T-cell populations was confirmed within *in vitro* killing assays. Firstly, CD8+T-cell clones specific to the HLA-Cw*0702 targets were calculated as significantly more avid than clones specific for HLA-A-restricted pp65-, UL69-, and UL105a-derived targets. Secondly, FRC-specific HLA-C clones efficiently lysed HCMV infected fibroblasts *in vitro*. Providing evidence for their efficacy in providing anti-viral protection *in vivo*. In conclusion the HLA-Cw*0702 specificities, in particular FRC-specific, have potential for development as an adoptive therapy to treat CMV disease in the post-transplant setting.

# Project 3 – Antigen driven stimulation of HLA-C specific T-cells as a potential mechanism for memory-inflation

## 4.11 - HLA-Cw*0702-restricted *ex vivo* PBMCs and specific CD8+T-cell clones are able to proliferate after antigen stimulation

One hypothesis for memory-inflation states that antigen driven stimulation within the lymph nodes by infected non-haematopoietic cells drives the proliferation and differentiation of CMV-specific $T_{CM}$. This results in a highly differentiated and cytotoxic $T_{EMRA}$ population that can enter the periphery to control reactivation. Studies in the murine model, in the absence of MCMV antigen, identified memory-inflated CD8+T-cells within the circulation as short lived with little proliferative capacity and continually replaced by CD8+T-cells [103]. These inflated populations then undergo extensive division upon antigen encounter [115, 123].

This study next sought to evaluate whether the proliferation of the HLA-Cw*0702 cells after antigen stimulation could be a factor in their peripheral accumulation within age. The proliferation of both *ex vivo* PBMCs (Fig-37) and HLA-C-specific CD8+T-cell clones (Fig-38) after incubation with peptide-loaded cell targets *in vitro* was examined. This was conducted by following the dilution of the CFSE dye incorporated into epitope-specific CD8+T-cells after cell division by flow cytometry (Fig-37). PBMCs isolated from individual seropositive donors with all three identified HLA-Cw*0702 CD8+T-cell populations, were CFSE labelled and co-cultured for 7 days at 37$^{o}$C with HLA-matched γ-irradiated LCLs that were either DMSO or peptide-loaded. PBMC only and PBMCs co-cultured with SEB-stimulated (final concentration 2mg/ml) negative and positive controls were included respectively (gating strategy provided in Fig-37A/B). As the three HLA-Cw*0702 populations were investigated within donors identified to have all three responses, only one SEB positive control was conducted up per donor. This positive control therefore represents the same value for all three HLA-Cw*0702-specific CD8+T-cell populations (Fig-37). PBMCs of donors with NLV-specific CD8+T-cells, that did not have HLA-Cw*0702-specific CD8+T-cells were included as a positive proliferation control [275].

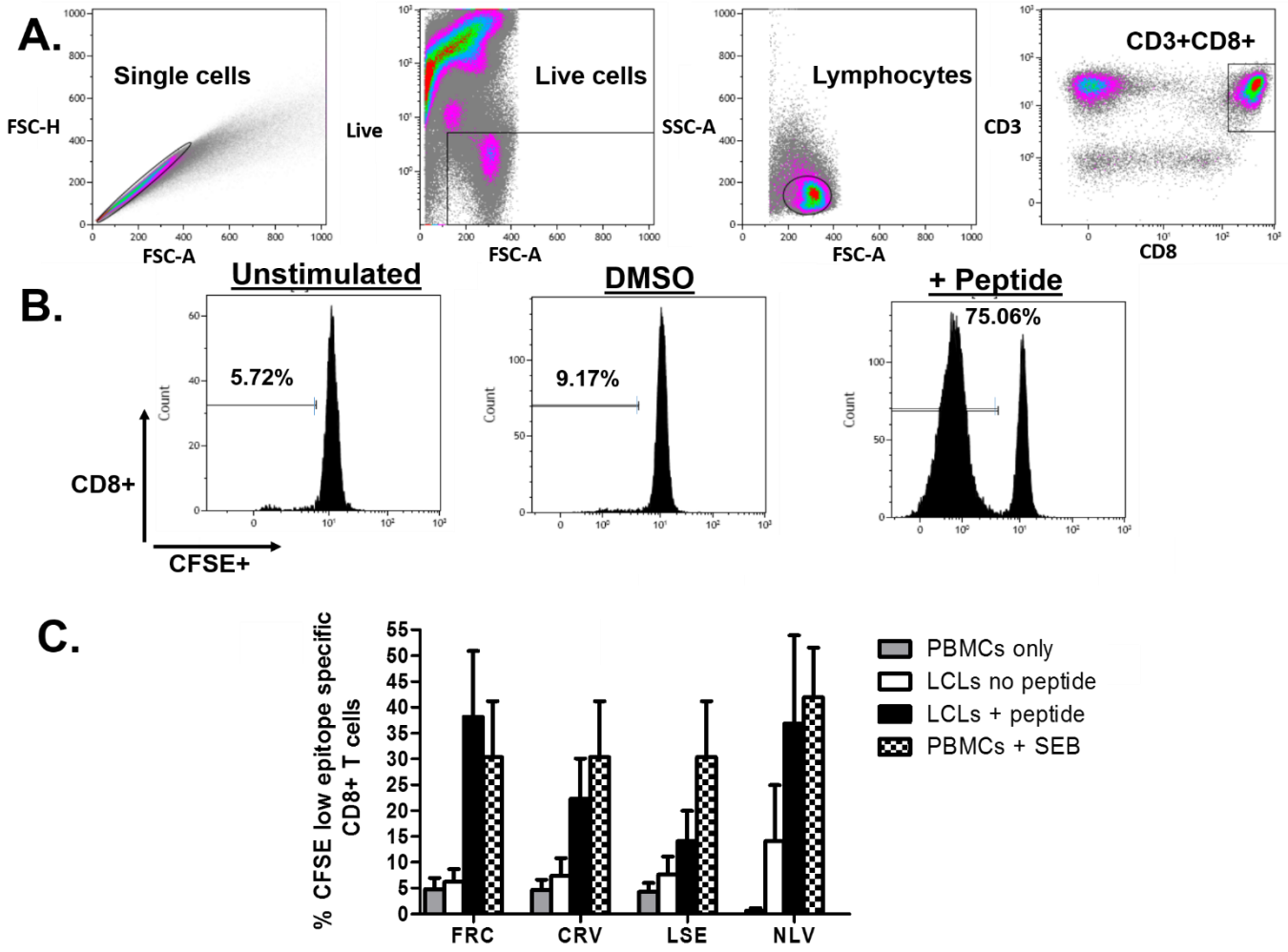


***Fig 37 – Proliferation capacity of HCMV-specific ex vivo PBMCS determined by CFSE staining.*** The ability of *ex vivo* HLA-Cw*0702 CD8+ T cell populations to proliferate in response to antigen was investigated and compared to the proliferation of HLA-A2-restricted NLV-specific CD8+T-cells. PBMCs were co-cultured with HLA-Matched LCLs that were either DMSO control or peptide-loaded for 7 days at 37ºC. PBMCs were left unstimulated or SEB stimulated (0.2mg/ml) as negative and positive controls respectively. Single, live, CD3+CD8+ lymphocytes were gated on in Kaluza 1.3 software. Within the CD8+T-cell population, CFSE low i.e. proliferating CD8+T-cells were identified. A/B) Gating strategy to identify proliferating i.e. CFSE low CD8+T-cells within PBMCs obtained from donor OD12 after co-culture with; media only (T-cells only) (left), DMSO-pulsed LCLs (middle) and peptide-pulsed LCLs (right). B) The representative histogram plots represent the percentage of CSFE CD8+T-cells C) Summary of the CFSE low CD8+T-cell staining obtained for PBMCs incubated with FRC-, CRV-, LSE- and NLV-loaded LCLs. n = 3 for FRC, CRV and LSE, n = 2 for NLV. Bars represent mean and error bars represent SEM.

A hierarchy of proliferation capacities of the *ex vivo* PBMCs elicited by the HLA-Cw*0702-restricted peptides was observed. The FRC peptide elicited the largest proliferation rates with an average $CFSE^{low}$ CD8+T-cell population after 7 days co-culture of 38.14% (Fig-37C). This was followed by an average of 22.31% for CRV and 14.11% for LSE. The NLV peptide elicited proliferation rates comparable to the FRC-peptide with an average of 36.88% $CFSE^{low}$ CD8+T-cell populations (Fig-37C).

Subsequently, CD8+T-cell clones were then also analysed for proliferation after incubation with peptide-loaded targets after 24-72 hours (Fig-38A/B). CFSE-labelled CD8+T-cell clones were co-cultured with peptide-loaded HLA-matched LCL targets for 24-72 hours.

The FRC-specific CD8+T-cell clone exhibited the highest rate of proliferation by 48 and 72 hours reaching 76.42% and 96.14% of the total CD8+T-cell clone population with a $CFSE^{low}$ phenotype (Fig-38A/B). 49.74% and 53.06% of an NLV-specific clone population were proliferating after 48 and 72 hours incubation with peptide-loaded target cells. UL69-derived RTD- and UL105a-derived YAD-specific clone proliferated in the ranges of 9.91% to 34.94% and 19.08-34.83% respectively of the total CD8+T-cell clone population (Fig-38B).

In summary*, ex vivo* PBMC CD8+T-cell responses specific for the HLA-Cw*0702 peptides are able to proliferate after antigen stimulation demonstrating a hierarchy of FRC>CRV>LSE with FRC comparable to that induced by the NLV peptide. Additionally, an FRC-specific CD8+T-cell clone population had higher proliferative capacity over a clone specific for the pp65-derived NLV, UL69-derived RTD and UL105a-derived YAD peptides *in vitro* after periods of short peptide stimulation (n = 1).

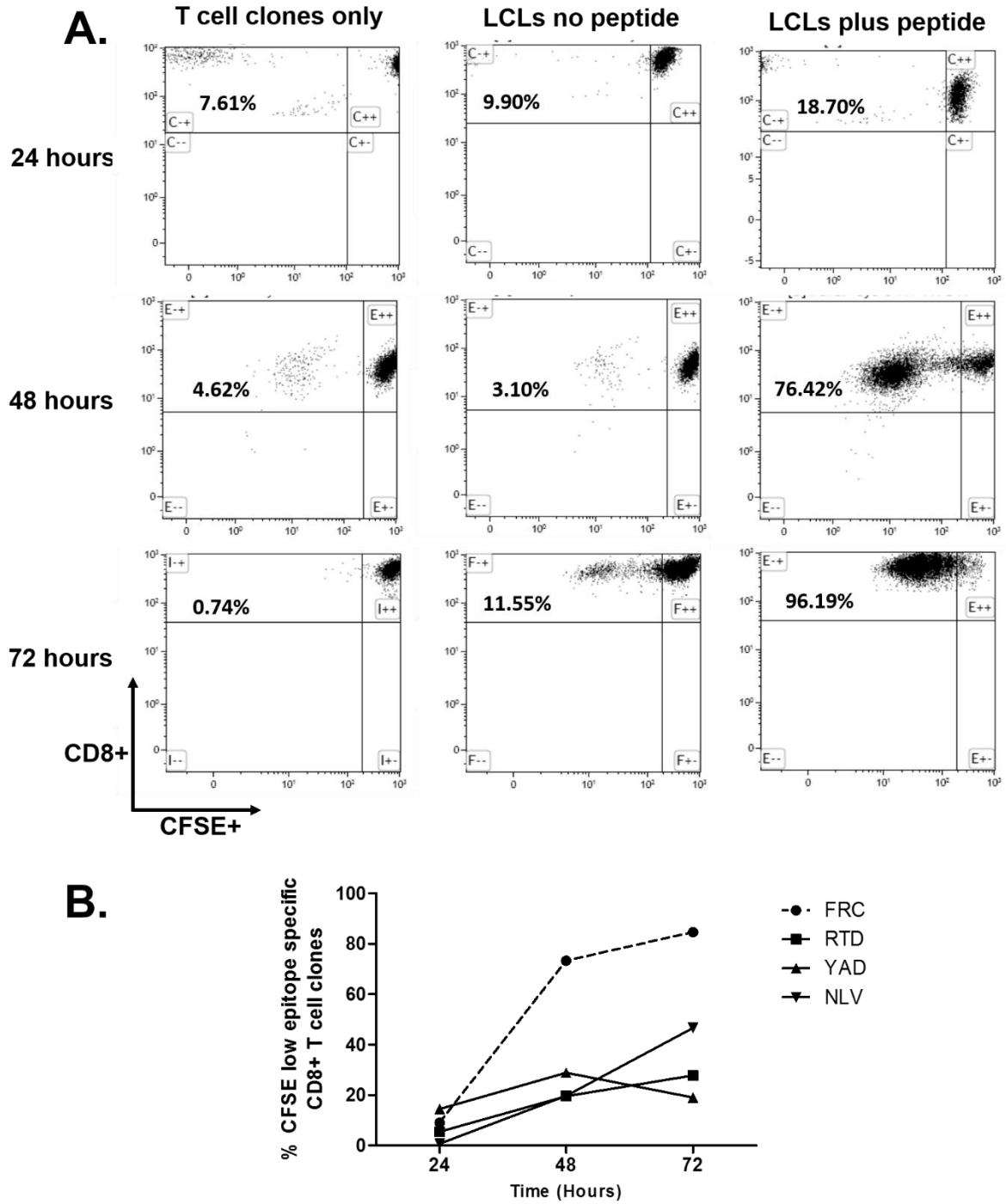


***Fig 38 – Proliferation capacity of HCMV-specific CD8+T-cell clones generated in vitro determined by CFSE staining by flow cytometry.*** The ability of *specific* HLA-Cw*0702 CD8+T-cell clones to proliferate in response to antigen was investigated and compared to the proliferation of HLA-A1 and HLA-A2-restricted CD8+T-cell clones. CD8+T-cell clones were incubated for 24-72 hours at 37ºC with peptide-loaded HLA-matched LCLs to analyse proliferation after antigen stimulation indicated by the dilution of CFSE dye. CFSE low i.e. proliferating CD8+T-cell clones were identified as outlined in Fig-37A/B. A) Representative dot plots of CFSE dilution by HCMV-specific CD8+T-cell clones after 24 (top row), 48 (middle row) and 72 hours (bottom row) incubation with; media only (T-cells only) (left column), DMSO-pulsed LCLs (middle) and peptide-pulsed LCLs (right column). Example shown is for the FRC-specific CD8+T-cell clone. B) Summary of the CFSE dilution obtained for CD8+T-cell clones specific for the FRC, NLV, RTD and YAD HCMV peptides (Table-7/8). In all cases n = 1 and, the downregulation values observed for the peptide stimulated tubes have had the background value subtracted.

## 4.12 - The UL28-derived HLA-Cw*0702-restricted HCMV-specific CD8+T-cell response becomes oligoclonal with age

Inflated HCMV memory CD8+T-cell populations are reported to be accumulations of CD8+T-cells with a restricted TCR Vβ usage [76, 92, 276]. One theory for this oligoclonal development is the selection of highly avid CD8+T-cell clones over the lifetime of the host that confer efficient control of viral reactivation events *in vivo*. It was thereupon assessed whether the HLA-Cw*0702 accumulations represent oligoclonal populations, supporting the preferential selection of a particular clone *in vivo*.

The *ex vivo* CD8+T-cell populations specific for the UL28-derived FRC peptide were characterised for their 'TCR β-chain V' (TCRβV) diversity by flow cytometry. PBMCs were peptide stimulated for 6 hours and surface stained with the TCR Vβ diversity repertoire kit (Becton Dickinson) containing MAbs to 24 TCRβV regions. PBMCS were then stained intracellularly for TNF-α production to identify FRC-specific CD8+T-cells. The positive gates for individual TCRβV usage were set upon the CD8+T-cells within the Kaluza 1.3 software and then applied to the FRC-specific CD8+T-cells (gating strategy provided in Fig-39).

A dominant usage of Vβ3 was obtained within a single donor of 29 years of age at 67.09% of the total epitope-specific CD8+T-cell response. Within older donors dominant Vβ3 usage was also observed at a higher magnitude within one donor of 81 years of age at 80.17% of the total epitope-specific CD8+T-cell response (Fig-40). Dominant Vβ3 usage was again observed at a smaller magnitude at 12.35% within a donor of 86 years of age (Fig-41). The range of Vβ3 usage within the FRC-specific CD8+T-cell populations was 7.7%-67.09% within younger and 0.62%-80.17% within older donors (Fig-40 vs 41).

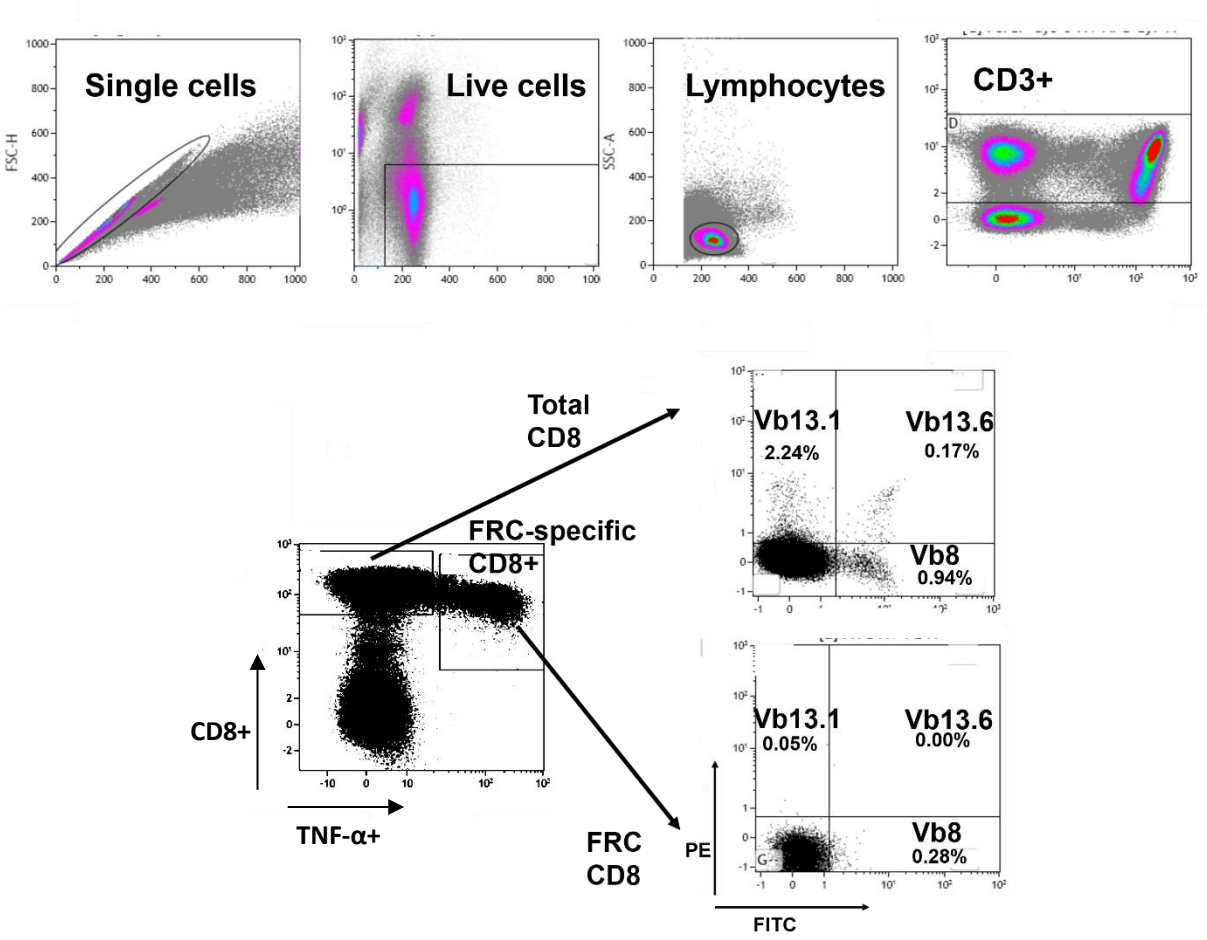


***Fig 39 – Gating strategy for phenotyping the TCRBV regions of the ex vivo HLA-Cw*-0702 specific CD8+T-cells by flow cytometry.*** PBMCs from donors with previously identified CD8+T-cell populations were characterised for TCR Vβ chain usage. Here the gating strategy utilised to identify the TCR Vβ usage within the *ex vivo* FRC-specific CD8+T-cell populations is provided. Single, live, CD3+CD8+ lymphocytes were gated upon sequentially in Kaluza 1.3 software. The FRC-specific CD8+T-cells were identified by TNF-α production after 6 hours peptide stimulation of HCMV seropositive donor PBMCs with previously identified *ex vivo* FRC-specific CD8+T-cell responses. Gates for TCRβV expression were set upon the total CD8+T-cell population and then applied to the FRC-specific CD8+T-cells. Individual TCRβV MAbs were conjugated to either, PE, FITC or PE+FITC (Beckman Coulter). The example provided demonstrates the staining obtained for the total CD8+T-cells (top graph) vs FRC-specific CD8+T-cells with tube E of the repertoire kit (Beckman Coulter). The percentages of CD8+T-cells within the total CD8+T-cell (top plot) and FRC-specific CD8+T-cell population (bottom plot) utilising that particular Vβ chain are provided in the quadrants on the representative flow plots.

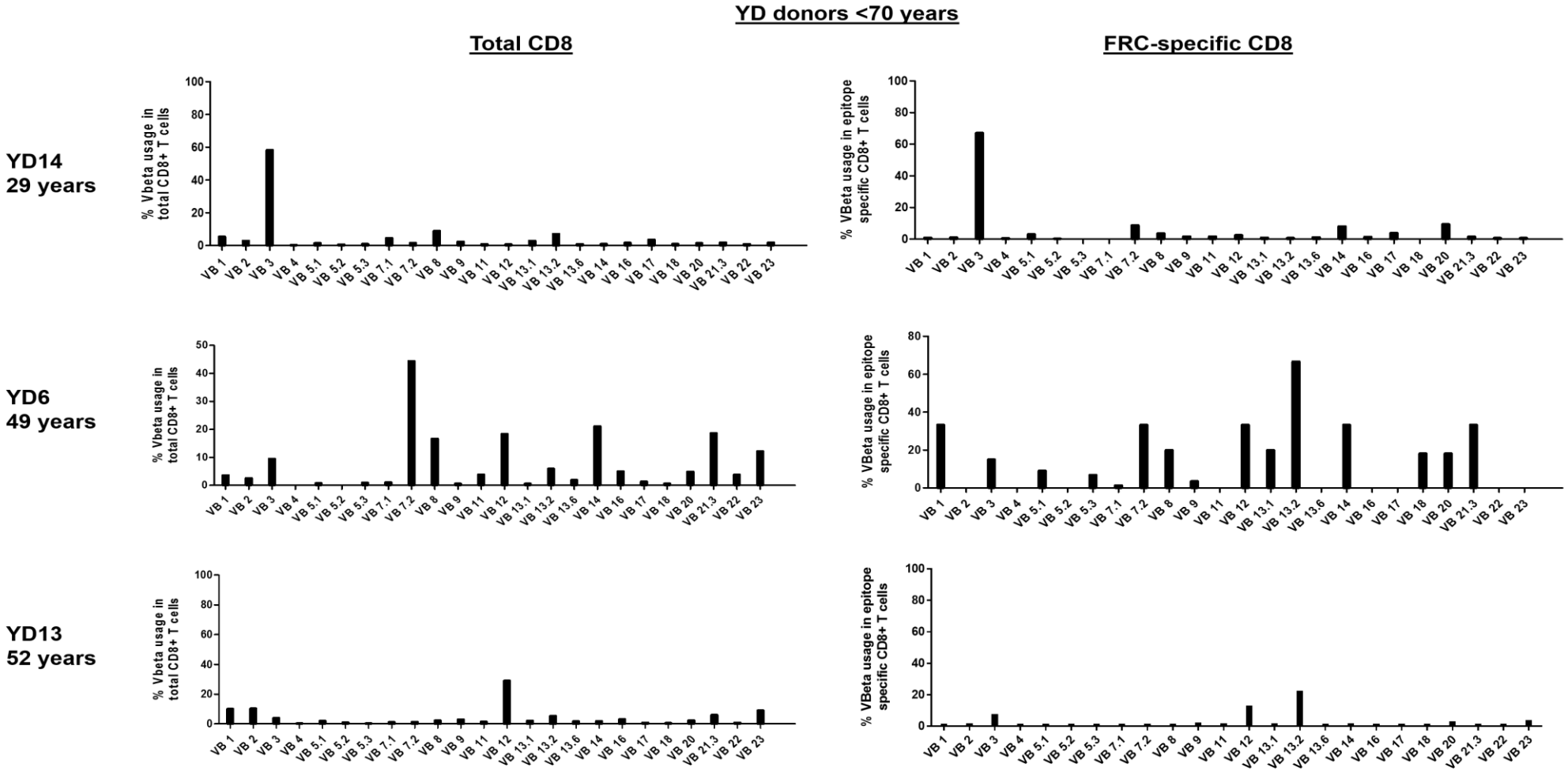


***Fig 40 – TCR VB staining obtained for FRC-specific CD8+T-cell donors in younger donors <70 years.*** The TCR Vβ usage within FRC-specific CD8+T-cell populations of PBMCs obtained from younger (<70 years) donors was investigated. PBMCs of donors with previously identified FRC-specific CD8+T-cell responses were peptide stimulated for 6 hours followed by staining with the TCR VB repertoire kit (Beckman Coulter) and ICS for TNF-α to identify the FRC-specific CD8+T-cells. The left hand graphs represents the staining obtained for the total CD8+T-cell population within individual donors The right hand graphs represent the TCRBV staining obtained for the FRC-specific CD8+T-cell populations. The donor's age is provided on the left hand side of the graph. n = 3 for donors <70 years.

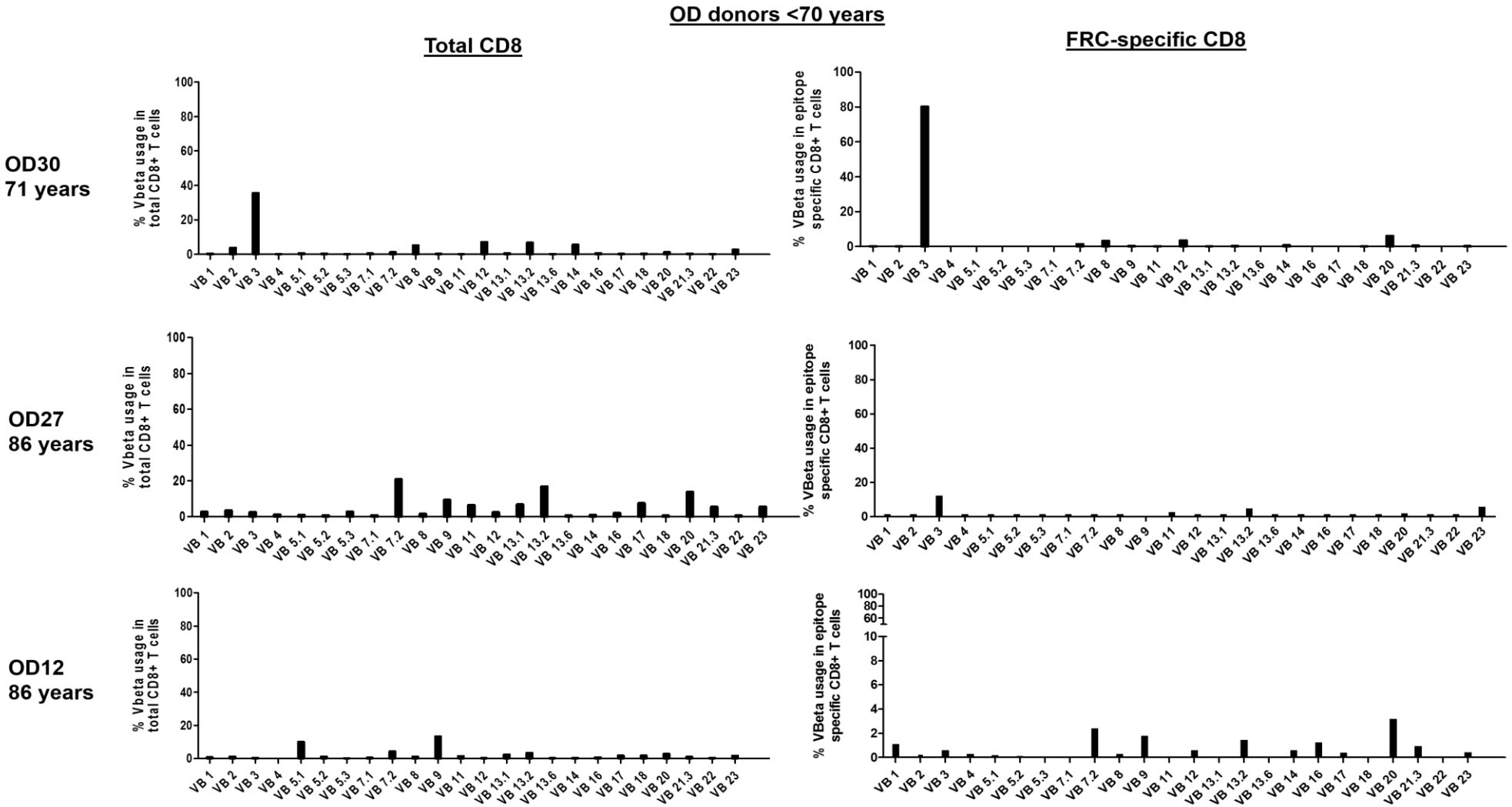


***Fig 41 –TCR VB staining obtained for FRC-specific CD8+T-cell donors in older donors >70 years.*** The TCR Vβ usage within FRC-specific CD8+T-cell populations of PBMCs obtained from older (>70 years) donors was investigated. PBMCs of donors with previously identified FRC-specific CD8+T-cell responses were peptide stimulated for 6 hours followed by staining with the TCR VB repertoire kit (Beckman Coulter) and ICS for TNF-α to identify the FRC-specific CD8+T-cells. The left hand graphs represent the staining obtained for the total CD8+T-cell population within individual donors. The right hand graphs represent the TCR Vβ staining obtained for the FRC-specific populations within individual donors. The donor's age is provided on the left hand side of the graph. n = 3 for donors >70 years.

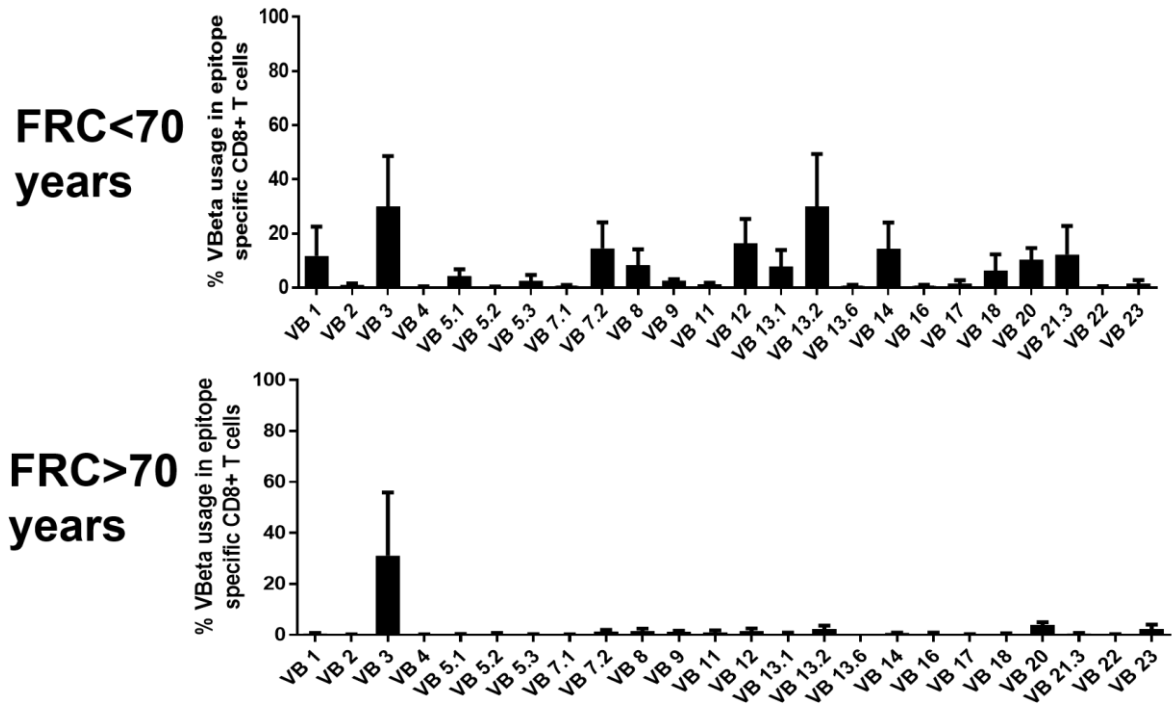


***Fig 42 – Summary of the* TCRβV *staining obtained for the ex vivo HCMV-specific CD8+T-cell responses.***
The average TCR Vβ usage of the FRC-specific CD8+T-cell populations between donors <70 vs >70 years of age. PBMCs of donors with previously identified FRC-specific CD8+T-cell responses were peptide stimulated for 6 hours followed by staining with the TCR VB repertoire kit (Beckman Coulter) and ICS for TNF-α to identify the FRC-specific CD8+T-cells. The graphs represent the summary of the TCR Vβ staining obtained for *ex vivo* FRC-specific CD8+T-cell populations within donors <70 years (top) vs >70 years (bottom) of age.

When the TCRβV staining was summarised, the average percentage of the FRC-specific CD8+T-cell population that uses Vβ3 remained almost identical with age (29.98% <70 years vs 31.05% >70 years) but the use of other Vβ chains reduced within the older donors (Fig-42).

To summarise, this section demonstrates the preferential usage of Vβ3 within inflationary *ex vivo* HLA-Cw*0702 FRC-specific CD8+T-cell populations within these six donors. However, a more diverse Vβ usage could be present within other donors not characterised or represented by a Vβ not included within the repertoire kit (Beckman Coulter). As such a larger donor cohort should be screened and donors followed longitudinally to observe whether the Vβ CD8+T-cells are maintained with age.

## 4.13 - Maintenance of surface HLA-C alleles at IE times of AD169 infection of fibroblasts *in vitro* when the US2-11 immunevasins are present

The observation of striking memory-inflated CD8+T-cell populations to three individual HCMV peptides restricted through a common HLA-Cw*0702 allele asked the question to what extent the HLA-restricting allele plays in the development of this HLA-C inflation.

Encouragingly, HLA-Cw*0702 alleles have been demonstrated as exempt from the immunomodulatory mechanisms of the US2-11 gene region products [139-141]**.**

As such, last to be investigated in this research chapter was the surface expression of HLA-C alleles on infected cells *in vitro*. The downregulation of HLA-C alleles from the surface of HCMV infected fibroblasts during a productive infection was determined by flow cytometry and compared to the total HLA-ABC alleles (Fig-43/44).

HLA-Cw*0702$^{+}$ MRC5 fibroblasts were infected with the AD169 or RV798 CMV strains for 6-72 hours. Fibroblasts were then trypsinised at the indicated time-points and stained for surface HLA-ABC (W6/32 monoclonal) vs HLA-C (DT9 monoclonal antibody – kindly provided by Dr Veronique Braud) alleles. The gating strategy is provided in Fig-43A.

The MFI of the HLA staining on the CMV infected fibroblasts was determined and expressed as a percentage of an uninfected fibroblast control MFI at each time point (percentage relative expression).

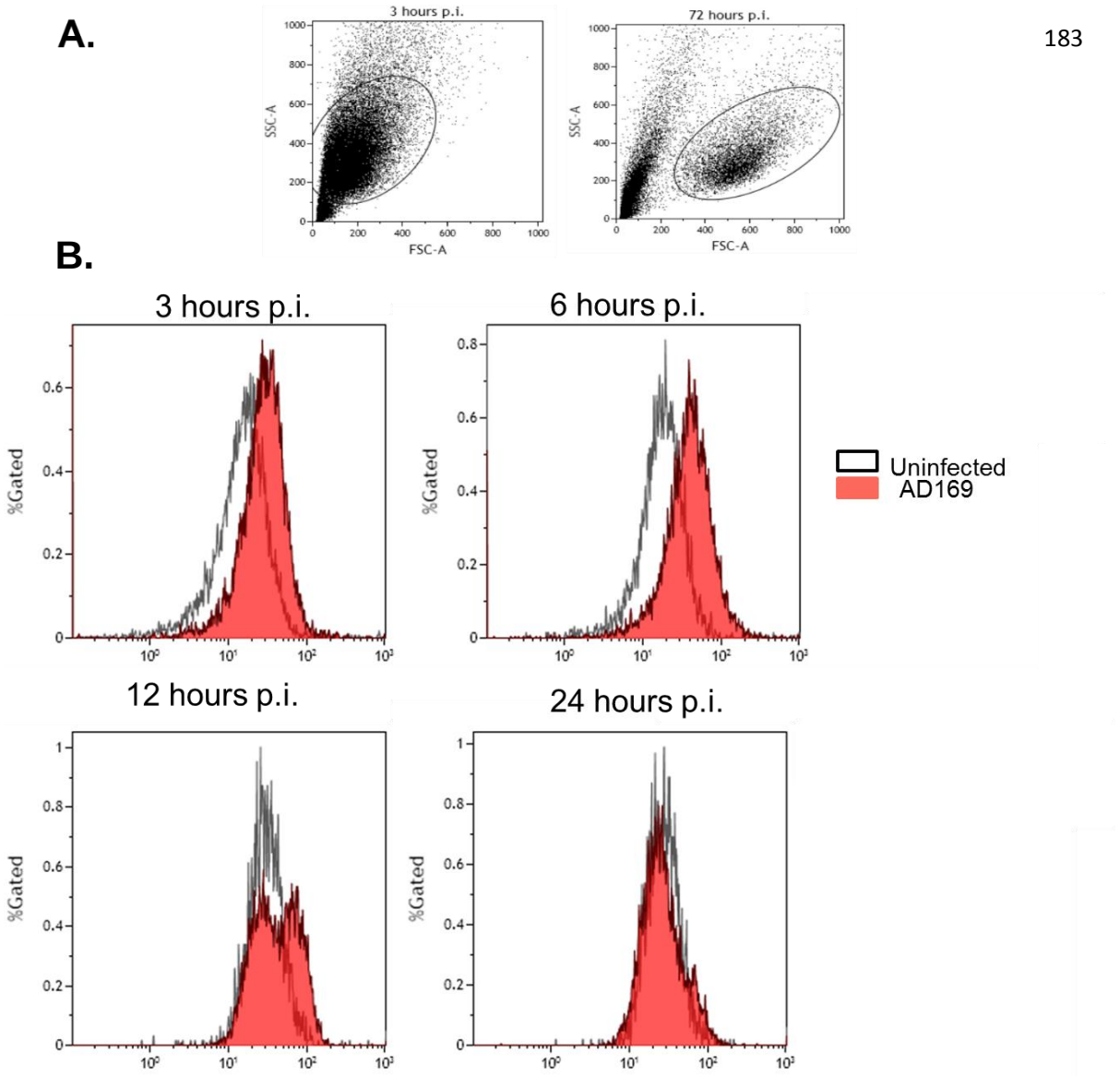


**Fig 43 – Representative surface HLA-C expression on HCMV infected MRC5 fibroblasts determined by flow cytometry over the course of a productive infection.** The levels of HLA-C alleles on the surface of HCMV infected fibroblasts *in vitro* during a productive infection were analysed by flow cytometry. A) Gating strategy for identifying HCMV infected fibroblasts at 3 vs 72 hours p.i. As infection progresses the size of the HCMV infected cells increases. For each time point, an individual uninfected fibroblast control was set up. The MFI of HLA staining on the fibroblasts was obtained and expressed as a percentage of the uninfected fibroblast control MFI (percentage relative expression) B) Representative histograms demonstrating surface HLA-C staining on AD169 infected MRC5 fibroblasts using the DT9 monoclonal antibody (Kindly provided by Dr Veronique Braud**)** at 3-24 hours p.i. The white histograms represent the HLA-C MFI obtained for uninfected fibroblasts. The red histograms represent the HLA-C MFI obtained for AD169 infected fibroblasts. The top row of representative histograms represent timepoints from one representative experiment and the bottom row of representative histograms indicates timepoints from a second representative experiment.

During an infection of fibroblasts with the AD169 strain, where the WT US2-11 gene region is present, the HLA-ABC (W6/32) MFI progressively decreased over the course of the infection (3-72 hours) compared to uninfected fibroblasts (Fig-44B). Conversely, the HLA-C MFI progressively increased from 3-12 hours p.i. with a significant increase at 6 hours p.i compared to the total HLA-ABC (W6/32) MFI (Fig43B, 44A/B). After this time-point, the MFI

obtained for HLA-C staining (DT9) also progressively decreased (Fig-43B/44B). It should be noted that the DT9 monoclonal antibody has cross-reactivity with HLA-E alleles. However, a previous study by Weekes et al demonstrated that HLA-E alleles were downregulated at IE time-points of CMV infection of fibroblasts [225]. Therefore it is anticipated that cross reactivity at these time-points is minimal.

During a ΔUS2-11 RV798 infection of MRC5 fibroblasts, the MFI obtained when staining for HLA-ABC (W6/32) increased up to 6-fold over the course of the infection relative to uninfected fibroblasts (Fig-44B). Interestingly, the HLA-C staining followed a similar trend to that observed during an AD169 infection, with a significant increase in the MFI obtained when staining for HLA-C (DT9) compared to HLA-ABC staining (W6/32) at 6-hours p.i followed by a progressive downregulation to reach an MFI comparable to uninfected fibroblasts (Fig-44B).

This indicates that the HLA-C alleles, at least those expressed on MRC5 fibroblasts, are not targeted by the US2-11 gene region products otherwise there would be a similar 6-fold increase in the DT9 MFI during an infection in their absence.

A second fibroblast cell line – HFFF2 – that is HLA-Cw*0702 negative was then characterised for surface HLA allele downregulation (Fig-44C). During IE-E times of an AD169 infection of HFFF2 fibroblasts both HLA-ABC and HLA-C MFI staining increased slightly compared to uninfected fibroblasts. After this time-point the HLA-ABC MFI decreased as the infection progressed whereas the HLA-C MFI was maintained at similar levels (Fig-44C).

During an RV798 infection of HFFF2 fibroblasts, the MFI obtained during staining for both HLA-ABC (W6/32) and HLA-C (DT9) increased progressively during infection 3-fold compared to uninfected fibroblasts (Fig-44C). This indicates that the HLA-C alleles on HFFF2 cell surfaces are targeted by the US2-11 gene region products preventing an increase in the DT9 MFI 3-fold during a WT infection.

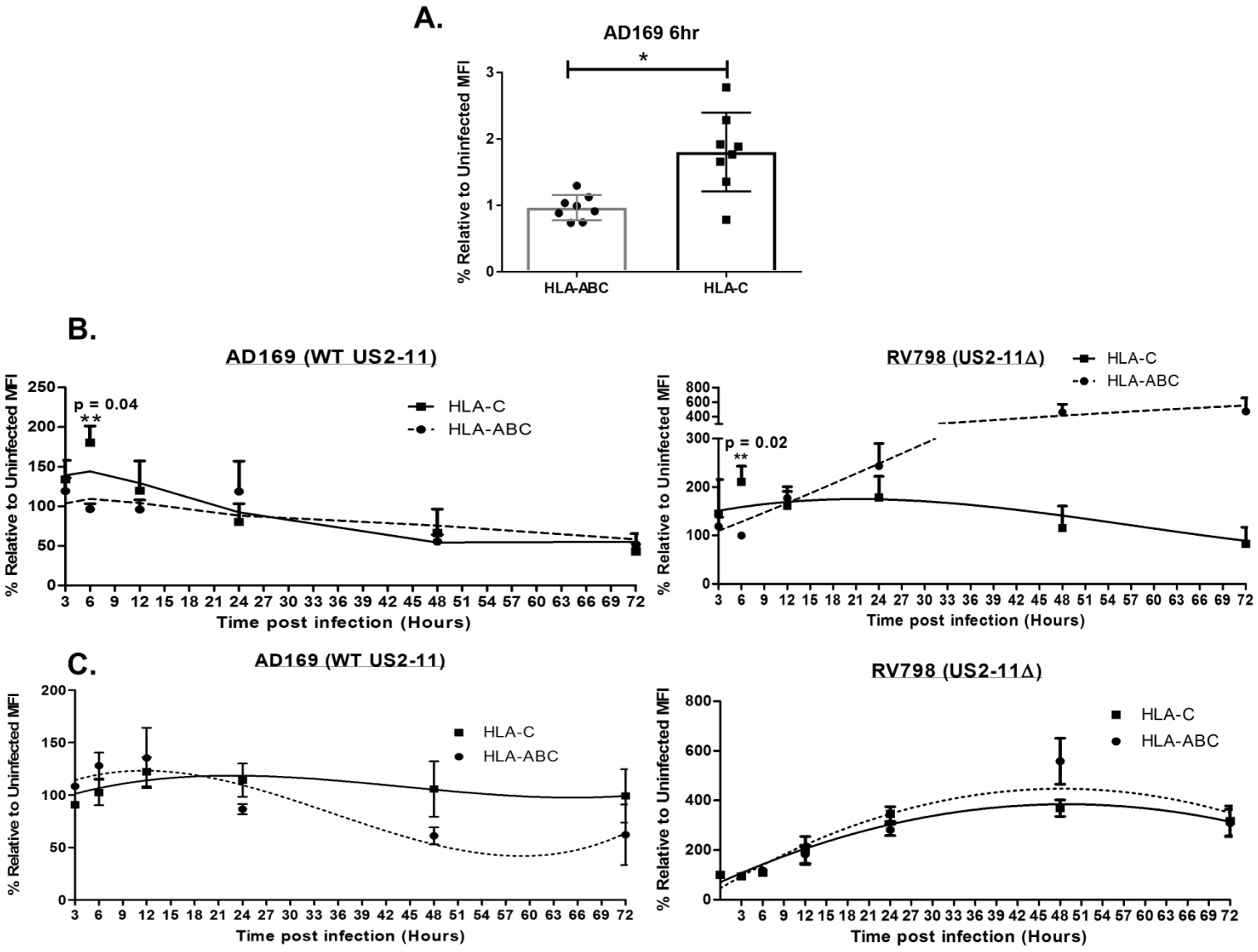


**Fig 44 – Summary of the surface expression of HLA-ABC alleles on infected MRC5 and HFFF2 fibroblasts during AD169 vs RV798 infections.** The surface expression of HLA-C vs HLA-ABC alleles on the surface of HCMV infected fibroblasts in the presence vs absence of the US2-11 immunevasins was analysed. At each time point, the MFI obtained on infected cells was expressed as a % of the MFI obtained on an uninfected control harvested at the same time as the infected cells. A) Summary of the HLA-ABC and HLA-C alleles on AD169 infected MRC5 fibroblasts at 6 hours p.i. Statistical significance was obtained using a Mann Whitney test within Graphpad Prism6 using * as a p-value < 0.05. B) Summary of the HLA-ABC and HLA-C staining on AD169 (left graph) vs RV798 (right graph) infected MRC5 HLA-Cw*0702 positive fibroblasts at 3-72 hours p.i. C) Summary of the HLA-ABC and HLA-C staining on AD169 (left graph) vs RV798 (right graph) infected HFFF2 fibroblasts at 3-72 hours p.i. B/C Error bars represent SEM. Lines represent a smoothed differentiation curve to demonstrate the trend of the data. n = 6-9 for MRC5 and n = 2-3 for HFFF2 cell lines per infection time point.

## 4.14 – HLA-C CD8+T-cell clones recognise cognate antigen that is naturally processed during a productive infection *in vitro*

After identifying that HLA-C alleles are upregulated at IE time-points of an *in vitro* infection of a HLA-Cw*0702$^{+}$ cell line, the ability of HLA-C specific CD8+T-cell clones to recognise naturally processed antigen on infected cells *in vitro* at IE time-points was assessed. In addition, it was evaluated which cell types may be presenting the HLA-Cw*0702 peptides *in vivo*. It has been hypothesised that CMV infected non-haematopoietic cells with access to the circulation such e.g. endothelial cells are the APCs driving memory-inflated CD8+T-cell populations [104, 123, 132].

The ability of haematopoietic vs non-haematopoietic cells to present HLA-C peptide to specific CD8+T-cell clones was thus investigated. Either monocytes isolated from donor PBMCs with identified HLA-Cw*0702 CD8+T-cell populations or fibroblasts were used in the assay. Two WT CMV strains were utilised - the AD169 strain that infects fibroblasts only due to mutations quickly acquired during passage *in vitro*, and the Merlin strain which is able to infect monocytes due to an intact UL128-131 region (Review [241]). Recognition was identified by IFN-γ release into the supernatant of an O/N co-culture of CD8+T-cell clones and infected target cells. This recognition was compared to recognition of RV798 infected cells, which are theoretically displaying all antigenic peptides of the virus. NLV-specific CD8+T-cell clones were included as comparison to a known inflationary CD8+T-cell population.

The FRC-, CRV- and LSE-specific CD8+T-cell clones recognised naturally processed peptide at all time-points IE-L (6-72hours p.i.) of an AD169 infection of HLA-Cw*0702$^{+}$ MRC5 fibroblasts (Fig-45). Recognition of RV798 infection of MRC5 fibroblasts was more pronounced i.e. higher magnitude of IFN-γ, and also occurred at all time-points of the infection (Fig-45). Interestingly, strong recognition of naturally processed HLA-C antigen on Merlin infected monocytes by FRC and CRV-specific clones occurred only at IE-E time-points (12-24 hours) of infection.

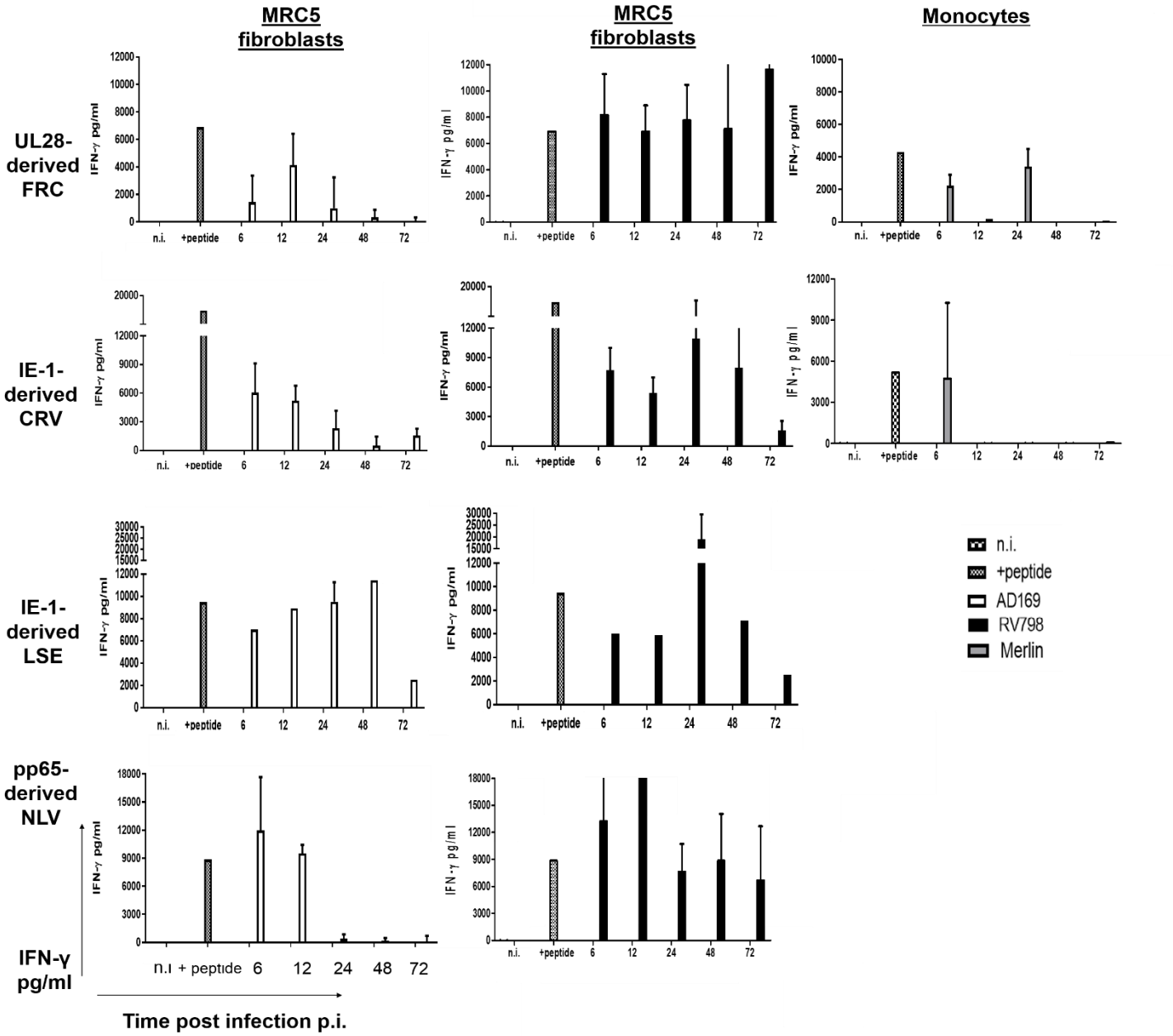


***Fig 45 – Recognition of fibroblasts and monocytes by HLA-C-restricted HCMV-specific CD8+T-cell clones during a productive in vitro infection***. The ability of HCMV-specific CD8+T-cell clones to recognise and engage naturally processed antigen during a HCMV infection *in vitro* was determined. MRC5 HLA-A2/Cw*0702$^{+}$ AD169 infected fibroblasts (left column), RV798 infected fibroblasts (middle column) or Merlin infected monocytes (right column) were infected for 6-72 hours at an MOI of 5. At the indicated time-points infected cells were incubated with 10 000 specific CD8+T-cell clones O/N indicated on the left of the figure. This was followed by an IFN-γ ELISA. Bars represent the mean IFN-γ production in pg/ml per time-point by specific CD8+T-cell clones and error bars SEM. n = 3-5 per time-point for fibroblasts FRC, n = 2-4 CRV n = 1-2 LSE and n = 2-4 NLV. For monocyte assays n = 2.

During an AD169 infection of MRC5 HLA-A2$^{+}$ fibroblasts, NLV-specific clones recognised naturally processed antigen strongly at IE-E time-points of infection (6-24hours) with small but reproducible IFN-γ release at E-L (48-72 hours p.i)(Fig-45). The same clones recognised NLV peptide at all time-points of an RV798 infection of the MRC5 HLA-A2$^{+}$ fibroblasts (Fig-45). Thus, both haematopoietic and non-haematopoietic cells can present HLA-C peptide to specific CD8+T-cell clones during an *in vitro* WT HCMV infection with two strains but non-haematopoietic cells are able to present HLA-C antigen to the end of a productive infection.

# Chapter 4

## Project 3 summary

This section of this investigative study aimed to assess some of the factors that may culminate in HLA-C memory-inflation; CD8+T-cell proliferation and oligoclonality, antigen recognition and the role of the restricting HLA allele.

Upon antigen stimulation of *ex vivo* PBMCS, a hierarchy of proliferation capability was attained; FRC>CRV>LSE-specific CD8+T-cells. This correlates with the hierarchy in the observed *ex vivo* magnitudes of CD8+T-cells detected towards these three HLA-Cw*0702-restricted peptides. Where a dominant TCR Vβ usage was observed within the *ex vivo* FRC-specific CD8+T-cell populations, it was for Vβ3 usage.

A potential mechanism driving HLA-C CD8+T-cell inflation was investigated. Preliminarily data demonstrated the upregulation of HLA-C on a fibroblast line that is positive for HLA-Cw*0702 at IE time-points of a HCMV infection *in vitro*. This is the restricting allele for the inflationary peptides investigated in this research and correlates with the peak expression of the proteins from which they are derived from [225]

Importantly, specific CD8+T-cell clones could recognise naturally processed cognate antigen during this window of HLA-C upregulation, and at all time-points of an AD169 infection of fibroblasts, and release IFN-γ. Furthermore, FRC- and CRV-specific CD8+T-cell clones were demonstrated to recognise naturally processed peptide during a Merlin strain infection of monocytes. These HLA-C peptides are hence efficiently generated during infection with two strains of CMV and HLA-C specific CD8+T-cell clones are able to exert anti-viral functions upon antigen engagement.

Altogether, these CD8+T-cell populations represent promising targets, in particular the UL28-derived FRC-specific CD8+T-cell populations, to include within adoptive immunotherapy regimens to treat CMV disease in the HSCT setting.

# CHAPTER 4 -DISCUSSION

**Identification of HLA-Cw*0702-restricted CMV CD8+T-cell memory-inflation**

Focus on the CD8+T-cell response to HCMV has been primarily devoted to the pp65 and IE-1 proteins and further restricted to HLA-A/-B restricted peptides derived from these immunodominant proteins. A recent investigation has shown that a HLA-C restricted CD8+T-cell population can be an important component of the overall CD8+T-cell repertoire dedicated to CMV control during latency [139] Thus emphasising that the focus of analysing the CMV CD8+T-cell response should be extended to HLA-C peptides.

This investigation identified memory CD8+T-cell inflation restricted through HLA-Cw*0702 specific for three antigens expressed at IE time-points of the CMV life cycle – the 'FRC', 'CRV' and 'LSE' peptides (Table-8, [77, 85, 139, 267]. These CMV CD8+T-cell populations dominated the total peripheral CD8+T-cell pool within older donors to individually reach 32% and 31% within a single donor producing IFN-γ and TNF-α respectively. Extraordinarily, the summation of these three populations within individual donors could exceed 56% of the circulating CD8+T-cells. Also, outstandingly, the HLA-Cw*0702 CD8+T-cells accounted for on average >7% of the peripheral $T_{EMRA}$ within donors <70 years of age and expanding to account for >20% within donors >70 years. As such, these CD8+T-cell populations represent one of the largest CD8+T-cell responses documented towards a viral pathogen to date. A hierarchy of CD8+T-cell responses directed towards the HLA-Cw*0702 peptides was observed where; FRC>CRV>LSE. This was in terms of the magnitude of the *ex vivo* CD8+T-cell responses.

**An increased $T_{EMRA}$ phenotype of inflated HLA-Cw*0702 T-cells with age – does this point to chronic antigen stimulation?**

The *ex vivo* CD8+T-cell responses to the three inflationary HLA-Cw*0702 peptides were phenotypically characterised in this work by flow cytometry and the results interpreted with

the age of our donor cohort. Additionally they were interpreted as the size of the specific HLA-Cw*0702 CD8+T-cell population accumulated. Throughout this investigation, the phenotypic results obtained support the antigen encounter theory of memory-inflation [115-117]. This hypothesis proposes that the frequent exposure of CD8+T-cells to antigen drives their accumulation and their phenotype down the differentiation pathway towards a $CD27^{-}CD28^{-}CCR7^{-}CD45RA^{+}$ phenotype. Some of the data obtained in this investigation supporting this theory will now be discussed.

LSE-specific CD8+T-cell populations demonstrated the smallest *ex vivo* magnitudes and proliferation. The total-epitope specific CD8+T-cells were split between $T_{EM}/T_{EMRA}$ ($CCR7^{-}CD45RA^{-}$) and intermediate/late ($CD27^{-}CD28^{+}/CD27^{+}CD28^{-}/CD27^{-}CD28^{-}$) antigen differentiated populations. This is suggestive that these populations are the least antigen stimulated of the HLA-Cw*0702 populations.

The inflationary FRC-specific CD8+T-cell populations demonstrated the largest *ex vivo* magnitudes, proliferation and exaggerated $T_{EMRA}$ phenotype ($CCR7^{-}CD27^{-}CD28^{-}CD45RA^{+}$) with age and population size. This implicates that they have been the most chronically stimulated of the HLA-Cw*0702 populations. Additionally, the loss of both CD27/CD28 has been reported as indicative of a history of high proliferative capacity [238]. Importantly, a FRC-specific CD8+T-cell clone demonstrated the highest *in vitro* proliferation in comparison to HLA-A-restricted CD8+T-cell clones, however this is very preliminary work and was conducted once. Additionally, as the age of the donor and size of the epitope-specific HLA-Cw*0702 CD8+T-cell populations increased, the HLA-Cw*0702 populations displayed an increased cytotoxic IFN-γ+TNF-α polyfunctional profile. CD8+T-cells capable of producing IL-2 were lost. This was similar to the NLV-specific CD8+T-cell profile. NLV-specific CD8+T-cells have previously been documented as antigen driven [71].

Taken together, this implies that the accumulated HLA-Cw*0702-restricted CD8+T-cell populations are further down the T-cell differentiation pathway in older age representing accumulations of later differentiated specific CD8+T-cells.

Further supporting the chronic stimulation hypothesis is the *ex vivo* phenotype of the stable CD8+T-cell populations in our donor cohort by the HLA-A1-restricted RTD and YAD peptides These displayed a greater percentage of earlier differentiated $T_{CM}$ and $T_{EM}$ CD8+T-cells capable of producing IL-2 compared to the HLA-Cw*0702 CD8+T-cells.

In further corroboration of antigen stimulation over the hosts lifetime, the HLA-Cw*-0702 CD8+T-cell populations increased NKG2D expression with age. NKG2D when expressed on CD8+T-cells is a marker of recent CD8+T-cell activation and has been documented to act as a co-stimulatory molecule in replacement of CD28 [277]. The same CD8+T-cells also maintained CX3CR1 expression with age. This CX3CR1 expression parallels previous data documenting this fractalkine receptor on CMV-specific CD8+T-cells which has been linked to their homing to endothelium where they cause endothelial damage [2, 72, 91]. It is plausible that CX3CR1 expression homes these CD8+T-cells to the endothelium to be continuously stimulated by antigen from latently infected CD8+T-cells over the host's lifetime. This drives the differentiation of the HLA-Cw*0702 CD8+T-cells to a late $T_{EMRA}$ phenotype whereby CD28 is downregulated. The progressive upregulation of NKG2D with age may therefore complement the loss of CD28 to provide activatory signals. However, the largest FRC-specific CD8+T-cell population that was phenotypically characterised displayed the most exaggerated $T_{EMRA}$ phenotype and downregulated CX3CR1 and NKG2D expression. It is therefore also plausible that larger accumulations of FRC-specific CD8+T-cells are at the end-stage of antigen driven differentiation and have also down-regulated the NKG2D co-stimulatory mechanism in preparation for cell turnover.

Lastly, the maintenance of Vβ3 usage, and loss of other Vβ usage, by the FRC-specific CD8+T-cells within older donors could possibly point to the repetitive antigen stimulation of a single clone over the lifetime of the infected host. However, this Vβ usage analysis has been conducted within a small donor cohort (n = 3 young <70 years and n = 3 older >70 years) and as such represents a preliminary analysis. To increase the accuracy of this TCR Vβ analysis, more donors should be investigated. It would also be interesting to determine

whether the FRC-specific Vβ3 populations within these donors represent CD8+T-cells of a high avidity. Thus providing a plausible selective advantage to the host for maintaining the Vβ3 populations within the periphery. Longitudinal TCR analysis of the FRC-specific CD8+T-cell populations would address whether the Vβ3 using clones are truly maintained into older age.

The *ex vivo* magnitudes and phenotypic results of these HLA-Cw*0702 CD8+T-cell responses were obtained after stimulating the PBMCs with peptide. It would be important, if such a reagent became available, to compare this 'activated' phenotype with the phenotype obtained with MHC-I tetramers. This would provide an indication of how many CD8+T-cells are non-functional but specific to these peptide epitopes. Additionally it will be important to investigate whether there are HLA-Cw*0702 epitope-specific T-cells producing regulatory cytokines such as IL-10.

**Factors involved in the generation of HLA-C CMV memory-inflation**

HLA-C memory-inflation observed within this study was confined to HLA-Cw*0702-restricted peptides. However, as evidenced by non-inflating CD8+T-cell population's specific for a fourth HLA-Cw*0702-restricted peptide 'SYR', that HLA-Cw*0702-restriction alone does not result in inflation. This peptide is derived from the UL33 protein expressed with L kinetics. This is in comparison to the IE-expressed antigens from which the three inflationary HLA-Cw*0702 peptides, characterised in this work, are derived from. Although, non-inflating CD8+T-cell responses were observed against another IE-expressed peptide restricted through HLA-Cw6 termed 'QIK'. Therefore it is not also simply a matter of IE kinetics for a peptide to elicit inflationary CD8+T-cell populations. This suggests it may be a combination of factors that culminate in IE-specific HLA-Cw*0702 memory-inflation with age. Some factors likely involved in the HLA-C inflation in this work will now be discussed.

- Abundance of mature MHC-I:peptide complexes on the cell surface

Several studies have concluded that the abundance of cognate peptide-epitope on the cell surface presented to CD8+T-cells determines the immunodominance of the resulting anti-viral CD8+T-cell response [278, 279]. A critical factor that determines cell surface density of MHC-I:peptide complexes is the binding affinity of peptides to MHC-I molecules on the ER [120, 280]. The lower surface expression of HLA-C alleles on host cell surfaces has been linked to a higher threshold of peptide binding to the HLA-C molecules within the ER causing less peptide:HLA-C complexes to reach the surface [255]. Efficient post-translational processing ensures that a mature peptide-epitope is generated able to bind to the MHC-I molecule in the ER lumen with sufficient affinity [120]. Although this manuscript has not directly assessed the differing processing of the peptides investigated in this manuscript, a previous study proved that the generation of the mature HLA-Cw*0702-restricted FRC vs. HLA-A1-restricted YAD peptide-epitopes from precursors is critically dependent upon separate processing pathways – being ERAp1 dependent and independent respectively [85]. ERAp1 is an important enzyme involved in the generation of mature MHC-I epitopes via the trimming of longer precursors within the endoplasmic reticulum [281, 282]. Importantly, ERAp1 is implicated in the development of *in vivo* CD8+T-cell immunodominance within mice [283]. However, Kim et al. also demonstrated that the HLA-Cw*1601 YLC and HLA-B7 WPK peptides (Table-7) - also investigated in this study and found to elicit non-inflationary and infrequent CD8+T-cell responses - were also ERAp1 dependent. Therefore, post-translational modification of the inflationary FRC peptide may contribute, but is not solely responsible for the resulting immunodominance of the FRC-specific over that of YAD-specific CD8+T-cell populations.

It is interesting to note, that the three HLA-Cw*0702 peptides displayed a hierarchy when MHC-I anchor residues and auxiliary residues were considered; FRC 5’ F**R**CPRRF**C****F** **3’,** CRV 5’ C**R**VLCCYV**L** 3’ and LSE 5’ LSEFCRVLV 3’ (anchor residues provided in bold and underlined, auxiliary residues underlined as identified by Rasmussen et al. [284]). We could therefore speculate that a higher number of both anchor residues and auxiliary residues

within the FRC peptide sequence, translates to a higher binding affinity to MHC-I, over CRV and LSE. This may result in a more stable MHC:peptide complex and increased cell surface expression of the FRC peptide to the CD8+T-cell response. This could explain the later differentiation phenotype and larger *ex vivo* CD8+T-cell responses against the FRC-peptide over CRV and LSE. In support of this, infection of mice with a recombinant-MCMV expressing the SIINFEKEL peptide abolished MCMV-specific memory-inflation in favour of SIINFEKLL-specific inflation. The authors hypothesised the higher affinity of the SINKFEKL peptide for its H-2K$^{b}$ alleles over endogenous MCMV peptides led to increased surface presentation [124].

- CD8+T-cell avidity

An important result in this study was the identification of the high functional avidity of HLA-C-specific CD8+T-cell clones generated *in vitro* in this investigation. CD8+T-cells that are specific for HLA-C targets are likely to be more avid to engage the low concentration of peptide:HLA-C complexes that presented on infected cell surfaces [254, 255]. In support of this, highly avid HCMV-specific CD8+T-cell populations have been demonstrated to be selected for and preferentially maintained by the host [126]. Day et al. analysed the focusing of the HCMV-specific CD8+T-cell response during a primary infection of renal transplant patients. They observed the maintenance of highly avid CD8+T-cell clones for pp65 and IE-1 compared to lower avidity clones. This affinity based survival and selection of HCMV CD8+T-cell clones has been demonstrated by a second research group who showed the selection of public TCRs specific for the pp65 NLV peptide between individuals that were highly avid [128]. The results of this study demonstrated the preferential maintenance of *ex vivo* CD8+T-cells using Vβ3 chains with age within the HLA-Cw*0702 FRC-specific CD8+T-cell population. It should be analysed whether this is the preferential systemic maintenance of a highly avid CD8+T-cell clone.

- Antigen presenting cell type

The consensus within the literature is that non-haematopoietic cells within either peripherally located tissues e.g. lungs or secondary lymphoid organs e.g. the lymph nodes, present HCMV antigen to CMV-specific CD8+T-cells that are of a $T_{CM}$ phenotype. Antigen stimulation of the $T_{CM}$ population results in rapid proliferation and differentiation to a CD8+T-cell population with a $T_{EMRA}$ phenotype that enters the periphery where they protect against CMV reactivation events and can accumulate [104, 123, 132].

The presentation of the HLA-Cw*0702 inflationary peptides to specific CD8+T-cell clones was investigated in both haematopoietic (monocytes) vs non-haematopoietic (fibroblasts) *in vitro*. The IE-1 and UL28 proteins, from which the three HLA-Cw*0702-restricted peptides are derived, are present within the incoming virion during primary infection and among the first to be expressed during infection. The IE-1 protein functions to initiate the viral lifecycle and the UL28 protein functions to export the resulting viral mRNAs from the nucleus to the cytoplasm for translation using the host machinery [248, 285]. These proteins may therefore theoretically be immediately available for degradation and enter the MHC-I pathway for direct presentation during a primary infection of cells. During AD169 infection, HLA-C-specific CD8+T-cells were activated by peptide at IE time-points in both cell types. However, it was the non-haematopoietic cells that presented the HLA-Cw*0702 antigens to the end of a productive infection (6-72 hours). Peptide recognition was only observed up to 12 and 24 hours p.i. for FRC- and CRV-specific CD8+T-cell clones respectively on infected monocytes.

These recognition profiles parallel the general consensus of non-haematopoietic cells driving memory-inflation by presenting HLA-C peptide at all time-points of an infection. [104, 123, 132]. Direct presentation by haematopoietic and non-haematopoietic cells could both be capable of the initial generation of HLA-Cw*-0702-specific CD8+T-cell responses

- Expression kinetics of the HCMV antigen

Several research groups have now identified that the expression kinetics of a CMV peptide is a key factor in its inflationary capacities. Dekhtiarenko et al. identified that only peptide-

epitopes fused to promoters expressed with IE-kinetics induced inflationary CD8+T-cell populations within MCMV infected mice [286]. Importantly, work by our research group characterised the accumulation of IE-1-specific CD8+T-cells within a healthy CMV infected donor cohort but not pp65-specifc. The authors hypothesised that the IE expression kinetics of the IE-1 protein gave the CD8+T-cells an advantage over the pp65-specific with regards to CD8+T-cell priming during a reactivation event. The inflationary peptides characterised in this work are derived from proteins expressed with IE- kinetics – the IE-1 and UL28 proteins. The IE kinetics of the HLA-Cw*-0702 peptides may as such play a role in whether the resulting CD8+T-cells will inflate or not.

- HLA restriction

Importantly, this work identified that in the presence of the US2-11 proteins, HLA-C alleles were significantly upregulated on the cell surface of infected fibroblasts that are HLA-Cw*0702$^{+}$HLA-Cw0501$^{+}$ at IE times of infection compared to the total HLA-ABC alleles. These were then progressively down-regulated over the course of the infection. During an RV798 infection of the same fibroblasts, the HLA-C alleles followed an almost identical pattern of significant upregulation at 6 hours p.i. followed by returning to levels similar to uninfected fibroblasts. Conversely, during RV798 infection the total HLA-ABC alleles increased 6-fold over the levels present on uninfected MFIs. If the US2-11 proteins were targeting these specific HLA-C alleles during infection it is likely that they would similarly increase 6-fold in the absence of the US2-11 proteins.

Within a second cell line that is HLA-Cw*0702 negative, HLA-C alleles appeared to be maintained at levels parallel to uninfected fibroblasts during an AD169 (WT US2-11) infection. During an RV798 infection, the HLA-C alleles increased 3-fold over the course of the infection. This implicates the US2-11 proteins as efficiently preventing these particular HLA-C alleles from 3-fold increased cell surface expression during HCMV infection.

Together this data alludes to the precise HLA allele targeting specificity of the US2-11 immunomodulatory proteins in differing cell lines. It indicates the US2-11 proteins as not targeting particular HLA-C alleles for downregulation within a HLA-Cw*0702$^{+}$ cell line. Additionally that WT HCMV infection may in fact induce HLA-C allele upregulation in the IE phase of HLA-Cw*0702$^{+}$ cell lines. However, the US2-11 proteins can prevent other HLA-C alleles increasing 3-fold during infection of a HLA-Cw*0702 negative cell line. Future research is focused on tracking HLA-Cw*0702 alleles during the course of a HCMV infection via transfection of a HLA-Cw*0702 construct into a HLA-C negative cell line.

The differential targeting of HLA alleles by the HCMV US2-11 gene products has been demonstrated elegantly by the research group of Ameres et al [139, 140]. Specifically, HLA-Cw*0702 alleles that are inhibitory ligands for the NK cell receptor KIR2DL3 were shown as less susceptible to downregulation by US3 [140] and US2/11 [139]. This translated to HLA-Cw*-0702 CRV-specific clones being efficiently able to kill infected cells whilst this HLA-Cw*0702 allele maintenance mediated the inhibition of NK-cell killing infected cells. An important finding with relevance to this study was that the US3 protein also did not target HLA-A3 alleles – a second NK cell inhibitory ligand [287].

The US3 protein is expressed during the viral lifecycle with IE kinetics [288, 289]. If the US3 protein is unable to target HLA-Cw*0702 alleles in an attempt to subvert NK-cell activation, this would provide a window whereby IE-expressed HLA-Cw*0702 peptides can be presented to CD8+T-cells. Indeed this was shown by Ameres et al during a fibroblast infection with a mutant strain deleted for all US immunevasins except US3 [140]. This translated functionally to an exacerbated recognition of infected cells by HLA-Cw*0702 clones at IE time-points. Secondly upon infection with strains expressing only US2 or US11, increased HLA-Cw*0702 CD8+T-cell recognition was observed at 24 hours p.i. This strongly suggests a time frame during the early stages of an infection where HLA-C CD8+T-cells have an advantage with regards to antigen stimulation.

When it is taken into account the US3 protein did also not affect a HLA-A3 allele that is an inhibitory receptor for NK cells, we hypothesise that the upregulation of NK-cell inhibitory receptors such as HLA-A3 and HLA-Cw*0702 on HCMV infected cells may allow for NK-cell evasion. However, this is at the expense of a HLA-Cw*0702-restricted CD8+T-cell population that is efficiently able to kill virally infected cells [139]**.**

**HLA-Cw*0702-restricted CD8+T-cells as an immunotherapy for HCMV disease**

IE-specific CD8+T-cells have been linked to an enhanced protection from MCMV disease in vivo [187]. Once CMV latency has been established, the majority of viral genomes are transcriptionally silent. However, murine studies into CMV reactivation have identified the random but frequent transcriptional activation of IE promoters during latency, particularly within the lungs [98, 119, 290, 291]. These reactivation events have led to the expression of IE gene products on the infected cell surface. IE-specific CD8+T-cells are importantly able to recognise these latency expressed transcripts leading to the termination of the viral reactivation event i.e. abortive not resulting in virion production [119]. As such, transcripts expressed after IE-E stage, i.e. L derived pp65 epitopes, are not generated and presented on the cell surface. It is likely that IE-specific CD8+T-cells would have an evolutionary advantage over those specific for L-expressed antigens with regards to engaging cognate antigen and undergoing antigen driven proliferation. Focus on developing novel immunotherapies to treat HCMV disease in the HSCT setting should be on including T-cell specificities towards IE-expressed antigens.

The results presented in this work indicate that the three HLA-Cw*0702 CD8+T-cell populations are excellent candidates for development as an adoptive immunotherapy to treat overt HCMV disease. The HLA-Cw*0702 FRC-specific CD8+T-cells could efficiently recognise and kill peptide naturally generated during an AD169 infection of fibroblasts and become activated after incubation with Merlin infected fibroblasts. This is indicative that the HLA-Cw*0702 inflationary peptides are generated efficiently during an infection with differing

strains of HCMV *in vivo*. This coupled with their cytotoxic potential, cytokine polyfunctionality, peptide recognition profile and avidity – FRC-specific CD8+T-cells represent extremely promising populations for inclusion within adoptive immunotherapy regimes. The main priorities are now, firstly, to develop these as such a therapy via the retroviral transduction of an FRC-specific TCR onto PBMCs *in vitro*. Secondly, testing whether the transduced populations are equally as efficacious as FRC-specific CD8+T-cell clones in removing virally infected cells.

**Proposed model for HCMV HLA-C CD8+T-cell memory-inflation**

To summarise, it is likely that a combination of the following factors (however not exclusively) leads to the preferential inflation of the HLA-Cw*0702-restricted CD8+T-cell populations;

1. IE kinetics of the peptide – expressed and presented in HLA-C during a reactivation event before termination of viral reactivation by CD8+T-cells
2. HLA-Cw*0702-restriction of the peptide – HLA-Cw*0702 upregulation on the cell surface during IE time-points allows interaction with NK-cell inhibitory receptors so that CMV latency can be established
3. The allele targeting specificity of the HCMV immunevasins during the IE time-points of a HCMV primary infection and reactivation event in differing cell types
4. High avidity of HLA-C CD8+T-cells - preferentially maintained by the host due to effective anti-viral function
5. High affinity of peptide for HLA-C binding in the ER - a result of the increased number of auxiliary and anchor residues within the mature ‘FRC’ peptide

This discussion will conclude with a proposed model for the preferential inflation of HLA-C restricted CD8+T-cell populations (Fig-46). During primary infection, HLA-AB and -C alleles on infected cells are able to prime the initial CD8+T-cell response generating a diverse repertoire comprising of CD8+T-cell clones with differing avidities. The HLA-Cw*0702 alleles, unaffected by the US2-11 gene region products, maintain-NK cell protection during

acute infection allowing the development of HCMV latency. During chronic infection, sporadic reactivations induce the upregulation of HLA-Cw*0702 alleles, preventing NK-cell removal of reactivating virus. At the same time the HLA-Cw*0702 alleles present the IE-expressed FRC, CRV and LSE-targets to the CD8 T-cells driving their accumulation, proliferation and oligoclonality. This results in CD8+T-cell elimination of the infected cell halting the generation of E-L transcripts for MHC-I presentation. Over the lifetime of the host these reactivation events drive the differentiation of the HLA-C CD8 T-cells to downregulate CCR7, CD27, CD28, re-express CD45RA and upregulate cytotoxic potential and pro-inflammatory cytokines. This leaves a large peripheral pool of highly avid and cytotoxic CD8+T-cells.

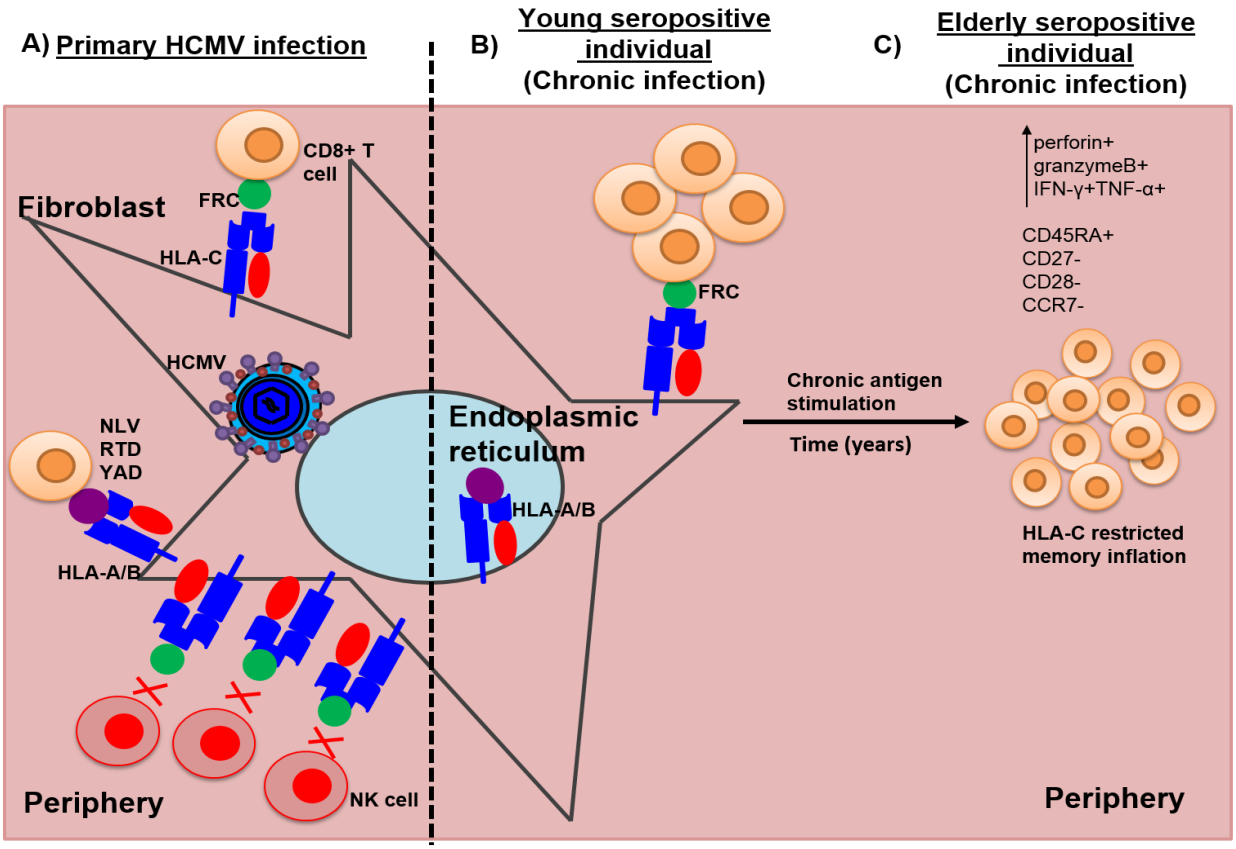


***Fig 46 –Proposed model for HLA-Cw*0702-restricted 'FRC' HCMV-mediated memory-inflation*** A) During primary HCMV infection HLA-A/-B and –C alleles prime the CD8+T-cell response with HCMV antigens derived from potentially all proteins of the virus. B) During chronic infection in young age, the virus selectively down regulates HLA-A and -B alleles leaving HLA-C on the surface as an NK-cell evasive mechanism. HLA-Cw*0702 alleles then re-stimulate the initial FRC-specific CD8+T-cell pool during viral reactivation. CD8+T-cells specific for L derived antigens presented through HLA-C are not primed due to the CD8+T-cell control of the infection after IE time-points. This leads to the accumulation of peripheral FRC-specific CD8+T-cells. C) In older donors, the frequency of HCMV reaction and therefore the frequency of HLA-Cw*0702 presentation of the FRC peptide determines the magnitude of FRC-specific CD8+T-cell memory-inflation within the periphery. Furthermore, the chronic antigen stimulation of the FRC-specific CD8+T-cells to upregulate expression of perforin, granzyme B, dual IFN+TNF+ cytokine polyfunctionality and progress to a late differentiated memory phenotype (CD45RA+CD27-CD28-CCR7-).

# CHAPTER 5

# THE DEVELOPMENT OF A HLA-CW*0702-RESTRICTED CD8+T-CELL POPULATION SPECIFIC FOR IE ANTIGEN AS AN IMMUNOTHERAPY FOR HCMV DISEASE IN THE HSCT SETTING

# CHAPTER 5 - INTRODUCTION

Development of CMV-mediated disease is strongly associated with the loss of CD8+T-cell control of the virus within immunocompromised transplant patients [292]. As a result, current immunotherapies for treatment of CMV disease are focused on recapitulating the CD8+T-cell immunity against CMV within these patients (Review [293]).

Recently, the concept that HLA-C alleles, in particular HLA-Cw*0702 and their presented peptides, are less affected by the HCMV MHC-I immune evasion gene region products has been proposed [139, 140]. We demonstrated that HLA-C-restricted CMV-specific CD8+T-cells are highly avid for cognate peptide, effective at killing CMV-infected targets and demonstrate high cytotoxicity and pro-inflammatory potential. This provides great promise for their adaption as an immunotherapy to treat HSCT patients with CMV reactivation.

Pp65 and IE-1-specific CD8+T-cells have previously been the focus of adoptive cell therapy for CMV disease and shown to have high efficacy within the murine model [187, 188] and human patients [64, 189-191]. However, this approach loses efficacy when a previously HCMV negative HSCT patient acquires HCMV after transplant or has low frequencies of circulating HCMV-specific CD8+T-cells. In this context it is difficult to isolate and expand the donor's memory CD8+T-cells. To overcome this a new approach, whereby the TCR of CMV-specific CD8+T-cell clones are transduced onto donor CD8+T-cells, has been adopted to recapitulate or generate an effective HCMV-specific CD8+T-cell effector pool [8, 195].

This investigative chapter concentrated on developing a UL28-derived FRC-specific CD8+T-cell population as a potential therapy. The premise of this was based upon IE expression kinetics, an enhanced *ex vivo* magnitude, killing efficacy and proliferation capacities over IE-1-derived HLA-Cw*0702 specific clones.

The DNA genome of HCMV encodes for approximately 200 ORFs and several distinct families of genes [294, 295]. The US22 CMV gene family consists of 13 members; UL23, UL24, UL26, UL28, UL29, UL36, UL43, IRS1, TRS1, US22, US23, US24, and US26. This

gene family is conserved among all the β-herpesviruses. The UL28 gene of the US22 family encodes for a protein product that is expressed with IE kinetics [225, 248, 285] as a bicistronic transcript with the UL29 protein which eventually becomes spliced. Interestingly, this protein has also been identified as a potential transcript that is expressed during latency [296].

The role of the UL28/29 bicistronic message is to stimulate the activity of the 'major immediate early protein' (MIEP) in cooperation with the UL38 protein [248]. To do this, the UL28/29 interacts with the 'Nucleosome remodelling and deacetylase complex' (NuRD) to allow viral replication to proceed during IE time-points of a primary HCMV infection. This results in the accumulation of CMV IE RNAs required for viral replication to proceed [248, 285].

It is therefore hopeful that any potential immunotherapies developed from a UL28-specific population may provide lifelong protection of the patient from reactivation events by encouraging removal of infected cells during the IE phase of an infection. Furthermore it is hypothesised that the transfer of a CD8+T-cell population transduced with the TCR obtained from a highly avid FRC-specific HLA-Cw*0702 CD8+T-cell clone will be selectively maintained by the patient's immune system. Thereby this may also enhance the duration of protection. This makes the UL28-derived FRC peptide an extremely promising HCMV target during a HCMV reactivation within HSCT transplant patients.

# CHAPTER 5 – RESULTS

## 5.1 - Sequencing the TCR of HLA-Cw*0702 specific CD8+T-cell clones

We aimed to test the efficacy of an immunotherapy for HCMV mediated disease in the HSCT transplant setting via the retroviral transduction of endogenous donor T-cells with a FRC-specific TCR sequenced from a specific CD8+T-cell clone. The first step towards this goal was to test the efficacy of the transduced TCR on PBMCs in *in vitro* functional assays.

To start, an FRC-specific clone with high avidity ($EC_{50}$ 250pg) and high cytotoxic potential was selected from our CD8+T-cell clone repertoire (Fig-48) termed FRC 1.9. Intracellular perforin and GranzymeB expression of this clone was 98.26% and 82.08% respectively as determined by flow cytometry (Fig-48). In addition we also selected one CRV- and one LSE-specific CD8+T-cell clone to analyse any similarities in chain usage between the HLA-Cw*0702 specific populations and to develop these as immunotherapies in future investigations (Table-9 both derived from donor YD13 of 52 years).

***Table 9 – VDJ gene usage of the α and β chains of HLA-Cw*0702 specific CD8+T-cell clones determined using the Clontech Smarter Race 5'/3' kit.*** The CDR3 gene region aa sequences are not provided due to ongoing work with these clones and the development of FRC 1.9 as an immunotherapy. The FRC clone was generated using PBMCs from donor YD6 of 49 years of age. The CRV and LSE clones were generated from donor YD13 of 52 years of age.

| Clone | | α chain | | β chain | | |
|---|---|---|---|---|---|---|
| Specificity | | V gene | J gene | V gene | J gene | D gene |
| 1.9 | FRC | TRAV30*01 | TRAJ43*01 | TRBV20-1*01 | TRBJ2-2*01 | TRBD2*01 |
| 3.26 | CRV | TRAV29 | TRAJ45*01 | TRBV4-3*01 | TRBJ2-1*01 | TRBD2*01 |
| 3.44 | LSE | TRAV29 | TRAJ433*01 | TRBV7-3*01 | TRBJ2-5*01 | TRBD2*01 |

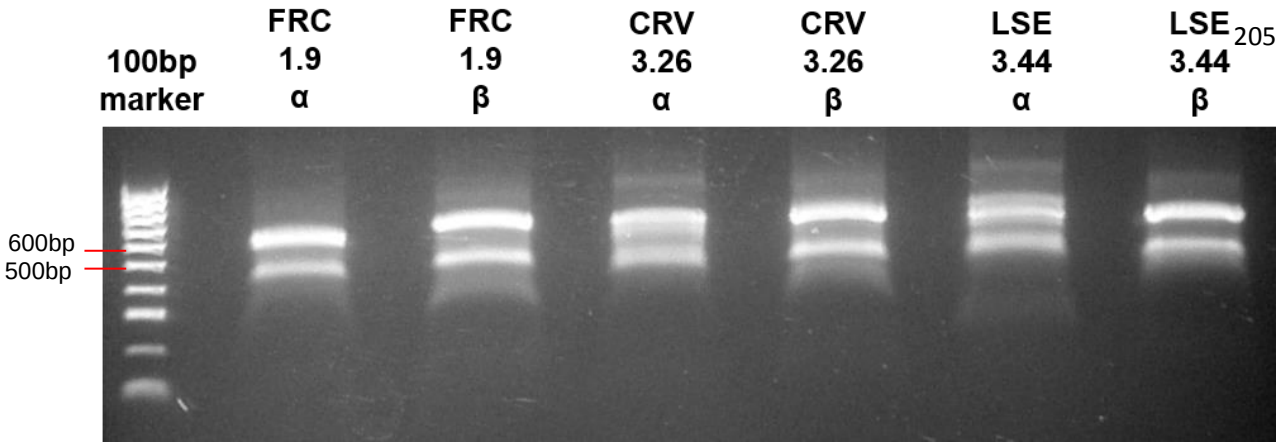


***Fig 47 – PCR α and β chains reactions separated by gel electrophoresis.*** The amplified cDNA product α and β reactions were run on a 1% agarose gel for 60 minutes at 120V. The FRC clone 1.9 α and β, CRV clone 3.26 α and β and LSE clone 3.44 α and β are provided from left to right. The two bands represent the same chain and sequence with the lower molecular weight representing a truncated version confirmed by sequencing, data not shown (University of Birmingham, DNA sequencing services)

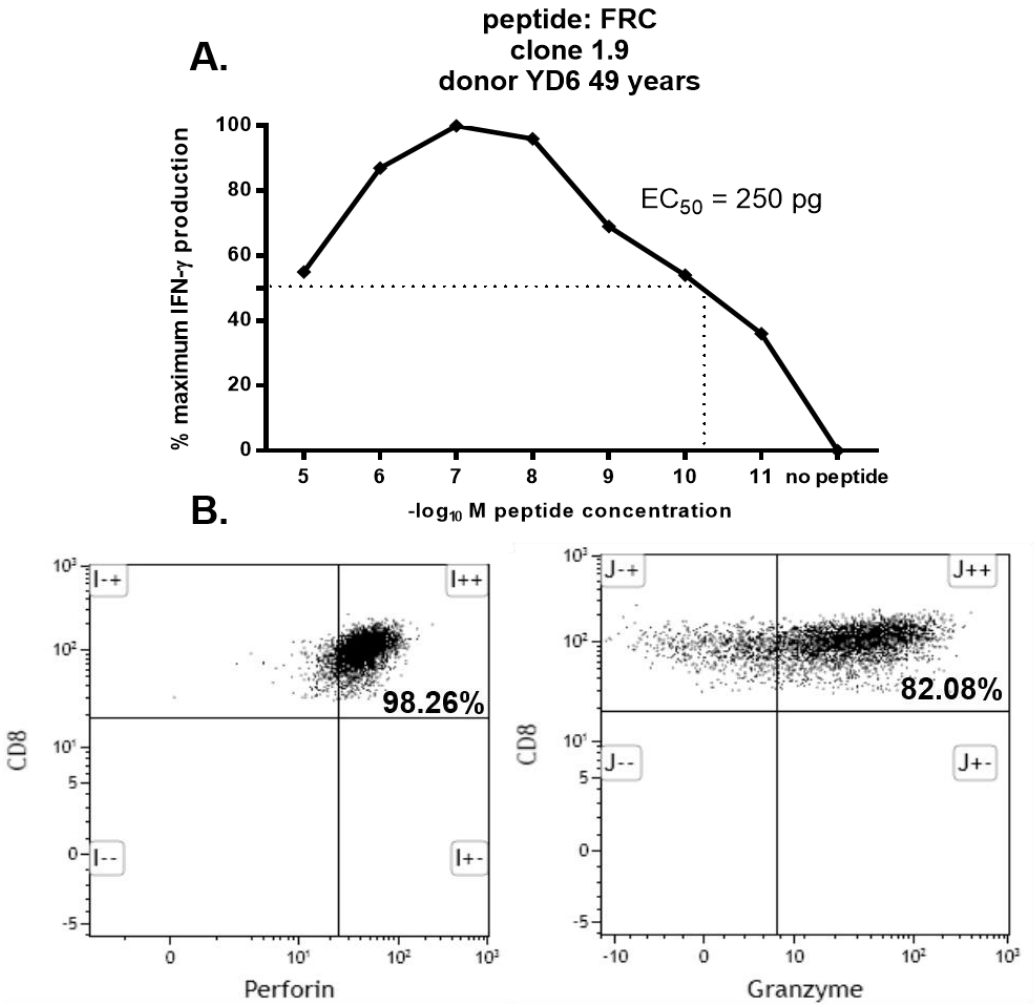


***Fig 48 – Avidity and cytotoxicity of FRC clone 1.9 from donor YD6.*** The characteristics of the FRC clone 1.9 selected for TCR sequencing and development of an immunotherapy for CMV disease. A) The $EC_{50}$ of the FRC 1.9 clone as determined after O/N co-culture with peptide-loaded LCLs (50 µg to 500 pg) followed by an IFN-γ ELISA. The $EC_{50}$ was determined as the concentration of peptide that indicated 50% maximal IFN-γ production. B) Intracellular perforin (left) and granzymeB (right) expression of the FRC 1.9 clone determined by flow cytometry with antibodies outlined in Table-4 after 6 hours FRC peptide stimulation.

Next the α and β chains of the TCR of the FRC 1.9 clone was elucidated using the Clontech Smarter Race 5'/3' kit. RNA was generated from a cell pellet of the CD8+T-cell clones, converted to cDNA, amplified by PCR and run by gel electrophoresis to visualise the separate α and β strands (Fig-47)(Materials and methods 2.2.17). This was to ensure that the PCR reaction correctly amplified the α and β strand cDNA products of 500-600 bp respectively. The DNA of the bands were extracted, cloned into pRACE plasmids and transformed into competent bacteria (Stellar competent cells, Clontech). Ampicillin resistant i.e. positively transformed colonies, were picked and subjected to mini preparations before a further plasmid DNA extraction and sequencing (Materials and methods 2.2.17)(University of Birmingham, DNA sequencing services).

When the PCR reactions were run by electrophoresis and visualised, two distinct bands were observed. DNA from both bands was excised and sequenced. The lower molecular weight band was found to be a truncated version of the α or β chain but otherwise the same sequence (data not shown).

The FRC clone 1.9 was determined to be utilising the Vα30 chain and the Vβ2 chain (Table-9). The sequencing of the β-chain was subsequently confirmed via flow cytometry staining of the FRC 1.9 clone with the Beckman coulter Vβ repertoire kit (Fig-49).

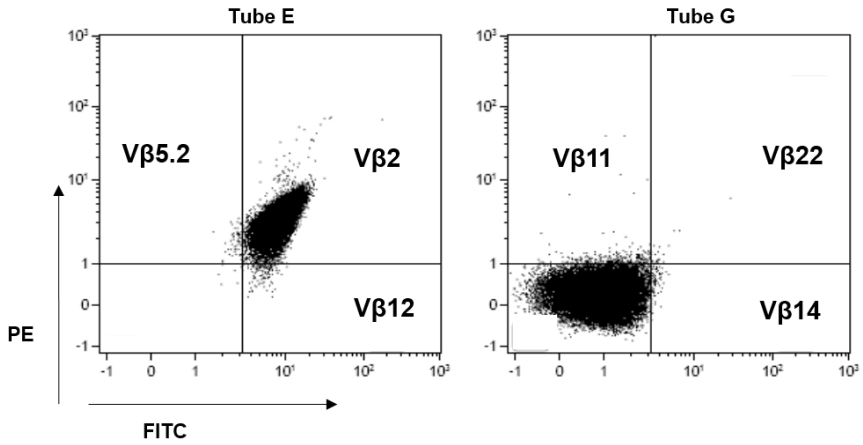


***Fig 49 – Confirmation of FRC 1.9 clone TCR Vβ2 sequencing by flow cytometry.*** A vial of liquid nitrogen cryopreserved FRC clone 1.9 was thawed and subjected to surface staining for CD3, CD8 and Vβ2. This was to validate the sequencing of the TCR using the SMARTer RACE kit (Table-2). Beckman Coulter, IOTest® Beta Mark TCR Vβ Repertoire Kit, events recorded on the LSR II (BD Biosciences) and analysed in Kaluza 1.3 software.

## 5.2 – Retroviral transduction of PBMCs with the FRC 1.9 CD8+T-cell clone TCR sequence

Once the sequence was ascertained, a gBlock DNA fragment was designed and purchased, and consisted of the codon optimised FRC clone 1.9 complete TCR sequence. This was then inserted into the pMP71 vector and transformed into competent TOP10 bacteria. Resistant colonies containing the FRC-pMP71 construct were subjected to endotoxin-free plasmid maxi preparations and the resulting plasmid used to transfect phoenix cells. The resulting retroviral supernatant was adhered to a retronectin coated plate, then α-CD137 and α-CD3 activated PBMC were added to the plate.

The transduced CD8+T-cells were incubated on the rectronectin plate for a minimum of 48 hours before being analysed by flow cytometry for expression of the transduced TCR on the cell surface (Fig-49).

As there is no HLA-Cw*0702 FRC MHC class I tetramer available to determine whether the transduction had worked, after 72 hours the transduced T-cells were subjected to staining with tube E of the IOTest® Beta Mark TCR Vβ Repertoire Kit which detected Vβ2 positive cells by dual PE/FITC staining.

After three attempts the highest transduction efficiency achieved was 4.75% (Fig-50). Unfortunately, the first transduction was lost due to contamination and in the subsequent transductions it was hard to determine if the transduction had indeed worked as the two separate buffy coats selected for transduction had a high percentage of Vβ2 positive CD8+T-cells making it hard to distinguish between the mock and transduced populations (Fig-50).

However, an interesting observation was the common usage of the Vα29 chain between the IE-1-derived CRV- and LSE-specific CD8+T-cell clones as these were generated from PBMCs of the same donor YD13 (Appendix Table-1).

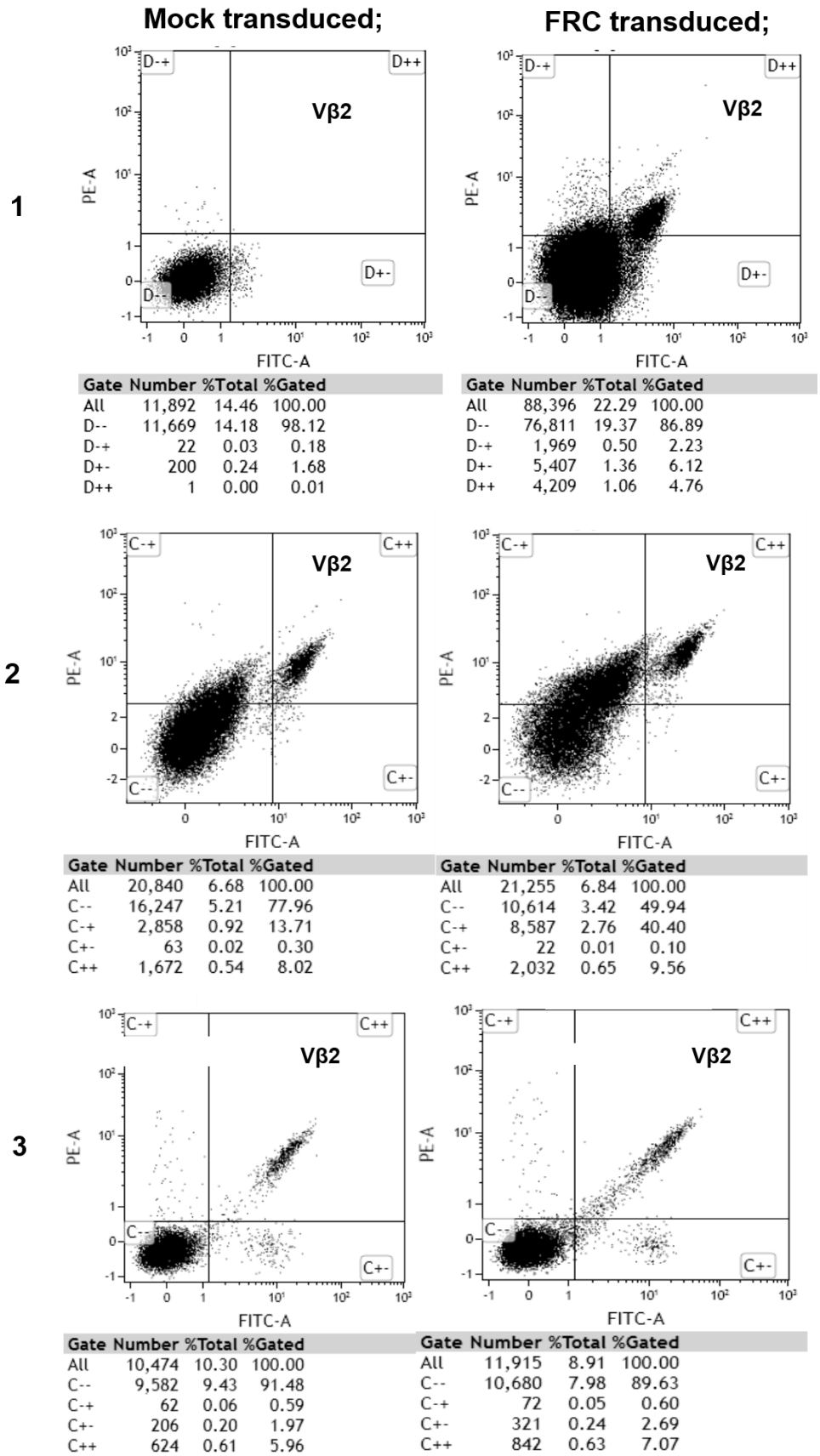


***Fig 50 – Retroviral transduction of PBMCs obtained from buffy coats with FRC-pMP71.*** Representative dot plots of the transduction efficiency of PBMCs with mock (DMEM media only, left column) or supernatant containing retrovirus expressing the FRC-pMP71 TCR construct (right column) indicated by Vβ2 staining (Tube E, IOTest® Beta Mark TCR Vβ Repertoire Kit). Vβ2 staining was determined as dual FITC and PE staining. The round of transduction is indicated to the left of the plots.

Therefore, DNA was extracted from PBMCs of the third transduction and analysed for the presence of the FRC-pMP71 construct expression by PCR. Primers were designed that bind specifically to the FRC gBlock transgene outlined in materials and methods Fig-6. As a positive control, the FRC gBlock fragment was spiked into the DNA isolated from the transduced T-cells. A band of the correct size was present in the positive DNA-spiked control but was clearly absent in the transduced cells (Fig-51). This suggests that the T cells were not successfully transduced with the transgene, or the transduction efficiency was very low.

Due to time constraints the transduction could not be repeated and the assessment of whether the FRC TCR transduced T-cells would be as efficacious as the *ex vivo* CD8+T-cell populations in removing CMV infected cells could not be assessed.

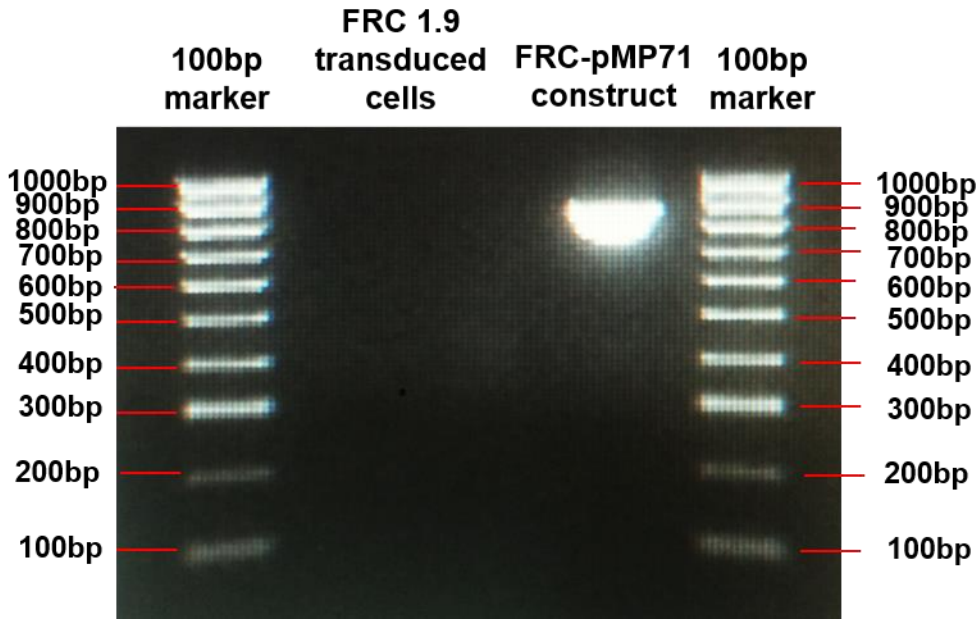


***Fig 51 – Analysis of the FRC-pMP71 transduced CD8+T-cells for the positive expression of the FRC 1.9 TCR.*** DNA was extracted from a DNA pellet of PBMCs from a buffy coat that were transduced with the retroviral supernatant expressing the FRC-pMP71 TCR construct. The DNA was then analysed for the presence of the FRC 1.9 TCR sequence via a PCR reaction with the Q5 polymerase (New England Biolabs) and the thermocycling conditions provided with the enzyme (left sample lane). The FRC gBlock fragment was spiked into the DNA obtained from the transduced T-cells as a positive control and ran under the same conditions (right sample lane).

# CHAPTER 5 – SUMMARY

The sequences of three HLA-Cw*0702-restricted CD8+T-cell clones were determined. A highly avid and cytotoxic FRC clone (1.9) was selected for further development as an immunotherapy that was generated *in vitro* from YD6 of 49 years.

The FRC clone 1.9 with an $EC_{50}$ of 250pg and perforin and granzymeB expression of 98.26% and 82.08% respectively was sequenced, and revealed to be utilising Vα30 and Vβ2 chains.

The CRV and LSE IE-1-specific CD8+T-cell TCR shared a common Vα29 chain usage.

Unfortunately the retroviral transduction of PBMCs obtained from a buffy coat preparation was suboptimal and therefore research on the testing of the functionality of FRC-pMP71 transduced CD8+T-cells *in vitro* was halted at this stage due to time constraints.

# CHAPTER 5 - DISCUSSION

Current anti-viral treatment of HCMV disease in the post-transplant setting that while effective is associated with high toxicity, expense and have been described as delaying the onset of CMV disease [297-299]. Thus improved treatment regimens are needed, in particular to treat HCMV disease in the post allogenic HSCT setting. The CD8+T-cell response dedicated to controlling CMV is known to be the critical component in protection from CMV-mediated disease [64]. As such, focus is dedicated on reconstituting the CMV-specific CD8+T-cell memory pool within immunocompromised transplant patients. The murine model of CMV adoptive therapy has proven invaluable for demonstrating both the efficacy and safety of this approach so that human clinical trials could be undertaken [8, 186, 188]. Phase I/II human clinical trials have since demonstrated the safety and efficacy of adoptively transferred donor CMV-specific CD8+T-cells to regenerate cellular immunity within human patients [64, 189, 190, 192, 194]**.** However, this approach can only be effective in the setting where the patient undergoing CMV reactivation was previously CMV positive and will therefore have a pre-established CD8+T-cell immunity that can be isolated. Recent focus has been on the transfer of the sequence of TCR from a previously characterised CMV CD8+T-cell population onto patient's endogenous CD8+T-cells. This allows for the transfer of CMV immunity into previously CMV negative patients.

**Advantages of a UL28-derived FRC-specific adoptive immunotherapy**

The protein of the CMV genome to target during viral reactivation or a primary CMV infection after a stem cell transplant is likely imperative for the efficacy of the treatment. The pp65 and IE-1 proteins have been the focus of antigens to direct the CD8+T-cell response towards. This is based upon the immunodominant CD8+T-cell responses identified to these antigens as a result of them being the most abundant tegument protein and first viral protein to be expressed during a viral life cycle respectively. However studies are contradictory on

whether pp65 or IE-1-specific cells are more efficacious when included within a treatment regimen. The immune evasion strategies encoded by HCMV theoretically make IE-expressed targets a more promising choice of CD8+T-cell target. The US2-11 gene region products are expressed in a temporal fashion from IE-L time-points of an infection [80, 81]. This makes it less likely that L-expressed HCMV antigens will be presented on the cell surface during CMV reactivation in disease once the full effects of the immunevasins are in place. Therefore the IE-1 antigen a represents a better target for therapy over the pp65 antigen, as by the time pp65 is expressed, there are reduced levels of HLA-A/-B alleles or the viral reactivation event has been controlled.

The presence of IE-1-specific CD8+T-cells within heart or lung patients was shown to correlate with protection from HCMV mediated disease [300]**.** The authors hypothesised that as a result of the IE-1 being the first protein expressed during the viral lifecycle, reactivation events are prevented from proceeding past the IE phase of the lifecycle. Therefore pp65-specific CD8+T-cells would be ineffective in recognising their L-expressed cognate peptide in this situation. Conversely, a research group has identified within allogenic stem cell transplant patients the greater production of the pro inflammatory cytokines IFN-γ and TNF-α by pp65-specific CD8+T-cell populations translating to a higher anti-viral function of these cells over IE-1-specific CD8+T-cell populations [301].

This research has identified immunodominant CD8+T-cell responses to a HLA-Cw*0702-restricted peptide ‘FRC’ derived from the UL28 protein that is generated with IE kinetics during the viral life cycle. To this end, this research focused on developing a TCR based therapy utilising the TCR sequence of a UL28-derived ‘FRC-specific CD8+T-cell clone. This was achieved via the amplification and sequencing of α and β chain cDNA generated from HLA-Cw*0702-specific CD8+ T-cell clones (SMARTer RACE 5'/3' Kit, Clontech). An alternative to this cDNA amplification method approach is next generation sequencing. This would have provided an unbiased TCR analysis of the total HLA-Cw*0702 epitope-specific CD8+T-cell populations. However in order to obtain a pure epitope-specific CD8+T-cell

population from PBMCs for such an experiment, an MHC-I tetramer would have been required which unfortunately we were unable to obtain. Thus we argue that the cDNA amplification method, in addition to the availability of highly avid CD8+T-cell clones specific to the inflationary HLA-C peptides generated *in vitro* within this work, was sufficient for the TCR sequencing purpose required for this research chapter. However for future research, if a HLA-Cw*0702 MHC-I tetramer was to be obtained next generation sequencing would be a valuable tool to analyse the total oligoclonality of these inflated HLA-Cw*0702 CD8+T-cell populations.

The properties of the UL28 protein from which the inflationary FRC peptide is derived from may provide several therapeutic benefits. Firstly, the UL28 protein is expressed with IE kinetics. This research investigation has hypothesised that the FRC peptide is presented frequently on infected cell surfaces at IE time-points due to the MHC-I targeting specificity of the US2-11 proteins and upregulation of HLA-C alleles during infection. Secondly, a mechanism whereby p53 expression in an infected host cell helps to enhance replication to generate large concentrations of mature virions during an infection life cycle has been proposed [302]. Importantly, the UL28 protein is implicated in stabilising p53 expression [303]**.** As UL28 has been described as a potential latency transcript this identifies a potential role of p53 regulation and hence enhanced viral production during latency. By targeting the UL28 protein, we may remove the advantageous effects of p53 on HCMV replication during a reactivation event in addition to transferring a highly avid TCR specificity.

However, a study has implicated that it is the intrinsic functional and phenotypic abilities of CMV-specific CD8+T-cell responses specific for a particular epitope within a HCMV protein important for protection from disease. For example, pp65 HLA-A2-restricted NLV peptide-specific CD8+T-cells provided higher protection from CMV disease compared to HLA-A4 QYD peptide-specific [304]. This provides premise for selecting epitope-specific CD8+T-cell responses for immunotherapy based upon superior anti-viral protection in addition to the HCMV target antigen.

Therapy consisting of CD8+T-cell clones or TCR specific to more than one HCMV antigen could possibly represent one method to enhance therapeutic benefits of adoptive immunotherapy. Impacting on the rationale behind a multi antigen specific immunotherapy, is a study by Holtappels et al. [305]. The authors identified that protection from CMV disease can be provided by subdominant CD8+T-cell specificities and that immunodominance of the transferred CD8+T-cell population is not a prerequisite for disease protection [188, 305, 306]. Holtppels et al. also observed that a combination of two cytotoxic cell line (CTLL) specificities did not enhance protection over a single specificity when transferred into CMV infected mice. Instead they determined that efficacy was dependent on the absolute number of functional CD8+T-cell transferred. Holtappels et al. did however state that the combination of two specificities did not decrease the overall anti-viral function. The inclusion of the HLA-Cw*0702-restricted FRC-specific TCR therapy should target infected cells in the IE stage of infection and potentially the L stages of an infection if the UL28 protein is confirmed as a latency transcript. It is hoped that in combination with HLA-A-restricted pp65-specificities this HLA-Cw*0702-specificity would enhance the detection of virally infected cells at IE vs L stages of the life cycle and reactivation. Therefore we are hopeful that the combination of UL28, pp65 and IE-1-specificities within a therapy regimen will translate to an enhanced detection of virally infected cells *in vivo* at all stages of a chronic infection.

The ultimate aim of adoptive T cell therapy is the transfer of T-cells that persist long term, proliferate after antigenic rechallenge and localise to sites of viral reactivation. A study by Scheinberg et al. has demonstrated that the successful reconstitution of HCMV-specific CD8+T-cells in the post HSCT setting depends upon the maintenance of CD8+T-cells with a less differentiated $T_{CM}$ phenotype rather than $T_{EMRA}$ populations [307]. Additionally they provided a correlation between $T_{CM}$ in the donor and protection of CMV reactivation. These findings were also recently corroborated by Mackay et al [308]. The majority of HCMV CD8+T-cells within the periphery are of the late differentiated $T_{EMRA}$ phenotype as were the

HLA-Cw*0702 FRC-specific CD8+T-cell populations. This research investigation did however identify a small proportion of earlier differentiated CD8+T-cells displaying a $T_{CM}$ phenotype ($CCR7^{+}CD45RA^{-}$) within the inflated RFC-specific HLA-Cw*0702 CD8+T-cell populations. Therefore, to utilise the HLA-Cw*0702 populations characterised in this work as an immunotherapy, we would wish to isolate these $T_{CM}$ cells for adoptive transfer. Alternatively $T_{CM}$ CD8+T-cells isolated from patients or HSCT donors would be transduced with the FRC-specific TCR characterised in this work for adoptive transfer. This will hopefully reconstitute HCMV-specific CD8+T-cells capable of long lived proliferation and expansion after antigenic rechallenge and homing to sites of viral reactivation.

**Future research**

To proceed with developing the HLA-Cw*0702 CD8+T-cell population as an immunotherapy the TCR transduction protocol should be optimised. Lastly, the resulting transduced cells should be tested *in vitro* for similar efficacy as *ex vivo* FRC-specific CD8+T-cell populations and CD8+T-cell clones in removing virally infected cells.

To summarise, the extremely promising phenotypic and characterisation results of FRC-specific *ex vivo* CD8+T-cell populations implies that FRC-specific TCR immunotherapy will be efficacious for inclusion within current adoptive regimens. The HLA-Cw*0702 allele is highly prevalent within the Caucasian population representing ~35% of individuals positive for this allele (http://www.allelefrequencies.net/default.asp). Thus expanding the current scope of patients eligible for treatment who are HLA-Cw*0702 positive. Furthermore we anticipate that the overall benefits of treatment of disease will be advanced via increasing the current HCMV targets to 3 protein antigens; pp65, IE-1 and UL28, each with differing roles and peak expression time-points during the viral life cycle. We hypothesise that the immunodominance and superior anti-viral effector functions *in vitro* will translate to an enhanced disease protection in the immunotherapy scenario. Lastly, as UL28 is postulated to be one of the few identified CMV latency transcripts, we hope that the benefits of this immunotherapy will translate through to latency and increase the long term efficacy**.**

# CHAPTER 6

# CHARACTERISATION OF CD8+T-CELLS TO ALTERNATIVE FRAME DERIVED ‘CRYPTIC’ HCMV CD8+T-CELL EPITOPES

# CHAPTER 6 - INTRODUCTION

Cryptic epitopes represent unique CD8+T-cell targets that are translated from alternative reading frames (ARFs) in both sense and antisense transcripts [309]. Their generation and immunogenicity *in vivo* has been identified within viral infections [310-317] autoimmune diseases [318] and several malignancies including melanoma [319, 320] and colorectal [321].

Cryptic epitope generation during viral infections has been most extensively studied for HIV [322], murine HIV [312, 315] and SIV infection [316]. Through these studies it was identified that CD8+T-cell populations specific for these unconventionally generated peptides are a frequent and dominant component of the anti-SIV response [317]. Additionally that they are important for protection of mice from retroviral disease [311, 323].

Frameshift mutations resulting in translation of a +1 shifted in frame protein has been demonstrated for a DNA virus – Herpes simplex virus (HSV) [310]. The resulting 'cryptic' protein was found to induce resistance of the HSV virus to acyclovir treatment [314].

Clearly, the CD8+T-cell response to viral pathogens is much more complex than previously understood and not restricted to in frame transcripts.

The use of the RV798 mutant strain (ΔUS2-11) of HCMV to infect APCs *in vitro* allowed the surface presentation of potentially all antigenic epitopes of the virus and led to the identification of previously uncharacterised peptide-epitopes [82, 85](Stanley Riddell. And Colleagues). These epitopes were derived from all phases of the lifecycle and are generated as in frame peptides.

The same work also led to the identification of peptide-epitopes that are not derived from in frame translation of the HCMV protein. Stanley Riddell and colleagues generated CD8+T-cell clones of an unknown specificity responding to RV798 infected fibroblasts. To identify the cognate CMV antigen, viruses KO for individual proteins were employed and loss of CD8+T-cell recognition used as indication that the deleted gene contained the clone

specificity. It was subsequently determined via the deletion of the US22 or US34 proteins that a fraction of the CD8+T-cell clones were specific for peptides derived from these antigens. However, upon transfection of the gene fragments into COS7 cells the peptide-epitope could not be identified. Subsequently, the entire nucleotide sequences of the US22 or US34 proteins was shifted by +1 (+1 ORF) and then +2 (+2 ORF) aa's from the conventional initial methionine translation start site. Upon transfection of gene fragments derived from the +2 ORF nucleotide sequences into COS7 cells, CD8+T-cell recognition was regained. The aa sequence of the epitopes giving rise to the CD8+T-cell recognition were determined and these novel epitopes were therefore termed 'cryptic' epitopes (Table-10).

It is currently unknown how frequently these would be presented to the immune response *in vivo* when the US2-11 gene region immunevasins may interfere with their reaching the cell surface or other unidentified mechanisms are preventing their alternative method of generation during the lifetime of the host.

# CHAPTER 6 - RESULTS

## 6.1 - *Ex vivo* CD8+T-cell responses to HCMV cryptic peptide-epitopes are readily detectable in healthy HCMV seropositive donors

This results chapter aimed to characterise the *ex vivo* CD8+T-cell responses to the two cryptic epitopes identified and kindly provided by Dr Stanley Riddell et al. with regards to kinetics, magnitude and phenotype (Table-10).

***Table 10 – 'Cryptic' HCMV epitopes used in this investigation.*** CD8+T-cell epitopes identified by Stanley Riddell et al that are translated in a +2 ORF. The protein antigen, amino acid position within the protein antigen, peptide sequence (peptide name is denoted by the first three amino acids of the sequence), restricting HLA allele, kinetics of expression and function of the protein antigen (if known) that the cryptic peptides are derived from are provided

| CMV Antigen | Location in the Virion [224] [324] | Function [224] | CTL Epitope | HLA Restricting Allele | Kinetics of Expression [225] |
|---|---|---|---|---|---|
| $US22_{612-620}$ | Tegument | ICP22 gene product E protein released by cells – role unknown [325] | **RPWPRRPAK*** | B701 | E |
| $US34_{76-105}$ | unknown | Unknown but dispensible for growth [224] | **APDSFIVSF*** | B3501 | n/a |

A total of 12 young and 17 older donors, classed as <70 vs >70 years of age, were screened for *ex vivo* CD8+T-cell responses by ICS to the cryptic peptides as previously outlined in materials and methods and gating strategy provided in Chapter 3, Fig-7 (Raw ICS provided in appendix Table 7-8). A BMedSci student, Miss Emily Briggs undertook her research project completing the first half of this chapter under the direct supervision of Miss Louise Hosie. The recognition of work completed by Miss Emily Briggs is indicated in figure legends. As previously, the background cytokine production detected in the unstimulated control were subtracted from the peptide sample tubes. This background ranged from 0.01-0.15%.

US22 **A.**

HLA-B7

RPW;

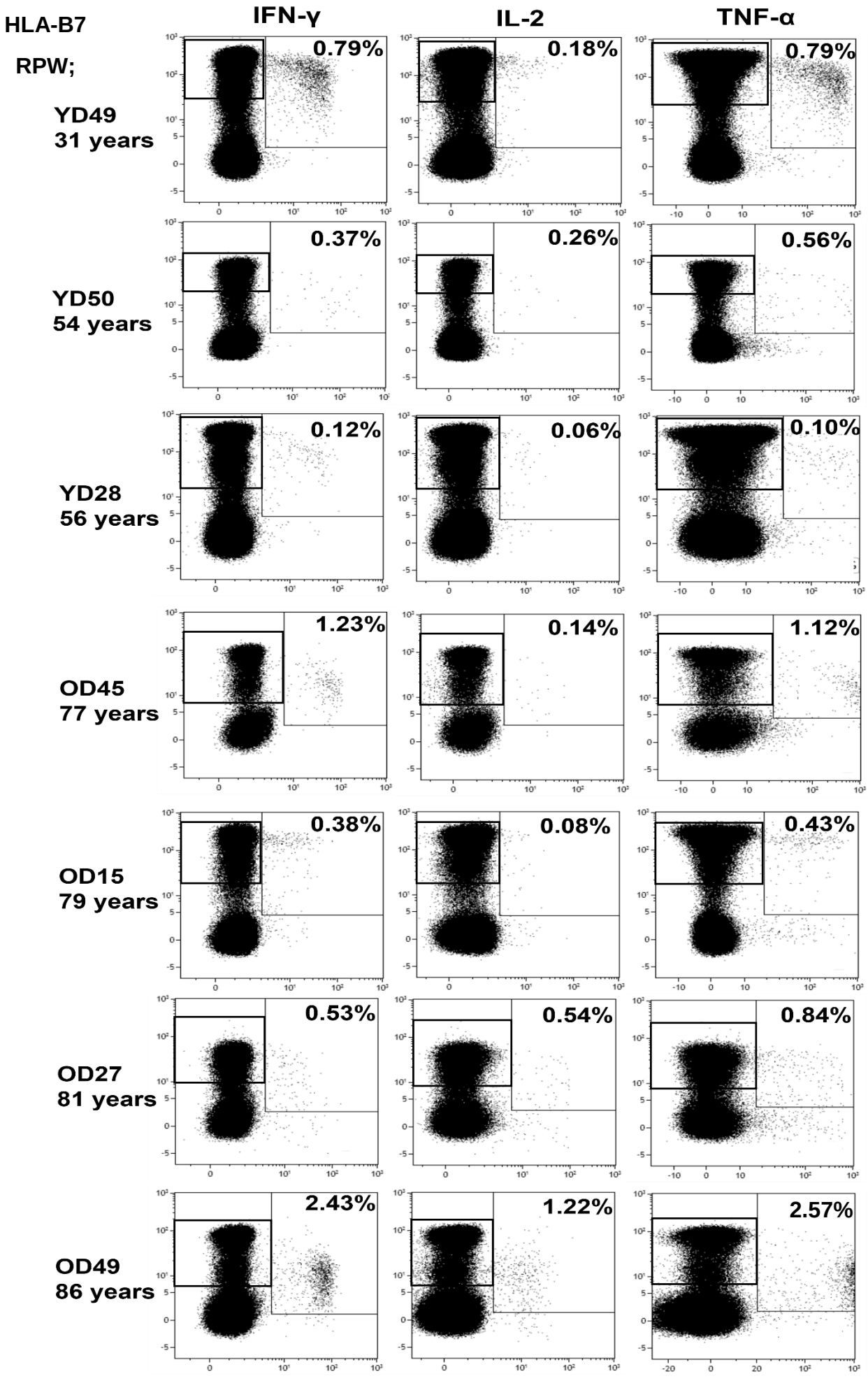

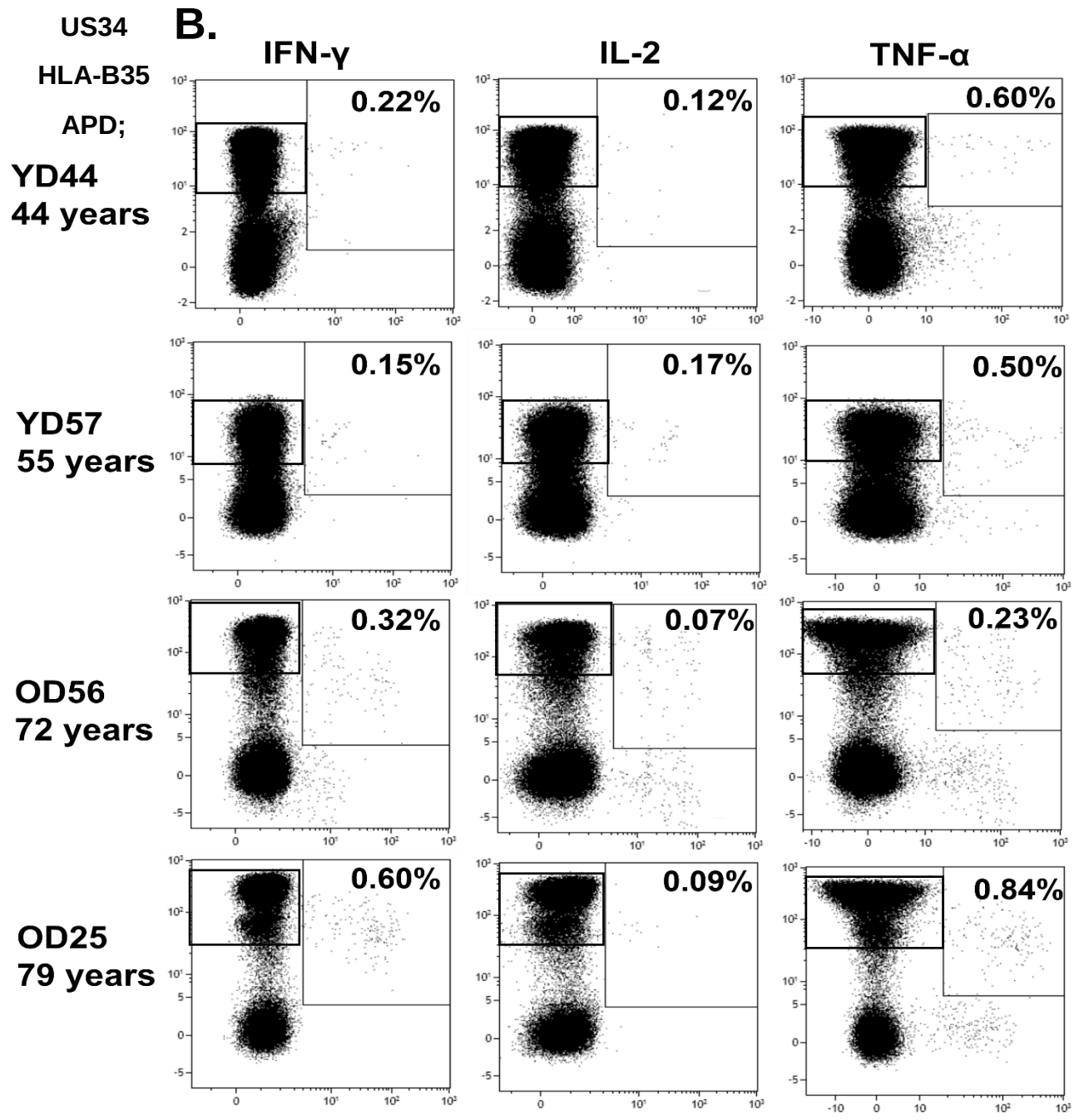


***Fig 52 – Representative dot plots of the ex vivo CD8+T-cell responses specific for the HCMV cryptic epitopes*** HCMV seropositive donors were screened for *ex vivo* CD8+T-cell responses to cryptic HCMV CD8+T-cell peptides restricted through HLA-B7 and HLA-B35 (Table-10). PBMCs of donors with HLA-B7- or HLA-B35-restriction were stimulated with RPW and APD cryptic peptide-epitopes for 6 hours followed by intracellular cytokine staining for IFN-γ (left), IL-2 (middle) and TNF-α (right) production to identify activated CD8+T-cells. As a positive control CD8+Tcells were stimulated with SEB to ensure the cytokine detection was working correctly. As a negative control CD8+T-cells were left unstimulated. The age of the donors is provided to the left of the plot. The gating strategy for identifying activating CD8+T-cells is provided in Chapter 3, Fig-7. The percentages represent the percentage of activated CD8+T-cells producing cytokine of the total CD8+T-cell response. RPW n = 22 and APD n = 12. Miss Emily Briggs n = 25 Miss Louise Hosie n = 4. In all cases, the percentages shown have had the unstimulated control percentages subtracted.

In total 32% (7/22) of donors responded to the HLA-B7-restricted US22-derived RPW peptide (Fig-52). The CD8+T-cell responses ranged from 0.37-2.43%, 0.06-1.22% and 0.43-2.57% producing IFN-γ, IL-2 and TNF-α (ICS results provided in Appendix Table-7-8)(Fig-53A/B). The average CD8+T-cell response size identified within the 7 seropositive donors was 0.84% IFN-γ, 0.35% IL-2 and 0.91% TNF-α (Fig-53B). The average RPW-specific CD8+T-cell responses producing IFN-γ, IL-2 and TNF-α increased non-significantly between donors <70 vs >70 years of age (Fig-53C)

A total of 33% (4/12) donors responded to the HLA-B35-restricted US34-derived APD peptide (Fig-52). The CD8+T-cell responses ranged from 0.15-0.60%, 0.07-0.17% and 0.23-0.67% producing TNF-α (Fig-53A/B). The average CD8+T-cell response size in the 4 donors was 0.32% IFN-γ, 0.11% IL-2 and 0.50% TNF-α (Fig-53B). Statistics could not be conducted on the APD-specific responses with age due to n =2 in both the <70 and >70 year donor cohorts, however, the IFN-γ production increased between donors aged <70 vs >70 years of age from 0.19%-0.44% (Fig-53C).

Overall the size of the *ex vivo* CD8+T-cell responses directed towards the cryptic epitopes were lower than those that have been observed towards conventional immunodominant epitopes derived from the pp65 and IE-1 immunodominant proteins (Appendix Table-1-6). The CD8+T-cell responses were however of a similar magnitude to those identified to the protected epitopes RTD and YAD (Appendix tables 1-6, Results chapter 3).

When the *ex vivo* cryptic-specific CD8+T-cell responses were correlated with the age of our donor cohort, the RPW-specific responses demonstrated a trend towards memory-inflation with age but however did not reach significance (Fig-53D). The increase in IFN-γ production with age elicited by the APD peptide almost reached significance ($p = 0.08$, Fig-53D).

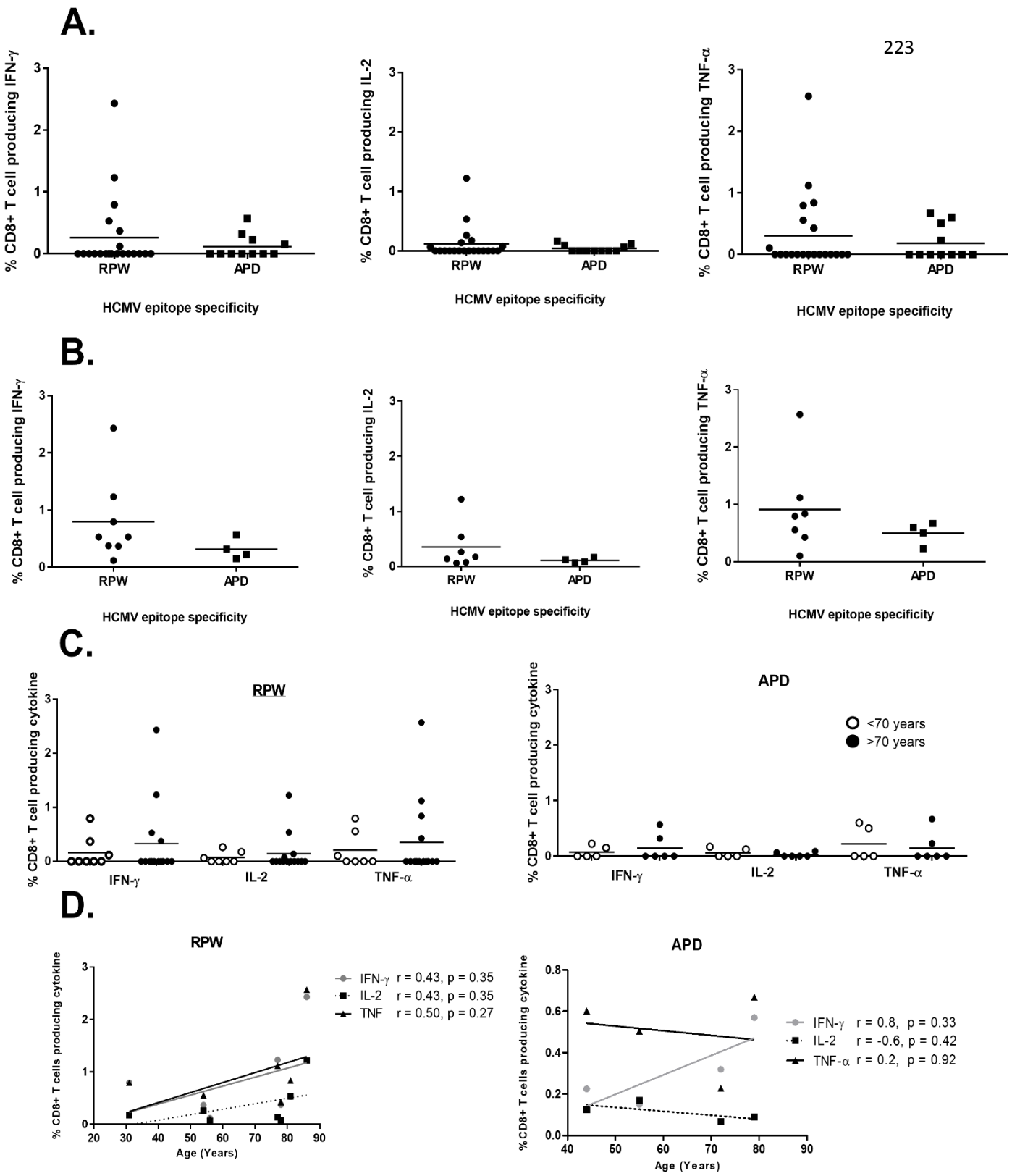


***Fig 53 – Summary of the ex vivo CD8+T-cell responses elicited by the cryptic HCMV peptide-epitopes.*** HCMV seropositive donors were screened for *ex vivo* CD8+T-cell responses to cryptic HCMV CD8+T-cell peptides restricted through HLA-B7 and HLA-B35. PBMCs of donors with HLA-B7 or HLA-B35 restriction were stimulated with RPW and APD cryptic peptide-epitopes for 6 hours followed by intracellular cytokine staining for TNF-α production to identify activated CD8+T-cells A) Summary of the negative and positive CD8+T-cell responses detected against the RPW and APD peptides (Table-10). B) Summary of the positive CD8+T-cell responses detected against the RPW and APD cryptic peptides. C) Summary of the RPW- (left graph) and APD- (right graph) specific *ex vivo* CD8+T-cell responses between donors <70 years (white circle) vs >70 years (black circles). In A/B/C lines represent SEM. D) Correlation of the RPW- (left graph) and APD- (right graph) specific CD8+T-cell IFN-γ, IL-2 and TNF-α production with the age of the donor cohort (years). Lines represent linear regression and p-values determined by Spearman's rank correlation within Graphpad Prism6. Miss Emily Briggs conducted n = 25 and Miss Louise Hosie n = 4. Graphs were constructed by Miss Louise Hosie.

## 6.2 - CD8+T-cells specific for the cryptic epitopes display a polyfunctional cytokine profile with RPW-specific CD8+T-cells demonstrating an enhanced cytotoxic potential with age

It was hypothesised that the CD8+T-cell responses to these cryptic CD8+T-cell epitopes may be generated less frequently during the host lifetime due to their unconventional method of translation. It was as such further hypothesised the specific *ex vivo* CD8+T-cell populations would show a phenotypically earlier differentiation state with higher CD28 expression and greater magnitudes of IL-2 production [326, 327].

### 6.2.1 – Cytokine polyfunctionality profile

First, the cytokine polyfunctionality i.e. the percentage of the CD8+T-cells within the cryptic epitope-specific populations capable of producing IFN-γ, IL-2 and TNF-α cytokines was determined. This was compared to the *ex vivo* cytokine profile of NLV-specific CD8+T-cells whom are described of belonging to an end stage T cell differentiation pathway ($T_{EMRA}$) producing little IL-2 associated with the loss of the CD28 co-receptor [326, 327].

The cryptic CD8+T-cell responses were comprised of a larger percentage of CD8+T-cells capable of producing all three cytokines investigated – IFN-$\gamma^+$, IL-$2^+$ and TNF-$\alpha^+$ - compared to the NLV-specific CD8+T-cell populations (RPW 13%, APD, 17% and NLV 4% $p = 0.079$) (Fig-54). Both cryptic epitopes elicited CD8+T-cell responses comprising a higher percentage of CD8+T-cells that were more singular TNF-$\alpha^+$ producing ($p = 0.058$) and less dual IFN-$\gamma^+$TNF-$\alpha^+$ producing than the NLV-specific CD8+T-cells (RPW 17%, APD 19% and NLV <1%, $p = 0.09$)(Fig-54).

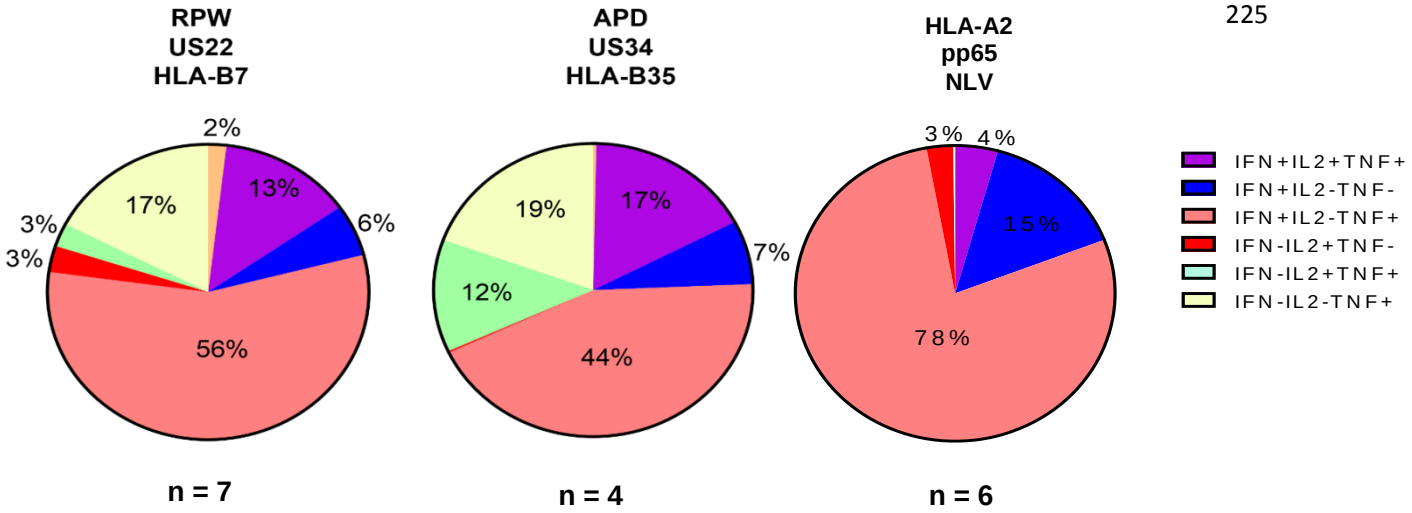


***Fig 54 – Cytokine polyfunctionality of the ex vivo cryptic-specific CD8+T-cell responses.*** The cytokine polyfunctionality profile of the cryptic-specific CD8+T-cell responses was determined after 6 hours peptide stimulation and intracellular cytokine staining for IFN-γ, IL-2 and TNF-α. This was followed by Boolean analysis in Kaluza 1.3 software and analysis of the output in Funky cell software [269]. Gating strategy provided in Fig-26 chapter 4. Miss Louise Hosie conducted the Boolean analysis of the raw ICS data conducted in major by Miss Emily Briggs. The ICS results for the NLV peptide was conducted by Miss Louise Hosie. Graphs were generated in Graphpad Prism 6. Statistical significance was investigated by Kruskall-Wallis test of the individual cytokine combinations between the HCMV-specific CD8+T-cell populations. The n numbers for each epitope-specific CD8+T-cell population are provided beneath the respective pie charts. The cytokine combinations are provided in the figure legend.

## 6.2.2 – Single marker phenotype

The single marker phenotype of the individual cryptic CD8+T-cell responses did not differ significantly from the phenotype of NLV-specific (Fig-55). The CD38 expression was decreased on the individual RPW and APD-specific CD8+T-cell responses in comparison to NLV-specific CD8+T-cells. When the cryptic CD8+T-cell responses were pooled, the CD38 expression was significantly reduced when assessed against the NLV-specific CD8+T-cell populations (Fig-55).

Compared to the NLV-specific CD8+T-cells there was a trend for decreased CD45RA and increased CD28 and CD45RO expression on the cryptic-specific CD8+T-cells (Fig-55).The RPW- and APD-specific CD8+T-cell responses exhibited intracellular stores of perforin and granzymeB at similar magnitudes to the NLV-specific (average perforin expression; 65.79%, 80.57% and 64.00% respectively, average granzymeB expression; 76.85%, 74.16%, 90.87% respectively, Fig-55).

.

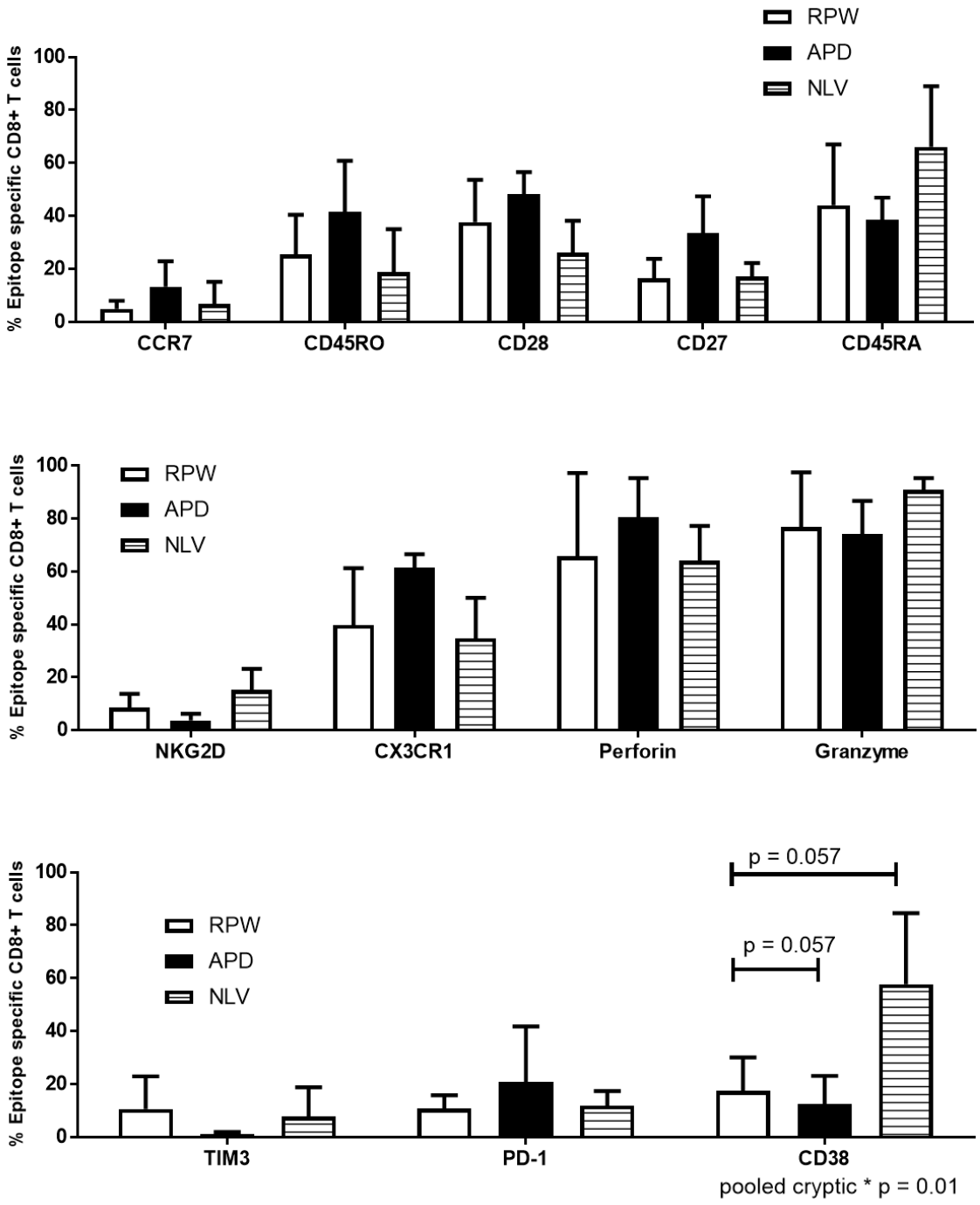


***Fig 55 –The phenotype of ex vivo CD8+T-cell responses specific for the cryptic CD8+T-cell responses determined by flow cytometry.*** The *ex vivo* CD8+T-cell phenotype of CD8+T-cells specific for the HLA-B7 'RPW' and HLA-B35-restricted 'APD' peptides was investigated. PBMCs of donors with HLA-B7- or HLA-B35-restriction were stimulated with RPW and APD cryptic peptide-epitopes for 6 hours followed by staining with the antibody panels outlined in Table-4. Intracellular cytokine staining was then conducted for TNF-α production to identify activated CD8+T-cells. Single, live, CD3+CD8+ lymphocytes were gated upon in Kaluza 1.3 software followed by CD8+TNF-α+ cells to identify the epitope-specific CD8+T-cells before phenotypic analysis. White bars represent APD-specific, black bars RPW-specific and lined bars NLV-specific CD8+T-cells. Bars represent mean and error bars SEM. Statistical significance was determined using multiple comparison Mann Whitney tests in Graphpad Prism 6 with * as a p-value < 0.05. RPW n = 4, APD n = 3 and NLV n = 4.

6.2.3 – Memory compartment phenotype

The memory CD8+T-cell phenotype of the *ex vivo* responses was next analysed by CCR7 vs CD45RA expression (Fig-56A). Both RPW- and APD-specific CD8+T-cell populations were comprised of a larger percentage of effector $T_{EM}$ cells (46.99% and 65.34% respectively) and a significantly smaller percentage of $T_{EMRA}$ cells (28.34% and 23.10% respectively) compared to the total NLV-specific CD8+T-cell population (Fig-56A).

6.2.4 – Antigen differentiation status

Last in this section, the antigen differentiation status of CD8+T-cells specific for the cryptic epitopes was analysed using CD27 vs CD28 expression to discriminate between early, intermediate or late differentiated populations [70] (Fig-56B). There were no significant differences between the RPW-, APD- and NLV-specific CD8+T-cell populations. The RPW-specific CD8+T-cell populations presented with a similar profile to the NLV-specific populations dominated by late differentiated CD8+T-cells (65.11% and 63.26% respectively) (Fig-56B). The APD-specific CD8+T-cells presented with a distribution of the total epitope-specific CD8+T-cells between early ($CD27^+CD28^+$), intermediate ($CD27^+CD28^-$/$CD27^-CD28^+$) and late differentiated T-cells (34.89% 3.02%/30.00% and 32.10% respectively) Fig-56B).

To summarise the cryptic-specific CD8+T-cell populations had a less activated *ex vivo* CD8+T-cell phenotype compared to NLV-specific CD8+T-cells. This was determined by a lower CD38 expression. Secondly, the cryptic-specific CD8+T-cell responses were comprised of a larger percentage of CD8+T-cells able to produce IL-2 compared to the pp65-specific CD8+T-cell populations. However the RPW- and APD-specific CD8+T-cells displayed similar levels of cytotoxic potential to the NLV-specific CD8+T-cells indicated by intracellular stores of perforin and granzymeB.

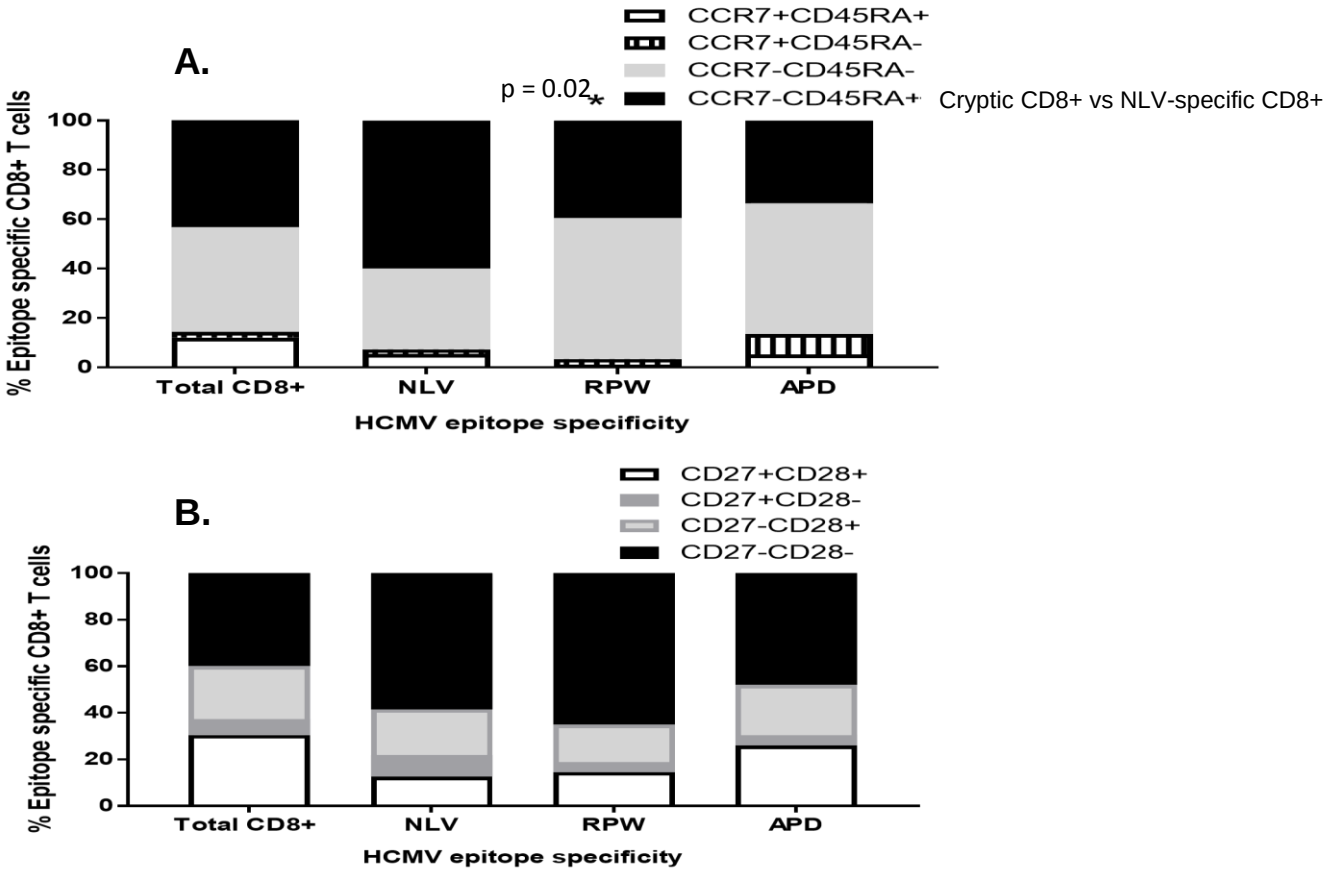


***Fig 56 – CCR7 vs CD45RA memory phenotype of the ex vivo CD8+T-cell phenotype of the specific cryptic epitope responses.*** PBMCs of donors with HLA-B7 or HLA-B35 restriction were stimulated with RPW and APD cryptic peptide-epitopes for 6 hours followed by intracellular cytokine staining for TNF-α production to identify activated CD8+T-cells. The cells were subjected to staining with the antibody panels outlined in Table-4. RPW and APD phenotyping - Miss Emily Briggs n = 7 and Miss Louise Hosie n = 1. The phenotyping of NLV-specific CD8+T-cell populations was conducted by Miss Louise Hosie. A) Memory phenotype of the *ex vivo* CD8+T-cell responses specific for the cryptic epitopes compared to pp65 derived NLV-specific CD8+T-cells. Memory compartments were identified as $T_N$ (CCR7+CD45RA+), $T_{CM}$ (CCR7+CD45RA-), $T_{EM}$ (CCR7-CD45RA-) and $T_{EMRA}$ (CCR7-CD45RA+). Statistical significance of the $T_{EMRA}$ populations was determined using multiple comparison Mann-Whitney tests in Graphpad prism 6 with * as a p value <0.05. B) Antigen differentiation status of the cryptic specific CD8+T-cell responses identified as early (CD27+CD28+), intermediate (CD27+CD28-/CD27-CD28+) and late (CD27-CD28-). RPW n = 4, APD n = 3 and NLV n = 6.

## 6.3 - The *ex vivo* CD8+ T cells specific for the HLA-B7- cryptic peptide become more cytotoxic and more differentiated with age

When correlated with age the RPW-specific responses trended towards inflation with age and the IFN-γ production elicited by the APD peptide increased significantly with age (Fig-53D). However due to low n numbers, the *ex vivo* CD8+T-cell phenotype of the RPW-specific CD8+T-cells was analysed in relation to the age of the donor (Fig-57). The panel previously used to phenotype HCMV-specific CD8+T-cells was investigated (Table-4)

### 6.3.1 – Single marker expression

The RPW-specific CD8+T-cells remained granzymeB$^{high}$ with age (46.56%-93.33%) and increased perforin expression (29.33%-97.29%). Levels of NKG2D increased slightly and PD-1 remained low with age (1.41%-13.94% and 6.17%-17.96% respectively, Fig-57A). CX3CR1 expression was dramatically increased with age (16.25%-63.39%, p = 0.08). Progressively the RPW-specific CD8+T-cells lost the co-stimulatory CD27 and CD28 molecules with age (27.51%-9.86% and 47.75%-14.20% respectively, Fig-57A). The T-cell homing marker CCR7 expression remained low (8.80%-6.11%, Fig-57A).

### 6.3.2 - Memory phenotype

Within two younger donors <70 years of age, the majority of RPW-specific CD8+T-cells were $T_{EM}$ (CCR7$^-$CD45RA$^-$ 67.62%, Fig-57B). Within two older donors >70 years, the percentage of $T_{EM}$ decreases (46.71%) and the percentage of $T_{EMRA}$ (CCR7$^-$CD45RA$^+$, 49.25%) increases (Fig-57B).

### 6.3.3 - Antigen differentiation status

The percentage of late differentiated (CD27$^-$CD28$^-$) CD8+T-cells within the RPW-specific CD8+T-cell population remained similar with age (63.47% YD donors vs 66.74% OD donors, Fig-57C). In addition, within two donors >70 years of age, the proportion of early differentiated CD8+T-cells decreased within the RPW-specific CD8+T-cell population (19.20% vs 9.77%, Fig-57C).

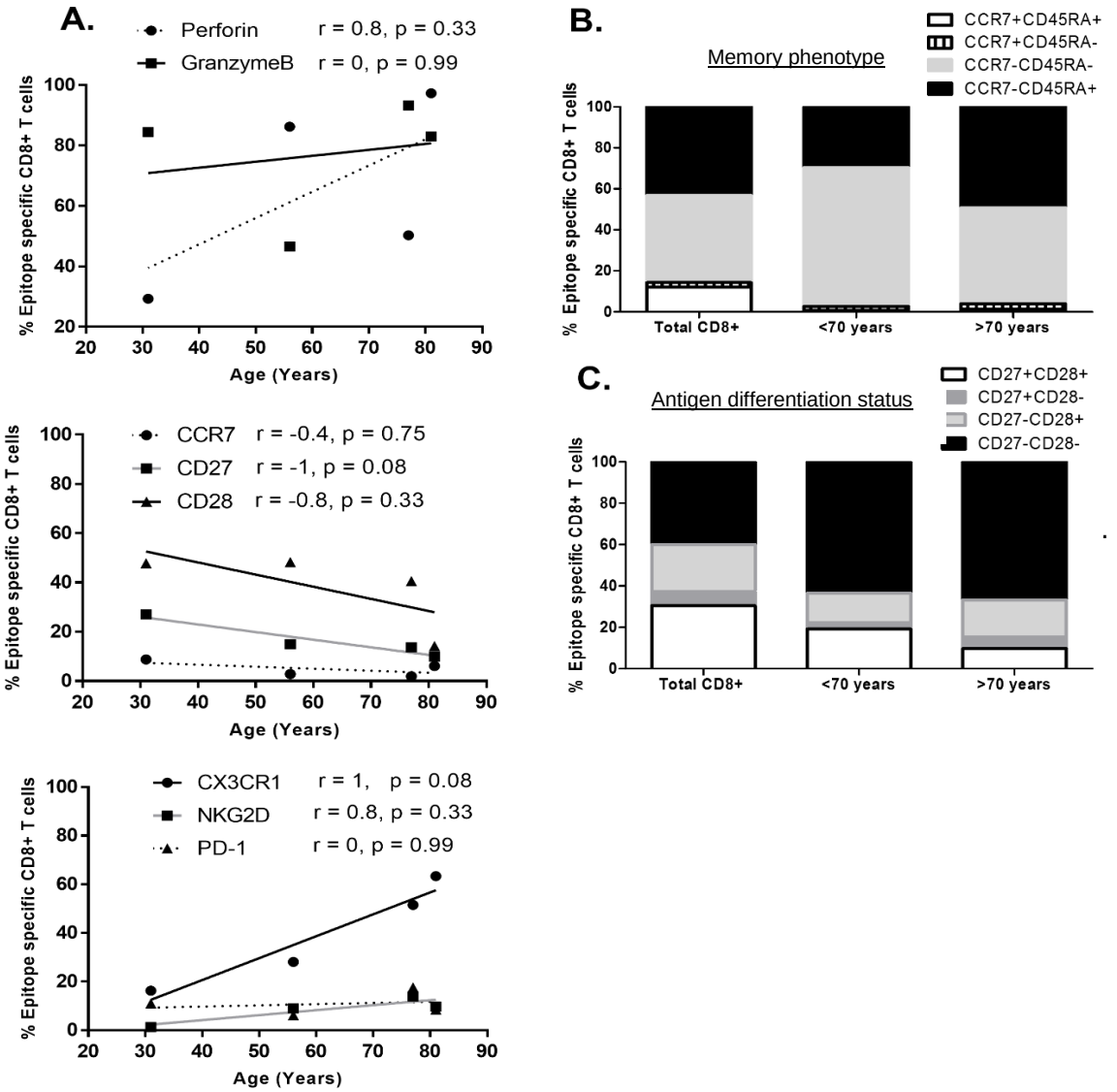


***Fig 57 – The ex vivo phenotype of cryptic RPW-specific CD8+T-cell responses with age*** Changes in the CD8+T-cells specific for the HLA-B7-restricted RPW cryptic peptide with age was analysed. PBMCs were stimulated with the RPW cryptic peptide-epitope for 6 hours followed by intracellular cytokine staining for TNF-α production to identify activated CD8+T-cells. The cells were subjected to staining with the antibody panels outlined in Table-4. Miss Emily Briggs phenotyped n = 7 and Miss Louise Hosie n = 1. The phenotyping of NLV-specific CD8+T-cell populations was conducted by Miss Louise Hosie A) Correlation of the expression of perforin, granzymeB, CD27, CD28, CCR7, CX3CR1, NKG2D and PD-1 expression on the *ex vivo* RPW-specific CD8+T-cell responses with age of the donors (years) by spearman's rank correlation. Lines represent linear regression. B) Memory phenotype of the *ex vivo* CD8+T-cell responses specific for the RPW cryptic epitope compared to NLV-specific. Memory compartments were identified as $T_N$ (CCR7+CD45RA+), $T_{CM}$ (CCR7+CD45RA-), $T_{EM}$ (CCR7-CD45RA-) And $T_{EMRA}$ (CCR7-CD45RA+). C) Antigen differentiation status of the RPW cryptic specific CD8+T-cell responses identified as early (CD27+CD28+), intermediate (CD27+CD28-/CD27-CD28+) and late (CD27-CD28-). RPW n = 4, APD n = 3 and NLV n = 6. The NLV phenotyping was conducted by Miss Louise Hosie. From herein research work on this chapter was conducted by Miss Louise Hosie.

To conclude, the *ex vivo* RPW-specific CD8+T-cells from four seropositive individuals demonstrated an increase in cytotoxic potential, whilst remaining low for PD-1 expression with age. The same CD8+T-cells acquired a more differentiated phenotype (loss of T-cell co-receptors CD27/CD28) with a concomitant increase in the endothelium homing marker CX3CR1. This indicates, that within these four individuals, the CD8+ T cells are becoming more stimulated by antigen with age.

## 6.4 - The functional avidity and peptide recognition profile of cryptic epitope-specific CD8+T-cell clones

To provide an indication of whether the cryptic peptide-epitopes could be directly presented to the immune system *in vivo,* it was next evaluated whether specific CD8+T-cell clones can recognise naturally processed cryptic peptide during an *in vitro* infection*.* CD8+T-cell clones specific for the RPW and APD peptides were generated from PBMCs obtained from donors YD49 (31 years) and OD25 (79 years) respectively.

First, the functional avidity of four RPW- and an APD-specific clone was calculated (Fig-58A). The $EC_{50}$ of the RPW clones ranged from 0.25μg – 250pg. The $EC_{50}$ of the APD clone was 0.005μg. This is in comparison to NLV-specific CD8+T-cell clones that ranged from 0.025μg-0.25μg (Chapter 3, Fig-16).

These CD8+T-cell clones were then utilised in a recognition assay to determine the recognition of cognate peptide generated during an *in vitro* CMV infection of haematopoietic non-haematopoietic cells (Fig-58B). This was conducted during infection with the WT US2-11 gene region AD169 and Merlin HCMV strains. Additionally, the recognition of peptide during a ΔUS2-11 RV798 infection was included due to their identification by Riddell et al. with this strain.

First, the recognition of fibroblasts i.e. non-haematopoietic cells was determined. RPW-specific CD8+T-cell clones recognised peptide presented on the cell surface of AD169 infected fibroblasts (MOI 5) at E-E/L time-points (12-48hrs p.i.). APD-specific clones also recognised peptide on the surface of AD169 infected fibroblasts at IE time-points (12hrs p.i.) and released a small concentration of IFN-γ at L time-points (72hrs p.i). During an RV798 infection, the cryptic RPW and APD epitopes were recognised at all time-points, excluding 48hrs p.i. for APD. In all cases the magnitude of IFN-γ production was larger compared to AD169 infection (Fig-58B).

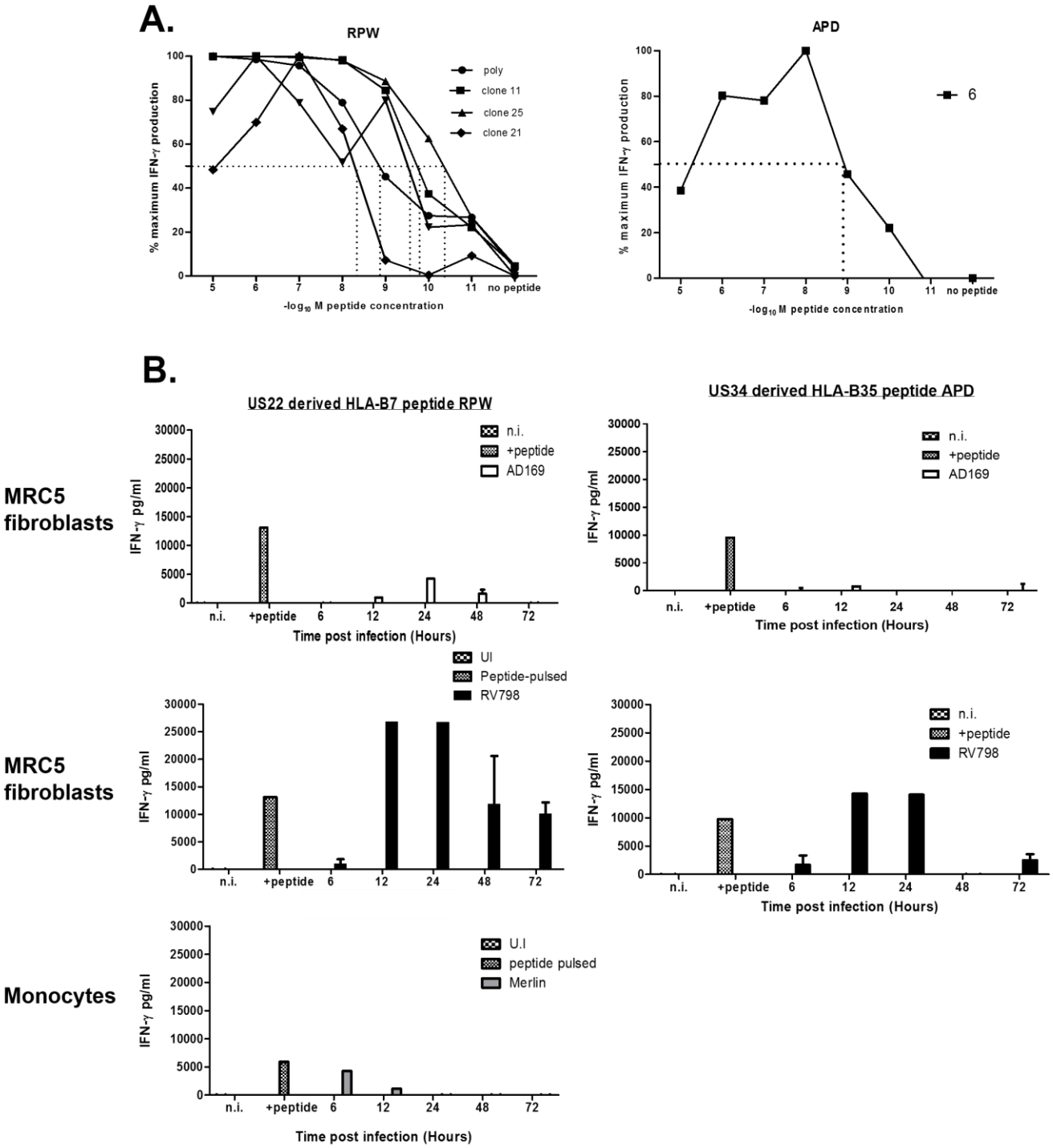


***Fig 58 – The $EC_{50}$ avidity and peptide recognition by HLA-B7 RPW- and HLA-B35 APD-specific CD8+T-cell clones* over the course of a productive HCMV infection** Cryptic epitope-specific CD8+T-cell clones were generated, their functional avidity determined and the recognition of peptide on the surface of HCMV infected cells *in vitro* assessed. CD8+T-cell clones were isolated from HCMV seropositive donor PBMCs after 3 hours peptide stimulation, IFN-γ secretion assay and a limiting dilution assay. A) The $EC_{50}$ of RPW- (left graph) and APD- (right graph) specific CD8+T-cell clones. The $EC_{50}$ was determined as the concentration of peptide that induced 50% maximal IFN-γ production (pg/ml) after O/N co-culture with peptide-loaded HLA-matched LCLs. Each line represents an individual clone. B) Cryptic CD8+T-cell recognition of cognate peptide during HCMV infection of fibroblasts and monocytes. Fibroblasts were infected with the AD169 or RV798 strains and monocytes infected with the Merlin strain for 6-72 hours at an MOI of 5. These were then co-cultured O/N with 10 000 CD8+T-cell clones. One clones tested per specificity, bars represent mean and error bars SEM. n = 2 experiments per fibroblast time-point. n = 1 per monocyte time-point.

The CD8+T-cell recognition of the RPW cryptic epitope during a primary CMV infection of haematopoietic cells was next analysed. Monocytes isolated from PBMCs of donors with previously identified RPW-specific CD8+T-cell responses were infected with the Merlin strain at an MOI of 5 for 6-72 hours prior to incubation with CD8+T-cell clones. RPW-specific CD8+T-cell clones recognised cognate peptide at IE (6-12 hours p.i.) only (Fig-58B).

To summarise, cryptic CD8+T-cell peptide-epitopes are presented *in vitro* directly during a primary infection of both haematopoietic and non-haematopoietic infections with three strains of HCMV – AD169, RV798 and Merlin. The peptides are efficiently recognised by specific CD8+T-cell clones generated *in vitro*.

## 6.5 – Cryptic RPW-specific CD8+T-cell clones effectively kill peptide-loaded and HCMV target cells

The adaptive immune system is efficiently able to recognise and generate a CD8+T-cell response to HCMV-derived cryptic epitopes generated in a non-canonical manner. However, it is as yet unclear the role that these CMV-specific CD8+T-cell populations play in the control of viral infection *in vivo*. Last in this results chapter, the functional and antiviral abilities of RPW-specific CD8+T-cell clones was investigated. In particular the proliferative and killing capacities. This was compared to NLV-specific clones already demonstrated as efficiently able to lyse cells and proliferate (Chapter 3 Fig-35/36).

First, the proliferative capacity of *ex vivo* RPW-specific CD8+T cells in response to antigen stimulation was elucidated (Fig-59). CFSE labelled PBMCs from donors with previously identified RPW-specific CD8+T-cell responses were co-cultured for 7 days with γ-irradiated peptide-pulsed HLA-matched LCLs. Proliferation was determined by analysing the dilution of CFSE on the PBMCs (gating strategy provided in Results chapter 4, Fig-37). PBMCs incubated with the RPW pulsed LCLs proliferated (18.3%-21.03%, n =2) but did not reach the proliferation levels observed with PBMCs incubated with NLV loaded targets (19.82%-53.94%, n = 2) (Fig-59A).

Secondly**,** the activation of RPW-specific CD8+T-cell clones after recognising cognate peptide during a primary fibroblast infection *in vitro* was assessed by flow cytometry. HLA-B7$^{+}$ MRC5 fibroblasts were infected with the Merlin strain at an MOI of 0.05 for 24 hours followed by incubation with RPW-specific CD8+T-cell clones for a further 48 hours. Following incubation, CD8+T-cell clones were removed from the infected cell monolayer and phenotyped by flow cytometry for CD25 upregulation. All RPW-specific clones demonstrated CD25 upregulation after incubation with Merlin infected fibroblasts (8.39%-73.43%, p = 0.11, Fig-59B).

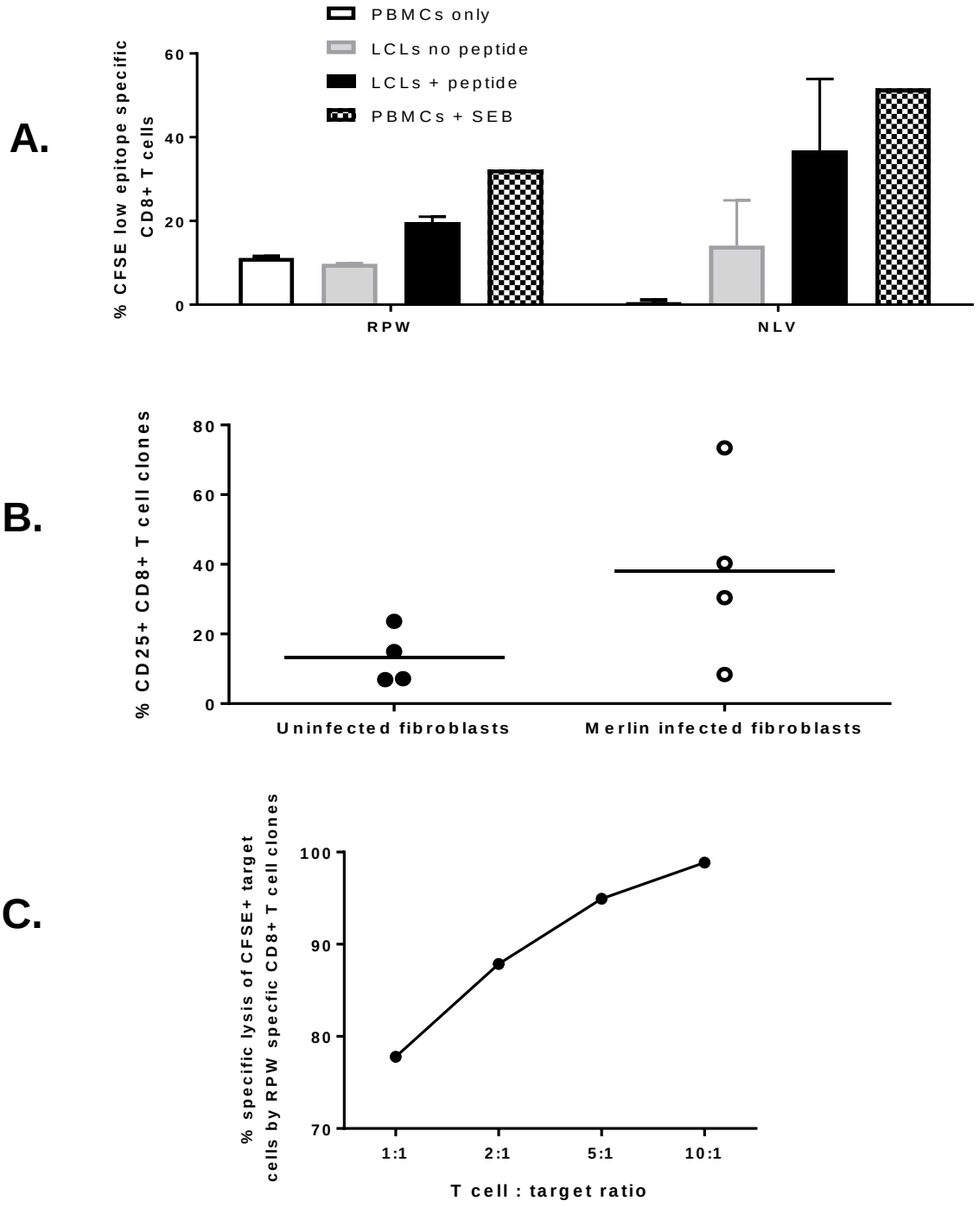


***Fig 59 – The in vitro functional activity of RPW-specific CD8+T-cell clones determined by CD25 upregulation and infected cell lysis.*** The proliferation of *ex vivo* RPW-specific CD8+T-cells and killing capacity of the RPW-specific CD8+T-cell clones was investigated. A) Proliferation of CFSE labelled RPW-specific PBMCs after incubation with peptide-loaded LCLs. Proliferation was determined by analysing the dilution of CFSE staining. Single, live, CD3+CD8+ lymphocytes were gated on in Kaluza 1,3 software. Within this population, CFSE low i.e. proliferating CD8+T-cells were identified. n = 2 for RPW and NLV B) Activation of RPW-specific CD8+T-cell clones after incubation with Merlin infected (MOI 0.05) MRC5 fibroblasts indicated by CD25 upregulation. Fibroblasts were infected with HCMV merlin strain at MOI 0.05 for 24 hours before the addition of specific CD8+T-cell clones for a further 48 hours and phenotyping of the CD8+T-cell clones by flow cytometry C) Specific lysis of RPW loaded LCLs by a RPW-specific CD8+T-cell clone. CFSE labelled, RPW peptide-loaded, HLA-matched LCLs were co-cultured with 10 000 CD8+T-cell clones at a 1-10:1 effector: target ratio O/N followed by analysis for PInegative CFSE POSITIVE target cells by flow cytometry. n = 1

Importantly, the ability of an RPW-specific CD8+T-cell clone to efficiently lyse HCMV infected cell targets was determined. An RPW-specific CD8+T-cell clone was incubated with CFSE labelled RPW-loaded HLA-B7+ LCLs O/N. The loss i.e. specific cell lysis, of viable CFSE positive PI negative targets was analysed the following day by flow cytometry (method outlined in chapter 2 materials and methods 2.2.8). The clone was found to efficiently kill RPW loaded targets *in vitro* ranging from 77.78% at a 1:1 to 98.85% at 10:1 effector:target cell ratio (n = 1) (Fig-59C).

# Chapter 6 - Summary

This work identified frequent *ex vivo* CD8+T-cell responses to novel peptides derived from the US22 and US34 proteins that are generated by a +2 amino acid shift in the translation from the cognate HCMV proteins (Table-9). These responses could reach 2.43% of the CD8+T-cell response producing TNF-α towards the US22-derived HLA-B7-restricted RPW peptide and 0.67% towards the US34-derived HLA-B35-restricted APD peptide. The *ex vivo* responses detected to these cryptic epitopes were largely Th1 cytokine producing but demonstrated larger ratios of Th1:IL-2 production than CD8+T cells specific for the immunodominant pp65 peptide NLV. The IFN-γ, IL-2 and TNF-α production elicited by the RPW peptide trended to a significant increase with age.

The phenotypic characterisation of these *ex vivo* CD8+T-cell responses found them to have high cytotoxic potential (intracellular perforin and granzymeB expression) with a significantly decreased CD38 expression compared to immunodominant pp65-specific CD8+T-cell responses. Both the RPW- and APD-specific responses were dominated by large $T_{EM}$ responses. The RPW-specific CD8+T-cell populations were comprised of a larger percentage of late antigen differentiated cells, with the APD-specific CD8+T-cell populations a distribution between early, intermediate and late differentiated cells.

As the age of the donor increased, the *ex vivo* CD8+T-cell responses directed towards the US22-derived RPW peptide shifted from a population comprised of mainly $T_{EM}$ CD8+T-cells to increase the percentage of $T_{EMRA}$. Additionally, the RPW-specific CD8+T-cell responses demonstrated an increase in CX3CR1 expression and progressive down-regulation of CD27/CD28 and CCR7.

The natural processing and surface presentation of these cryptic peptides on both haematopoietic (monocytes) and non-haematopoietic cells (fibroblasts) was established during a WT CMV infection *in vitro*. Cryptic peptide-specific CD8+T-cell clones produced IFN-γ in response to recognising their cognate peptides on these cell *in vitro*. This was conducted with strains of the virus where the WT US2-11 MHC-I immunomodulatory region

was present and compared to the RV798 mutant strain. The use of the RV798 strain to infect APCs originally led to the identification of the cryptic HCMV epitopes.

Most importantly, the efficient lysis of HCMV infected fibroblasts was demonstrated by an RPW-specific CD8+T-cell clone and RPW-specific clones became activated after incubation with merlin strain infected fibroblasts.

Altogether, cryptic CD8+T-cell responses appear an important part of the anti HCMV CD8+T-cell repertoire.

# CHAPTER 6 - DISCUSSION

To our knowledge, this work represents the first characterisation of *ex vivo* CD8+T-cell responses directed towards two cryptic epitopes – US22-derived RPW and US34-derived APD – produced by Human Cytomegalovirus, originally identified by our collaborator Dr Stanley Riddell and colleagues.

The HLA-B7-restricted RPW peptide is derived from the HCMV US22 protein which forms part of the infectious virion tegument [324]. The US22 gene encodes for the HWLF1 reading frame whose translation produces the nuclear located ICP22 protein which becomes released from infected cells at E (24hrs) and L (72hrs) time-points [325]. The role of this protein is unknown however removal of the US22 gene from HCMV was found as dispensable for growth [224]. The US22 gene has been identified as having peak expression at E-EL (24-48 hours p.i.) time-points of an infection [225].

The HLA-B35-restricted APD peptide is derived from the US34 protein. Little is known about the role this protein plays *in vivo*, however, removal of this protein from the virus has been demonstrated as dispensable for growth of the virus *in vitro* [224]. Within the literature it has not yet been determined what kinetics the US34 gene is expressed with.

This work characterised the CD8+T-cell responses towards these peptides with regards to kinetics, magnitude and frequency within HCMV seropositive donors and found that *ex vivo* CD8+T-cells to these peptides were frequent within HCMV infected healthy donors. The RPW-specific CD8+T-cells ranged from 0.37-2.43%, 0.06-1.22% and 0.43-2.57% producing IFN-γ, IL-2 and TNF-α respectively of the total CD8+T-cell response. The APD-specific CD8+T-cell responses ranged from 0.15-0.60%, 0.07-0.17% and 0.23-0.67% producing IFN-γ, IL-2 and TNF-α respectively of the total CD8+T-cell response.

**A hypothesis for the generation of HCMV cryptic CD8+T-cel peptide-epitopes**

Previously, cryptic epitope generation has been identified with RNA viruses [313, 315, 316, 322] whose generation during these infections has been hypothesised as resulting from errors in ribosomal reading during translation. It has also been identified during malignancies and autoimmune diseases [318, 319, 321].

Both HIV and Influenza are viruses with a small RNA genome and the generation of cryptic epitopes from both sense and antisense alternative reading frames is a plausible method for these viral pathogens to generate several protein products from a small number of transcripts maximising the encoding potential. Out of frame translation within a +1 ORF context has also been demonstrated for a DNA virus Herpes Simplex Virus 'HSV' [310, 314]. This virus was demonstrated to induce a +1 frameshift mutation at a ribosome error prone site within the thymidine kinase protein that in 1% of cases resulted in viral escape from acyclovir treatment. More recently, a cryptic presented epitope has been identified from the murine m54 protein but the role of this epitope *in vivo* has not been determined [328]. It was, however, determined that the CD8+T-cell responses directed towards this alternative epitope gained immunodominance after the deletion of typical dominant CD8+T-cell populations within infected mice.

This asks the question to why CMV, a large DNA virus encoding for ~192 unique ORFS with the potential to encode for functional in frame proteins [73], would also generate cryptic epitopes from an already large antigenic repertoire. It also asks why cryptic epitopes would be generated from protein antigens that are not associated with viral immunevasion and are dispensable for viral replication [224].

As such, two theories are proposed. The first that the generation of these cryptic epitopes occurs during primary infection of cell types *in vivo*. This would allow the generation of an initial CD8+T-cell peripheral pool specific for theses epitopes. During latency the virus 'switches' off this mechanism of cryptic epitope generation so that the immune system has

generated a CTL response that is unlikely to encounter their antigen again during latency. Thereby representing an immunevasion mechanism.

The second hypothesis is that the alternatively translated proteins from which these CD8+T-cell epitopes are generated from play an important and as yet undetermined role in the viral life cycle *in vivo*. For example, cryptic translation of the secreted ICP22 protein encoded by the US22 gene could generate variants with differing roles outside of the virally infected cell. Future research is to establish CMV CD8+T-cell peptide-epitopes of the canonically translated US22 and US34 proteins and to compare the recognition of these during a WT infection *in vitro* vs cryptic peptides derived from the same gene region.

There are several mechanisms whereby alternatively derived cryptic epitopes may arise [329]. Transcriptional mechanisms include; the ‘Pepton Hypothesis’ whereby an unidentified non-traditional RNA polymerase, not utilising the canonical eukaryotic methionine start codon, starts translation at a distinct site which is cleaved to peptides [330]. Others include the presence of cryptic promoters within a gene.

Translational mechanisms for cryptic epitope generation include; ribosomal errors where a non-start codon is read as a translation initiation start site, ribosomal jumping/shifting halfway through translation of a transcript and the credited ‘DRiP theory’ [331-333].

The DRiPs hypothesis proposed by Jonathan Yewdell [331] states that the majority of antigenic peptide presented on the cell surface within MHC-I molecules are derived from the neosynthesis and degradation of defective or abandoned ribosomal products of both self and viral proteins. Not from the degradation of stable long term proteins. This hypothesis was then extended [332] by the proposal of an ‘immunoribosome’ that may be closely linked to the immunoproteasome and TAP-mediated peptide transport. This ‘immunoribosome’ is dedicated to generating peptide-epitopes quickly from newly synthesised protein products under times of cell stress such as a viral infection. This would provide an advantage to the infected cells for the rapid presentation of IE viral peptides to mediate efficient removal by

CD8+T-cells of infected cells. This work by Yewdell et al. has focused primarily on viral proteins derived from the Influenza virus and has as yet to be demonstrated for other viral pathogens such as CMV.

This DRiPs hypothesis has been elegantly demonstrated by other research groups who demonstrated that MHC-I molecules within the ER are exposed primarily to peptides originating from newly synthesised proteins [334]. Furthermore that the presentation of an immunodominant viral antigen requires neosynthesis and not the degradation of stable proteins present within the virus particles that enter the cell. This indicates that surface antigens are derived from a pool of newly synthesised proteins and not the long lived protein form that enters the cell with the incoming virion [335].

The peptides investigated within this PhD study are derived from when the amino acid sequence is 'read' +2 amino acids from the canonical start methionine. The shifting of both the US22 and US34 nucleotide sequences +2 in frame creates a downstream internal ATG site which the ribosome can start translation from (Fig-60). This allows the translation of alternative US22 or US34 protein products containing the amino acid sequence for the HLA-B7 RPW and HLA-B35 APD peptides. A study has previously used ribosomal profiling to identify that the generation of several polypeptides from the same gene occurs frequently during CMV infection [336]. In particular relevance, the study identified several internal out of frame ORFs within previously identified ORFs. The translation from these internal sites led to the generation of out of frame proteins as is the case with the cryptic peptides characterised within this investigation. However the mechanism causing the ribosome to frameshift to these internal ORFs during viral translation, such as slippery sequences within the HCMV genome, were not investigated.

The research group of Shastri and colleagues have effectively demonstrated the misreading of the initial methionine start residue for translation by ribosomes as a leucine [337-340]. When the authors attempted to define the mechanism behind this, they observed a distinct ribosome complex that preferentially scans for the CUG leucine residue rather than AUG

methionine. Furthermore that the incorporation of the leucine residue does not involve the host 'eukaryotic translation factor 2' which halts host translation in time of viral stress. The author's hypothesized that this novel mechanism of CUG-initiated translation would allow for the cryptic translation of viral antigens during times of cellular viral stress when translation would otherwise be shut off by host factors.


***Fig 60 – Schematic of the cryptic translation of the US22 and US34 by identifying internal methionine residues as start codons.*** The canonical methionine start codon is indicated in bold and underlined blue. The protein sequence encoded by translation is provided beneath the nucleotide sequence. The start site of the +2 ORF is provided in bold and underlined red. The 'cryptic' protein sequence resulting from translation from this ATG start site is provided beneath the nucleotide sequence. The peptide sequence of the cryptic CD8+T-cell epitopes investigated in this study are provided in capital letters and underlined. The sequences used here are obtained from the merlin strain of CMV obtained from pubmed - NCBI Reference Sequence: NC_006273.2

The fact that CD8+T-cell responses directed to these cryptic epitopes can be found between several different donors, would imply that their generation and identification was not fortuitous and there is a common mechanism of generation between donors. Relevantly, a study has implicated HCMV promoter sequences as supporting an enhanced number of cryptic translation events compared to an SV40 promoter in the context of a DNA vaccine encoding the Hepatitis B polymerase in an alternative ORF [341]. Importantly this translation led to the generation of immunogenic peptides from the alternative frame protein within the DNA vaccine.

This investigation has not yet attempted to address the mechanism behind the US22 and US34 cryptic translation. We could nonetheless speculate based upon the evidence within the literature, a hypothesised model for HCMV cryptic epitope generation. When HCMV first infects a cell this cell enters a state of cellular stress and attempts to switch off translation. HCMV then utilises distinct cellular ribosome machinery that functions in the absence of host translation 'enhancers' to produce its protein products. However, this is at the expense of +2 ORF protein products that have not yet been determined as having role in the viral life cycle. In addition, the HCMV promoter sequences, demonstrated to enhance cryptic translation, may also increase the generation of these alternative protein products. These newly synthesised cryptic protein products are then substrates for the MHC-I pathway as proposed by the DRiPs hypothesis ultimately leading to the surface presentation of RPW/APD:MHC-I complexes.

**The phenotype and peptide recognition profile of cryptic-specific CD8+T-cells indicates antigen encounter during an infected host's lifetime**

The demonstration of direct presentation of the cryptic epitopes to specific CD8+T-cell clones during infection with three strains of the virus; AD169, RV798 and Merlin, strongly implies that they are indeed generated and presented naturally *in vivo* and may be a common phenomenon of CMV strains. Additionally, infection with the RV798 virus led to an enhanced magnitude of IFN-γ by cryptic-specific CD8+T-cell clones. In this regard, the

cryptic epitopes are generated and presented with similar kinetics that follows their protein expression profile to normally translated CMV protein peptides such as NLV from the pp65 protein whose recognition is also enhanced during an RV798 infection. This also implicates the viral US2-11 gene region in dampening but not completely abrogating the initial CD8+T-cell effector functions towards cryptic peptide presenting infected host cells.

Phenotypic characterisation of the *ex vivo* CD8+T-cell populations specific for the cryptic peptides revealed that they consist of a higher percentage of CD8+T-cells producing all three cytokines investigated in this study – IFN-γ, IL-2 and TNF-α. A lower CD38 expression on cryptic CD8+T-cell populations indicates that these are not as activated as NLV-specific CD8+T-cells within the periphery. Additionally, these cryptic peptides could be hypothesised as less frequently generated during an *in vivo* infection resulting in a less chronically stimulated phenotype of the specific CD8+T-cell population within the periphery than inflated immunodominant CD8+T-cell epitopes. This is supported by a significantly smaller percentage of $T_{EMRA}$ CD8+T-cells within the total cryptic-epitope specific populations compared to NLV-specific CD8+T-cell populations. However, the total RPW-specific CD8+T-cell populations did exhibit an increase of $T_{EMRA}$ CD8+T-cells with age - suggesting they are in fact encountering antigen over a period of time. The increase in CX3CR1 expression on RPW-specific CD8+T-cells with the age of donor would also indicate that these cytotoxic CD8+T-cells could efficiently migrate towards and control viral reactivation events within the periphery.

This raises the question to the cell type capable of presenting these cryptic peptides *in vivo*. As such the recognition was determined in this here work of naturally presented cryptic peptide on haematopoietic non-haematopoietic cells *in vitro*. The RPW peptide was recognised at IE (6 hours p.i. onwards) time-points of an AD169 primary CMV infection of haematopoietic monocytes but only from 12 hours p.i. onwards within non-haematopoietic fibroblasts. This would insinuate that both cell types are capable of presenting the cryptic peptides *in vivo* however they may be generated at different time-points during the viral life

cycle in differing cell types. The US22 protein, from which the HLA-B7 RPW peptide is derived, is present within the tegument of infectious virus particles [324, 325]. The RPW peptide should theoretically be immediately, i.e. 6 hours p.i., available for presentation In MHC-I in essentially all CMV permissible cell types. Fibroblasts could therefore contain cellular factors or viral factors that prevent the generation of these cryptic epitopes until time-points past 12 hours p.i. within this cell type. It may also represent a product of the RPW specific clone tested for CD8+T-cell recognition.

**Future research**

Research should be focused on the precise mechanism that may induce the ribosome to recognise a methionine codon that is +2 nucleotides out of the normal translation frame in preference to the initial methionine codon of the US22 or US34 genes. Furthermore, it should be focused on determining how frequently this occurs. It ought to be investigated whether HCMV encodes for any further cryptic CD8+T-cell epitopes and to what extent these contribute to the overall CD8+T-cell repertoire. To this end, it would be interesting to treat HCMV infected cells with aminoglycosides to enhance ribosomal errors and therefore gain a full picture of the extent of cryptic CMV epitopes [342]. Research should lastly be aimed at determining whether the alternative protein products generated by cryptic translation of the US22 or US34 genes have an important role in the viral life cycle *in vivo* or represent products of the virus attempting to translate its gene products within stressed host cells.

At present, research into the anti-CMV CD8+T-cell response could be massively underestimating the antigenic profile of HCMV by focusing upon in frame peptides. CD8+T-cell population's specific for cryptically generated peptide-epitopes are clearly important contributors to immune responses *in vivo*. They may play an important role in controlling viral infection *in vivo* as demonstrated by the efficient removal of virus-infected targets *in vitro* in this study. The clear message is that the overall understanding and known breadth of the immune response to this highly antigenic human DNA pathogen is still severely understated.

# CHAPTER 7

# INVESTIGATION INTO HCMV AS A VACCINE VECTOR FOR CANCER THERAPY

# CHAPTER 7 - INTRODUCTION

Cytomegaloviruses persist for the lifetime of the host whereby it is hypothesised these viruses induce low grade chronic antigen presentation resulting in a powerful cellular CD8+T-cell immune response that inflates with age [3, 88, 343]. The resulting long lived memory CD8+T-cells are highly cytotoxic and polyfunctional with age [110]. Together this makes CMV an attractive vector for vaccination in the hopes that such immune responses can be induced towards a gene insert and will be maintained indefinitely.

Louis Picker et al. pioneered research into CMV as a vaccine therapy for the vaccination of a viral disease, in particular 'Simian Immunodeficiency Virus' (SIV) as a prerequisite for whether such a vaccine construct would be applicable for the treatment of HIV disease. These studies demonstrated the undeniable efficacy of such a vaccine construct in the protection of vaccinated Rhesus Macaques from lethal SIV challenge. It was indeed the induction of long lived $T_{EM}$ CD8+T-cells as a result of chronic antigen presentation induced by the CMV vector that the author's attributed to the control and protection from lethal SIV strain disease.

Importantly for the context of this research chapter, CMV based vaccines have also been successfully used in studies and clinical trials for malignancies [208, 344, 345].

The research groups of Qiu et al. and Xu et al. have utilised CMV as a vaccine therapy to investigate the efficacy of this viral pathogen in directing the immune system to melanoma within mice [208, 344, 345]. The results of Qiu et al. were very promising and demonstrated the superior efficacy of a recombinant MCMV vector over a vesicular stomatitis virus (VSV) vector with regards to CD8+T-cell duration and protection from melanoma [344]. Additionally, Xu et al demonstrated that antibodies were the critical factor in protection from melanoma revealing the broad immunostimulatory effects of a CMV based vaccine.

CMV has therefore been established as a potential and promising vaccine vector for inducing durable cellular and humoral responses to tumour gene inserts. The question now arises which cancer antigen to target.

CTAgs are a family of tumour associated antigens that are preferentially expressed in immuneprivilidged sites or upregulated preferentially on several malignancies making them ideal and attractive targets for cancer immunotherapy [211]. The first member of this family of tumour antigens was identified by Van der Bruggen et al. termed MAGE-A1 [346]. Subsequent members were identified by either T-cell cloning methods or serologically with cDNA libraries generated from tumours screened with anti-tumour antibodies obtained from patients termed ‘Serological analysis of cDNA expression libraries (SEREX) [347]. Using this method Chen et al. identified the CTAG1 gene encoding for the ‘New York esophageal squamous cell carcinoma 1’ (NYESO1) [215].

The NYESO1 protein has since been the focus of numerous clinical trials [217] as a result of its potent immunogenicity to the immune system during malignancies [217, 348] and the correlation of its expression on tumours with poor prognosis [214, 349, 350].

This research chapter aimed to develop a therapy for NYESO1 expressing malignancies utilising HCMV as a vaccine vector to induce NYESO1-specific CD8+T-cells.

# CHAPTER 7 - RESULTS

## 7.1 - Generation of a HCMV-NYESO1 vaccine vector utilising the pALIIII 'Bacterial Artificial Chromosome' (BAC) construct

In collaboration with Dr Richard Stanton (School of Medicine, University of Cardiff), a HCMV BAC construct containing the NYESO1 gene was generated termed 'pALIIII-NYESO1' which would produce recombinant HCMV expressing NYESO1 (HCMV-NYESO1) when transfected into mammalian cells.

The pALIIII construct was constructed from a Merlin strain background and has mutations within the UL128-131 region [221]. This UL128-131 gene region is critical for CMV tropism *in vivo* and its removal restricts CMV infection to fibroblasts. The virus construct generated in this study was replication efficient to allow for the preparation of viral HCMV-NYESO1 stocks to test during *in vitro* assays. The RL13 gene was found to be a potent inhibitor of CMV replication in fibroblasts *in vitro* [221]. Therefore the replacement of the RL13 gene with the NYESO1 gene was hypothesised to increase yields of viral stocks of the recombinant HCMV-NYESO1 after transfection of pALIIII-NYESO1 into fibroblasts.

The pALIIII-NYESO1 construct was generated via a recombineering event within competent bacteria between an NYESO1 construct containing 80bp of homology to the HCMV RL13 gene (Table-6) and the endogenous RL13 gene within the pALIIII HCMV BAC construct. SW102 competent bacteria containing the pALIIII BAC were incubated for 15 minutes at 42$^{o}$C to induce the lambda phage recombination genes. The NYESO1 DNA construct with RL13 homology was then electroporated into the bacteria and the bacteria recovered and selected on media containing chloramphenicol. Positively pALIIII-NYESO1 transformed bacterial colonies, identified by a white opaque colour (materials and methods section 2.2.17) underwent plasmid isolation preparations. The resulting plasmid DNA was digested with the HinDIII restriction enzyme and electrophoresed to ensure that the integrity of the HCMV genome had not been significantly altered after the NYESO1 insert (Fig-61). This was

established by comparison to the digested pALIIII construct (previously characterised [221]), Fig-61).

Once established that the NYESO1 insert had not disrupted the HCMV genome, plasmids were sequenced for the correct NYESO1 sequence (University of Birmingham, Genomics service). Two selected plasmids (p3 and p11) both had the correct sequence alignment (data not shown).

After the confirmation of the correct NYESO1 sequence in the BAC, the pALIIII-NYESO1 was transfected into HFFF2 fibroblasts to produce recombinant HCMV. Plasmid 3 was selected for transduction into HFFF2 fibroblasts to generate a viral stock of HCMV-NYESO1 for *in vitro* assays. The titre of the HCMV-NYESO1 viral stock was quantified by a plaque assay of HFFF2 fibroblasts to be 1 x $10^7$ pfu/ml (data not shown).

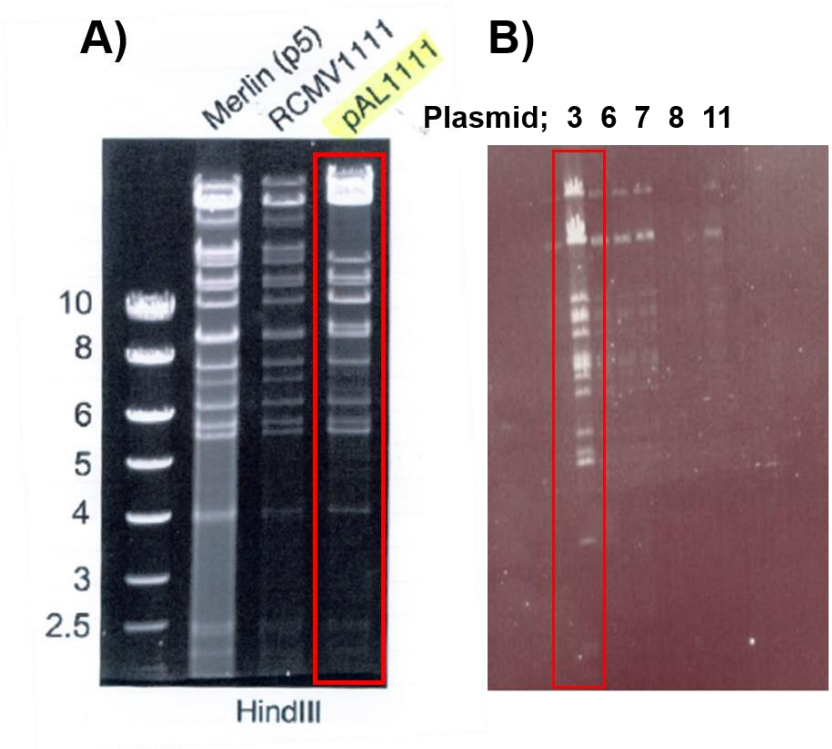


***Fig 61 – Characterisation of the correct NYESO1 gene insert into the CMV pALIIII construct*** Plasmids isolated from pALIII-NYESO1 transformed bacterial colonies were restriction digested with HinDIII to ensure the structural integrity of the HCMV genome was not lost after the recombination between RL13 and NYESO1. A) Restriction digest of the pALIIII BAC generated and digested by Dr Richard Stanton (A) [221] vs B) Restriction digest of plasmid isolated from pALIII-NYESO1 transformed bacterial colonies. Restriction digestion preparations were run for 16 hours on a 0.8% agarose gel at 60V.

## 7.2 - Generation of NYESO1-specific CD8+T-cell clones to assess the immunogenicity of a HCMV-NYESO1 vaccine construct

To determine whether NYESO1 was generated and expressed during an *in vitro* infection with recombinant HCMV-NYESO1 and an indication of whether such a CTAg expressing CMV strain would be immunogenic to the immune system, CD8+T-cell recognition assays were conducted.

For this, NYESO1-specific CD8+T-cell clones needed to be generated *in vitro*.

The levels of detectable CTAg specific CD8+T-cells within the periphery are extremely rare or non-detectable within healthy donors [351]. This is a result of NYESO1 expression being restricted to immuneprivilidged sites such as the testis**.**

In a collaboration with Dr Hayden Pearce (University of Birmingham, work recognised within Fig-62), rare CTAg specific CD8+T-cells within healthy donors were enriched and then isolated using a protocol as published [229]. This was achieved by utilising DCs loaded with an NYESO1 peptide to stimulate naïve CD8+T-cells isolated from an autologous buffy coat preparation over a course of 10 days in culture. This was followed by either; a 2 week co-culture with γ-irradiated peptide-loaded LCLs and PBMCs from buffy coat preparations followed by CD137 sorting, or a further weeks co-culture. This was to expand the low frequency of NYESO1-specific cells so that a limiting dilution cloning could be conducted. Expanded wells after limiting dilution were then grown further *in vitro* for functional testing. The entire procedure is outline in Fig-62.

The immunodominant HLA-A2-restricted **SLL**MWITQC peptide (aa position 157-165) was selected as the target peptide in this investigation [352-354].

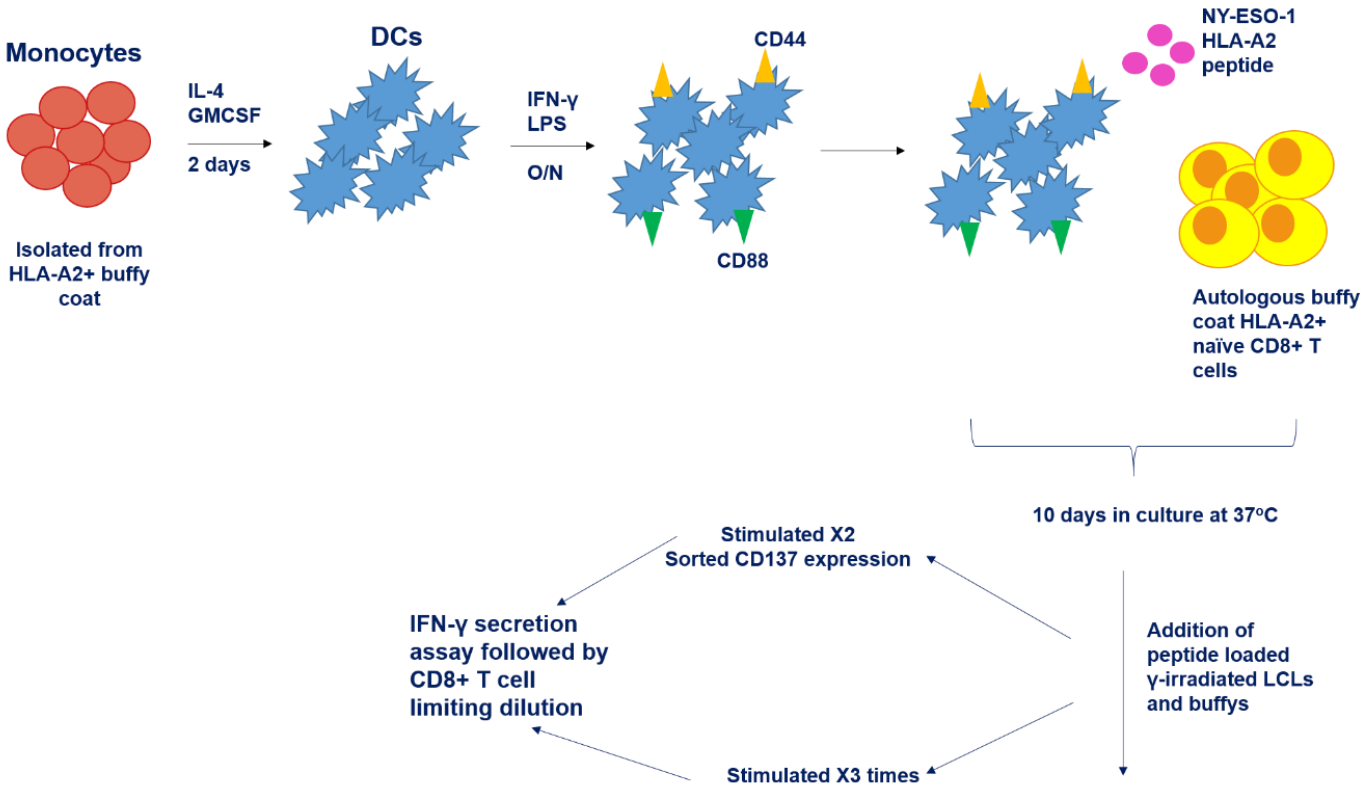


***Fig 62 – Schematic of the generation of NYESO1-specific CD8+T-cells generated from PBMCs obtained from a HLA-A2-restricted buffy coat preparation.*** Monocytes were isolated from buffy coat preparations by allowing them to adhere to a 24 well plate after 3 hours incubation at 37ºC. These were then differentiated into monocytes over a period of 2 days via the addition of IL-4 and GMCSF and matured O/N via the addition of IFN-γ and LPS. Activated DCs will have upregulated CD44 and CD88 molecules important for mature DC function. Naïve CD8+T-cells were subsequently isolated (Miltenyi Biotech, Table-2) from the autologous HLA-A2+ buffy coat preparation as the monocytes and these incubated the DCs who had been peptide-pulsed with a HLA-A2-restricted NYESO1 peptide SLM. This co-culture was left at 37ºC for 10 days. After this cultures were either stimulated (one stimulation per 7 days) twice with peptide-loaded γ-irradiated LCLs and buffy coat PBCs and sorted for CD137 expression followed by a limiting dilution cloning or stimulated three times followed by a limiting dilution cloning. After 2 weeks at 37oC, CD8+T-cell clones that expand within the wells of a 96-well plate after the limiting dilution were subjected to IFN-γ ELISA after O/N co-culture with peptide-loaded HLA-matched LCLs to determine their specificity. Specific clones were expanded in vitro via stimulation with peptide-loaded γ-irradiated LCLs and buffy preparation PBMCs. Dr Hayden Pearce devised the DC stimulation protocol, isolated both the monocytes and naive CD8+T-cells and provided the buffy coat PBMCs to generate the NYESO1 clones from. Miss Louise Hosie conducted the stimulations, limiting dilution assay and functional work of the obtained clones.

Through this method, a total of 10 expanded wells were observed. These were then tested for specificity by an IFN-γ ELISA after co-culture with SLL peptide-loaded HLA-A2$^+$ LCLs (5 representative clones are provided in Fig-63A). Of these 10 clones, 2 were found to have specificity towards the SLL NYESO1 peptide i.e. they produced more IFN-γ in response to SLL peptide-loaded target cells than control DMSO loaded target cells. The 37.1 clone was obtained from the CD137 sorting method prior to limiting dilution and the γ2 clone obtained by limiting dilution after the 3 week co-culture method (Fig-63A, method Fig-62).

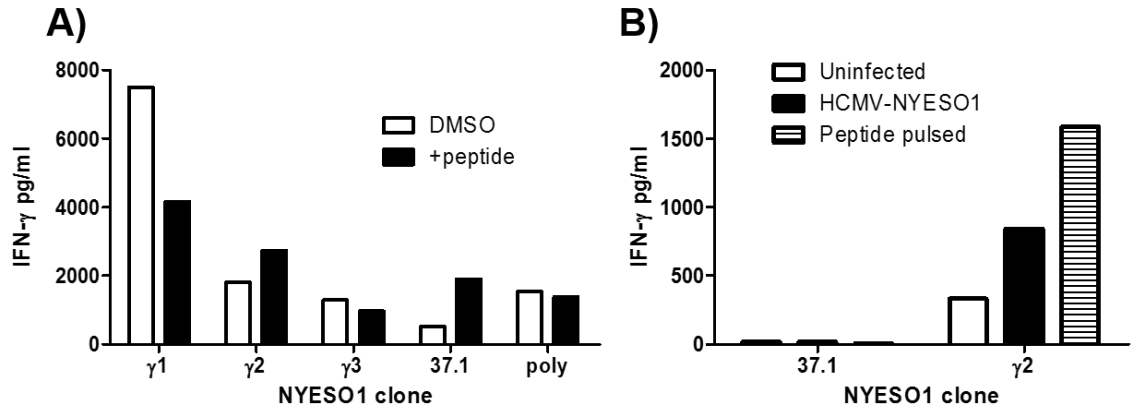


***Fig 63 – NYESO1 CD8+T-cell clone peptide specificity and recognition of naturally processed NYESO1 antigen during an in vitro HCMV-NYESO1 infection of fibroblasts.*** NYESO1-specific CD8+T-cell clones were tested for their ability to recognise peptide-loaded and HCMV-NYESO1 infected cell targets *in vitro* A) Peptide specificity check of NYESO1-specific CD8+T-cell clones obtained after 2 weeks culture *in vitro* with NYESO1 peptide-loaded DCs which was re stimulated with NYESO1 peptide-loaded γ-irradiated LCLs and PBMCs from buffy coat preparations. Specificity was determined by and IFN-γ ELISA after an O/N co-culture of NYESO1 CD8+T-cell clones. B) Specific lysis of HCMV-NYESO1 infected MRC5 fibroblasts by the γ2 specific CD8+T-cell clone. HLA-A2+ restricted MRC5 fibroblasts were infected with HCMV-NYESO1 at an MOI of 5 for 8 hours followed by O/N co-culture with 10 000 of either the 37.1 or γ2 NYESO1-specific clone. This was followed by an IFN-γ ELISA to detect a positive recognition of NYESO1 peptide by the CD8+T-cell clones. n = 1 for both A) and B). In all cases each condition was tested in duplicate.

Both of the specific clones were tested for the recognition of naturally generated NYESO1 peptide during an *in vitro* infection of MRC5 fibroblasts (n = 1, Fig-63B). The fibroblasts were infected with HCMV-NYESO1 for 8 hours at an MOI of 5 and incubated with 10 000 NYESO1-specific CD8+T-cell clones O/N. Positive recognition was determined by measuring IFN-γ release into the supernatant by an ELISA. The γ2 clone was able to efficiently release IFN-γ in response to incubation with HCMV-NYESO1 infected cells - 50% of the maximal IFN-γ production elicited after incubation with peptide-pulsed LCLs (Fig-63B). Unfortunately the 37.1 clone did not specifically recognise peptide on infected cells,

however, due to time constraints the mechanism behind this was not investigated. The γ2 clone was subsequently tested for the specific cell lysis of SLL peptide-loaded HLA-A2$^+$ LCLs. The γ2 clone was able to lyse 8.26% to 16.69% of peptide-loaded targets which decreased from 1:1 to 10:1 ratios (n =2 for 1:1 and n =1 for all other ratios, Fig-64). The γ2 CD8+T-cell clone was lastly assessed for the ability to lyse HCMV-NYESO1 infected fibroblasts *in vitro*. Fibroblasts were infected with the HCMV-NYESO1 viral construct at an MOI of 5 for 24 hours followed by CFSE labelling and the addition of NYESO1-specific CD8+T-cell clones at 1, 2, 5 and 10:1 effector target ratios O/N. Importantly, specific cell lysis of HCMV-NESO1 infected targets was determined by analysing the loss of CFSE positive, PI negative, i.e. viable target cells, by flow cytometry compared to DMSO-pulsed control fibroblasts. Continued specificity of the clone was confirmed by the inclusion of a fibroblast that had been peptide-pulsed with the SLM peptide. Specific cell lysis reached comparable levels to the positive control of vaccine infect fibroblasts at a 10:1 ratio (44.28% vs 46.23% respectively, Fig-64). Further work should focus effort on conducting this assay with an increased number of NYESO1-specific CD8+T-cell clones.

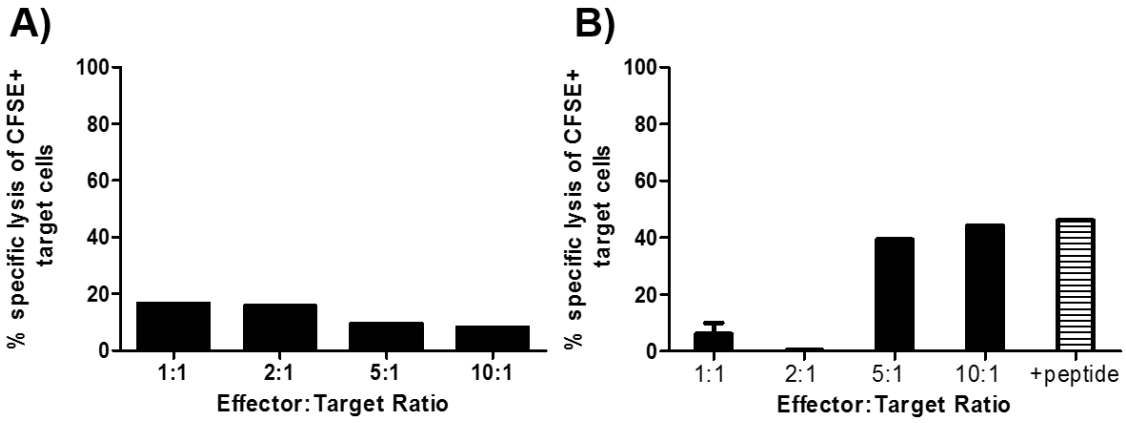


***Fig 64 – Specific cell lysis of NYESO1 peptide-loaded targets or HCMV-NYESO1 vaccine infected fibroblasts in vitro by the γ2 specific CD8.*** The NYESO1-specfic γ2 CD8+T-cell clone was evaluated for specific cell lysis of peptide-loaded and HCMV-NYESO1 infected target cells. A) Specific lysis of 20 000 peptide-loaded HLA-A2+ LCLs in vitro. 20 000 CFSE labelled HLA-A2$^+$ LCLs were peptide-loaded with the SLM NYESO1 peptide for 1 hour at 37$^o$C followed by O/N incubation at 1, 2, 5 and 10:1 effector:target ratios with γ2 NYESO1-specific T-cell clones. Specific cell lysis was determined as the loss of CFSE positive PI negative target cells by flow cytometry. B) Specific cell lysis of 20 000 HCMV-NYESO1 infected cells at an MOI of 5 incubated with 1-10:1 effector target ratios of CD8+T-cell clones. The lysis of fibroblasts peptide-pulsed with 1 μg/ml final concentration of SLM NYESO1 peptide for 1 hour prior to the addition of γ2 NYESO1-specific T cell clones was included as a positive control. A) n = 1 per effector:target ratio. B) n = 2 for 1:1 and n = 1 2:1, 5:1 and 10:1. In A/B) each ratio was tested in duplicate.

# CHAPTER 7 - SUMMARY

In a collaboration with Dr Richard Stanton (University of Cardiff), this research generated a vaccine construct for the treatment of NYESO1 positive malignancies based on a HCMV BAC construct (pALIIII [221]) containing the NYESO1 CTAg gene in place of the RL13 gene termed 'pALIIII-NYESO1'. This construct was used to generate a recombinant HCMV virus that expresses NYESO1 - HCMV-NYESO1 - when mammalian cells were stably transfected *in vitro*. The correct insertion of NYESO1 was determined by the sequencing of plasmids isolated from bacteria transformed with the pALIIII-NYESO1 BAC construct.

Positive expression of the NYESO1 protein was provided from the recognition of HCMV-NYESO1 infected cells by an NYESO1-specific CD8+T-cell clone generated *in vitro* in this investigation. This clone was specific for the immunodominant HLA-A2-restricted SLM NYESO1 peptide.

Significantly, the lytic ability of the NYESO1-specific CD8+T-cell clone was demonstrated against NYESO1-derived SLM peptide-loaded LCL targets and critically against HCMV-NYESO1 infected fibroblasts *in vitro*.

This research, though preliminary at present (n=1 CD8+T-cell clone tested and killing assay conducted) provides encouraging results that such a HCMV-NYESO1 vaccine construct could be immunogenic *in vivo* stimulating the low frequency of NYESO1-specific CD8+T-cell precursors that can then effectively remove NYESO1 expressing cancer cells.

# CHAPTER 7 - DISCUSSION

The previous success of CMV as a vaccine vector [208, 344, 345] coupled with both the high immunogenicity [348, 352, 355] and the association of the CTAg NYESO1 protein with poor survival outcomes [214, 349, 350], prompted our development of a HCMV vaccine construct expressing NYESO1.

The ubiquitous expression of NYESO1 on several tumours that can reach a high percentage would make the application of such a HCMV-NYESO1 vaccine widespread. A high percentage of tumours including; synovial sarcoma (80%) [356], ovarian (45%) [357], melanoma (17-43%) [217, 350, 358] and esophageal (32%) [359] amongst others have been reported positive for NYESO1 expression [217].

The NYESO1 protein was historically discovered by Chen et al., utilising the SEREX method – screening patient serum with CDNA molecules derived from tumour samples [215]. Unfortunately the role of the NYESO1 protein is still unknown, by large a fact that there are no known animal homologues of this protein. However, since its discovery NYESO1 has been the focus of in excess of 30 clinical trials (review [217]).

Previous clinical trials with viral constructs to induce NYESO1 immune responses utilising either a combined Vaccinia/Fowlpox [360, 361] or Lentiviral/Vaccinia vector regimes have been conducted. Whilst successful, a downfall of these trials was the requirement of prime-boost regimens. For example, a Vaccinia construct followed by a Fowlpox [360, 361] or a Lentiviral construct followed by a Vaccinia [218], in order to maintain the protective NYESO1 CD8+T-cell immune response [218, 361]. The use of a CMV-based vector in this situation should enhance the duration of the protective immune response after a single dose as studies with a spread-deficient MCMV strain have demonstrated the maintained capacity for memory-inflation [114]. Moreover, these previous viral constructs contained an immunodominant NYESO1 peptide and not the full NYESO1 protein. The HCMV-NYESO1

construct in this investigation was generated with the complete NYESO1 gene – meaning that any potential CD8+T-cell epitopes of NYESO1 can be generated and induce immune responses after vaccination.

The work conducted in this chapter at present represents preliminary data with regards to the *in vitro* antigenic testing of the HCMV-NYESO1 vaccine construct. Importantly the research presented in this investigation demonstrated the lytic capability of NYESO1-specific CD8+T-cells in removing HCMV-NYESO1 infected fibroblasts *in vitro*. This investigation has therefore developed a useful tool to study the efficacy of this vaccine construct *in vitro*. The results of the CD8+T-cell recognition assay imply that the NYESO1 protein expressed by the recombinant HCMV-NYESO1 is antigenic. It further demonstrates that the HCMV-NYESO1 infected fibroblast can process NYESO1 peptides within the MHC-I pathway and could potentially stimulate robust T-cell responses to NYESO1 *in vivo*. This is extremely promising for its efficacy *in vivo* in directing NYESO1-specific CD8+T-cells to NYESO1 expressing malignancies. Future research is concentrated on obtaining NYESO1-specific CD8+T-cells from the blood of patients with NYESO1 expressing malignancies and testing these during *in vitro* vaccine infection assays. This will represent a more physiological indication of whether this vaccine construct could stimulate CTAg-specific CD8+T-cells within patients *in vivo*. This will furthermore increase the data size of the current investigation and ensure the positive NYESO1-recogniton results are not a product of the specific NYESO1-clone isolated in this work.

Previously Valmori et al. identified NYESO1-specific CD8+T-cells utilising MHC-I tetramer technology, but however, only after prior peptide stimulation of PBMCs obtained from melanoma patients [220]. Thus confirming the low precursor frequency of NYESO1-specific CD8+T-cells. Additionally, the authors did not demonstrate the ability of such tetramer stained cells to specifically lyse tumour targets *in vivo*. Our construct was determined to activate a specific CD8+T-cell clone *in vitro* resulting in the specific lysis of HCMV-NYESO1

infected cells. This offers preliminary evidence that the HCMV-NYESO1 vaccine construct could stimulate low magnitudes of NYESO1-specific CD8+T-cells.

The HCMV-NYESO1 vaccine will theoretically induce robust CD8+T-cell responses for the lifetime of the host. Additionally vaccination of patients with the HCMV-NYESO1 may allow for the isolation of several different NYESO1-specific TCRs. This opens the possibility to sequence NYESO1 TCRS that confer protection for their retroviral transfer onto patient's endogenous T-cells for adoptive immunotherapy. This would be of advantage for patients whom relapse. The transfer of NYESO1 TCR transduced CD8+T-cells has earlier been shown as efficacious against myeloma within a phase I/II clinical trial whose persistence was correlated with the clinical efficacy observed in 80% of patients [362].

The Merlin strain engineered in this research expresses the WT US2-11 gene region [221]. This asks the question to how NYESO1 derived peptides will be naturally processed and presented when these US proteins interfere with MHC-I processing. CMV has a wide tropism and it is currently unknown the extent of the MHC-I targeting efficacy of these proteins in all cell types. NYESO1-derived peptides could be directly presented on the surface of such cells. Additionally, cross presentation of CMV antigens has been demonstrated both *in vivo* and *in vitro*. It is plausible DCs may activate CD8+T-cells by acquiring NYESO1 peptides from apoptotic debris of vaccine infected cells.

As discussed previously, the presence of the US immunevasin homologues within RhCMV are required for superinfection of macaques [134]. This demonstrates the capacity of the US proteins in evading the anti-CMV cytotoxic CD8+T-cell response within seropositive individuals. These findings have implications for the development of the HCMV-NYESO1 vaccine in this research. In the context of HCMV as a vaccine vector, the presence of the US genes would allow for the vaccination of seropositive individuals with previously established infections. This therefore argues premise for the inclusion of the WT US gene region within

CMV based vaccine vectors to evade pre-existing immunity and establish an infection foci resulting in repeated priming and activation of CTAg CD8+T-cells.

Several challenges would have to be overcome before such a HCMV-NYESO1 vaccine would gain safety and regulatory approval. Despite an asymptomatic infection within immunocompetent hosts, CMV represents a major cause of pathogenesis in both pregnant and immunocompromised individuals. Additionally, there may be problems with the public's perception of utilising a human pathogen in its own right as a vaccine vector. The vaccine construct generated in this investigation was replication competent to allow for the generation of recombinant viral stocks to test immunogenicity during *in vitro* assays. Therefore the next steps in the generation of this vaccine would be to inactivate the recombinant HCMV-NYESO1 to prevent spread to the unvaccinated population, and test the immunogenicity of such an inactivated construct in a murine model. In parallel to the approach adopted in this work, Hansen et al. utilised strains of the RhCMV that are deleted for the UL128-131 HCMV homologues [12]. This reduced virus tropism to generate a safer attenuated vaccine strain. The vectors demonstrated reduced replication within cell types responsible for viral dissemination whilst inducing and maintaining protective CD8+T-cell responses.

The safety of HCMV-NYESO1 would consequently need to be robustlessly investigated before human clinical trials could be conducted. The expression of NYESO1 in normal cells - restricted to early spermatogonia and lost with further differentiation of these sperm cells - support the safety of a vaccine *in vivo* as these locations are highly immuneprivilidged [363]. However, a study did describe positive results for low mRNA detection within pancreas, placenta, liver and breast tissue but no protein expression [364]. Even more encouraging, a genome wide investigation for the NYESO1 protein found no evidence of expression within normal healthy tissue other than immuneprivilidged sites e.g. brain/testis [365]. Any HCMV-NYESO1 vaccine strain that would be tested in a clinical trial would inevitably be made

competent only for one round of replication to reduce immune mediated damage, spread to the unvaccinated population and prevent recombination events with endogenous HCMV strains. This would allow infected cells to present NYESO1-derived peptides and generate a peripheral memory pool. After this time-point, no healthy cells (excluding the testis) should express NYESO1 peptides. Thus restricting damage caused to normal healthy NYESO1 expressing cells and ensure specificity to NYESO1 expressing tumours.

NYESO1 is arguably one of the most immunogenic cancer associated antigens that have been discovered to date. This investigation has focused primarily on the CD8+T-cell immune response to this vaccine, namely, due to limiting time and the availability of an immunodominant NYESO1 epitope SLL. NYESO1 is known for inducing cellular immune responses including CD4+T-cell [355] and a humoral response [366]. It is anticipated that further therapeutic benefits would be provided from the CD4+T-cell and antibody responses induced by the HCMV-NYESO1 recombinant virus.

A major hurdle preventing the use of HCMV as a vaccine vector within human trials is the global burden of congenital disease and reactivation within SOT and HIV patients [52, 54]. HCMV vaccines must therefore factor in the differing clinical situations and pathogenicity between immunocompetent and compromised individuals. However this study has provided promising results for the first steps towards the generation of a HCMV vaccine vector to target NYESO1 expressing malignancies. It is hoped that such a vaccine vector will maintain a potent cellular response exceeding that induced naturally during cancer with regards to the cellular [220, 352, 355] and humoral responses [366].

# CHAPTER 8 – FINAL DISCUSSION

Cytomegaloviruses (CMVs) represent a family of herpesviruses (β) that have evolved with their mammalian hosts to establish lifelong latent infections. Typically these infections are well controlled within immunocompetent hosts and the immune compartment critical for maintaining this control is the CD8+T-cell response. The loss of this cellular compartment within patients e.g. end stage AIDS patients or HSCT and SOT transplant patients, leads to the development of disseminated CMV replication culminating in organ disease.

The large antigenic repertoire of HCMV and the presence of a vast array of immunevasins that interfere with MHC-I presentation, namely the US2-11 gene region, makes the global CD8+T-cell response to HCMV difficult to completely delineate. It is undetermined to what extent the US2-11 gene products can reduce viral peptide:MHC-I presentation to the immune response in all cell types permissible to CMV. However CD8+T-cell responses specific for HCMV antigens across all phases of the viral lifecycle (IE-L) including those expressed after the US2-11 proteins, have been identified [58, 230]. Therefore CD8+T-cells specific for L-expressed antigens are still being primed *in vivo* despite the concerted actions of the US2-11 gene region.

It has been demonstrated that MCMV-specific CD8+T-cells can be primed early during infection of salivary gland non-haematopoietic cells that still display MHC-I on their surface despite the presence of MHC-I immunevasins [250]. It is also now known that the US2-11 gene region products cannot uniformly target all HLA alleles with the same efficacy and therefore some cells with a particular haplotype may be able to present CMV antigens on their surface in the context of MHC-I. As such CD8+T-cells can be directly primed by HCMV infected cells that are not as uniformly targeted by the US2-11 gene products. Secondly,

cross presentation of HCMV antigens via the uptake of apoptotic bodies of HCMV infected cells is also likely an important priming route [169, 171].

This investigation characterised *ex vivo* CD8+T-cell responses towards HCMV peptide-epitopes discovered during an RV798 (ΔUS2-11) strain infection of fibroblasts. These were found to be a frequent component of the total CD8+T-cell repertoire. These peptides were demonstrated to be both directly presented, and in the case of a UL69-derived peptide, cross presented to CD8+T-cell clones *in vitro*. Additionally, an immunodominant CD8+T-cell response towards a newly characterised HLA-Cw*0702-restricted UL28-derived peptide termed 'FRC' was identified. As such, the global CD8+T-cell response to CMV is likely underestimated using WT US2-11 strains and fibroblasts as the staple *in vitro* cell line.

Secondly, the CD8+T-cell response to CMV is made more complex by the identification of two epitopes of the virus derived from non-canonical translation methods of the US22 and US34 proteins (Riddell at al. Unpublished data). These were termed 'cryptic' peptides. *Ex vivo* CD8+T-cell responses towards these cryptic epitopes are frequent within HCMV-seropositive donors and can lyse infected cell targets *in vitro*. They also may accumulate within the periphery with age. This work has therefore also shown that by restricting studies to *in frame* derived peptides, research may be missing important CD8+ T-cells for CMV control *in vivo*. The treatment of cells with drugs that enhance translational errors will provide insight into the global capability of HCMV to produce cryptic peptide during an infection. The role of such proteins in the viral life cycle should be determined.

Within health, the CD8+T-cell repertoire dominates the total peripheral CD8+T-cell response – termed memory-inflation [86, 87, 100, 343, 367]. Currently, the factors governing memory-inflation are not definitively understood and are the focus of several research groups. The murine model has proven invaluable for dissecting the CMV antigens to which inflation occurs and the factors involved [105]. Within humans, cross-sectional studies have delineated that memory-inflated CD8+T-cells display a unique phenotype indicative of chronic antigen stimulation. They are defined as highly differentiated $T_{EMRA}$ cells, maintain

their functionality *ex vivo* and with age demonstrating high cytotoxicity and uniquely express CX3CR1 [68, 72, 87, 107, 110].

Memory-inflation is therefore undoubtedly the result of chronic low-level antigen persistence as a result of viral reactivation driving the accumulation of the T-cells to the late compartment. There are currently two scenarios proposed within the literature of how this chronic antigen stimulation occurs *in vivo*. The first depicts non-haematopoietic cells in secondary lymphoid organs, particularly the LN as stimulating CMV-specific $T_{CM}$. This results in the activation, proliferation, differentiation and the migration of the T-cells to the periphery and peripheral tissues. The second depicts that the $T_{CM}$ originating from the LN are restimulated by latently infected endothelium with access to the systemic circulation.

These models however do not explain why stable vs inflationary CD8+T-cell population's specific for differing epitopes within the same CMV protein can arise. As such several factors have been linked to the development of inflationary CD8+T-cell populations including; expression kinetics of the antigen, affinity of peptide for MHC-I, abundance of mature processed peptide and surface peptide:MHC-I concentration. Importantly, this work has hypothesised that the HLA-restriction of a peptide may impact upon the frequency of the presentation of the peptide within latently infected cells. This is due to the HLA haplotype of a particular infected cell type and the HLA targeting specificity of the US2-11 proteins. Almost certainly, properties of the CMV-specific CD8+T-cell itself will also determine whether the resulting population inflates or contracts such as peptide avidity and proliferation capacities.

This here work has identified three memory inflated CD8+T-cell populations specific for IE antigen derived from the IE-1 or UL28 proteins and restricted through HLA-Cw*0702. These inflated HLA-Cw*0702 CD8+T-cells demonstrated several of the factors reported as important for memory-inflation generation that we believe is responsible for their preferential inflation *in vivo*.

The inflated *ex vivo* HLA-Cw*0702 CD8+T-cell responses, towards the UL28-derived FRC peptide in particular, demonstrated; a $T_{EMRA}$ phenotype and retained a high cytotoxic potential with age. Specific CD8+T-cell clones to the HLA-Cw*0702 inflationary peptides demonstrated very high functional avidity, recognised peptide presented on non-haematopoietic fibroblasts and lysed these HCMV infected targets. The antigens from which the HLA-Cw*0702-restricted peptides are derived from are expressed with IE kinetics and are theoretically immediately accessible to the MHC-I pathway. Importantly, the HLA-Cw*0702-restriction of the peptides is likely critical as these alleles have been identified as less targeted by the US2-11 gene region. Lastly, HLA-C alleles were demonstrated in this study to be present on the infected cell surface during IE infection time-points correlating with the peak expression of the CMV antigens from which the inflationary targets are derived. This would allow a window of opportunity for the restimulation of HLA-C CD8+T-cells which may contribute to their accumulation within the periphery. As such, this investigation has identified particularly promising CD8+ T-cell candidates for immunotherapy. It is hoped these qualities and potential HLA-C allele upregulation during reactivation events will translate to a higher recognition of infected cells and therefore efficacy.

A more thorough understanding of how these inflated $T_{EMRA}$ HCMV-specific CD8+T-cell populations are generated and persist over time into old age will facilitate the development of CMV for therapeutic uses. In particular; which antigens to target for the treatment of CMV disease, which CMV genes to replace with therapeutic genes that will drive inflationary populations i.e. IE genes and manipulating this immune response towards malignancies.

Several features of the CMV virus make it an advantageous and extremely promising vector to target malignancies such as; lifelong cellular immunity with a cytotoxic $T_{EMRA}$ phenotype, ability to superinfect a previously HCMV seropositive individual and the capability of manipulating the CMV genome by BAC technology to introduce therapeutic genes. Studies

have demonstrated the use of recombinant CMV expressing tumour antigens as inducing a protective immune response from tumour challenge in murine models [209, 344].

This work, in collaboration with Dr Richard Stanton (University of Cardiff), generated a recombinant HCMV strain that expresses the NYESO1 CTAg. *In vitro* assays demonstrated this recombinant virus to be antigenic to a CD8+T-cell clone which effectively removed HCMV-NYESO1 infected cells. This provides the promising first steps towards developing this recombinant HCMV strain as a vaccine for cancer therapy.

If HCMV is to be treated in the post-transplant setting, then it is critically important to understand how the human immune system can efficiently control this virus during health. By doing so, the correct CD8+T-cell populations conferring the most efficacious and during protection can be recapitulated within immunocompromised patients. Additionally, if HCMV is to be used as a therapeutic agent for malignancies, it must first be understood the capacity of this virus to induce highly functional CD8+T-cell responses that will be maintained for life to provide tumour protection.

**Append ix Table 1 – CD8+T-cell IFN-γ production elicited by HCMV protected and pp65/IE-1 peptides after peptide stimulation of PBMCs from YD donors <70 years.** The numbers provided indicate the percentage of CD8+T-cells responding to peptide stimulation with IFN-γ production of the total CD8+ T cell population.

| Sex | Age (when PBMCs tested) | | A1-RTD | A1-YAD | A3-RVD | A11-RSA | B7-RPR | B7-SPS | B7-YPR | B35-HPF | B44-NEG | B51-DAR | B51-TLM | B51-IPH | B51-WPK | Cw7-FRC | Cw7-SYR | Cw7-CRV | Cw7-LSE | Cw16-YLC | B7-RPH | B7-TPR | A2-NLV | A1-VLE | A1-YSE | A1-VTE |
|---|---|---|---|---|---|---|---|---|---|---|---|---|---|---|---|---|---|---|---|---|---|---|---|---|---|---|
| M | 48 | YD1 | | | | 0.10 | | | | 0.15 | | | | | | | | | | | | | | | | |
| M | 48 | YD2 | 0.04 | 0.04 | | | | | | | 0.13 | | | | | | | | | 0.13 | | | | | 0.00 | 0.00 |
| M | 59 | YD3 | 0 | 0.05 | | | | | | | | | | | | | | | | | | | | | | |
| F | 27 | YD4 | 0.04 | 0 | | | | | | | | | | | | | | | | | | | | | | |
| M | 53 | YD5 | 0.19 | 0.22 | 0.13 | | | | | | | | | | | 0.10 | 0 | 0.00 | | | | | | | 0.00 | 0.14 |
| F | 49 | YD6 | | | | | 0.07 | 0.12 | 0.04 | | | | | | | 0.29 | 0.10 | 0.00 | | | | | | | | |
| F | 30 | YD7 | | | 0.09 | | | | | 0.19 | | | | | | | | | | | | | | | | |
| F | 52 | YD8 | 0 | 0.17 | | | | | | | | | | | | | | | | | | | | | | |
| F | 47 | YD9 | | | 0 | | | | | | | | | | | | | | | | | | | | | |
| M | 49 | YD10 | 0 | 0 | | | | | | | 0.07 | | | | | | | | | | | | | | | |
| F | 45 | YD11 | 0.27 | 0.13 | | 0.14 | | | | | | | | 0.09 | 0.32 | | | | | | | | | | 0.00 | 0.00 |
| F | 44 | YD12 | | | | | | | | 0 | | | | | | | | | | | | | | | | |
| F | 52 | YD13 | | | 0 | | 0 | 0 | 0 | | | | | | | 0.69 | 0 | 0.16 | 0.00 | | 0.16 | 0.29 | | | | |
| F | 29 | YD14 | | | | | 0 | 0 | 0 | | 0.08 | | | | | 0.10 | 0 | 0.06 | 0.21 | 0 | 0.00 | 0.00 | | | | |
| F | 30 | YD15 | 0.07 | 0.10 | | | | | | | | | | | | | | 0.00 | | | | | | | 0.00 | 0.00 |
| F | 44 | YD16 | | | | | 0.00 | 0.00 | 0.00 | | | | | | | 0.03 | | | | | | | | | | |
| F | 49 | YD17 | | | | | 0.00 | 0.00 | 0.00 | | | | | | | 0.18 | 0.00 | | | | | | | | | |
| | 40 | YD18 | 0.04 | 0.04 | | | | | | | | | | | | | | | | | | | 0.00 | 0.00 | | |
| | 40 | YD19 | | | | 0.00 | 0.00 | 0.00 | 0.00 | | | 0.00 | 0.00 | 0.00 | 0.00 | 0.05 | 0.00 | | | | | | | | | |
| M | 44 | YD20 | | | | | | | | 0.13 | | | | | | | | | | | | | | | | |
| | <70 | YD21 | | | | | 0.04 | 0.04 | 0.07 | | | | | | | 0.33 | 0.07 | 0.03 | | | | | | | | |
| | 51 | YD22 | | | | | | | | 0.00 | | | | | | | | | | | | | | | | |
| F | 51 | YD23 | 0.19 | | | | | | | | | | | | | | | | | | | | | | | |
| | <70 | YD24 | | | | | | | | | | | | | | 0.12 | 0.06 | | | | | | | | | |
| F | 33 | YD25 | | | | | | | | | | | | | | | | | | 0.05 | | | | | | |
| | <70 | YD26 | 0.00 | 0.00 | 0.00 | 0.00 | 0.00 | 0.00 | 0.00 | | | 0.00 | 0.00 | | | 0.20 | 0.00 | | | | | | | | | |
| | <70 | YD27 | | | | 0.00 | 0.00 | 0.00 | | | | 0.00 | 0.00 | | 0.00 | 0.00 | 0.00 | | | | | | 0.09 | 0.06 | | |
| | 55 | YD28 | | | | | 0.18 | 0.09 | 0.09 | | | | | | | 0.12 | | 0.09 | 0.06 | | 0.18 | 0.27 | | | | |
| | <70 | YD29 | | | | 0.00 | | | | | 0.00 | 0.00 | 0.00 | 0.00 | 0.00 | 0.18 | 0.00 | | | | | | | | | |
| M | 56 | YD30 | | | | | | | | | | | | | | 0.10 | | | | | | | | | | |
| M | 52 | YD31 | | | 0.07 | | 0.00 | 0.00 | 0.00 | | | | | | | 1.29 | | | | | | | | | | |
| | <70 | YD32 | | | 0.05 | | 0.11 | 0.06 | 0.00 | | | | | | | 0.09 | 0.05 | | | | | | 0.00 | 0.00 | | |
| | 27 | YD33 | | | | | | | | | 0.00 | | | | | | | | | | | | | | | |
| | 47 | YD34 | 0.00 | 0.00 | | 0.00 | | | | 0.00 | | | | | | | | | | | | | | | | |
| | 26 | YD35 | | | 0.00 | | 0.00 | 0.00 | 0.00 | | | 0.00 | 0.00 | 0.00 | 0.00 | | | | | | 0.00 | 0.00 | 0.07 | | | |
| | <70 | YD36 | | | | | | | | | | | | | | | | | | | 0.00 | 0.00 | 0.00 | 0.00 | | |
| | 37 | YD37 | | | | | | | | | | | | | | | | | | | | | 0.00 | 0.00 | | |
| | 30 | YD38 | | | | | 0.00 | 0.00 | 0.00 | | | | | | | | | | | | 0.00 | 0.00 | 0.00 | 0.00 | | |
| | 47 | YD39 | | | | | | | | | | | | | | | | | | | | | 0.00 | 0.00 | | |
| | 47 | YD40 | | | | | | | | | | | | | | | | | | | | | | | | |
| | 44 | YD41 | | | 0.00 | | | | | | | | | | | | | | | | | | | | | |
| | 49 | YD42 | | | | | | | | 0.00 | 0.00 | | | | | | | | | | | | 0.00 | 0.00 | | |
| | 37 | YD43 | | | | | | | | | 0.00 | | | | | | | | | | | | 0.00 | 0.00 | | |
| | 44 | YD44 | | | | | | | | 0.00 | 0.00 | | | | | | | | | | | | 0.00 | 0.00 | | |
| M | 23 | YD47 | 0.00 | 0.00 | | | | | | | | 0.00 | 0.00 | 0.00 | 0.00 | | | | | | | | | | | |
| M | <70 | YD48 | | | | | | | | | 0.00 | | | | | | | | | | | | 0.12 | | | |
| F | 31 | YD49 | 0.00 | 0.00 | 0.00 | 0.00 | 0.00 | 0.00 | 0.00 | | | | | | | 0.13 | 0.00 | 0.00 | 0.00 | | 0.00 | 0.00 | | | | |
| M | 54 | YD50 | | | | | 0.06 | 0.06 | 0.06 | | | | | | | 0.41 | | 0.06 | 0.06 | | 0.42 | 0.29 | | | | |
| M | 68 | YD51 | 0.29 | 0.09 | | | | | | | | | | | | | | | | | | | | | | |
| M | <70 | YD52 | | | | | | | | | | | | | | 0.05 | | 0.00 | 0.32 | | | | | | | |
| F | <70 | YD53 | | | | | | | | | | | | | | 0.00 | 0.27 | 0.09 | 0.00 | | | | | | | |
| M | <70 | YD54 | | | | | | | | | | | | | | 0.15 | 0.15 | 0.44 | 0.04 | | | | | | | |
| M | 23 | YD55 | | | | | | | | | | | | | | 0.00 | | 0.00 | 0.00 | | | | | | | |
| F | 63 | YD56 | 0.09 | 0.09 | | | | | | | | | | | | 0.16 | 0.04 | 0.00 | 0.00 | | | | | | | |

***Append ix Table 2 – CD8+T-cell IL-2 production elicited by HCMV protected and pp65/IE-1 peptides after peptide stimulation of PBMCs from YD donors <70 years.*** The numbers provided indicate the percentage of CD8+T-cells responding to peptide stimulation with IL-2 production of the total CD8+ T cell population.

| Sex | Age (when PBMCs tested) | | A1-RTD | A1-YAD | A3-RVD | A11-RSA | B7-RPR | B7-SPS | B7-YPR | B35-HPF | B44-NEG | B51-DAR | B51-TLM | B51-IPH | B51-WPK | Cw7-FRC | Cw7-SYR | Cw16-YLC | Cw7-CRV | Cw7-LSE | B7-RPH | B7-RPR | A2-NLV | A1-VLE | A1-YSE | A1-VTE |
|---|---|---|---|---|---|---|---|---|---|---|---|---|---|---|---|---|---|---|---|---|---|---|---|---|---|---|
| M | 48 | YD1 | | | | 0.05 | | | | 0.05 | | | | | | | | | | | | | | | | |
| M | 48 | YD2 | 0 | 0.04 | | | | | | | 2.31 | | | | | | | 0.04 | | | | | | | 0.00 | 0.00 |
| M | 59 | YD3 | 0.28 | 0.05 | | | | | | | | | | | | | | | | | | | | | | |
| F | 27 | YD4 | 0.03 | 0 | | | | | | | | | | | | | | | | | | | | | | |
| M | 53 | YD5 | 0 | 0.16 | 0 | | | | | | | | | | | 0 | 0 | | 0.00 | | | | | | 0.00 | 0.14 |
| F | 49 | YD6 | | | | | 0 | 0.08 | 0 | | | | | | | 1.28 | 0.04 | | 0.00 | | | | | | | |
| F | 30 | YD7 | | | 0 | | | | | 0.14 | | | | | | | | | | | | | | | | |
| F | 52 | YD8 | 0 | 0.16 | | | | | | | | | | | | | | | | | | | | | | |
| F | 47 | YD9 | | | 0 | | | | | | | | | | | | | | | | | | | | | |
| M | 49 | YD10 | 0 | 0 | | | | | | | 0.07 | | | | | | | | | | | | | | | |
| F | 45 | YD11 | 0.17 | 0.13 | | 0.27 | | | | | | 0.00 | 0.00 | 0.00 | 0.00 | | | | | | | | | | 0.00 | 0.00 |
| F | 44 | YD12 | | | | | | | | 0 | | | | | | | | | | | | | | | | |
| F | 52 | YD13 | | | 0 | | 0 | 0 | 0 | | | | | | | 2.09 | 0 | | 0.16 | 0.00 | 0.16 | 0.29 | | | | |
| F | 29 | YD14 | | | | | 0.00 | 0 | 0 | | 0 | | | | | 0.39 | 0 | 0.14 | 0.06 | 0.21 | 0.00 | 0.00 | | | | |
| F | 30 | YD15 | 0.02 | 0 | | | | | | | | | | | | | | | 0.00 | | | | | | 0.00 | 0.00 |
| F | 44 | YD16 | | | | | 0.00 | 0.00 | 0.00 | | | | | | | 0.03 | | | | | | | | | | |
| F | 49 | YD17 | | | | | 0.00 | 0.16 | 0.00 | | | | | | | 0.38 | | | | | | | | | | |
| | 40 | YD18 | 0.00 | 0.00 | | | | | | | | | | | | | | | | | | | 0.00 | 0.00 | | |
| | 40 | YD19 | | | | | | | | 0.00 | | | | | | | | | | | | | | | | |
| M | 44 | YD20 | | | | | 0.09 | 0.04 | 0.00 | | | | | | | 4.14 | 0.00 | | | | | | | | | |
| | <70 | YD21 | | | | | | | | 0.00 | | | | | | | | | 0.03 | | | | | | | |
| | 51 | YD22 | 0.15 | | | | | | | | | | | | | | | | | | | | | | | |
| F | 51 | YD23 | | | | | | | | | | | | | | 0.71 | 0.00 | | | | | | | | | |
| | <70 | YD24 | | | | | | | | | | | | | | | | 0.00 | | | | | | | | |
| F | 33 | YD25 | | | | 0.00 | 0.00 | 0.00 | | | | 0.00 | 0.00 | | | 0.36 | 0.00 | | | | | | | | | |
| | <70 | YD26 | 0.00 | 0.00 | 0.00 | 0.00 | 0.00 | 0.00 | 0.00 | | | 0.00 | 0.00 | | 0.00 | 1.71 | 0.00 | | | | | | | | | |
| | <70 | YD27 | 0.00 | 0.00 | | | | | | | | | | | | | | | | | | | 0.09 | 0.06 | | |
| | 55 | YD28 | | | | | 0.33 | 0.20 | 0.42 | | | | | | | 1.86 | | | 0.09 | 0.06 | 0.18 | 0.27 | | | | |
| | <70 | YD29 | | | | 0.48 | | | | | 0.58 | 0.00 | 0.00 | 0.00 | 0.00 | 1.79 | 1.34 | | | | | | | | | |
| M | 56 | YD30 | | | | | | | | | | | | | | 1.73 | | | | | | | | | | |
| M | 52 | YD31 | | | 5.65 | | 0.00 | 0.00 | 0.00 | | | | | | | 18.18 | 0.00 | | | | | | | | | |
| | <70 | YD32 | | | | | 0.00 | 0.00 | 0.00 | | | | | | | 0.00 | 0.00 | | | | | | 0.00 | 0.00 | | |
| | 27 | YD33 | | | | | | | | | 0.00 | | | | | | | | | | | | | | | |
| | 47 | YD34 | 0.00 | 0.00 | | 0.00 | | | | 0.00 | | | | | | | | | | | | | | | | |
| | 26 | YD35 | | | 0.00 | | 0.00 | 0.00 | 0.00 | | | 0.00 | 0.00 | 0.00 | 0.00 | | | | | | 0.00 | 0.00 | 0.07 | | | |
| | <70 | YD36 | | | | | | | | | | | | | | 0.00 | 0.00 | | | | 0.00 | 0.00 | 0.00 | 0.00 | | |
| | 37 | YD37 | | | | | | | | | | | | | | 0.00 | 0.00 | | | | | | 0.00 | 0.00 | | |
| | 30 | YD38 | | | | | 0.00 | 0.00 | 0.00 | | | | | | | | | | | | 0.00 | 0.00 | 0.00 | 0.00 | | |
| | 47 | YD39 | | | | | | | | | | | | | | | | | | | | | 0.00 | 0.00 | | |
| | 47 | YD40 | | | | | | | | | | | | | | | | | | | | | | | | |
| | 44 | YD41 | | | 0.00 | | | | | | | | | | | | | | | | | | | | | |
| | 49 | YD42 | | | | | | | | 0.00 | 0.00 | | | | | | | | | | | | 0.00 | 0.00 | | |
| | 37 | YD43 | | | | | | | | | 0.00 | | | | | | | | | | | | 0.00 | 0.00 | | |
| | 44 | YD44 | | | | | | | | 0.00 | 0.00 | | | | | | | | | | | | 0.00 | 0.00 | | |
| M | 23 | YD47 | 0.00 | 0.00 | | | | | | | | 0.00 | 0.00 | 0.00 | 0.00 | | | | | | | | | | | |
| M | <70 | YD48 | | | | | | | | | 0.32 | | | | | | | | | | | | 0.12 | | | |
| F | 31 | YD49 | 0.00 | 0.00 | 0.00 | 0.00 | 0.00 | 0.00 | 0.00 | | | | | | | 1.42 | 0.00 | | 0.00 | 0.00 | 0.00 | 0.00 | | | | |
| M | 54 | YD50 | | | | | 0.00 | 0.28 | 0.34 | | | | | | | 4.69 | | | 0.06 | 0.06 | 0.42 | 0.29 | | | | |
| M | 68 | YD51 | | | | | | | | | | | | | | | | | | | | | | | | |
| M | <70 | YD52 | | | | | | | | | | | | | | 0.13 | | | 0.00 | 0.32 | | | | | | |
| F | <70 | YD53 | | | | | | | | | | | | | | 0.00 | 0.03 | | 0.09 | 0.00 | | | | | | |
| M | <70 | YD54 | | | | | | | | | | | | | | 5.28 | 0.07 | | 0.44 | 0.04 | | | | | | |
| M | 23 | YD55 | | | | | | | | | | | | | | 1.72 | | | 0.00 | 0.00 | | | | | | |
| F | 63 | YD56 | 0.12 | 0.21 | | | | | | | | | | | | 1.14 | 0.00 | | | | | | | | | |

***Append ix Table 3 – CD8+T-cell TNF-α production elicited by HCMV protected and pp65/IE-1 peptides after peptide stimulation of PBMCs from YD donors <70 years.*** The numbers provided indicate the percentage of CD8+T-cells responding to peptide stimulation with TNF-α production of the total CD8+ T cell population.

| Sex | Age (when PBMCs tested) | | A1-RTD | A1-YAD | A3-RVD | A11-RSA | B7-RPR | B7-SPS | B7-YPR | B35-HPF | B44-NEG | B51-DAR | B51-TLM | B51-IPH | B51-WPK | Cw7-FRC | Cw7-SYR | Cw7-CRV | Cw7-LSE | Cw16-YLC | B7-RPH | B7-TPR | A2-NLV | A1-VLE | A1-YSE |
|---|---|---|---|---|---|---|---|---|---|---|---|---|---|---|---|---|---|---|---|---|---|---|---|---|---|
| M | 48 | YD1 | | | | 0.05 | | | | 0.10 | | | | | | | | | | | | | | | |
| M | 48 | YD2 | 0.16 | 0.28 | | | | | | | 3.98 | | | | | | | | | 0.33 | | | | | 0.00 |
| M | 59 | YD3 | 0.05 | 0 | | | | | | | | | | | | | | | | | | | | | |
| F | 27 | YD4 | 0.04 | 0 | | | | | | | | | | | | | | | | | | | | | |
| M | 53 | YD5 | 0.16 | 0.27 | 0.12 | | | | | | | | | | | 0.15 | 0 | 0.00 | | | | | | | 0.00 |
| F | 49 | YD6 | | | | | 0 | 0.04 | 0.04 | | | | | | | 1.25 | 0.07 | 0.89 | 1.46 | | | | | | |
| F | 30 | YD7 | | | 0.92 | | | | | 0.56 | | | | | | | | | | | | | | | |
| F | 52 | YD8 | 0 | 0.64 | | | | | | | | | | | | | | | | | | | | | |
| F | 47 | YD9 | | | 0 | | | | | | | | | | | | | | | | | | | | |
| M | 49 | YD10 | 0 | 0 | | | | | | | 0.18 | | | | | | | | | | | | | | |
| F | 45 | YD11 | 0.42 | 0.16 | | 0.36 | | | | | | 0.00 | 0.00 | 0.00 | 0.00 | | | | | | | | | | 0.00 |
| F | 44 | YD12 | | | | | | | | 0 | | | | | | | | | | | | | | | |
| F | 52 | YD13 | | | 0 | | 0 | 0 | 0 | | | | | | | 2.25 | 0 | 1.48 | 1.33 | | 0.67 | 0.28 | | | |
| F | 29 | YD14 | | | | | 1.21 | 0 | 0 | | 0 | | | | | 0.47 | 0 | 0.25 | 0.21 | 0.28 | 0.00 | 0.00 | | | |
| F | 30 | YD15 | 0.02 | 0.02 | | | | | | | | | | | | | | 0.00 | | | | | | | 0.00 |
| F | 44 | YD16 | | | | | 0.00 | 0.00 | 0.00 | | | | | | | 0.03 | | | | | | | | | |
| F | 49 | YD17 | | | | | 0.00 | 0.00 | 0.00 | | | | | | | 0.24 | 0.00 | | | | | | | | |
| | 40 | YD18 | 0.00 | 0.04 | | | | | | | | | | | | | | | | | | | 0.00 | 0.00 | |
| | 40 | YD19 | | | | | | | | 0.00 | | | | | | | | | | | | | | | |
| M | 44 | YD20 | | | | | 0.11 | 0.09 | 0.07 | | | | | | | 3.81 | 0.05 | 7.58 | | | | | | | |
| | <70 | YD21 | | | | | | | | 0.00 | | | | | | | | | | | | | | | |
| | 51 | YD22 | 0.15 | | | | | | | | | | | | | | | | | | | | | | |
| F | 51 | YD23 | | | | | | | | | | | | | | 0.84 | 0.00 | | | | | | | | |
| | <70 | YD24 | | | | | | | | | | | | | | | | | | 0.00 | | | | | |
| F | 33 | YD25 | | | | 0.00 | 0.00 | 0.00 | | | | 0.00 | 0.00 | | | 0.65 | 0.00 | | | | | | | | |
| | <70 | YD26 | 0.00 | 0.00 | 0.00 | 0.00 | 0.00 | 0.00 | 0.00 | 0.00 | 0.00 | 0.00 | 0.00 | 0.00 | 0.00 | 0.00 | 0.00 | | | 0.00 | | | | | |
| | <70 | YD27 | 0.00 | 0.00 | | | | | | | | | | | | | | | | | | | 1.95 | 0.58 | |
| | 55 | YD28 | | | | | 0.24 | 0.09 | 0.15 | | | | | | | 2.27 | | 4.39 | 1.62 | | 4.72 | 2.97 | | | |
| | <70 | YD29 | | | | 0.00 | | | | | 0.00 | 0.00 | 0.00 | 0.00 | 0.00 | 1.26 | 0.00 | | | | | | | | |
| M | 56 | YD30 | | | | | | | | | | | | | | 1.84 | | | | | | | | | |
| M | 52 | YD31 | | | 4.69 | | 0.00 | 0.00 | 0.00 | | | | | | | 18.93 | | | | | | | | | |
| | <70 | YD32 | | | 0.03 | | 0.17 | 0.07 | 0.05 | | | | | | | 0.36 | 0.07 | | | | | | | | |
| | 27 | YD33 | | | | 0.00 | | | | 0.00 | 0.00 | | | | | | | | | | | | 0.00 | 0.00 | |
| | 47 | YD34 | 0.00 | 0.00 | | | | | | | | | | | | | | | | | | | | | |
| | 26 | YD35 | | | 0.00 | | 0.00 | 0.00 | 0.00 | | | 0.00 | 0.00 | 0.00 | 0.00 | | | | | | 0.00 | 0.00 | 0.81 | | |
| | <70 | YD36 | | | | | | | | | | | | | | 0.00 | 0.00 | | | | 0.00 | 0.00 | 0.00 | 0.00 | |
| | 37 | YD37 | | | | | | | | | | | | | | 0.00 | 0.00 | | | | | | 0.00 | 0.00 | |
| | 30 | YD38 | | | | | 0.00 | 0.00 | 0.00 | | | | | | | | | | | | 0.00 | 0.00 | 0.10 | 0.00 | |
| | 47 | YD39 | | | | | | | | | | | | | | | | | | | | | 0.15 | 0.00 | |
| | 47 | YD40 | | | | | | | | | | | | | | | | | | | | | | | |
| | 44 | YD41 | | | 0.00 | | | | | | | | | | | | | | | | | | | | |
| | 49 | YD42 | | | | | | | | 0.00 | 0.00 | | | | | | | | | | | | 0.00 | 0.00 | |
| | 37 | YD43 | | | | | | | | | 0.00 | | | | | | | | | | | | 0.00 | 0.00 | |
| | 44 | YD44 | | | | | | | | 0.00 | 0.00 | | | | | | | | | | | | 0.00 | 0.00 | |
| M | 23 | YD47 | 0.00 | 0.00 | | | | | | | | 0.00 | 0.00 | 0.00 | 0.00 | | | | | | | | | | |
| M | <70 | YD48 | | | | | | | | | 0.00 | | | | | | | | | | | | 1.89 | | |
| F | 31 | YD49 | 0.00 | 0.00 | 0.00 | 0.00 | 0.00 | 0.00 | 0.00 | | | | | | | 1.53 | 0.00 | 0.21 | 0.36 | | 0.29 | 5.35 | | | |
| M | 54 | YD50 | | | | | 0.00 | 0.17 | 0.11 | | | | | | | 3.69 | | 1.36 | 1.50 | | 1.96 | 1.92 | | | |
| M | 68 | YD51 | | | | | | | | | | | | | | | | | | | | | | | |
| M | <70 | YD52 | | | | | | | | | | | | | | 0.32 | | 2.59 | 2.34 | | | | | | |
| F | <70 | YD53 | | | | | | | | | | | | | | 0.00 | 0.22 | 0.47 | 0.07 | | | | | | |
| M | <70 | YD54 | | | | | | | | | | | | | | 5.05 | 0.12 | 0.35 | 0.03 | | | | | | |
| M | 23 | YD55 | | | | | | | | | | | | | | 1.18 | | 1.67 | 0.61 | | | | | | |
| F | 63 | YD56 | 0.25 | 0.31 | | | | | | | | | | | | 1.21 | 0.15 | | | | | | | | |

***Append ix Table 4 – CD8+T-cell IFN-γ production elicited by HCMV protected and pp65/IE-1 peptides after peptide stimulation of PBMCs from OD donors >70 years*** The numbers provided indicate the percentage of CD8+T-cells responding to peptide stimulation with IFN-γ production of the total CD8+ T cell population.

| Sex | Age (when PBMCs tested) | | A1-RTD | A1-YAD | A3-RVD | A11-RSA | B7-RPR | B7-SPS | B7-YPR | B35-HPF | B44-NEG | B51-DAR | B51-TLM | B51-IPH | B51-WPK | Cw7-FRC | Cw7-SYR | Cw7-CRV | Cw-LSE | Cw16-YLC | B7-RPH | B7-TPR | A2-NLV | A1-VLE | A1-YSE | A1-VTE |
|---|---|---|---|---|---|---|---|---|---|---|---|---|---|---|---|---|---|---|---|---|---|---|---|---|---|---|
| | 78 | OD04 | 0 | 0 | | | | | | | 0 | | | | | | | | | 0 | | | | | 0.00 | 0.49 |
| F | 86 | ODO7 | 0 | 0 | | | 0 | 0 | 0 | | | | | | | 32.25 | 0 | 1.63 | | 12.19 | | | | | | |
| | 80 | ODO1 | | | 0 | | | | | | 0 | | | | | 0 | 0.05 | 0.00 | 0.00 | 0.09 | 0.00 | 0.00 | | | | |
| | 83 | OD08 | 0.58 | 0 | | | 0 | 0 | 0 | | | | | | | 0 | 0.34 | | | 0 | | | | | | |
| F | 86 | OD12 | | | | | 0 | 0 | 0 | | 0.06 | | | | | 1.68 | 0 | 20.83 | 16.70 | 0 | 5.55 | 0.30 | | | | |
| | 77 | OD21 | 0 | 0 | | | | | | | | | | | | | | | | | | | 0.77 | 0.00 | 0.00 | 0.00 |
| | 81 | OD28 | 0.15 | 0.05 | | | | | | | | | | | | | | | | 0.08 | | | 3.96 | | | |
| | | OD10 | 0 | 0 | | | | | | | | | | | | | | | | | | | | | 0.00 | 0.00 |
| F | 79 | OD11 | 0 | 0.28 | | | | 0.10 | 0.19 | 0.19 | | | | | | 4.88 | 0.08 | | | 0.40 | | | | | | |
| F | 81 | OD27 | | | | 0.06 | 0.06 | 0 | 0 | | 0 | | | | | 6.91 | 0 | 10.56 | 0.59 | 0.24 | 1.97 | 0.64 | 0.83 | 2.58 | | |
| | 79 | OD25 | 0 | 0.05 | | 0.03 | | | | 0 | | | | | | | | | | | | | | | | |
| | 74 | OD24 | | | | | 0 | 0 | 0 | | | | | | | | | | | | | | | | | |
| F | 71 | OD30 | | | | 0.64 | 0 | 0 | 0 | | | | | | | 4.81 | 0 | 12.71 | 6.11 | 0.56 | 0.75 | 0.00 | 1.41 | | | |
| | 69 | 0D37 | | | | | | | | 0.0000 | | | | | | | | | | | | | | | | |
| | 86 | OD40 | | | | | 0.00 | 0.00 | 0.00 | | | | | | | | | | | | | | | | | |
| | 72 | OD44 | | | | | 0.00 | 0.00 | 0.00 | 0.0000 | | | | | | | | | | | | | | | | |
| | 76 | 38CW | | | | | 0.00 | 0.00 | | | | | | | | 0.00 | 0.00 | | | | | | | | | |
| | 77 | OD47 | | | 0.15 | | 0.00 | 0.00 | 0.00 | 0.00 | | | | | | | | | | | | | | | | |
| | 86 | 0D49 | | | 1.76 | | 0.00 | 0.00 | 0.00 | 0.00 | | | | | | | | | | | | | | | | |
| | 66 | OD50 | | | | | | | | | 0.00 | | | | | | | | | | | | | | | |
| | 96 | OD52 | 0.00 | 0.00 | | | 0.00 | 0.00 | 0.00 | | | 0.00 | 0.00 | 0.00 | 0.00 | | | | | | 0.00 | 0.00 | | | | |
| | 75 | OD55 | | | | | 0.00 | 0.00 | 0.00 | | | | | | | 0.00 | 0.00 | | | | 0.00 | 0.00 | | | | |
| F | 87 | OD61 | | | | | 0.00 | 0.00 | 0.00 | | | 0.00 | 0.00 | 0.00 | 0.00 | 1.01 | 0.00 | | | | 0.45 | 2.33 | | | | |
| | 80 | OD54 | | | | | | | | 0.00 | | 0.00 | 0.00 | 0.00 | 0.00 | | | | | | | | | | | |
| | 68 | OD70 | | | 0.00 | | 0.00 | 0.00 | 0.00 | | | 0.00 | 0.00 | 0.00 | 0.00 | 0.00 | 0.00 | 2.28 | 0.00 | | 0.00 | 0.81 | 0.00 | 0.00 | | |
| | 87 | OD68 | | | | 0.00 | | | | | | | | | | | | | | | | | | | | |
| F | 70 | OD53 | | | | 0.36 | | | | | 0.00 | | | | | 0.00 | | 0.00 | 0.00 | | 0.00 | 0.00 | | | | |
| M | 88 | OD71 | 0.00 | 0.00 | | 0.00 | | | | | | 0.00 | 0.00 | 0.00 | 0.00 | 5.13 | 0.08 | 0.00 | | | 0.00 | 0.00 | | | 0.00 | 0.00 |
| | 74 | OD63 | 0.00 | 0.00 | | 0.00 | | | | | | 0.00 | 0.00 | 0.00 | 0.00 | | | | | | | | | | | |
| F | 70 | OD59 | | | | | 0.00 | 0.00 | 0.00 | 0.00 | 0.00 | | | | | 0.62 | 0.00 | | | | 0.00 | 1.94 | | | | |
| F | 78 | OD62 | 0.00 | 0.00 | | 0.00 | 0.00 | 0.00 | 0.00 | | | 0.00 | 0.00 | 0.00 | 0.00 | 16.89 | 0.00 | | | | 0.22 | 0.78 | | 0.00 | | |
| | 72 | OD56 | | | | | | | | 0.00 | 0.00 | | | | | | | | | | | | 0.24 | 2.38 | | |
| | 80 | OD14 | | | | | | | | | | | | | | | | | | | | | 2.57 | 0.00 | | |
| | 78 | OD15 | 0.00 | 0.00 | 0.00 | | 0.00 | 0.00 | 0.00 | | | | | | | | | | | | 0.00 | 1.29 | | | 0.00 | 0.15 |
| | 71 | OD06 | | | 0.00 | | | 0.00 | 0.00 | | 0.00 | | | | | 0.00 | 0.00 | | 0.00 | 0.00 | 0.13 | 0.10 | | | | |
| | 77 | OD45 | | | | | 0.00 | 0.00 | 0.00 | | 0.00 | | | | | | | | | | 1.06 | 4.75 | 0.00 | 0.00 | | |
| | 77 | OD46 | | | 0.00 | | 0.00 | 0.00 | 0.00 | | 0.00 | | | | | | | | | | 1.46 | 1.74 | 0.30 | 0.44 | | |

***Append ix Table 5– CD8+T-cell IL-2 production elicited by HCMV protected and pp65/IE-1 peptides after peptide stimulation of PBMCs from OD donors >70 years.*** The numbers provided indicate the percentage of CD8+T-cells responding to peptide stimulation with IL-2 production of the total CD8+ T cell population.

| Sex | Age (when PBMCs tested) | | A1-RTD | A1-YAD | A3-RVD | A11-RSA | B7-RPR | B7-SPS | B7-YPR | B35-HPF | B44-NEG | B51-DAR | B51-TLM | B51-IPH | B51-WPK | Cw7-FRC | Cw7-SYR | Cw7-CRV | Cw7-LSE | Cw16-YLC | B7-RPH | B7-TPR | A2-NLV | A1-VLE | A1-YSE | A1-VTE |
|---|---|---|---|---|---|---|---|---|---|---|---|---|---|---|---|---|---|---|---|---|---|---|---|---|---|---|
| | 78 | OD04 | 0 | 0.07 | | | | | | | 0 | | | | | | | | | 0 | | | | | 0.00 | 0.00 |
| F | 86 | OD07 | 0 | 0 | | | 0 | 0 | 0 | | | | | | | 4.23 | 0 | | | 1.16 | | | | | | |
| | 80 | OD01 | | | 0 | | | | | | 0.04 | | | | | 0.07 | 0.05 | 0.00 | 0.00 | 0.04 | 0.00 | 0.00 | | | | |
| | 83 | OD08 | 0.21 | 0 | | | 0 | 0 | 0 | | | | | | | 0 | 0.19 | | | 0 | | | | | | |
| F | 86 | OD12 | | | | | 0 | 0 | 0 | | 0.06 | | | | | 0.12 | 0 | 10.81 | 0.10 | 0 | 9.58 | 7.44 | | | | |
| | 77 | OD21 | 0 | 0 | | | | | | | | | | | | | | | | | | | 0.08 | 0.00 | 0.00 | 0.00 |
| | 81 | OD28 | 0.10 | 0.05 | | | | | | | | | | | | | | | | 0.03 | | | 0.84 | | | |
| | | OD10 | 0 | 0 | | | | | | | | | | | | | | | | | | | | | 0.00 | 0.00 |
| F | 79 | OD11 | 0 | 0 | | | | | 0 | 0 | | | | | | 0.29 | 0 | | | 0 | | | | | | |
| F | 81 | OD27 | | | | 0 | 0 | 0 | 0 | | 0.07 | | | | | 0.86 | 0 | 1.80 | 0.03 | 0 | 0.37 | 0.00 | 0.00 | 0.39 | | |
| | 79 | OD25 | 0 | 0.08 | | 0 | | | | 0 | | | | | | | | | | | | | | | | |
| | 74 | OD24 | | | | | 0 | 0 | 0 | | | | | | | | | | | | 0.00 | 0.00 | 0.00 | 0.00 | | |
| F | 71 | OD30 | | | | 0.22 | 0 | 0 | 0 | | | | | | | 0.58 | 0 | 0.53 | 0.02 | 0.09 | 0.25 | 0.00 | 0.40 | | | |
| | 69 | 0D37 | | | | | | | | 0.0729 | | | | | | | | | | | | | | | | |
| | 86 | 0D40 | | | | | 0.06 | 0.14 | 0.06 | | | | | | | | | | | | | | | | | |
| | 72 | 0D44 | | | | | 0.05 | 0.10 | 0.05 | 0.12 | | | | | | | | | | | | | | | | |
| | 76 | 38CW | | | | | 0.00 | 0.07 | | | | | | | | 0.00 | 0.01 | | | | | | | | | |
| | 77 | OD47 | | | 0.00 | | 0.04 | 0.00 | 0.00 | 0.04 | | | | | | | | | | | | | | | | |
| | 86 | OD49 | | | 0.00 | | 0.00 | 0.00 | 0.00 | 0.00 | | | | | | | | | | | | | | | | |
| | 66 | OD50 | | | | | | | | | 0.00 | | | | | | | | | | | | | | | |
| | 96 | OD52 | 0.00 | 0.00 | | | 0.00 | 0.00 | 0.00 | | | 0.00 | 0.00 | 0.00 | 0.00 | | | | | | 0.00 | 0.00 | | | | |
| | 75 | OD55 | | | | | 0.00 | 0.00 | 0.00 | | | | | | | 0.00 | 0.00 | | | | 0.00 | 0.00 | | | | |
| F | 87 | OD61 | | | | | 0.00 | 0.00 | 0.00 | | | 0.00 | 0.00 | 0.00 | 0.00 | 0.00 | 0.00 | | | | 0.00 | 0.00 | | | | |
| | 80 | OD54 | | | | | | | | | | 0.00 | 0.00 | 0.00 | 0.00 | | | | | | | | | | | |
| | 68 | OD70 | | | 0.00 | | 0.00 | 0.00 | 0.00 | | | 0.00 | 0.00 | 0.00 | 0.00 | 0.00 | 0.00 | 0.00 | 0.00 | | 0.00 | 0.10 | 0.00 | 0.00 | | |
| | 87 | OD68 | | | | 0.00 | | | | | | | | | | | | | | | | | | | | |
| F | 70 | OD53 | | | | 0.05 | | | | | 0.00 | | | | | 0.00 | | 0.00 | | | 0.00 | 0.00 | | | | |
| M | 88 | OD71 | 0.00 | 0.00 | | 0.00 | | | | | | 0.00 | 0.00 | 0.00 | 0.00 | 0.11 | 0.00 | 0.00 | | | | | | | 0.00 | 0.00 |
| | 74 | OD63 | 0.00 | 0.00 | | 0.00 | | | | | | 0.00 | 0.00 | 0.00 | 0.00 | | | | | | | | | | | |
| F | 70 | OD59 | | | | | 0.00 | 0.00 | 0.00 | 0.00 | 0.00 | | | | | 0.00 | 0.00 | | | | 0.00 | 0.13 | | | | |
| F | 78 | OD62 | 0.00 | 0.00 | | 0.00 | 0.00 | 0.00 | 0.00 | | | 0.00 | 0.00 | 0.00 | 0.00 | 0.50 | 0.00 | | | | 0.00 | 0.08 | | 0.00 | | |
| | 72 | OD56 | | | | | | | | 0.00 | 0.00 | | | | | | | | | | | | 0.00 | 0.29 | | |
| | 80 | OD14 | | | | | | | | | | | | | | | | | | | | | 0.00 | 0.00 | | |
| | 78 | OD15 | 0.00 | 0.00 | 0.00 | | 0.00 | 0.00 | 0.00 | | | | | | | | | | | | 0.00 | 0.19 | | | 0.00 | 0.08 |
| | 71 | OD06 | | | 0.00 | | | 0.00 | 0.00 | | 0.00 | | | | | | 0.84 | | 0.00 | 0.16 | 0.00 | 0.00 | | | | |
| | 77 | DR | | | | | 0.00 | 0.00 | 0.00 | | 0.00 | | | | | | | | | | 0.00 | 1.02 | 0.00 | 0.00 | | |
| | 77 | RR | | | 0.00 | | 0.00 | 0.00 | 0.00 | | 0.00 | | | | | | | | | | 0.47 | 0.46 | 0.08 | 0.00 | | |

***Append ix Table 6 – CD8+T-cell TNF-α production elicited by HCMV protected and pp65/IE-1 peptides after peptide stimulation of PBMCs from OD donors >70 years.*** The numbers provided indicate the percentage of CD8+T-cells responding to peptide stimulation with TNF-α production of the total CD8+ T cell population.

| Sex | Age (when PBMCs tested) | | A1-RTD | A1-YAD | A3-RVD | A11-RSA | B7-RPR | B7-SPS | B7-YPR | B35-HPF | B44-NEG | B51-DAR | B51-TLM | B51-IPH | B51-WPK | Cw7-FRC | Cw7-SYR | Cw7-CRV | Cw-LSE | Cw16-YLC | B7-RPH | B7-TPR | A2-NLV | A1-VLE | A1-YSE | A1-VTE |
|---|---|---|---|---|---|---|---|---|---|---|---|---|---|---|---|---|---|---|---|---|---|---|---|---|---|---|
| | 78 | OD04 | 0 | 0 | | | | | | | 0 | | | | | | | | | 0 | | | | | 0.00 | 0.49 |
| F | 86 | ODO7 | 0 | 0 | | | 0 | 0 | 0 | | | | | | | 32.25 | 0 | 1.63 | | 12.19 | | | | | | |
| | 80 | ODO1 | | | 0 | | | | | | 0 | | | | | 0 | 0.05 | 0.00 | 0.00 | 0.09 | 0.00 | 0.00 | | | | |
| | 83 | OD08 | 0.58 | 0 | | | 0 | 0 | 0 | | | | | | | 0 | 0.34 | | | 0 | | | | | | |
| F | 86 | OD12 | | | | | 0 | 0 | 0 | | 0.06 | | | | | 1.68 | 0 | 20.83 | 16.70 | 0 | 5.55 | 0.30 | | | | |
| | 77 | OD21 | 0 | 0 | | | | | | | | | | | | | | | | | | | 0.77 | 0.00 | 0.00 | 0.00 |
| | 81 | OD28 | 0.15 | 0.05 | | | | | | | | | | | | | | | | 0.08 | | | 3.96 | | | |
| | | OD10 | 0 | 0 | | | | | | | | | | | | | | | | | | | | | 0.00 | 0.00 |
| F | 79 | OD11 | 0 | 0.28 | | | | 0.10 | 0.19 | 0.19 | | | | | | 4.88 | 0.08 | | | 0.40 | | | | | | |
| F | 81 | OD27 | | | | 0.06 | 0.06 | 0 | 0 | | 0 | | | | | 6.91 | 0 | 10.56 | 0.59 | 0.24 | 1.97 | 0.64 | 0.83 | 2.58 | | |
| | 79 | OD25 | 0 | 0.05 | | 0.03 | | | | 0 | | | | | | | | | | | | | | | | |
| | 74 | OD24 | | | | | 0 | 0 | 0 | | | | | | | | | | | | | | | | | |
| F | 71 | OD30 | | | | 0.64 | 0 | 0 | 0 | | | | | | | 4.81 | 0 | 12.71 | 6.11 | 0.56 | 0.75 | 0.00 | 1.41 | | | |
| | 69 | 0D37 | | | | | | | | 0.0000 | | | | | | | | | | | | | | | | |
| | 86 | OD40 | | | | | 0.00 | 0.00 | 0.00 | | | | | | | | | | | | | | | | | |
| | 72 | OD44 | | | | | 0.00 | 0.00 | 0.00 | 0.0000 | | | | | | | | | | | | | | | | |
| | 76 | 38CW | | | | | 0.00 | 0.00 | | | | | | | | 0.00 | 0.00 | | | | | | | | | |
| | 77 | OD47 | | | 0.15 | | 0.00 | 0.00 | 0.00 | 0.00 | | | | | | | | | | | | | | | | |
| | 86 | 0D49 | | | 1.76 | | 0.00 | 0.00 | 0.00 | 0.00 | | | | | | | | | | | | | | | | |
| | 66 | OD50 | | | | | | | | | 0.00 | | | | | | | | | | | | | | | |
| | 96 | OD52 | 0.00 | 0.00 | | | 0.00 | 0.00 | 0.00 | | | 0.00 | 0.00 | 0.00 | 0.00 | | | | | | 0.00 | 0.00 | | | | |
| | 75 | OD55 | | | | | 0.00 | 0.00 | 0.00 | | | | | | | 0.00 | 0.00 | | | | 0.00 | 0.00 | | | | |
| F | 87 | OD61 | | | | | 0.00 | 0.00 | 0.00 | | | 0.00 | 0.00 | 0.00 | 0.00 | 1.01 | 0.00 | | | | 0.45 | 2.33 | | | | |
| | 80 | OD54 | | | | | | | | 0.00 | | 0.00 | 0.00 | 0.00 | 0.00 | | | | | | | | | | | |
| | 68 | OD70 | | | 0.00 | | 0.00 | 0.00 | 0.00 | | | 0.00 | 0.00 | 0.00 | 0.00 | 0.00 | 0.00 | 2.28 | 0.00 | | 0.00 | 0.81 | 0.00 | 0.00 | | |
| | 87 | OD68 | | | | 0.00 | | | | | | | | | | | | | | | | | | | | |
| F | 70 | OD53 | | | | 0.36 | | | | | 0.00 | | | | | 0.00 | | 0.00 | 0.00 | | 0.00 | 0.00 | | | | |
| M | 88 | OD71 | 0.00 | 0.00 | | 0.00 | | | | | | 0.00 | 0.00 | 0.00 | 0.00 | 5.13 | 0.08 | 0.00 | | | 0.00 | 0.00 | | | 0.00 | 0.00 |
| | 74 | OD63 | 0.00 | 0.00 | | 0.00 | | | | | | 0.00 | 0.00 | 0.00 | 0.00 | | | | | | | | | | | |
| F | 70 | OD59 | | | | | 0.00 | 0.00 | 0.00 | 0.00 | 0.00 | | | | | 0.62 | 0.00 | | | | 0.00 | 1.94 | | | | |
| F | 78 | OD62 | 0.00 | 0.00 | | 0.00 | 0.00 | 0.00 | 0.00 | | | 0.00 | 0.00 | 0.00 | 0.00 | 16.89 | 0.00 | | | | 0.22 | 0.78 | | 0.00 | | |
| | 72 | OD56 | | | | | | | | 0.00 | 0.00 | | | | | | | | | | | | 0.24 | 2.38 | | |
| | 80 | OD14 | | | | | | | | | | | | | | | | | | | | | 2.57 | 0.00 | | |
| | 78 | OD15 | 0.00 | 0.00 | 0.00 | | 0.00 | 0.00 | 0.00 | | | | | | | | | | | | 0.00 | 1.29 | | | 0.00 | 0.15 |
| | 71 | OD06 | | | 0.00 | | | 0.00 | 0.00 | | 0.00 | | | | | 0.00 | 0.00 | | 0.00 | 0.00 | 0.13 | 0.10 | | | | |
| | 77 | OD45 | | | | | 0.00 | 0.00 | 0.00 | | 0.00 | | | | | | | | | | 1.06 | 4.75 | 0.00 | 0.00 | | |
| | 77 | OD46 | | | 0.00 | | 0.00 | 0.00 | 0.00 | | 0.00 | | | | | | | | | | 1.46 | 1.74 | 0.30 | 0.44 | | |

***Appendix fig 1 - Calculation of the average increase of the HLA-Cw*0702-restricted CD8+T-cells in the periphery with increment decades of the donor cohort***

A)

| 20-40 years | | |
|---|---|---|
| Donor | IFN | TNF |
| YD14 | 0.39 | 0.47 |
| YD49 | 1.42 | 1.53 |
| YD25 | 0.36 | 0.65 |
| YD55 | 1.72 | 1.18 |
| YD52 | 0.13 | 0.32 |
| **Average** | **0.81** | **0.96** |

| 40-60 years | | |
|---|---|---|
| Donor | IFN | TNF |
| YD6 | 1.28 | 1.25 |
| YD16 | 0.03 | 0.03 |
| YD17 | 0.38 | 0.24 |
| YD20 | 4.14 | 3.81 |
| YD50 | 4.69 | 3.69 |
| YD5 | 0 | 0.15 |
| YD13 | 2.09 | 2.25 |
| YD23 | 0.71 | 0.84 |
| YD30 | 1.76 | 1.84 |
| YD31 | 18.18 | 18.93 |
| YD28 | 1.86 | 2.27 |
| **Average** | **3.19** | **3.21** |
| **% increase from 20-40 years** | **2.39** | **2.25** |

| 60-80 years | | |
|---|---|---|
| Donor | IFN | TNF |
| YD56 | 1.14 | 1.21 |
| OD59 | 0.62 | 0.45 |
| OD11 | 4.88 | 6.03 |
| YD54 | 5.28 | 5.05 |
| OD30 | 4.81 | 6.15 |
| OD53 | 0.00 | 0.18 |
| OD62 | 16.89 | 17.89 |
| **Average** | **4.80** | **5.28** |
| **% increase from 40-60 years** | **1.48** | **1.98** |

| 80-100 years | | |
|---|---|---|
| Donor | IFN | TNF |
| OD07 | 32.25 | 31.07 |
| OD12 | 1.68 | 17.71 |
| OD27 | 6.91 | 7.34 |
| OD61 | 1.01 | 0.00 |
| OD71 | 5.13 | 6.52 |
| **Average** | **9.40** | **12.53** |
| **% increase from 60-80 years** | **4.59** | **7.25** |

| Average increase in FRC-specific CD8+ T cells | | |
|---|---|---|
| Age (years) | Relative Increase in CD8+FRC+IFN+ | Relative Increase in CD8+FRC+TNF+ |
| 20-40 | - | - |
| 40-60 | 2.36 | 2.34 |
| 60-80 | 1.48 | 1.98 |
| 80-100 | 4.59 | 7.25 |
| **per decade average** | **1.41** | **1.93** |

B)

| 20-40 years | | |
|---|---|---|
| Donor | IFN | TNF |
| YD14 | 0.29 | 0.25 |
| YD49 | 0.08 | 0.21 |
| YD55 | 2.10 | 1.67 |
| YD52 | 2.44 | 2.59 |
| **Average** | **1.23** | **1.18** |

| 40-60 years | | |
|---|---|---|
| Donor | IFN | TNF |
| YD6 | 0.92 | 0.89 |
| YD13 | 1.60 | 1.48 |
| YD20 | 5.96 | 7.58 |
| YD50 | 1.57 | 1.36 |
| YD28 | 3.56 | 4.39 |
| **Average** | **2.72** | **3.14** |
| **% increase from 20-40 years** | **1.50** | **1.96** |

| 60-80 years | | |
|---|---|---|
| Donor | IFN | TNF |
| OD70 | 2.28 | 3.88 |
| OD30 | 12.71 | 12.75 |
| YD53 | 0.51 | 0.47 |
| YD54 | 0.01 | 0.35 |
| **Average** | **3.88** | **4.36** |
| **% increase from 40-60 years** | **1.16** | **1.22** |

| 80-100 years | | |
|---|---|---|
| Donor | IFN | TNF |
| OD07 | 1.63 | 1.47 |
| OD12 | 20.83 | 21.43 |
| OD27 | 10.56 | 10.56 |
| **Average** | **11.01** | **11.16** |
| **% increase from 60-80 years** | **7.13** | **6.79** |

| Average increase in CRV-specific CD8+ T cells | | |
|---|---|---|
| Age (years) | Relative Increase in CD8+CRV+IFN+ | Relative Increase in CD8+CRV+TNF+ |
| 20-40 | - | - |
| 40-60 | 1.50 | 1.96 |
| 60-80 | 5.47 | 5.96 |
| 80-100 | 7.13 | 6.79 |
| **per decade average** | **2.35** | **2.45** |

C)

| 20-40 years | | |
|---|---|---|
| Donor | IFN | TNF |
| YD49 | 0.07 | 0.36 |
| YD55 | 0.69 | 0.61 |
| YD52 | 1.78 | 2.34 |
| **Average** | **0.85** | **1.10** |

| 40-60 years | | |
|---|---|---|
| Donor | IFN | TNF |
| YD6 | 0.29 | 1.46 |
| YD13 | 1.15 | 1.33 |
| YD50 | 1.31 | 1.5 |
| YD28 | 0.83 | 1.62 |
| **Average** | **0.89** | **1.48** |
| **% increase from 20-40 years** | **0.05** | **0.37** |

| 60-80 years | | |
|---|---|---|
| Donor | IFN | TNF |
| OD30 | 6.11 | 8.23 |
| YD53 | 0.03 | 0.07 |
| YD54 | 0.01 | 0.03 |
| **Average** | **2.05** | **2.77** |
| **% increase from 40-60 years** | **1.16** | **1.30** |

| 80-100 years | | |
|---|---|---|
| Donor | IFN | TNF |
| OD12 | 16.70 | 14.09 |
| OD27 | 0.59 | 0.73 |
| **Average** | **8.65** | **7.41** |
| **% increase from 60-80 years** | **2.54** | **-0.82** |

| Average increase in LSE-specific CD8+ T cells | | |
|---|---|---|
| Age (years) | Relative Increase in CD8+LSE+IFN+ | Relative Increase in CD8+LSE+TNF+ |
| 20-40 | - | - |
| 40-60 | 0.05 | 0.37 |
| 60-80 | 1.16 | 1.30 |
| 80-100 | 6.59 | 4.54 |
| **per decade average** | **1.30** | **1.04** |

***Appendix Table 7 and 8 – CD8+T-cell cytokine production elicited by HCMV cryptic epitopes in YD (<70 years, Table 7) and OD (>70years, Table 8) donors***

| YD <70 years | | | | | | | | |
|---|---|---|---|---|---|---|---|---|
| | | | IFN | | IL-2 | | TNF | |
| Sex | Donor | Age | RPW | APD | RPW | APD | RPW | APD |
| F | YD49 | 31 | 0.79426083 | | 0.17530532 | | 0.79487179 | |
| F | YD7 | 30 | | 0 | | 0 | | 0 |
| F | YD12 | 44 | 0 | 0 | 0 | 0 | 0 | 0 |
| | YD44 | 44 | | 0.22472653 | | 0.12376238 | | 0.60185915 |
| M | YD50 | 54 | 0.36897893 | | 0.26499966 | | 0.55540318 | |
| M | YD28 | 56 | 0.11763584 | | 0.06321113 | | 0.10302406 | |
| M | YD57 | 60 | 0 | | 0 | | 0 | |
| | YD58 | 55 | | 0.15012848 | | 0.16869292 | | 0.50352165 |
| | YD59 | 23 | 0 | | 0 | | 0 | |
| | YD60 | <70 | | 0 | | 0 | | 0 |
| F | YD61 | <70 | 0 | | | | | |
| F | YD13 | 52 | 0 | | 0 | | 0 | |

| OD >70 years | | | | | | | | |
|---|---|---|---|---|---|---|---|---|
| | | | IFN | | IL-2 | | TNF | |
| Sex | Donor | Age | RPW | APD | RPW | APD | RPW | APD |
| | OD06 | 71 | 0 | | 0 | | 0 | |
| F | OD59 | 67 | 0 | 0 | 0 | 0 | 0 | 0 |
| | OD30 | 71 | 0 | 0 | 0 | 0 | 0 | 0 |
| | OD47 | 77 | 0 | 0 | 0 | 0 | 0 | 0 |
| | OD46 | 77 | 0 | | 0 | | 0 | |
| | OD45 | 77 | 1.23045169 | | 0.13864079 | | 1.11774654 | |
| F | OD12 | 86 | 0 | | 0 | | 0 | |
| | OD49 | 86 | 2.43001443 | 0 | 1.22014688 | 0 | 2.56823678 | 0 |
| | OD52 | 96 | 0 | | 0 | | 0 | |
| | OD25 | 79 | | 0.56970989 | | 0.08889736 | | 0.66804687 |
| | OD55 | 75 | 0 | | 0 | | 0 | |
| | OD56 | 72 | | 0.31901174 | | 0.06565858 | | 0.22812212 |
| F | OD61 | 87 | 0 | | 0 | | 0 | |
| F | OD27 | 81 | 0.52778233 | | 0.53655265 | | 0.83924468 | |
| F | OD62 | 78 | 0 | | 0 | | 0 | |
| M | OD15 | 78 | 0.37603409 | | 0.0751503 | | 0.4258517 | |

# CHAPTER 10 - BIBLIOGRAPHY


1. Reddehase, M.J.e.o.c. and N.e.o.c. Lemmermann, *Cytomegaloviruses : from molecular pathogenesis to intervention*. Updated and upgraded second edition. ed. 2013.
2. van de Berg, P.J., et al., *Cytomegalovirus-induced effector T cells cause endothelial cell damage.* Clin Vaccine Immunol, 2012. **19**(5): p. 772-9.
3. Redeker, A., S.P. Welten, and R. Arens, *Viral inoculum dose impacts memory T-cell inflation.* Eur J Immunol, 2013.
4. Wall, N.A., et al., *Cytomegalovirus seropositivity is associated with increased arterial stiffness in patients with chronic kidney disease.* PLoS One, 2013. **8**(2): p. e55686.
5. Pawelec, G., *Immunosenenescence: role of cytomegalovirus.* Exp Gerontol, 2014. **54**: p. 1-5.
6. Sansoni, P., et al., *New advances in CMV and immunosenescence.* Exp Gerontol, 2014.
7. Derhovanessian, E., et al., *Cytomegalovirus-associated accumulation of late-differentiated CD4 T-cells correlates with poor humoral response to influenza vaccination.* Vaccine, 2013. **31**(4): p. 685-90.
8. Thomas, S., et al., *Evaluating Human T-Cell Therapy of Cytomegalovirus Organ Disease in HLA-Transgenic Mice.* PLoS Pathog, 2015. **11**(7): p. e1005049.
9. Reddehase, M.J., *Antigens and immunoevasins: opponents in cytomegalovirus immune surveillance.* Nat Rev Immunol, 2002. **2**(11): p. 831-44.
10. Schleiss, M.R., *Animal models of congenital cytomegalovirus infection: an overview of progress in the characterization of guinea pig cytomegalovirus (GPCMV).* Journal of Clinical Virology, 2002. **25, Supplement 2**(0): p. 37-49.
11. Hansen, S.G., et al., *Profound early control of highly pathogenic SIV by an effector memory T-cell vaccine.* Nature, 2011. **473**(7348): p. 523-527.
12. Hansen, S.G., et al., *Cytomegalovirus Vectors Violate CD8+ T Cell Epitope Recognition Paradigms.* Science, 2013. **340**(6135): p. 1237874-1237874.
13. Hansen, S.G., et al., *Effector memory T cell responses are associated with protection of rhesus monkeys from mucosal simian immunodeficiency virus challenge.* Nature Medicine, 2009. **15**(3): p. 293-299.
14. Sinzger, C., M. Digel, and G. Jahn, *Cytomegalovirus cell tropism.* Curr Top Microbiol Immunol, 2008. **325**: p. 63-83.
15. Sinclair, J., *Human cytomegalovirus: Latency and reactivation in the myeloid lineage.* J Clin Virol, 2008. **41**(3): p. 180-5.
16. Bissinger, A.L., et al., *Human cytomegalovirus as a direct pathogen: Correlation of multiorgan involvement and cell distribution with clinical and pathological findings in a case of congenital inclusion disease.* Journal of Medical Virology, 2002. **67**(2): p. 200-206.
17. Varnum, S.M., et al., *Identification of proteins in human cytomegalovirus (HCMV) particles: the HCMV proteome.* J Virol, 2004. **78**(20): p. 10960-6.
18. Rogers, N., *A dormant danger: New therapies target a ubiquitous pathogen known as cytomegalovirus.* Nat Med, 2015. **21**(10): p. 1104-5.

19. Jean Beltran, P.M. and I.M. Cristea, *The life cycle and pathogenesis of human cytomegalovirus infection: lessons from proteomics.* Expert Rev Proteomics, 2014. **11**(6): p. 697-711.
20. Crough, T. and R. Khanna, *Immunobiology of human cytomegalovirus: from bench to bedside.* Clin Microbiol Rev, 2009. **22**(1): p. 76-98, Table of Contents.
21. Luckheeram, R.V., et al., *CD4⁺T cells: differentiation and functions.* Clin Dev Immunol, 2012. **2012**: p. 925135.
22. Hewitt, E.W., *The MHC class I antigen presentation pathway: strategies for viral immune evasion.* Immunology, 2003. **110**(2): p. 163-9.
23. Vantourout, P. and A. Hayday, *Six-of-the-best: unique contributions of γδ T cells to immunology.* Nat Rev Immunol, 2013. **13**(2): p. 88-100.
24. Dustin, M.L. and D. Depoil, *New insights into the T cell synapse from single molecule techniques.* Nat Rev Immunol, 2011. **11**(10): p. 672-84.
25. Dustin, M.L. and E.O. Long, *Cytotoxic immunological synapses.* Immunol Rev, 2010. **235**(1): p. 24-34.
26. Kagi, D., et al., *Fas and perforin pathways as major mechanisms of T cell-mediated cytotoxicity.* Science, 1994. **265**(5171): p. 528-30.
27. Turner, S.J., et al., *Structural determinants of T-cell receptor bias in immunity.* Nat Rev Immunol, 2006. **6**(12): p. 883-94.
28. Lefranc, M.P., et al., *IMGT®, the international ImMunoGeneTics information system® 25 years on.* Nucleic Acids Res, 2015. **43**(Database issue): p. D413-22.
29. Wherry, E.J. and R. Ahmed, *Memory CD8 T-cell differentiation during viral infection.* J Virol, 2004. **78**(11): p. 5535-45.
30. Badovinac, V.P., B.B. Porter, and J.T. Harty, *Programmed contraction of CD8+ T cells after infection.* Nat Immunol, 2002. **3**(7): p. 619-626.
31. Sallusto, F., J. Geginat, and A. Lanzavecchia, *Central memory and effector memory T cell subsets: function, generation, and maintenance.* Annu Rev Immunol, 2004. **22**: p. 745-63.
32. Mueller, S.N., et al., *Memory T cell subsets, migration patterns, and tissue residence.* Annu Rev Immunol, 2013. **31**: p. 137-61.
33. Macagno, A., et al., *Isolation of human monoclonal antibodies that potently neutralize human cytomegalovirus infection by targeting different epitopes on the gH/gL/UL128-131A complex.* J Virol, 2010. **84**(2): p. 1005-13.
34. Sallusto, F., J. Geginat, and A. Lanzavecchia, *CentralMemory andEffectorMemoryT CellSubsets: Function, Generation, and Maintenance.* Annual Review of Immunology, 2004. **22**(1): p. 745-763.
35. Hosking, M.P., et al., *CD8+ memory T cells appear exhausted within hours of acute virus infection.* J Immunol, 2013. **191**(8): p. 4211-22.
36. Tchilian, E.Z. and P.C. Beverley, *Altered CD45 expression and disease.* Trends Immunol, 2006. **27**(3): p. 146-53.
37. Carrasco, J., et al., *CD45RA on human CD8 T cells is sensitive to the time elapsed since the last antigenic stimulation.* Blood, 2006. **108**(9): p. 2897-905.
38. Mueller, S.N. and L.K. Mackay, *Tissue-resident memory T cells: local specialists in immune defence.* Nat Rev Immunol, 2016. **16**(2): p. 79-89.
39. Schenkel, J.M. and D. Masopust, *Tissue-resident memory T cells.* Immunity, 2014. **41**(6): p. 886-97.

40. Jackson, S.E., G.M. Mason, and M.R. Wills, *Human cytomegalovirus immunity and immune evasion.* Virus Research, 2011. **157**(2): p. 151-160.
41. Compton, T., et al., *Human cytomegalovirus activates inflammatory cytokine responses via CD14 and Toll-like receptor 2.* J Virol, 2003. **77**(8): p. 4588-96.
42. Vivier, E., et al., *Innate or adaptive immunity? The example of natural killer cells.* Science, 2011. **331**(6013): p. 44-9.
43. Marcenaro, E., et al., *NK cells and their receptors during viral infections.* Immunotherapy, 2011. **3**(9): p. 1075-86.
44. Smith, M.S., et al., *Human cytomegalovirus induces monocyte differentiation and migration as a strategy for dissemination and persistence.* J Virol, 2004. **78**(9): p. 4444-53.
45. Sinclair, J. and M. Reeves, *The intimate relationship between human cytomegalovirus and the dendritic cell lineage.* Front Microbiol, 2014. **5**: p. 389.
46. Sun, J.C., A. Ma, and L.L. Lanier, *Cutting edge: IL-15-independent NK cell response to mouse cytomegalovirus infection.* J Immunol, 2009. **183**(5): p. 2911-4.
47. Foley, B., et al., *Cytomegalovirus reactivation after allogeneic transplantation promotes a lasting increase in educated NKG2C+ natural killer cells with potent function.* Blood, 2012. **119**(11): p. 2665-2674.
48. Jackson, S.E., G.M. Mason, and M.R. Wills, *Human cytomegalovirus immunity and immune evasion.* Virus Res, 2011. **157**(2): p. 151-60.
49. Jacob, C.L., et al., *Neutralizing antibodies are unable to inhibit direct viral cell-to-cell spread of human cytomegalovirus.* Virology, 2013. **444**(1-2): p. 140-7.
50. Parry, H.M., et al., *Cytomegalovirus viral load within blood increases markedly in healthy people over the age of 70 years.* Immun Ageing, 2016. **13**: p. 1.
51. Bunde, T., et al., *Protection from cytomegalovirus after transplantation is correlated with immediate early 1–specific CD8 T cells.* The Journal of Experimental Medicine, 2005. **201**(7): p. 1031-1036.
52. Gamadia, L.E., et al., *Properties of CD4(+) T cells in human cytomegalovirus infection.* Hum Immunol, 2004. **65**(5): p. 486-92.
53. Einsele, H., et al., *Infusion of cytomegalovirus (CMV)-specific T cells for the treatment of CMV infection not responding to antiviral chemotherapy.* Blood, 2002. **99**(11): p. 3916-22.
54. Walter, E.A., et al., *Reconstitution of Cellular Immunity against Cytomegalovirus in Recipients of Allogeneic Bone Marrow by Transfer of T-Cell Clones from the Donor.* New England Journal of Medicine, 1995. **333**(16): p. 1038-1044.
55. Li, C.R., et al., *Recovery of HLA-restricted cytomegalovirus (CMV)-specific T-cell responses after allogeneic bone marrow transplant: correlation with CMV disease and effect of ganciclovir prophylaxis.* Blood, 1994. **83**(7): p. 1971-9.
56. Widmann, T., et al., *Levels of CMV Specific CD4 T Cells Are Dynamic and Correlate with CMV Viremia after Allogeneic Stem Cell Transplantation.* PLOS ONE, 2008. **3**(11): p. e3634.
57. Sylwester, A.W., et al., *Broadly targeted human cytomegalovirus-specific CD4+ and CD8+ T cells dominate the memory compartments of exposed subjects.* J Exp Med, 2005. **202**(5): p. 673-85.
58. Elkington, R., et al., *Ex vivo profiling of CD8+-T-cell responses to human cytomegalovirus reveals broad and multispecific reactivities in healthy virus carriers.* J Virol, 2003. **77**(9): p. 5226-40.

59. Pourgheysari, B., et al., *The Cytomegalovirus-Specific CD4+ T-Cell Response Expands with Age and Markedly Alters the CD4+ T-Cell Repertoire. Journal of Virology*, 2007. **81**: p. 7759-7765.
60. Pachnio, A., et al., *The Cellular Localization of Human Cytomegalovirus Glycoprotein Expression Greatly Influences the Frequency and Functional Phenotype of Specific CD4+ T Cell Responses.* J Immunol, 2015. **195**(8): p. 3803-15.
61. Pachnio, A., et al., *Cytomegalovirus Infection Leads to Development of High Frequencies of Cytotoxic Virus-Specific CD4+ T Cells Targeted to Vascular Endothelium.* PLoS Pathog, 2016. **12**(9): p. e1005832.
62. Verma, S., et al., *Cytomegalovirus-Specific CD4 T Cells Are Cytolytic and Mediate Vaccine Protection.* J Virol, 2016. **90**(2): p. 650-8.
63. Reddehase, M.J., et al., *CD8-positive T lymphocytes specific for murine cytomegalovirus immediate-early antigens mediate protective immunity.* J Virol, 1987. **61**(10): p. 3102-8.
64. Riddell, S.R., et al., *Restoration of viral immunity in immunodeficient humans by the adoptive transfer of T cell clones.* Science, 1992. **257**(5067): p. 238-41.
65. Chen, G., et al., *CD8 T cells specific for human immunodeficiency virus, Epstein-Barr virus, and cytomegalovirus lack molecules for homing to lymphoid sites of infection.* Blood, 2001. **98**(1): p. 156-64.
66. Doisne, J.M., et al., *CD8+ T cells specific for EBV, cytomegalovirus, and influenza virus are activated during primary HIV infection.* J Immunol, 2004. **173**(4): p. 2410-8.
67. Gamadia, L.E., et al., *Primary immune responses to human CMV: a critical role for IFN-gamma-producing CD4+ T cells in protection against CMV disease.* Blood, 2003. **101**(7): p. 2686-92.
68. van Lier, R.A., I.J. ten Berge, and L.E. Gamadia, *Human CD8(+) T-cell differentiation in response to viruses.* Nat Rev Immunol, 2003. **3**(12): p. 931-9.
69. Harari, A., et al., *Distinct profiles of cytotoxic granules in memory CD8 T cells correlate with function, differentiation stage, and antigen exposure.* J Virol, 2009. **83**(7): p. 2862-71.
70. Appay, V., et al., *Memory CD8+ T cells vary in differentiation phenotype in different persistent virus infections.* Nat Med, 2002. **8**(4): p. 379-85.
71. Khan, N., et al., *Comparative analysis of CD8+ T cell responses against human cytomegalovirus proteins pp65 and immediate early 1 shows similarities in precursor frequency, oligoclonality, and phenotype.* J Infect Dis, 2002. **185**(8): p. 1025-34.
72. Hertoghs, K.M., et al., *Molecular profiling of cytomegalovirus-induced human CD8+ T cell differentiation.* J Clin Invest, 2010. **120**(11): p. 4077-90.
73. Murphy, E., et al., *Reevaluation of human cytomegalovirus coding potential.* Proc Natl Acad Sci U S A, 2003. **100**(23): p. 13585-90.
74. Rodgers, B., et al., *Immunoaffinity purification of a 72K early antigen of human cytomegalovirus: analysis of humoral and cell-mediated immunity to the purified polypeptide.* J Gen Virol, 1987. **68 ( Pt 9)**: p. 2371-8.
75. McLaughlin-Taylor, E., et al., *Identification of the major late human cytomegalovirus matrix protein pp65 as a target antigen for CD8+ virus-specific cytotoxic T lymphocytes.* Journal of Medical Virology, 1994. **43**(1): p. 103-110.
76. Khan, N., et al., *Cytomegalovirus Seropositivity Drives the CD8 T Cell Repertoire Toward Greater Clonality in Healthy Elderly Individuals.* The Journal of Immunology, 2002. **169**(4): p. 1984-1992.

77. Moss, P. and N. Khan, *CD8+ T-cell immunity to cytomegalovirus.* Human Immunology, 2004. **65**(5): p. 456-464.
78. Vescovini, R., et al., *Massive load of functional effector CD4+ and CD8+ T cells against cytomegalovirus in very old subjects.* J Immunol, 2007. **179**(6): p. 4283-91.
79. Waller, E.C., et al., *Dynamics of T cell memory in human cytomegalovirus infection.* Med Microbiol Immunol, 2008. **197**(2): p. 83-96.
80. Ahn, K., et al., *Human cytomegalovirus inhibits antigen presentation by a sequential multistep process.* Proc Natl Acad Sci U S A, 1996. **93**(20): p. 10990-5.
81. Noriega, V., et al., *Diverse immune evasion strategies by human cytomegalovirus.* Immunol Res, 2012. **54**(1-3): p. 140-51.
82. Manley, T.J., *Immune evasion proteins of human cytomegalovirus do not prevent a diverse CD8+ cytotoxic T-cell response in natural infection.* Blood, 2004. **104**(4): p. 1075-1082.
83. Jones, T.R., et al., *Multiple independent loci within the human cytomegalovirus unique short region down-regulate expression of major histocompatibility complex class I heavy chains.* Journal of Virology, 1995. **69**(8): p. 4830-4841.
84. Khan, N., et al., *Identification of cytomegalovirus-specific cytotoxic T lymphocytes in vitro is greatly enhanced by the use of recombinant virus lacking the US2 to US11 region or modified vaccinia virus Ankara expressing individual viral genes.* J Virol, 2005. **79**(5): p. 2869-79.
85. Kim, S., et al., *Human cytomegalovirus microRNA miR-US4-1 inhibits CD8(+) T cell responses by targeting the aminopeptidase ERAP1.* Nat Immunol, 2011. **12**(10): p. 984-91.
86. Karrer, U., et al., *Memory inflation: continuous accumulation of antiviral CD8+ T cells over time.* J Immunol, 2003. **170**(4): p. 2022-9.
87. Khan, N., et al., *Cytomegalovirus Seropositivity Drives the CD8 T Cell Repertoire Toward Greater Clonality in Healthy Elderly Individuals. The Journal of Immunology* 2002. **169**: p. 1984-1992.
88. O'Hara, G.A., et al., *Memory T cell inflation: understanding cause and effect.* Trends Immunol, 2012. **33**(2): p. 84-90.
89. Lang, A., J.D. Brien, and J. Nikolich-Zugich, *Inflation and long-term maintenance of CD8 T cells responding to a latent herpesvirus depend upon establishment of latency and presence of viral antigens.* J Immunol, 2009. **183**(12): p. 8077-87.
90. Ouyang, Q., et al., *An age-related increase in the number of CD8+ T cells carrying receptors for an immunodominant Epstein-Barr virus (EBV) epitope is counteracted by a decreased frequency of their antigen-specific responsiveness.* Mech Ageing Dev, 2003. **124**(4): p. 477-85.
91. Vescovini, R., et al., *Massive load of Functional Effector CD4+ and CD8+ T Cells against Cytomegalovirus in Very Old Subjects. The Journal of Immunology* 2007. **179**: p. 4283-4291.
92. Moss, P. and N. Khan, *CD8+ T-Cell Immunity to Cytomegalovirus. Human Immunology*, 2004. **65**: p. 456-464.
93. Klenerman, P. and A. Oxenius, *T cell responses to cytomegalovirus.* Nat Rev Immunol, 2016. **16**(6): p. 367-77.
94. Cicin-Sain, L., et al., *Cytomegalovirus Infection Impairs Immune Responses and Accentuates T-cell Pool Changes Observed in Mice with Aging.* PLoS Pathogens, 2012. **8**(8): p. e1002849.

95. Holtappels, R., et al., *Cytomegalovirus misleads its host by priming of CD8 T cells specific for an epitope not presented in infected tissues.* J Exp Med, 2004. **199**(1): p. 131-6.
96. Powers, C. and K. Früh, *Rhesus CMV: an emerging animal model for human CMV.* Med Microbiol Immunol, 2008. **197**(2): p. 109-15.
97. Mestas, J. and C.C.W. Hughes, *Of Mice and Not Men: Differences between Mouse and Human Immunology.* The Journal of Immunology, 2004. **172**(5): p. 2731.
98. Grzimek, N.K., et al., *Random, asynchronous, and asymmetric transcriptional activity of enhancer-flanking major immediate-early genes ie1/3 and ie2 during murine cytomegalovirus latency in the lungs.* J Virol, 2001. **75**(6): p. 2692-705.
99. Arens, R., et al., *Cutting edge: murine cytomegalovirus induces a polyfunctional CD4 T cell response.* J Immunol, 2008. **180**(10): p. 6472-6.
100. Lang, K.S., et al., *High frequency of human cytomegalovirus (HCMV)-specific CD8+ T cells detected in a healthy CMV-seropositive donor.* Cell Mol Life Sci, 2002. **59**(6): p. 1076-80.
101. Kern, F., et al., *Target structures of the CD8(+)-T-cell response to human cytomegalovirus: the 72-kilodalton major immediate-early protein revisited.* J Virol, 1999. **73**(10): p. 8179-84.
102. Kern, F., et al., *Cytomegalovirus (CMV) phosphoprotein 65 makes a large contribution to shaping the T cell repertoire in CMV-exposed individuals.* J Infect Dis, 2002. **185**(12): p. 1709-16.
103. Snyder, C.M., et al., *Memory Inflation during Chronic Viral Infection Is Maintained by Continuous Production of Short-Lived, Functional T Cells.* Immunity, 2008. **29**(4): p. 650-659.
104. Torti, N., et al., *Non-hematopoietic cells in lymph nodes drive memory CD8 T cell inflation during murine cytomegalovirus infection.* PLoS Pathog, 2011. **7**(10): p. e1002313.
105. Munks, M.W., et al., *Four distinct patterns of memory CD8 T cell responses to chronic murine cytomegalovirus infection.* J Immunol, 2006. **177**(1): p. 450-8.
106. Gamadia, L.E., et al., *Differentiation of cytomegalovirus-specific CD8+ T cells in healthy and immunosuppressed virus carriers.* Blood, 2001. **98**(3): p. 754-761.
107. Gillespie, G.M.A., et al., *Functional Heterogeneity and High Frequencies of Cytomegalovirus-Specific CD8+ T Lymphocytes in Healthy Seropositive Donors. Journal of Virology* 2000. **74**: p. 8140-8150.
108. Wills, M.R., et al., *Identification of naive or antigen-experienced human CD8(+) T cells by expression of costimulation and chemokine receptors: analysis of the human cytomegalovirus-specific CD8(+) T cell response.* J Immunol, 2002. **168**(11): p. 5455-64.
109. La Rosa, C., et al., *Primary response against cytomegalovirus during antiviral prophylaxis with valganciclovir, in solid organ transplant recipients.* Transpl Int, 2011. **24**(9): p. 920-31.
110. Chiu, Y.L., et al., *Cytotoxic polyfunctionality maturation of cytomegalovirus-pp65-specific CD4 + and CD8 + T-cell responses in older adults positively correlates with response size.* Sci Rep, 2016. **6**: p. 19227.
111. Wills, M.R., et al., *Human Virus-Specific CD8+ CTL Clones Revert from CD45ROhigh to CD45RAhigh In Vivo: CD45RAhighCD8+ T Cells Comprise Both Naive and Memory Cells.* The Journal of Immunology, 1999. **162**(12): p. 7080-7087.

112. Kurz, S.K. and M.J. Reddehase, *Patchwork Pattern of Transcriptional Reactivation in the Lungs Indicates Sequential Checkpoints in the Transition from Murine Cytomegalovirus Latency to Recurrence.* Journal of Virology, 1999. **73**(10): p. 8612-8622.
113. Kurz, S.K., et al., *Focal Transcriptional Activity of Murine Cytomegalovirus during Latency in the Lungs.* Journal of Virology, 1999. **73**(1): p. 482-494.
114. Snyder, C.M., et al., *Sustained CD8+ T cell memory inflation after infection with a single-cycle cytomegalovirus.* PLoS Pathog, 2011. **7**(10): p. e1002295.
115. Snyder, C., et al., *Memory Inflation during Chronic Viral Infection Is Maintained by Continuous Production of Short-Lived, Functional T cells. Immunity* 2008. **29**: p. 650-659.
116. Loewendorf, A.I., et al., *Dissecting the requirements for maintenance of the CMV-specific memory T-cell pool.* Viral Immunol, 2011. **24**(4): p. 351-5.
117. Beswick, M., et al., *Antiviral therapy can reverse the development of immune senescence in elderly mice with latent cytomegalovirus infection.* J Virol, 2013. **87**(2): p. 779-89.
118. Snyder, C.M., *Buffered memory: a hypothesis for the maintenance of functional, virus-specific CD8+ T cells during cytomegalovirus infection.* Immunologic Research, 2011. **51**(2-3): p. 195-204.
119. Simon, C.O., et al., *CD8 T cells control cytomegalovirus latency by epitope-specific sensing of transcriptional reactivation.* J Virol, 2006. **80**(21): p. 10436-56.
120. Yewdell, J.W., *Confronting complexity: real-world immunodominance in antiviral CD8+ T cell responses.* Immunity, 2006. **25**(4): p. 533-43.
121. Ferrington, D.A. and D.S. Gregerson, *Immunoproteasomes: structure, function, and antigen presentation.* Prog Mol Biol Transl Sci, 2012. **109**: p. 75-112.
122. Hutchinson, S., et al., *A dominant role for the immunoproteasome in CD8+ T cell responses to murine cytomegalovirus.* PLoS One, 2011. **6**(2): p. e14646.
123. Smith, C.J., H. Turula, and C.M. Snyder, *Systemic hematogenous maintenance of memory inflation by MCMV infection.* PLoS Pathog, 2014. **10**(7): p. e1004233.
124. Farrington, L.A., et al., *Competition for antigen at the level of the APC is a major determinant of immunodominance during memory inflation in murine cytomegalovirus infection.* J Immunol, 2013. **190**(7): p. 3410-6.
125. Turula, H., et al., *Competition between T cells maintains clonal dominance during memory inflation induced by MCMV.* Eur J Immunol, 2013. **43**(5): p. 1252-63.
126. Day, E.K., et al., *Rapid CD8+ T cell repertoire focusing and selection of high-affinity clones into memory following primary infection with a persistent human virus: human cytomegalovirus.* J Immunol, 2007. **179**(5): p. 3203-13.
127. Schwanninger, A., et al., *Age-related appearance of a CMV-specific high-avidity CD8+ T cell clonotype which does not occur in young adults.* Immun Ageing, 2008. **5**: p. 14.
128. Trautmann, L., et al., *Selection of T cell clones expressing high-affinity public TCRs within Human cytomegalovirus-specific CD8 T cell responses.* J Immunol, 2005. **175**(9): p. 6123-32.
129. Weekes, M.P., et al., *The Memory Cytotoxic T-Lymphocyte (CTL) Response to Human Cytomegalovirus Infection Contains Individual Peptide-Specific CTL Clones That Have Undergone Extensive Expansion In Vivo.* Journal of Virology, 1999. **73**(3): p. 2099-2108.

130. Griffiths, S.J., et al., *Age-associated increase of low-avidity cytomegalovirus-specific CD8+ T cells that re-express CD45RA.* J Immunol, 2013. **190**(11): p. 5363-72.
131. Arens, R., et al., *Differential B7-CD28 costimulatory requirements for stable and inflationary mouse cytomegalovirus-specific memory CD8 T cell populations.* J Immunol, 2011. **186**(7): p. 3874-81.
132. Seckert, C.K., et al., *Antigen-presenting cells of haematopoietic origin prime cytomegalovirus-specific CD8 T-cells but are not sufficient for driving memory inflation during viral latency.* J Gen Virol, 2011. **92**(Pt 9): p. 1994-2005.
133. Torti, N., et al., *Batf3 transcription factor-dependent DC subsets in murine CMV infection: differential impact on T-cell priming and memory inflation.* Eur J Immunol, 2011. **41**(9): p. 2612-8.
134. Hansen, S.G., et al., *Evasion of CD8+ T cells is critical for superinfection by cytomegalovirus.* Science, 2010. **328**(5974): p. 102-6.
135. Wiertz, E.J., et al., *Sec61-mediated transfer of a membrane protein from the endoplasmic reticulum to the proteasome for destruction.* Nature, 1996. **384**(6608): p. 432-8.
136. Wiertz, E.J., et al., *The human cytomegalovirus US11 gene product dislocates MHC class I heavy chains from the endoplasmic reticulum to the cytosol.* Cell, 1996. **84**(5): p. 769-79.
137. Schust, D.J., et al., *Trophoblast class I major histocompatibility complex (MHC) products are resistant to rapid degradation imposed by the human cytomegalovirus (HCMV) gene products US2 and US11. Journal of Experimental Medicine* 1998. **188**: p. 497-503.
138. Gewurz, B.E., et al., *Human cytomegalovirus US2 endoplasmic reticulum-lumenal domain dictates association with major histocompatibility complex class I in a locus-specific manner.* J Virol, 2001. **75**(11): p. 5197-204.
139. Ameres, S., et al., *Presentation of an immunodominant immediate-early CD8+ T cell epitope resists human cytomegalovirus immunoevasion.* PLoS Pathog, 2013. **9**(5): p. e1003383.
140. Ameres, S., et al., *CD8 T cell-evasive functions of human cytomegalovirus display pervasive MHC allele specificity, complementarity, and cooperativity.* J Immunol, 2014. **192**(12): p. 5894-905.
141. Barel, M.T., et al., *Human cytomegalovirus-encoded US2 differentially affects surface expression of MHC class I locus products and targets membrane-bound, but not soluble HLA-G1 for degradation.* J Immunol, 2003. **171**(12): p. 6757-65.
142. Hesse, J., et al., *Suppression of CD8+ T-cell recognition in the immediate-early phase of human cytomegalovirus infection.* Journal of General Virology, 2013. **94**(Pt 2): p. 376-386.
143. Ahn, K., et al., *The ER-Luminal Domain of the HCMV Glycoprotein US6 Inhibits Peptide Translocation by TAP.* Immunity, 1997. **6**(5): p. 613-621.
144. Hegde, N.R., et al., *Inhibition of HLA-DR assembly, transport, and loading by human cytomegalovirus glycoprotein US3: a novel mechanism for evading major histocompatibility complex class II antigen presentation.* J Virol, 2002. **76**(21): p. 10929-41.
145. Lehner, P.J., et al., *The human cytomegalovirus US6 glycoprotein inhibits transporter associated with antigen processing-dependent peptide translocation.* Proc Natl Acad Sci U S A, 1997. **94**(13): p. 6904-9.

146. Park, B., et al., *The HCMV membrane glycoprotein US10 selectively targets HLA-G for degradation.* J Exp Med, 2010. **207**(9): p. 2033-41.
147. Kalejta, R.F., *Tegument proteins of human cytomegalovirus.* Microbiol Mol Biol Rev, 2008. **72**(2): p. 249-65, table of contents.
148. Kalejta, R.F., *Functions of human cytomegalovirus tegument proteins prior to immediate early gene expression.* Curr Top Microbiol Immunol, 2008. **325**: p. 101-15.
149. Gilbert, M.J., et al., *Cytomegalovirus selectively blocks antigen processing and presentation of its immediate-early gene product.* Nature, 1996. **383**(6602): p. 720-2.
150. Huh, Y.H., et al., *Binding STAT2 by the acidic domain of human cytomegalovirus IE1 promotes viral growth and is negatively regulated by SUMO.* J Virol, 2008. **82**(21): p. 10444-54.
151. Kotenko, S.V., et al., *Human cytomegalovirus harbors its own unique IL-10 homolog (cmvIL-10).* Proc Natl Acad Sci U S A, 2000. **97**(4): p. 1695-700.
152. He, R., et al., *Characterization of the transcripts of human cytomegalovirus UL144.* Virology Journal, 2011. **8**(1): p. 299.
153. Jones, T.R. and L. Sun, *Human cytomegalovirus US2 destabilizes major histocompatibility complex class I heavy chains.* J Virol, 1997. **71**(4): p. 2970-9.
154. Jones, T.R., et al., *Human cytomegalovirus US3 impairs transport and maturation of major histocompatibility complex class I heavy chains.* Proc Natl Acad Sci U S A, 1996. **93**(21): p. 11327-33.
155. Furman, M.H., et al., *The human cytomegalovirus US10 gene product delays trafficking of major histocompatibility complex class I molecules.* J Virol, 2002. **76**(22): p. 11753-6.
156. Welte, S.A., et al., *Selective intracellular retention of virally induced NKG2D ligands by the human cytomegalovirus UL16 glycoprotein.* Eur J Immunol, 2003. **33**(1): p. 194-203.
157. Dunn, C., et al., *Human cytomegalovirus glycoprotein UL16 causes intracellular sequestration of NKG2D ligands, protecting against natural killer cell cytotoxicity.* J Exp Med, 2003. **197**(11): p. 1427-39.
158. Beck, S. and B.G. Barrell, *Human cytomegalovirus encodes a glycoprotein homologous to MHC class-I antigens.* Nature, 1988. **331**(6153): p. 269-72.
159. Ulbrecht, M., et al., *Cutting edge: the human cytomegalovirus UL40 gene product contains a ligand for HLA-E and prevents NK cell-mediated lysis.* J Immunol, 2000. **164**(10): p. 5019-22.
160. Wilkinson, G.W., et al., *Modulation of natural killer cells by human cytomegalovirus.* J Clin Virol, 2008. **41**(3): p. 206-12.
161. Long, E.O., et al., *Controlling natural killer cell responses: integration of signals for activation and inhibition.* Annu Rev Immunol, 2013. **31**: p. 227-58.
162. Chapman, T.L., A.P. Heikema, and P.J. Bjorkman, *The Inhibitory Receptor LIR-1 Uses a Common Binding Interaction to Recognize Class I MHC Molecules and the Viral Homolog UL18.* Immunity, 1999. **11**(5): p. 603-613.
163. Cerwenka, A. and L.L. Lanier, *NKG2D ligands: unconventional MHC class I-like molecules exploited by viruses and cancer.* Tissue Antigens, 2003. **61**(5): p. 335-343.
164. Nattermann, J., et al., *HIV-1 infection leads to increased HLA-E expression resulting in impaired function of natural killer cells.* Antivir Ther, 2005. **10**(1): p. 95-107.
165. Jung, S., et al., *In vivo depletion of CD11c+ dendritic cells abrogates priming of CD8+ T cells by exogenous cell-associated antigens.* Immunity, 2002. **17**(2): p. 211-20.

166. Tan, J.K.H. and H.C. O'Neill, *Maturation requirements for dendritic cells in T cell stimulation leading to tolerance versus immunity.* Journal of Leukocyte Biology, 2005. **78**(2): p. 319-324.
167. Joffre, O.P., et al., *Cross-presentation by dendritic cells.* Nat Rev Immunol, 2012. **12**(8): p. 557-69.
168. Snyder, C.M., et al., *Cross-presentation of a spread-defective MCMV is sufficient to prime the majority of virus-specific CD8+ T cells.* PLoS One, 2010. **5**(3): p. e9681.
169. Arrode, G., et al., *Incoming human cytomegalovirus pp65 (UL83) contained in apoptotic infected fibroblasts is cross-presented to CD8(+) T cells by dendritic cells.* J Virol, 2000. **74**(21): p. 10018-24.
170. Arrode, G., et al., *Cross-Presentation of Human Cytomegalovirus pp65 (UL83) to CD8+ T Cells Is Regulated by Virus-Induced, Soluble-Mediator-Dependent Maturation of Dendritic Cells. Journal of Virology* 2002. **76**: p. 142-150.
171. Busche, A., et al., *Priming of CD8+ T cells against cytomegalovirus-encoded antigens is dominated by cross-presentation. Journal of Immunology* 2013. **190**: p. 2767-2777.
172. Pinto, A.K., et al., *Coordinated function of murine cytomegalovirus genes completely inhibits CTL lysis.* J Immunol, 2006. **177**(5): p. 3225-34.
173. Savva, G.M., et al., *Cytomegalovirus infection is associated with increased mortality in the older population.* Aging Cell, 2013. **12**(3): p. 381-7.
174. Chou, J.P. and R.B. Effros, *T cell replicative senescence in human aging.* Curr Pharm Des, 2013. **19**(9): p. 1680-98.
175. Olsson, J., et al., *Age-related change in peripheral blood T-lymphocyte subpopulations and cytomegalovirus infection in the very old: the Swedish longitudinal OCTO immune study.* Mechanisms of Ageing and Development, 2001. **121**(1–3): p. 187-201.
176. Wikby, A., et al., *An immune risk phenotype, cognitive impairment, and survival in very late life: impact of allostatic load in Swedish octogenarian and nonagenarian humans.* J Gerontol A Biol Sci Med Sci, 2005. **60**(5): p. 556-65.
177. Strindhall, J., et al., *The inverted CD4/CD8 ratio and associated parameters in 66-year-old individuals: the Swedish HEXA immune study.* Age (Dordr), 2013. **35**(3): p. 985-91.
178. Wallace, D.L., et al., *Human cytomegalovirus-specific CD8+ T-cell expansions contain long-lived cells that retain functional capacity in both young and elderly subjects.* Immunology, 2011. **132**(1): p. 27-38.
179. Gillespie, G.M.A., et al., *Functional Heterogeneity and High Frequencies of Cytomegalovirus-Specific CD8+ T Lymphocytes in Healthy Seropositive Donors.* Journal of Virology, 2000. **74**(17): p. 8140-8150.
180. Wallace, D.L., et al., *Human cytomegalovirus-specific CD8(+) T-cell expansions contain long-lived cells that retain functional capacity in both young and elderly subjects.* Immunology, 2011. **132**(1): p. 27-38.
181. van de Berg, P.J., et al., *A fingerprint left by cytomegalovirus infection in the human T cell compartment.* J Clin Virol, 2008. **41**(3): p. 213-7.
182. Ahmed, A., *Antiviral treatment of cytomegalovirus infection.* Infect Disord Drug Targets, 2011. **11**(5): p. 475-503.
183. Jacobsen, T. and N. Sifontis, *Drug interactions and toxicities associated with the antiviral management of cytomegalovirus infection.* Am J Health Syst Pharm, 2010. **67**(17): p. 1417-25.

184. Limaye, A.P., et al., *Emergence of ganciclovir-resistant cytomegalovirus disease among recipients of solid-organ transplants.* Lancet, 2000. **356**(9230): p. 645-9.
185. Razonable, R.R. and C.V. Paya, *Herpesvirus infections in transplant recipients: current challenges in the clinical management of cytomegalovirus and Epstein-Barr virus infections.* Herpes, 2003. **10**(3): p. 60-5.
186. Holtappels, R., et al., *Experimental preemptive immunotherapy of murine cytomegalovirus disease with CD8 T-cell lines specific for ppM83 and pM84, the two homologs of human cytomegalovirus tegument protein ppUL83 (pp65).* J Virol, 2001. **75**(14): p. 6584-600.
187. Pahl-Seibert, M.F., et al., *Highly protective in vivo function of cytomegalovirus IE1 epitope-specific memory CD8 T cells purified by T-cell receptor-based cell sorting.* J Virol, 2005. **79**(9): p. 5400-13.
188. Holtappels, R., et al., *CD8 T-cell-based immunotherapy of cytomegalovirus infection: "proof of concept" provided by the murine model.* Med Microbiol Immunol, 2008. **197**(2): p. 125-34.
189. Walter, E.A., et al., *Reconstitution of cellular immunity against cytomegalovirus in recipients of allogeneic bone marrow by transfer of T-cell clones from the donor.* N Engl J Med, 1995. **333**(16): p. 1038-44.
190. Cobbold, M., et al., *Adoptive transfer of cytomegalovirus-specific CTL to stem cell transplant patients after selection by HLA-peptide tetramers.* J Exp Med, 2005. **202**(3): p. 379-86.
191. Feuchtinger, T., et al., *Adoptive transfer of pp65-specific T cells for the treatment of chemorefractory cytomegalovirus disease or reactivation after haploidentical and matched unrelated stem cell transplantation.* Blood, 2010. **116**(20): p. 4360-7.
192. Peggs, K.S., et al., *Directly selected cytomegalovirus-reactive donor T cells confer rapid and safe systemic reconstitution of virus-specific immunity following stem cell transplantation.* Clin Infect Dis, 2011. **52**(1): p. 49-57.
193. Sellar, R.S. and K.S. Peggs, *Therapeutic strategies for cytomegalovirus infection in haematopoietic transplant recipients: a focused update.* Expert Opin Biol Ther, 2014. **14**(8): p. 1121-6.
194. Peggs, K.S., et al., *Adoptive cellular therapy for early cytomegalovirus infection after allogeneic stem-cell transplantation with virus-specific T-cell lines.* Lancet, 2003. **362**(9393): p. 1375-7.
195. Schub, A., et al., *CMV-specific TCR-transgenic T cells for immunotherapy.* J Immunol, 2009. **183**(10): p. 6819-30.
196. Thomas, S., et al., *Strong and sustained effector function of memory- versus naïve-derived T cells upon T-cell receptor RNA transfer: implications for cellular therapy.* Eur J Immunol, 2012. **42**(12): p. 3442-53.
197. Fischer, W., et al., *Coping with Viral Diversity in HIV Vaccine Design: A Response to Nickle et al.* PLoS Comput Biol, 2008. **4**(1): p. e15.
198. Draper, S.J. and J.L. Heeney, *Viruses as vaccine vectors for infectious diseases and cancer.* Nat Rev Microbiol, 2010. **8**(1): p. 62-73.
199. Garcia Casado, J., et al., *Lentivector immunization induces tumor antigen-specific B and T cell responses in vivo.* Eur J Immunol, 2008. **38**(7): p. 1867-76.
200. Kass, E., et al., *Induction of protective host immunity to carcinoembryonic antigen (CEA), a self-antigen in CEA transgenic mice, by immunizing with a recombinant vaccinia-CEA virus.* Cancer Res, 1999. **59**(3): p. 676-83.

201. Paredes, A.M. and D. Yu, *Human Cytomegalovirus: Bacterial Artificial Chromosome (BAC) Cloning and Genetic Manipulation.* 2012.
202. Warden, C., Q. Tang, and H. Zhu, *Herpesvirus BACs: Past, Present, and Future.* Journal of Biomedicine and Biotechnology, 2011. **2011**: p. 1-16.
203. Borst, E.M., et al., *Cloning of the human cytomegalovirus (HCMV) genome as an infectious bacterial artificial chromosome in Escherichia coli: a new approach for construction of HCMV mutants.* J Virol, 1999. **73**(10): p. 8320-9.
204. Paredes, A.M. and D. Yu, *Human cytomegalovirus: bacterial artificial chromosome (BAC) cloning and genetic manipulation.* Curr Protoc Microbiol, 2012. **Chapter 14**: p. Unit14E.4.
205. Messerle, M., et al., *Cloning and mutagenesis of a herpesvirus genome as an infectious bacterial artificial chromosome.* Proceedings of the National Academy of Sciences, 1997. **94**(26): p. 14759-14763.
206. Karrer, U., et al., *Expansion of protective CD8+ T-cell responses driven by recombinant cytomegaloviruses.* J Virol, 2004. **78**(5): p. 2255-64.
207. Tsuda, Y., et al., *A Replicating Cytomegalovirus-Based Vaccine Encoding a Single Ebola Virus Nucleoprotein CTL Epitope Confers Protection against Ebola Virus.* PLoS Negl Trop Dis, 2011. **5**(8): p. e1275.
208. Xu, G., et al., *Cytomegalovirus-based cancer vaccines expressing TRP2 induce rejection of melanoma in mice.* Biochemical and Biophysical Research Communications, 2013. **437**(2): p. 287-291.
209. Klyushnenkova, E.N., et al., *A cytomegalovirus-based vaccine expressing a single tumor-specific CD8+ T-cell epitope delays tumor growth in a murine model of prostate cancer.* J Immunother, 2012. **35**(5): p. 390-9.
210. Tierney, R., et al., *A single-dose cytomegalovirus-based vaccine encoding tetanus toxin fragment C induces sustained levels of protective tetanus toxin antibodies in mice.* Vaccine, 2012. **30**(20): p. 3047-3052.
211. Scanlan, M.J., et al., *Cancer/testis antigens: an expanding family of targets for cancer immunotherapy.* Immunological reviews, 2002. **188**: p. 22-32.
212. Simpson, A.J., et al., *Cancer/testis antigens, gametogenesis and cancer.* Nat Rev Cancer, 2005. **5**(8): p. 615-25.
213. Almeida, L.G., et al., *CTdatabase: a knowledge-base of high-throughput and curated data on cancer-testis antigens.* Nucleic Acids Res, 2009. **37**(Database issue): p. D816-9.
214. Gure, A.O., et al., *Cancer-testis genes are coordinately expressed and are markers of poor outcome in non-small cell lung cancer.* Clin Cancer Res, 2005. **11**(22): p. 8055-62.
215. Chen, Y.T., et al., *A testicular antigen aberrantly expressed in human cancers detected by autologous antibody screening.* Proc Natl Acad Sci U S A, 1997. **94**(5): p. 1914-8.
216. Jäger, E., et al., *Induction of primary NY-ESO-1 immunity: CD8+ T lymphocyte and antibody responses in peptide-vaccinated patients with NY-ESO-1+ cancers.* Proceedings of the National Academy of Sciences, 2000. **97**(22): p. 12198-12203.
217. Gnjatic, S., et al., *NY-ESO-1: review of an immunogenic tumor antigen.* Adv Cancer Res, 2006. **95**: p. 1-30.
218. Palmowski, M.J., et al., *Intravenous injection of a lentiviral vector encoding NY-ESO-1 induces an effective CTL response.* J Immunol, 2004. **172**(3): p. 1582-7.

219. Jäger, E., et al., *Recombinant vaccinia/fowlpox NY-ESO-1 vaccines induce both humoral and cellular NY-ESO-1-specific immune responses in cancer patients.* Proceedings of the National Academy of Sciences, 2006. **103**(39): p. 14453-14458.
220. Valmori, D., et al., *Naturally occurring human lymphocyte antigen-A2 restricted CD8+ T-cell response to the cancer testis antigen NY-ESO-1 in melanoma patients.* Cancer Res, 2000. **60**(16): p. 4499-506.
221. Stanton, R.J., et al., *Reconstruction of the complete human cytomegalovirus genome in a BAC reveals RL13 to be a potent inhibitor of replication.* Journal of Clinical Investigation, 2010. **120**(9): p. 3191-3208.
222. Rabin, H., et al., *Spontaneous release of a factor with properties of T cell growth factor from a continuous line of primate tumor T cells. The Journal of Immunology*, 1981. **127**: p. 1852-1856.
223. Bunce, M., et al., *Phototyping: comprehensive DNA typing for HLA-A, B, C, DRB1, DRB3, DRB4, DRB5 & DQB1 by PCR with 144 primer mixes utilizing sequence-specific primers (PCR-SSP).* Tissue Antigens, 1995. **46**(5): p. 355-67.
224. Dunn, W., et al., *Functional profiling of a human cytomegalovirus genome.* Proc Natl Acad Sci U S A, 2003. **100**(24): p. 14223-8.
225. Weekes, M.P., et al., *Quantitative temporal viromics: an approach to investigate host-pathogen interaction.* Cell, 2014. **157**(6): p. 1460-72.
226. Gibson, D.G., et al., *Enzymatic assembly of DNA molecules up to several hundred kilobases.* Nat Methods, 2009. **6**(5): p. 343-5.
227. Swift, S., et al., *Rapid production of retroviruses for efficient gene delivery to mammalian cells using 293T cell-based systems.* Curr Protoc Immunol, 2001. **10**(10).
228. Frecha, C., et al., *Advances in the field of lentivector-based transduction of T and B lymphocytes for gene therapy.* Mol Ther, 2010. **18**(10): p. 1748-57.
229. Wölfl, M. and P.D. Greenberg, *Antigen-specific activation and cytokine-facilitated expansion of naive, human CD8+ T cells.* Nature protocols, 2014. **9**(4): p. 950-966.
230. Sylwester, A.W., et al., *Broadly targeted human cytomegalovirus-specific CD4+ and CD8+ T cells dominate the memory compartments of exposed subjects. The Journal of Experimental Medicine*, 2005. **202**: p. 673-685.
231. Wills, M.R., et al., *Human virus-specific CD8+ CTL clones revert from CD45ROhigh to CD45RAhigh in vivo: CD45RAhighCD8+ T cells comprise both naive and memory cells.* J Immunol, 1999. **162**(12): p. 7080-7.
232. Halenius, A., C. Gerke, and H. Hengel, *Classical and non-classical MHC I molecule manipulation by human cytomegalovirus: so many targets—but how many arrows in the quiver?* Cell Mol Immunol, 2015. **12**(2): p. 139-53.
233. Gold, M.C., et al., *The murine cytomegalovirus immunomodulatory gene m152 prevents recognition of infected cells by M45-specific CTL but does not alter the immunodominance of the M45-specific CD8 T cell response in vivo. Journal of Immunology* 2002. **169**: p. 359-365.
234. Elkington, R., et al., *Ex Vivo Profiling of CD8+ T Cell Responses to Human Cytomegalovirus Reveals Broad and Multispecific Reactivities in Healthy Virus Carriers.*
235. Almanzar, G., et al., *Long-term cytomegalovirus infection leads to significant changes in the composition of the CD8+ T-cell repertoire, which may be the basis for an imbalance in the cytokine production profile in elderly persons.* J Virol, 2005. **79**(6): p. 3675-83.

236. Jackson, S.E., et al., *Diverse specificities, phenotypes, and antiviral activities of cytomegalovirus-specific CD8+ T cells.* J Virol, 2014. **88**(18): p. 10894-908.
237. Sallusto, F., et al., *Two subsets of memory T lymphocytes with distinct homing potentials and effector functions.* Nature, 1999. **401**(6754): p. 708-12.
238. Romero, P., et al., *Four functionally distinct populations of human effector-memory CD8+ T lymphocytes.* J Immunol, 2007. **178**(7): p. 4112-9.
239. Picker, L.J., et al., *Control of lymphocyte recirculation in man. I. Differential regulation of the peripheral lymph node homing receptor L-selectin on T cells during the virgin to memory cell transition.* J Immunol, 1993. **150**(3): p. 1105-21.
240. Sierro, S., R. Rothkopf, and P. Klenerman, *Evolution of diverse antiviral CD8+ T cell populations after murine cytomegalovirus infection.* Eur J Immunol, 2005. **35**(4): p. 1113-23.
241. Wilkinson, G.W., et al., *Human cytomegalovirus: taking the strain.* Med Microbiol Immunol, 2015. **204**(3): p. 273-84.
242. Luo, J., et al., *Modulation of the Cellular Distribution of Human Cytomegalovirus Helicase by Cellular Factor Snapin.* Journal of Virology, 2013. **87**(19): p. 10628-10640.
243. Woon, H.G., et al., *Identification of putative functional motifs in viral proteins essential for human cytomegalovirus DNA replication.* Virus Genes, 2008. **37**(2): p. 193-202.
244. Sinzger, C., M. Digel, and G. Jahn, *Cytomegalovirus cell tropism. Current Topics in Microbiology and Immunology* 2008. **325**: p. 63-83.
245. Wooldridge, L., et al., *Tricks with tetramers: how to get the most from multimeric peptide–MHC.* Immunology, 2009. **126**(2): p. 147-164.
246. Hosking, M.P., C.T. Flynn, and J.L. Whitton, *Antigen-specific naive CD8+ T cells produce a single pulse of IFN-γ in vivo within hours of infection, but without antiviral effect.* J Immunol, 2014. **193**(4): p. 1873-85.
247. Brehm, M.A., K.A. Daniels, and R.M. Welsh, *Rapid production of TNF-alpha following TCR engagement of naive CD8 T cells.* J Immunol, 2005. **175**(8): p. 5043-9.
248. Mitchell, D.P., et al., *Human cytomegalovirus UL28 and UL29 open reading frames encode a spliced mRNA and stimulate accumulation of immediate-early RNAs.* J Virol, 2009. **83**(19): p. 10187-97.
249. Arrode, G., et al., *Cross-presentation of human cytomegalovirus pp65 (UL83) to CD8+ T cells is regulated by virus-induced, soluble-mediator-dependent maturation of dendritic cells.* J Virol, 2002. **76**(1): p. 142-50.
250. Thom, J.T., et al., *The Salivary Gland Acts as a Sink for Tissue-Resident Memory CD8(+) T Cells, Facilitating Protection from Local Cytomegalovirus Infection.* Cell Rep, 2015. **13**(6): p. 1125-36.
251. Winkler, M. and T. Stamminger, *A specific subform of the human cytomegalovirus transactivator protein pUL69 is contained within the tegument of virus particles.* J Virol, 1996. **70**(12): p. 8984-7.
252. Manley, T.J., et al., *Immune evasion proteins of human cytomegalovirus do not prevent a diverse CD8+ cytotoxic T-cell response in natural infection. Blood*, 2004. **104**: p. 1075-1082.
253. Jarvis, M.A. and J.A. Nelson, *Human Cytomegalovirus Tropism for Endothelial Cells: Not All Endothelial Cells Are Created Equal.* Journal of Virology, 2007. **81**(5): p. 2095-2101.

254. Turner, S., et al., *Sequence-based typing provides a new look at HLA-C diversity.* J Immunol, 1998. **161**(3): p. 1406-13.
255. Neisig, A., C.J. Melief, and J. Neefjes, *Reduced cell surface expression of HLA-C molecules correlates with restricted peptide binding and stable TAP interaction.* J Immunol, 1998. **160**(1): p. 171-9.
256. Blais, M.-E., T. Dong, and S. Rowland-Jones, *HLA-C as a mediator of natural killer and T-cell activation: spectator or key player? Immunology* 2011. **133**: p. 1-7.
257. Tan, A.T., et al., *Immunoprevalence and immunodominance of HLA-Cw*0801-restricted T cell response targeting the hepatitis B virus envelope transmembrane region.* J Virol, 2014. **88**(2): p. 1332-41.
258. Mkhwanazi, N., et al., *Immunodominant HIV-1-specific HLA-B- and HLA-C-restricted CD8+ T cells do not differ in polyfunctionality.* Virology, 2010. **405**(2): p. 483-91.
259. Apps, R., et al., *Influence of HLA-C expression level on HIV control.* Science, 2013. **340**(6128): p. 87-91.
260. Thomas, R., et al., *HLA-C cell surface expression and control of HIV/AIDS correlate with a variant upstream of HLA-C.* Nat Genet, 2009. **41**(12): p. 1290-4.
261. Khan, N., et al., *Herpesvirus-specific CD8 T cell immunity in old age: cytomegalovirus impairs the response to a coresident EBV infection.* J Immunol, 2004. **173**(12): p. 7481-9.
262. Reddehase, M.J.e.o.c. and N.e.o.c. Lemmermann, *Cytomegaloviruses : from molecular pathogenesis to intervention*. Updated and upgraded second edition. ed.
263. Ljunggren, H.G. and K. Kärre, *In search of the 'missing self': MHC molecules and NK cell recognition.* Immunol Today, 1990. **11**(7): p. 237-44.
264. Specht, A., et al., *Counteraction of HLA-C-mediated immune control of HIV-1 by Nef.* J Virol, 2010. **84**(14): p. 7300-11.
265. Cohen, G.B., et al., *The selective downregulation of class I major histocompatibility complex proteins by HIV-1 protects HIV-infected cells from NK cells.* Immunity, 1999. **10**(6): p. 661-71.
266. Horowitz, A., et al., *Regulation of Adaptive NK Cells and CD8 T Cells by HLA-C Correlates with Allogeneic Hematopoietic Cell Transplantation and with Cytomegalovirus Reactivation.* J Immunol, 2015. **195**(9): p. 4524-36.
267. Slezak, S.L., et al., *CMV pp65 and IE-1 T cell epitopes recognized by healthy subjects.* J Transl Med, 2007. **5**: p. 17.
268. Lachmann, R., et al., *Polyfunctional T cells Accumulate in Large Human Cytomegalovirus-Specific T Cell Responses. Journal of Virology*, 2012. **86**: p. 1001-1009.
269. Larsen, M., et al., *Evaluating cellular polyfunctionality with a novel polyfunctionality index.* PLoS One, 2012. **7**(7): p. e42403.
270. Cerdan, C., et al., *CD28 costimulation up-regulates long-term IL-2R beta expression in human T cells through combined transcriptional and post-transcriptional regulation.* J Immunol, 1995. **154**(3): p. 1007-13.
271. Hamann, D., et al., *Phenotypic and functional separation of memory and effector human CD8+ T cells.* J Exp Med, 1997. **186**(9): p. 1407-18.
272. Barber, A. and C.L. Sentman, *NKG2D receptor regulates human effector T-cell cytokine production.* Blood, 2011. **117**(24): p. 6571-81.
273. Schalich, J., et al., *Analysis of the human cytomegalovirus pp65-directed T-cell response in healthy HLA-A2-positive individuals.* Biol Chem, 2008. **389**(5): p. 551-9.

274. Solache, A., et al., *Identification of three HLA-A*0201-restricted cytotoxic T cell epitopes in the cytomegalovirus protein pp65 that are conserved between eight strains of the virus.* J Immunol, 1999. **163**(10): p. 5512-8.
275. Sinclair, E., et al., *CMV antigen-specific CD4+ and CD8+ T cell IFNgamma expression and proliferation responses in healthy CMV-seropositive individuals.* Viral Immunol, 2004. **17**(3): p. 445-54.
276. Ouyang, Q., et al., *Dysfunctional CMV-specific CD8(+) T cells accumulate in the elderly. Experimental Gerontology* 2004. **39**: p. 607-613.
277. Groh, V., et al., *Costimulation of CD8alphabeta T cells by NKG2D via engagement by MIC induced on virus-infected cells.* Nat Immunol, 2001. **2**(3): p. 255-60.
278. York, I.A., et al., *Endoplasmic reticulum aminopeptidase 1 (ERAP1) trims MHC class I-presented peptides in vivo and plays an important role in immunodominance.* Proc Natl Acad Sci U S A, 2006. **103**(24): p. 9202-7.
279. Pudney, V.A., et al., *CD8+ immunodominance among Epstein-Barr virus lytic cycle antigens directly reflects the efficiency of antigen presentation in lytically infected cells. The Journal of Experimental Medicine*, 2005. **201**: p. 349-360.
280. Yewdell, J.W. and J.R. Bennink, *Immunodominance in major histocompatibility complex class I-restricted T lymphocyte responses.* Annu Rev Immunol, 1999. **17**: p. 51-88.
281. Saric, T., et al., *An IFN-[gamma]-induced aminopeptidase in the ER, ERAP1, trims precursors to MHC class I-presented peptides.* Nat Immunol, 2002. **3**(12): p. 1169-1176.
282. Chang, S.C., et al., *The ER aminopeptidase, ERAP1, trims precursors to lengths of MHC class I peptides by a "molecular ruler" mechanism.* Proc Natl Acad Sci U S A, 2005. **102**(47): p. 17107-12.
283. Rastall, D.P., et al., *ERAP1 functions override the intrinsic selection of specific antigens as immunodominant peptides, thereby altering the potency of antigen-specific cytolytic and effector memory T-cell responses.* Int Immunol, 2014. **26**(12): p. 685-95.
284. Rasmussen, M., et al., *Uncovering the peptide-binding specificities of HLA-C: a general strategy to determine the specificity of any MHC class I molecule.* J Immunol, 2014. **193**(10): p. 4790-802.
285. Terhune, S.S., et al., *Human Cytomegalovirus UL29/28 Protein Interacts with Components of the NuRD Complex Which Promote Accumulation of Immediate-Early RNA.* PLoS Pathog, 2010. **6**(6): p. e1000965.
286. Dekhtiarenko, I., et al., *The context of gene expression defines the immunodominance hierarchy of cytomegalovirus antigens.* J Immunol, 2013. **190**(7): p. 3399-409.
287. Pende, D., et al., *The natural killer cell receptor specific for HLA-A allotypes: a novel member of the p58/p70 family of inhibitory receptors that is characterized by three immunoglobulin-like domains and is expressed as a 140-kD disulphide-linked dimer.* J Exp Med, 1996. **184**(2): p. 505-18.
288. Hesse, J., et al., *Suppression of CD8+ T-cell recognition in the immediate-early phase of human cytomegalovirus infection.* J Gen Virol, 2013. **94**(Pt 2): p. 376-86.
289. Tenney, D.J. and A.M. Colberg-Poley, *Human cytomegalovirus UL36-38 and US3 immediate-early genes: temporally regulated expression of nuclear, cytoplasmic, and polysome-associated transcripts during infection.* J Virol, 1991. **65**(12): p. 6724-34.

290. Kurz, S.K., et al., *Focal transcriptional activity of murine cytomegalovirus during latency in the lungs.* J Virol, 1999. **73**(1): p. 482-94.
291. Kurz, S.K. and M.J. Reddehase, *Patchwork pattern of transcriptional reactivation in the lungs indicates sequential checkpoints in the transition from murine cytomegalovirus latency to recurrence.* J Virol, 1999. **73**(10): p. 8612-22.
292. Reusser, P., et al., *Cytotoxic T-lymphocyte response to cytomegalovirus after human allogeneic bone marrow transplantation: pattern of recovery and correlation with cytomegalovirus infection and disease.* Blood, 1991. **78**(5): p. 1373-80.
293. Moss, P. and A. Rickinson, *Cellular immunotherapy for viral infection after HSC transplantation.* Nat Rev Immunol, 2005. **5**(1): p. 9-20.
294. Murphy, E., et al., *Coding potential of laboratory and clinical strains of human cytomegalovirus.* Proc Natl Acad Sci U S A, 2003. **100**(25): p. 14976-81.
295. Chee, M.S., et al., *Analysis of the protein-coding content of the sequence of human cytomegalovirus strain AD169.* Curr Top Microbiol Immunol, 1990. **154**: p. 125-69.
296. Rossetto, C.C., M. Tarrant-Elorza, and G.S. Pari, *Cis and trans acting factors involved in human cytomegalovirus experimental and natural latent infection of CD14 (+) monocytes and CD34 (+) cells.* PLoS Pathog, 2013. **9**(5): p. e1003366.
297. Biron, K.K., *Antiviral drugs for cytomegalovirus diseases.* Antiviral Res, 2006. **71**(2-3): p. 154-63.
298. Razonable, R.R., *Antiviral drugs for viruses other than human immunodeficiency virus.* Mayo Clin Proc, 2011. **86**(10): p. 1009-26.
299. Boeckh, M., et al., *Late cytomegalovirus disease and mortality in recipients of allogeneic hematopoietic stem cell transplants: importance of viral load and T-cell immunity.* Blood, 2003. **101**(2): p. 407-14.
300. Bunde, T., et al., *Protection from cytomegalovirus after transplantation is correlated with immediate early 1-specific CD8 T cells.* J Exp Med, 2005. **201**(7): p. 1031-6.
301. Bao, L., et al., *Expansion of cytomegalovirus pp65 and IE-1 specific cytotoxic T lymphocytes for cytomegalovirus-specific immunotherapy following allogeneic stem cell transplantation.* Biol Blood Marrow Transplant, 2008. **14**(10): p. 1156-62.
302. Casavant, N.C., et al., *Potential role for p53 in the permissive life cycle of human cytomegalovirus.* J Virol, 2006. **80**(17): p. 8390-401.
303. Savaryn, J.P., et al., *Human cytomegalovirus pUL29/28 and pUL38 repression of p53-regulated p21CIP1 and caspase 1 promoters during infection.* J Virol, 2013. **87**(5): p. 2463-74.
304. Giest, S., et al., *Cytomegalovirus-specific CD8(+) T cells targeting different HLA/peptide combinations correlate with protection but at different threshold frequencies.* Br J Haematol, 2010. **148**(2): p. 311-22.
305. Holtappels, R., et al., *Reconstitution of CD8 T Cells Protective against Cytomegalovirus in a Mouse Model of Hematopoietic Cell Transplantation: Dynamics and Inessentiality of Epitope Immunodominance.* Front Immunol, 2016. **7**: p. 232.
306. Ye, M., C.S. Morello, and D.H. Spector, *Strong CD8 T-cell responses following coimmunization with plasmids expressing the dominant pp89 and subdominant M84 antigens of murine cytomegalovirus correlate with long-term protection against subsequent viral challenge.* J Virol, 2002. **76**(5): p. 2100-12.
307. Scheinberg, P., et al., *The transfer of adaptive immunity to CMV during hematopoietic stem cell transplantation is dependent on the specificity and phenotype of CMV-specific T cells in the donor.* Blood, 2009. **114**(24): p. 5071-80.

308. Mackay, L.K., et al., *Hobit and Blimp1 instruct a universal transcriptional program of tissue residency in lymphocytes.* Science, 2016. **352**(6284): p. 459-63.
309. Mayrand, S.M. and W.R. Green, *Non-traditionally derived CTL epitopes: exceptions that prove the rules?* Immunol Today, 1998. **19**(12): p. 551-6.
310. Hwang, C.B., et al., *A net +1 frameshift permits synthesis of thymidine kinase from a drug-resistant herpes simplex virus mutant.* Proc Natl Acad Sci U S A, 1994. **91**(12): p. 5461-5.
311. Mayrand, S.M., D.A. Schwarz, and W.R. Green, *An alternative translational reading frame encodes an immunodominant retroviral CTL determinant expressed by an immunodeficiency-causing retrovirus.* J Immunol, 1998. **160**(1): p. 39-50.
312. Mayrand, S.M., et al., *Anti-Gag cytolytic T lymphocytes specific for an alternative translational reading frame-derived epitope and resistance versus susceptibility to retrovirus-induced murine AIDS in F(1) mice.* Virology, 2000. **272**(2): p. 438-49.
313. Bullock, T.N. and L.C. Eisenlohr, *Ribosomal scanning past the primary initiation codon as a mechanism for expression of CTL epitopes encoded in alternative reading frames.* J Exp Med, 1996. **184**(4): p. 1319-29.
314. Griffiths, A., et al., *Translational compensation of a frameshift mutation affecting herpes simplex virus thymidine kinase is sufficient to permit reactivation from latency.* J Virol, 2003. **77**(8): p. 4703-9.
315. Cardinaud, S., et al., *Identification of cryptic MHC I-restricted epitopes encoded by HIV-1 alternative reading frames.* J Exp Med, 2004. **199**(8): p. 1053-63.
316. Maness, N.J., et al., *AIDS virus specific CD8+ T lymphocytes against an immunodominant cryptic epitope select for viral escape.* J Exp Med, 2007. **204**(11): p. 2505-12.
317. Maness, N.J., et al., *CD8+ T cell recognition of cryptic epitopes is a ubiquitous feature of AIDS virus infection.* J Virol, 2010. **84**(21): p. 11569-74.
318. Saulquin, X., et al., *+1 Frameshifting as a novel mechanism to generate a cryptic cytotoxic T lymphocyte epitope derived from human interleukin 10.* J Exp Med, 2002. **195**(3): p. 353-8.
319. Rimoldi, D., et al., *Efficient simultaneous presentation of NY-ESO-1/LAGE-1 primary and nonprimary open reading frame-derived CTL epitopes in melanoma.* J Immunol, 2000. **165**(12): p. 7253-61.
320. Wang, R.F., et al., *Utilization of an alternative open reading frame of a normal gene in generating a novel human cancer antigen.* J Exp Med, 1996. **183**(3): p. 1131-40.
321. Saeterdal, I., et al., *Frameshift-mutation-derived peptides as tumor-specific antigens in inherited and spontaneous colorectal cancer.* Proc Natl Acad Sci U S A, 2001. **98**(23): p. 13255-60.
322. Bet, A., et al., *The HIV-1 antisense protein (ASP) induces CD8 T cell responses during chronic infection.* Retrovirology, 2015. **12**: p. 15.
323. Ho, O. and W.R. Green, *Cytolytic CD8+ T cells directed against a cryptic epitope derived from a retroviral alternative reading frame confer disease protection.* J Immunol, 2006. **176**(4): p. 2470-5.
324. Adair, R., et al., *The products of human cytomegalovirus genes UL23, UL24, UL43 and US22 are tegument components.* J Gen Virol, 2002. **83**(Pt 6): p. 1315-24.
325. Mocarski, E.S., L. Pereira, and A.L. McCormick, *Human cytomegalovirus ICP22, the product of the HWLF1 reading frame, is an early nuclear protein that is released from cells.* J Gen Virol, 1988. **69 ( Pt 10)**: p. 2613-21.

326. Borthwick, N.J., et al., *Loss of CD28 expression on CD8(+) T cells is induced by IL-2 receptor gamma chain signalling cytokines and type I IFN, and increases susceptibility to activation-induced apoptosis.* Int Immunol, 2000. **12**(7): p. 1005-13.
327. Powell, J.D., et al., *Molecular regulation of interleukin-2 expression by CD28 co-stimulation and anergy.* Immunol Rev, 1998. **165**: p. 287-300.
328. Holtappels, R., et al., *Identification of an atypical CD8 T cell epitope encoded by murine cytomegalovirus ORF-M54 gaining dominance after deletion of the immunodominant antiviral CD8 T cell specificities.* Med Microbiol Immunol, 2015. **204**(3): p. 317-26.
329. Starck, S.R. and N. Shastri, *Non-conventional sources of peptides presented by MHC class I.* Cell Mol Life Sci, 2011. **68**(9): p. 1471-9.
330. Boon, T. and A. Van Pel, *T cell-recognized antigenic peptides derived from the cellular genome are not protein degradation products but can be generated directly by transcription and translation of short subgenic regions. A hypothesis.* Immunogenetics, 1989. **29**(2): p. 75-9.
331. Yewdell, J.W., L.C. Antón, and J.R. Bennink, *Defective ribosomal products (DRiPs): a major source of antigenic peptides for MHC class I molecules?* J Immunol, 1996. **157**(5): p. 1823-6.
332. Yewdell, J.W. and C.V. Nicchitta, *The DRiP hypothesis decennial: support, controversy, refinement and extension.* Trends Immunol, 2006. **27**(8): p. 368-73.
333. Yewdell, J.W., *DRiPs solidify: progress in understanding endogenous MHC class I antigen processing.* Trends Immunol, 2011. **32**(11): p. 548-58.
334. Reits, E.A., et al., *The major substrates for TAP in vivo are derived from newly synthesized proteins.* Nature, 2000. **404**(6779): p. 774-8.
335. Khan, S., et al., *Cutting edge: neosynthesis is required for the presentation of a T cell epitope from a long-lived viral protein.* J Immunol, 2001. **167**(9): p. 4801-4.
336. Stern-Ginossar, N., et al., *Decoding Human Cytomegalovirus.* Science, 2012. **338**(6110): p. 1088-1093.
337. Malarkannan, S., et al., *Presentation of out-of-frame peptide/MHC class I complexes by a novel translation initiation mechanism.* Immunity, 1999. **10**(6): p. 681-90.
338. Schwab, S.R., et al., *Constitutive display of cryptic translation products by MHC class I molecules.* Science, 2003. **301**(5638): p. 1367-71.
339. Schwab, S.R., et al., *Unanticipated antigens: translation initiation at CUG with leucine.* PLoS Biol, 2004. **2**(11): p. e366.
340. Starck, S.R., et al., *A distinct translation initiation mechanism generates cryptic peptides for immune surveillance.* PLoS One, 2008. **3**(10): p. e3460.
341. Schirmbeck, R., et al., *Translation from cryptic reading frames of DNA vaccines generates an extended repertoire of immunogenic, MHC class I-restricted epitopes.* J Immunol, 2005. **174**(8): p. 4647-56.
342. Goodenough, E., et al., *Cryptic MHC class I-binding peptides are revealed by aminoglycoside-induced stop codon read-through into the 3' UTR.* Proc Natl Acad Sci U S A, 2014. **111**(15): p. 5670-5.
343. Kim, J., A.R. Kim, and E.C. Shin, *Cytomegalovirus Infection and Memory T Cell Inflation.* Immune Netw, 2015. **15**(4): p. 186-90.
344. Qiu, Z., et al., *Cytomegalovirus-Based Vaccine Expressing a Modified Tumor Antigen Induces Potent Tumor-Specific CD8(+) T-cell Response and Protects Mice from Melanoma.* Cancer Immunol Res, 2015. **3**(5): p. 536-46.

345. Qiu, Z., J.M. Grenier, and K.M. Khanna, *Reviving virus based cancer vaccines by using cytomegalovirus vectors expressing modified tumor antigens.* Oncoimmunology, 2016. **5**(1): p. e1056974.
346. van der Bruggen, P., et al., *A gene encoding an antigen recognized by cytolytic T lymphocytes on a human melanoma.* Science, 1991. **254**(5038): p. 1643-7.
347. Gure, A.O., et al., *SSX: a multigene family with several members transcribed in normal testis and human cancer.* Int J Cancer, 1997. **72**(6): p. 965-71.
348. Ademuyiwa, F.O., et al., *NY-ESO-1 cancer testis antigen demonstrates high immunogenicity in triple negative breast cancer.* PLoS One, 2012. **7**(6): p. e38783.
349. Iura, K., et al., *Cancer-testis antigens PRAME and NY-ESO-1 correlate with tumour grade and poor prognosis in myxoid liposarcoma.* J Pathol Clin Res, 2015. **1**(3): p. 144-59.
350. van Rhee, F., et al., *NY-ESO-1 is highly expressed in poor-prognosis multiple myeloma and induces spontaneous humoral and cellular immune responses.* Blood, 2005. **105**(10): p. 3939-44.
351. Alanio, C., et al., *Enumeration of human antigen-specific naive CD8+ T cells reveals conserved precursor frequencies.* Blood, 2010. **115**(18): p. 3718-25.
352. Jäger, E., et al., *Simultaneous humoral and cellular immune response against cancer-testis antigen NY-ESO-1: definition of human histocompatibility leukocyte antigen (HLA)-A2-binding peptide epitopes.* J Exp Med, 1998. **187**(2): p. 265-70.
353. Held, G., et al., *Dissecting cytotoxic T cell responses towards the NY-ESO-1 protein by peptide/MHC-specific antibody fragments.* Eur J Immunol, 2004. **34**(10): p. 2919-29.
354. Dutoit, V., et al., *Multiepitope CD8(+) T cell response to a NY-ESO-1 peptide vaccine results in imprecise tumor targeting.* J Clin Invest, 2002. **110**(12): p. 1813-22.
355. Gnjatic, S., et al., *Survey of naturally occurring CD4+ T cell responses against NY-ESO-1 in cancer patients: correlation with antibody responses.* Proc Natl Acad Sci U S A, 2003. **100**(15): p. 8862-7.
356. Jungbluth, A.A., et al., *Monophasic and biphasic synovial sarcomas abundantly express cancer/testis antigen NY-ESO-1 but not MAGE-A1 or CT7.* Int J Cancer, 2001. **94**(2): p. 252-6.
357. Odunsi, K., et al., *NY-ESO-1 and LAGE-1 cancer-testis antigens are potential targets for immunotherapy in epithelial ovarian cancer.* Cancer Res, 2003. **63**(18): p. 6076-83.
358. Vaughan, H.A., et al., *Immunohistochemical and molecular analysis of human melanomas for expression of the human cancer-testis antigens NY-ESO-1 and LAGE-1.* Clin Cancer Res, 2004. **10**(24): p. 8396-404.
359. Akcakanat, A., et al., *NY-ESO-1 expression and its serum immunoreactivity in esophageal cancer.* Cancer Chemother Pharmacol, 2004. **54**(1): p. 95-100.
360. Odunsi, K., et al., *Efficacy of vaccination with recombinant vaccinia and fowlpox vectors expressing NY-ESO-1 antigen in ovarian cancer and melanoma patients.* Proc Natl Acad Sci U S A, 2012. **109**(15): p. 5797-802.
361. Jäger, E., et al., *Recombinant vaccinia/fowlpox NY-ESO-1 vaccines induce both humoral and cellular NY-ESO-1-specific immune responses in cancer patients.* Proc Natl Acad Sci U S A, 2006. **103**(39): p. 14453-8.
362. Rapoport, A.P., et al., *NY-ESO-1-specific TCR-engineered T cells mediate sustained antigen-specific antitumor effects in myeloma.* Nat Med, 2015. **21**(8): p. 914-21.

363. Satie, A.P., et al., *The cancer-testis gene, NY-ESO-1, is expressed in normal fetal and adult testes and in spermatocytic seminomas and testicular carcinoma in situ.* Lab Invest, 2002. **82**(6): p. 775-80.
364. Sugita, Y., et al., *NY-ESO-1 expression and immunogenicity in malignant and benign breast tumors.* Cancer Res, 2004. **64**(6): p. 2199-204.
365. Hofmann, O., et al., *Genome-wide analysis of cancer/testis gene expression.* Proc Natl Acad Sci U S A, 2008. **105**(51): p. 20422-7.
366. Stockert, E., et al., *A survey of the humoral immune response of cancer patients to a panel of human tumor antigens.* J Exp Med, 1998. **187**(8): p. 1349-54.
367. Khan, N., et al., *T cell recognition patterns of immunodominant cytomegalovirus antigens in primary and persistent infection.* J Immunol, 2007. **178**(7): p. 4455-65.